ROCK, TILL, AND ICE: A PROVENANCE STUDY OF THE BYRD GLACIER AND THE CENTRAL AND WESTERN ROSS SEA, ANTARCTICA

Emerson Fowler Palmer

Submitted to the faculty of the Graduate School
in partial fulfillment of the requirements
for the degree
Master of Science
in the Department of Earth Sciences,
Indiana University

February 2008

Accepted by the Faculty of Indiana University, in fulfillment of the requirements for the degree of Master of Science.

_____

Kathy J. Licht, PhD., Chair

_____

Andrew P. Barth, PhD.

_____

R. Jeffery Swope, PhD.

_____

Gabriel M. Filippelli, PhD.

Acknowledgments

I'd like to thank:

Dr. Kathy Licht for her support as an undergraduate, for giving me the opportunity to work on this project as a graduate student, and for being such a great mentor and friend.

Dr. Andrew Barth for teaching me the geology in the field and for giving me my first opportunity at scientific research. The day you taught us how the Cretaceous follows the Jurassic in a chalkboard of desert dust is one I will never forget.

Dr. Jeffery Swope for teaching me the fundamentals of earthen matter and comedy. Your curiosity and enthusiasm for science has been a great inspiration to myself, and so many other students here at IUPUI. You make science fun and interesting. You are a true Professor of science.

Dr. Art Mirsky for not only his instruction, but for good conversion over a cup of coffee. Thank you for your time and teaching.

Dr. Bob Hall for my first A+. My first geology class here at IUPUI was your last. I hope I can give someone an A+ in my last class.

Dr. Gary Rossenberg for showing me that creativity, and its appreciation, has a pure and proper place in the scientific world.

Dr. Lenore Tedesco, Bob Hall, Kara Salazar, Lani Pascual, and Lora Shrake of CEES for the opportunity to work as an intern. It was an indispensable part of my undergraduate education at IUPUI and lots of fun as well. I foresee great things from all of you.

Dr. Joseph Pachut for teaching me cladistics and graduated equilibrium. While much more is left to learn in evolutionary theory, to the miseducated, these ideas provide a light where once there was darkness.

My friends and fellow students: Kenneth Brown, Ivy Caito, Leda Casey, Christy Carter, Phillip Chapman, Megan Flaherty, Nicole Fohey, Dustin Graves, Kristen Hughes, Kate Kramer, Jay Lederer, Cheryl Nazareth, Sarah Needy, Derek Newkirk, Joe Phillips, Kelly Probst, Robin Raftis, Kate Randolf, Josh Richards, Jennifer Sembach, Andrew Smith, Michael Smith, Rachael Troyer, Andy Wolf, Laura Wagner, Jeremy Webber, and Andy Wolf.

Lora Shrake for being my best friend and confidant during the time I was researching and writing this project. Thanks for being there.

The rest of the 2005 Antarctic field party: Peter Braddock, Dr. John Goodge, Deven Brecke, Jim Haffey, and Chuck Slade.

The staff of McMurdo Station, Antarctica and the National Science Foundation for the funding and support that made this research possible.

My mother Dr. Carolyn Fowler, who was never able to see the product of these last few years. I miss her very much.

"If one advances confidently in the direction of his dreams, and endeavors to live the life which he has imagined, he will meet with a success unexpected in common hours."

David Henry Thoreau

Abstract

Petrography of the sand fraction, particle size analysis, and detrital zircon U/Pb isotope data, and pebble count data were collected from Byrd Glacier moraines and central/western Ross Sea till in order to study the glacially-driven sedimentological dynamics of the Byrd Glacier and to trace material transported from the Byrd Glacier into the Ross embayment. Most of the petrographic data show evidence of local derivation with the exception of the sites from the Lonewolf Nunataks as indicated by exotic rock types within the sand and pebble fractions. This, in conjunction with particle-size data of the samples from the Lonewolf Nunataks indicate that material from underneath the East Antarctic Ice Sheet (EAIS) is being transported to the surface and deposited in this area.

The U/Pb ages of zircons from the Byrd Glacier show dominant populations of Ross to Pan-African ages (~533 - 610 Ma) with varying populations of older (Grenville to Archean) zircons. Late Precambrian (~588 – 610 Ma) aged detrital zircons in samples from the head of the Byrd Glacier are older than other dated grains found in the vicinity and may be evidence of early development of the Ross belt or represent evidence of sub-glacial extension of the Mozambique structure found in Dronning Maud Land.

The west central Ross Sea till samples have a variety of mineral and lithic fragments that include a dominant population of polymict at certain depth intervals. Detrital zircon data suggests the potential provenance of two of these intervals may be derived from Marie Byrd Land and possibly the Byrd Glacier. Using sand petrography and U/Pb detrital zircon age dating, positive correlation was found between specific samples from the head of the Byrd Glacier and the western Ross Sea.

The ice-sheet flow models of Stuiver et al. (1981), Licht and Fastook (1998), and Licht et al. (2005) each show potential support from aspects of this study. It is possible that dynamic ice-flow regime changes of the West and East Antarctic Ice Sheets into the Ross Sea may have occurred some time during the LGM as suggested by geochemical and petrographical evidence found within intervals of central and western Ross Sea cores.

Table of Contents

List of Figures:

List of Tables:

List of Appendices:

List of Plates:

1. Introduction

The Ross Sea (Figure 1) receives nearly one third of all ice discharging from the continent of Antarctica (Anderson, 1999). More fresh water has accumulated as part of Antarctica's ice sheets than anywhere on Earth. With the scientific debate over global climate-change transitioning from validity to one of prognosis and abatement, an improved comprehension and knowledge of Antarctic ice sheet dynamics is of utmost importance. With the ongoing increase in population and development of global coastal regions, the potential for significant economic, political, and social tensions are certain if future sea levels increase.

The East and West Antarctic Ice Sheets cover most of the Antarctic continent with the majority of bedrock exposure limited to the coastal areas. Due to the marine-based nature of the West Antarctic ice sheet (WAIS), global climate-change may potentially facilitate its collapse. The WAIS has a large volume of grounded ice below sea level; therefore the potential exists for the WAIS to become unsTable if sea level rises due to an increase in average global temperatures (Hollin, 1962; Alley and Whillians, 1991; MacAyeal, 1992; Bentley, 1997; Bindschadler, 1997a; 1997b; and Oppenheimer, 1998; Alley and Bindschadler, 2001).

The WAIS has three major drainage systems. These drainages discharge ice that terminates at floating ice shelves. It has been proposed that these ice shelves cause a "back pressure," which limits the outflow speed, therefore increasing the volume of inland-grounded ice (Weertman, 1974). Though debated, melting of these ice shelves could cause this backpressure to reduce resulting in accelerated ice discharge from the

WAIS and a subsequent retreat of the ice sheet's grounding line (Mercer, 1977; Thomas et al., 1979; and Van der Veen, 1985).

The recent 2002 collapse of a section of the Larsen B Ice Shelf along the Antarctic Peninsula has been followed by a two to six-fold increase in the centerline velocities of four glaciers flowing into the ice shelf. A decrease in the elevation of these glaciers has also been observed in conjunction with their increased velocity using satellite laser altimetry (Scambos et al., 2004). These observations of the smaller Larsen B Ice Shelf give us insight into the potential future of the WAIS.

A rapid retreat of the grounding line could cause a collapse of the WAIS, releasing much of its 3.8 million km^3 of ice. This would increase global sea levels by 5 to 6 meters (Bentley, 1997). The time frame for such a scenario has been considered to be as little as 100 years, while others have postulated times of 400, 500, up to 1200 years (Thomas et al., 1979; Bentley, 1981; and Bindshadler, 1997). While no solid evidence has been found to imply that the WAIS has catastrophically collapsed after the LGM (Conway et al., 1999; Licht, 2004) evidence of an open marine environment during the Pleistocene has been found under the Ross sector of the WAIS suggesting a possible partial collapse (Scherer et al., 1998).

The effect of such a drastic rise in sea level would have devastating consequences on coastal cities. Therefore in-depth studies constraining past behavior of the WAIS and the East Antarctic ice sheets (EAIS) are necessary in order to gain insights into their dynamics, history, and potential future. Understanding the behavior of these two systems in the Ross Embayment during the last glacial maximum (LGM) will help our

conception of past and future behavior of the WAIS, including the cause of late Holocene eustatic sea-level rise (Flemming, et al., 1998; Conway, et al., 1999).

Previous studies have attempted to reconstruct and model ice dynamics of the East and West Antarctic ice sheets during and since the LGM (e.g., Stuiver et al., 1981; Licht and Fastook, 1998; Denton and Hughes, 2000; 2002). Stuiver et al.'s (1981) conceptual model (Figure 2*)* suggests that ice draining from the WAIS during the LGM was the dominant contributor to the Ross Ice Sheet, including the central and western Ross Sea. Licht and Fastook's (1998) and Denton and Hughes (2000) model (Figure 2*)*, constrained by data collected to determine maximum ice extent during the LGM (Licht et al., 1996; 1999), suggests an EAIS-dominated regime in the central and western Ross Sea.

Previous provenance studies (Anderson et al., 1992; Licht et al., 2005; and Farmer et al., 2006) provide a foundation on which paleo ice-flow lines can be determined. Licht et al. (2005) and Farmer et al. (2006) studied tills from East and West Antarctic and the Ross Sea in an attempt to assess WAIS and EAIS dynamics during the LGM. Geochemical and petrographic data from these two studies show evidence of mixing in the central Ross Sea from material originating from both East and West Antarctica. Due to the lack of sample density, these studies could not provide conclusive evidence for detailed LGM flow-line reconstructions. In particular, a detailed flow-line reconstruction was not determined for the Byrd Glacier of East Antarctica, which is the largest of the East Antarctic outlet glaciers. The Byrd Glacier has the highest ice discharge of any glacier in the Transantarctic Mountains, with

recorded velocities of ~850 m a^{-1} in 1978/79 to ~650 m a^{-1} in 2000/01 (Stearns and Hamilton, 2005).

Improving our knowledge of the Byrd Glacier as a potential source area to the Ross Sea and placing better constraint on the the provenance of western and central Ross Sea tills will give us insight into the Byrd Glacier's paleo ice-flow path during the LGM. Determining the Byrd Glacier's paleo ice-flow pattern, along with similar studies of other major outlet glaciers in the TAM, will assist in reconstructions of the EAIS during the LGM. The combination of sand petrography and/or geochronology has been used to determine provenance in basins and river systems (e.g., Geslin et al., 1999) and for the Laurentide Ice Sheet (e.g., Grousset et al., 1993; Gwiazda et al., 1996; Hemming et al., 1998; 2000; 2002). Therefore, a comprehensive provenance study of till from the Byrd Glacier and western/central Ross Sea will better constrain paleo ice-flow paths and contribute Antarctic ice sheet models.

This study will expand upon previous work done (Licht et al., 2005) by analyzing the sand petrography, pebble composition, and particle-size of Byrd Glacier and central and western Ross Sea tills and will include detrital zircon U/Pb age dating, in order to delineate the paleo ice-flow path of the Byrd Glacier during the LGM and to gain insight into the subglacial geology of the East Antarctic craton. The hypotheses of this study are:

1. Sand composition from till found at the head and margins of the Byrd Glacier is distinctive and similar sand can be identified in sediment cores containing till from the central and/or western Ross Sea.

2. U/Pb detrital zircon age distributions or distinctive age populations from till samples along the margins and head of the Byrd Glacier can be positively matched and/or correlated with U/Pb detrital zircon ages from till samples from the central and/or western Ross Sea.

2. Physical setting

The continent of Antarctica is divided into two regions (East and West) by the 3,300 km long Transantarctic Mountains (TAM) and is covered by two interacting ice sheets (Figure 1). The EAIS has a mean thickness of 2,226 m while the WAIS averages 1,306 m thick (British Antarctic Survey, 2005). The majority of the WAIS's ice is grounded on bedrock that, due to isostatic pressure and rifting, is below sea level while much of the rest is floating as part of the Ross and Ronne Filchner ice shelves (Oppenheimer, 1998). West Antarctica is now an archipelago which sustains the only extant full-bodied marine ice sheet in the world with a base over one kilometer below sea level near its center (Anderson, 1984). More recent studies suggest the base may be even deeper at over 2 – 3 kilometers (Gogineni et al., 2006). The EAIS has a portion of its mass grounded below sea level as well, but not to the degree of the WAIS.

The Byrd Glacier, which drains the EAIS, has a maximum vertical relief of over 2100 meters from its lowest point to its highest (Figures 3 and 4). The Byrd Glacier's deepest subglacial basin has a maximum depth of ~1600 meters below sea level. The glacier bed then rises to 500 meters above sea level over a positive slope of around +2 before falling into a secondary basin. As seen in the profile in Figure 3, the ice moving through the Byrd Glacier travels through these two basins, with a maximum positive slope of around +3, and over two ridges before emerging into the Ross Ice Shelf.

The edge of Antarctica's ice sheets are commonly grounded on the continental shelves at an average depth of 500 m or are floating above the seafloor with water

depths ranging from 400 to 1000 m (Anderson et al., 1984). The Ross Sea is the most sampled area of the Antarctic continental shelf. The shelf is characterized by a series of ridges and troughs that trend northeast/southwest (Figure 4), which Hughes (1973) interpreted to be the result of multiple ice-stream advances and retreats. The Ross Sea continental shelf is tilted toward the continent as the result of repeating episodes of glacially driven erosion have moved material from the inner to the outer shelf (Johnson et al., 1982; Anderson et al., 1984; ten Brink et al., 1995; Shipp et al., 1999). The maximal extension of grounded ice into the Ross Sea during the LGM has been accessed using piston cores and seismic data by determining the contact between till and glacial marine sediments in addition to locating geomorphic features of glacial material residing over regional erosion surfaces and located at the shelf break in the eastern Ross Sea around the midshelf in the western Ross Sea (Kellogg, et al., 1979; Anderson et al., 1980; 1984; 1992; Domack et al., 1999; Licht et al., 1996; 1999; and Shipp et al., 1999).

2.1. East Antarctic cratonic history

The East Antarctic Shield is one of Earth's oldest cratons. The EAIS covers most of the shield, yet outcrops of basement can be found around its outer margin that confirm a history dating back to the Archean (Tingey, 1991). The TAM are an orogenic belt that extends along nearly one-third of the shield margin and are mostly composed of deformed Neoproterozoic and lower Paleozoic sedimentary sequences of the Ross Orogen overlain by Gondwanan sediments (Goodge and Fanning, 2002). From Byrd Glacier to the Shackleton Range (Figure 1), Cambrian shallow-marine

sediments (Byrd Group) are overlain by Ordovician-Devonian coarse-grained post-orogenic clastic deposits. These in turn are unconformably overlain by the Devonian - Triassic Beacon Supergroup, including the Jurassic Ferrar dolerite or Ferrar Group (Laird, 1987).

The drainage basin for the Byrd Glacier covers a large area from the adjacent East Antarctic Craton and TAM. In order to put the detrital zircon age data into context, a basic understanding of the orogenic history of the Antarctic shield is necessary. The East Antarctic craton has undergone several orogenic events throughout its history beginning with the Napier Orogeny around 4000 Ma (Sobotovich et al., 1976; Grikurov, 1982; Kamenev, 1982; and Ravich, 1982), which was followed by crustal thickening of the Rayner Orogeny around 3500 Ma (Grikurov, 1982, Ravich, 1982). Following the Rayner orogeny, the Humboldt Orogeny (Grikurov, 1982) began around 3000 Ma creating extensive exposures of rock that can be found in Queen Maud Land and MacRobertson Land (Figure 1). The Insel Orogeny followed the Humboldt around 2650 ± 150 Ma (Grikurov, 1982) from which large regions of crust were produced by the reworking of older crust and are distinguished by amphibolite-grade metamorphism (Anderson, 1999).

Evidence of several of these events can be found in the metamorphic and igneous rocks of the Nimrod Group (~3000 Ma), southeast of the Byrd Glacier. The Nimrod Group forms the basement rock of the TAM and crops out only in the central region of the TAM (Figures 5 and 6). The Precambrian history of the Nimrod Group began with production of Archean juvenile magmatic crust around 3150 – 3000 Ma (Humbolt Orogeny). This was followed by metamorphism between 2955 – 2900 Ma,

and anatectic magmatism around 2500 Ma (Insel Orogeny). An episode of additional magmatism, metamorphism, and eclogite formation occurred between 1730 – 1720 (Nimrod Orogeny), followed by clastic sedimentation beginning after 1700 Ma (Goodge and Fanning, 2002).

The later Ross Orogeny was characterized by high-pressure, high-temperature Late Precambrian to Early Cambrian metamorphism, deformation, and abundant orogenic magmatism between 540 – 520 Ma (i.e., Goodge and Dallmeyer, 1992; 1996; Goodge et al., 1993a; 1993b). The Ross Orogeny overprints the Nimrod Group's pre-Ross history. Pre-Ross events have been interpreted with SHRIMP U/Pb dating of zircon, thanks to zircon's persistence though later metamorphic events. The refractory properties of zircon make it possible for the crystal to preserve internal structures that reveal multiple growth events caused by igneous and/or metamorphic crystallization, resorption, and one or more overgrowth periods (Goodge et al., 2004).

During the Lower Cambrian, the Shackleton Limestone of the Byrd Group (Figure 5) was deposited unconformably over the Goldie Formation of the Beardmore Group. The Beardmore Group does not outcrop in the Byrd Glacier area but does so along the Nimrod Glacier to the south. The Shackleton Limestone consists of a thick carbonate sequence containing a lower unit of unfossiliferous carbonate interbedded with quartzite. The Douglas conglomerate, Starshot, and Dick Formations lie stratigraphically above the Shackleton Limestone, but their conformity and locations of contact are still debated (Myrow et al., 2002). These rocks make up the southern margin of the Byrd Glacier (Figure 6).

During and after the Ross Orogeny, the Precambrian and Paleozoic bedrock underwent intense erosion and is now overlain by unconformable Gondwanan sediments consisting of the Devonian – Triassic Beacon Supergroup and the Jurassic intrusive-igneous Ferrar Group (Barrett, 1972, 1991; Collinson and Pennington, 1986; Bernet and Gaupp, 2005). The Beacon Supergroup is subdivided into the Taylor and Victoria Groups (Figure 7). The Taylor group consists of Devonian quartzarenites including red-beds along its base, middle, and top (Barrett, 1972; 1991). The Victoria Group sits unconformably over the Taylor group and consists of abasal tillite, which is overlain by the Weller Coal measures (Bernet and Gaupp, 2005). The Ferrar Group consists of continental flood basalts with compositions of dolerite and basalt which are related to the Gondwanan break-up after deposition of the Beacon Supergroup (Wilson, 1989; Wilhelm, 1994; Balance and Watters, 2002).

The Byrd Glacier overlies a discontinuity in the trend of the Ross Orogen in the TAM (Stump et al., 2004) (Figure 6). Outcrops along the southern margin of the Byrd Glacier expose the Lower Cambrian to Ordovician Shackleton Limestone and Starshot Group siliciclastic rocks (Figure 6) (Goodge et al., 2004). Bedrock along the northern margin of the Byrd Glacier mostly comprise crystalline rocks which Grindley and Laird (1969) mapped using aerial photo interpretation as Cambro-Orodovician Granite Harbour Intrusives (Figure 6). A reconnaissance survey along the north side of the Byrd Glacier by Borg (1989) found amphibolite-grade schist and gneiss, which were named the Horney Formation. Little else is known of this area (Stump et al., 2004).

Stump et al. (2006), propose a tectonic model in which rifting in the Byrd Glacier area and the western cratonic margin occurred ~670 Ma leaving the Beardmore microcontinent (Borg and Depaulo, 1991) obliquely converged in the Byrd Glacier area. This rifting was then followed by subduction of the Beardmore microcontinent along the cratonic margin of East Antarctica during the Late Neoproterozoic and Early Cambrian. They propose that subduction of the microcontinent began ~550 Ma followed by carbonate and clastic deposition from 525 – 512 Ma.

3. Previous Provenance Studies

Several provenance studies have been performed in the Ross Embayment. A previous study by Anderson et al. (1992) performed petrographic studies on central and western Ross Sea tills. The three components used for their study included rock clasts, coarse sand, and heavy mineral components. The study found differences in the sand composition of Ross Sea tills, therefore making it possible to divide the Ross Sea into NE-SW trending provinces (1 – 7) and, according to Anderson et al (1992), "confirm reasonably well with paleodrainage models constructed independently by Stuvier et al. (1981) (Figure 2), and Denton et al. (1989)."

Cores from this study fall into provinces four, five, and six. Province 4 includes core NBP94-01-02. The cores in province 5 include ELT27-14, ELT32-20, and ELT32-21. Core NBP94-07-39 is located in province 6.

More recent studies by Licht et al. (2005) used coarse sand (0.5 – 2mm) petrography to determine provenance of both terrestrial and Ross Sea tills. Farmer et al. (2006) used trace elements, Nd, Sr, and Pb isotopes of the < 0.63 μm fraction of the same samples as the Licht et al. (2005) study to examine till composition in finer fractions.

The Licht et al. (2005) study found the sand fraction of western Ross Sea tills were minerologically and lithologically similar to tills from East Antarctica with similar amounts of quartz, sedimentary, mafic intrusive, and metamorphic lithic fragments. Tills from the eastern Ross Sea (Figure 8) were found to be similar to West Antarctic tills with both having high amounts of quartz grains with low to absent quantities of mafic and extrusive igneous lithic fragments. Till samples from the central Ross Sea

displayed characteristics of both East and West Antarctic tills suggesting a confluence of East and West Antarctic ice in the central Ross Sea during the LGM. However, their samples from East Antarctic outlet glaciers were limited with only one sample studied from the Byrd Glacier.

The Farmer et al. (2006) study found ε_{Nd} values for West Antarctic and southern TAM tills to range from -5.6 to -9.9. ε_{Nd} values from central TAM tills ranged from -11.9 to -14.9. Western Ross Sea tills had ε_{Nd} values from -5.8 to -7.5 while eastern Ross Sea tills had ε_{Nd} values of -3.8 to -6.9. Central Ross Sea tills had ε_{Nd} values of -7.1 to -12.5.

Both studies conclude that tills from the East and West Antarctic are compositionally unique, that till from the western and eastern Ross Sea are compositionally unique and derived from East and West Antarctic sources respectively, and that central Ross Sea till is the result of a confluence of material from both East and West Antarctica, which places constraint on the paleo ice-flow paths of material flowing from both the WAIS and the EAIS into the Ross Sea during the LGM.

4. Methods

4.1. Sample acquisition

Three distinct sub-samples of till and clasts were collected from moraines at seven localities along the margin and head of the Byrd Glacier (Figure 9). At each sample site three individual till and pebble samples were collected and assigned a designation of A, B, and C (plates 1 and 2). Due to limited exposure and time restraints only two pebble samples were collected at LW and at CJ and HB only two till samples were collected (plates 1 and 2). For each sub-sample, a representative one to two square meter area was chosen where approximately 100 clasts, 2.5 to 10 centimeters in diameter, were collected. Approximately one liter of till was also collected after first discarding the top 2 – 3 centimeters of surface material. Additionally 11 samples from five Ross Sea cores (Table 1) located in the south central and western Ross Sea were requested from Florida State University's Antarctic Research Center (Figure 9). These were added to the dataset reported by Licht et al. (2005) for better spatial coverage.

Each till sample was prepared for a suite of four different analytical measurements. These analyses include particle-size analysis, petrography of the sand-sized fraction, U/Pb age dating of detrital zircons, and isotopic analysis of the silt and clay-sized fraction. Dr. Lang Farmer performed U-Pb and Nd-Sm isotope analysis of the clay fraction at the University of Colorado.

4.2. Particle-size analysis

For particle-size analysis, ~30 – 40 grams were sub-sampled from the bulk till and freeze-dried. The weight of coarse fraction was then determined using dry sieves and 2 g of the < 2000 μm fraction was then heated for 30 minutes with 5 ml of 30% H_2O_2 to remove organic material. This process was repeated and the samples were then stored after adding 8 ml of 25 g/L magnesium chloride. The samples were then sieved through a 125 μm sieve and the > 125 μm fraction was examined using a Leica® MZ95 stereoscope to remove any organic material in the process. Each sample was then recombined and placed in a beaker with 600 ml of DI water and left to settle for 24 hours. Afterward, the supernatant was removed and the remaining sediment was centrifuged in 50 ml centrifuge tubes for 10 minutes at 8000 rpm. Twenty ml of 2.5-g/L sodium metaphosphate was added before sample storage.

Following the initial H_2O_2 preparation, the 2 g samples were split from 1/2 to 1/8 and analyzed using a Malvern Mastersizer 2000 laser particle-size analyzer. Each sample was measured (percent by volume) 3 – 5 times for its clay, silt, and sand-sized content ranging from 0.02 – 2000 μm. These results were averaged to produce a single size distribution for each sample (Table 2).

4.3. Sand petrography

The method implemented by Lederer (2003) was used to mount the 0.5 – 2.0 mm sand fraction for petrographic analysis. Each sample was then point counted using the Indiana point counting method (Suttner, 1974; Suttner et al., 1981) for determination of provenance, and for correlation to petrographic data of the 0.5 – 2 mm fraction previously reported from central and western Ross Sea cores (Lederer, 2003; Licht et al., 2005). The point counting was done using a Leitz® Laborlux 12 Pol S microscope with a Leitz® Wetzler graduated point counting stage. Each grain within the thin section was counted and recorded to determine each sample's total content of mineral and lithic fragments. The preferred minimum criterion for total grains was 300 grains for each sample site (3 total samples) although the in a few of the Ross Sea samples, this criterion was not met due to limited material.

Detailed identification criteria from Lederer's (2003) study of the mineral and lithic fragment classification can be seen in Table 3. All of Lederer's thin sections used in this study were recounted and compared to his results. The differences and error statistics can be seen in Table 4. Overall there were large differences in the percentage of several categories. The categories with the most discrepancy (difference %) were quartz (28%), polymict (12.3%), metamorphic (10.5%), and felsic igneous lithic fragments (7%).

Lederer (2003) did not include polymict lithic fragments as a point counting category. After recounting and reviewing the 2003 data, what is categorized as polymict in this study was categorized as mudstone in the former. Therefore the difference % comparisons are made between mudstones (2003) and polymict (2007).

Further review of the point count data from the previous 2003 study indicate that most errors can be attributed to different categorization and/or misidentification between quartz, felsic igneous, and intermediate igneous fragments, specifically the proper categorization of mudstone vs. claystone lithic fragments and also mafic igneous vs. metamorphic lithic fragments resulted in the largest differences.

4.4. Pebble Analysis

The pebble samples were cleaned and assigned to a rock-type category (Table 5). The clasts were then organized according to shape and roundness and groups were counted (Appendix A). Thin sections were also made of the most common clasts in each sample sub-set to verify proper identification.

4.5. Detrital Zircon Analysis

The 0.063 – 0.149 mm fraction from 12 samples was sent to the Iowa State University Wet Chemistry Lab for zircon separation using heavy liquids. The samples were returned in three separations: high magnetic, Methylene Iodide (MI) sink, and MI float. The zircon grains normally reside in the MI Sink due to the higher density of zircon. The zircon grains were then sent to the University of Arizona Laserchron Center for further separation.

U and Pb isotopic compositions of zircons were analyzed by laser ablation multicollector inductively coupled plasma mass spectrometry (LA-MC-ICPMS) at the Arizona LaserChron Center. The analyses involve ablation of zircon with a New Wave/Lambda Physik DUV193 Excimer laser (operating at a wavelength of 193 nm) using a spot diameter of 20 – 30 microns, depending on average zircon size within each

sample. The ablated material is carried in helium into the plasma source of a GVI Isoprobe ICP-MS, which is equipped with a flight tube of sufficient width that U, Th, and Pb isotopes are measured simultaneously. All measurements are made in static mode, using $10e^{11}$ ohm Faraday detectors for ^{238}U, ^{232}Th, ^{208}Pb, and ^{206}Pb, a $10e^{12}$ ohm faraday collector for ^{207}Pb, and an ion-counting channel for ^{204}Pb. Ion yields are ~1.0 mv per ppm. Each analysis consists of one 20-second integration on peaks with the laser off (for backgrounds), 20 one-second integrations with the laser firing, and a 30 second delay to purge the previous sample and prepare for the next analysis. The resulting ablation pit is ~15 microns in depth.

For each analysis, the errors in determining $^{206}Pb/^{238}U$ and $^{206}Pb/^{204}Pb$ result in a measurement error of ~1 – 2% (at 2-sigma level) in the $^{206}Pb/^{238}U$ age. The errors in measurement of $^{206}Pb/^{207}Pb$ and $^{206}Pb/^{204}Pb$ also result in ~1 – 2% (at 2-sigma level) uncertainty in age for grains that are > 1.0 Ga, but the uncertainty is substantially larger for younger grains due to low intensity of the ^{207}Pb signal. For most analyses, the cross-over in precision of $^{206}Pb/^{238}U$ and $^{206}Pb/^{207}Pb$ ages occurs at 0.8 – 1.0 Ga. Common Pb correction is accomplished by using the measured ^{204}Pb and assuming an initial Pb composition from Stacey and Kramers (1975) (with uncertainties of 1.0% for $^{206}Pb/^{204}Pb$ and 0.3% for $^{207}Pb/^{204}Pb$). Our measurement of ^{204}Pb is unaffected by the presence of ^{204}Hg because backgrounds are measured on peaks (thereby subtracting any background ^{204}Hg and ^{204}Pb), and because very little Hg is present in the argon gas.

Inter-element fractionation of Pb/U is generally ~20%, whereas fractionation of Pb isotopes is generally ~2%. In-run analysis of fragments of a large zircon crystal

(generally every fifth measurement) with known age of 564 ± 4 Ma (2-sigma error) is used to correct for this fractionation. The uncertainty resulting from the calibration correction is generally 1 – 2% (2-sigma) for both $^{206}Pb/^{207}Pb$ and $^{206}Pb/^{238}U$ ages. Complete analytical data are reported in Appendix C. Uncertainties shown in these Tables are at the 1-sigma level, and include only measurement errors.

Interpreted ages are based on $^{206}Pb/^{238}U$ for < 1000 Ma grains and on $^{206}Pb/^{207}Pb$ for > 1000 Ma grains. Analyses that are > 30% discordant (by comparison of $^{206}Pb/^{238}U$ and $^{206}Pb/^{207}Pb$ ages) or > 5% reverse discordant are not considered further. The resulting interpreted ages are shown on relative age-probability diagrams (from Ludwig, 2003). These diagrams show each age with its uncertainty (as a normal distribution) and sum all ages from a sample into a single cumulative probability curve.

5. Results

5.1. Particle-size Data

The particle-size data (0.5 – 2.0 mm) collected from the Byrd Glacier tills show a variety of distributions among the sample sites (Table 2). The bedrock for samples sites LW, LW2, BN, and BR is all mapped as Beacon Supergroup (Figure 6), yet all three have very different particle-size distributions (Figure 11). The area for sample site MT is mapped as Cambro-Ordovician limestone while the areas of CJ and HB are mapped as Granite Harbour Intrusives. While these areas contain different bedrock, the glacial processes acting upon them should be similar since all three areas are located along the trunk of the Byrd Glacier.

Lonewolf (LW and LW2) and Mt. Tuatara (MT) have a higher clay and silt content than the sites along the northern margin and head of the Byrd Glacier (BN, BR, CJ and HB) (Figure 11). The northern sites along the Byrd Glacier (BN, BR, CJ, and HB) are relatively consistent, with all sites containing large amounts of sand (Table 2). CJ and HB are almost completely devoid of clay size sediment.

Multiple samples from each site can be used to assess intrasite variability. LW has more sand and less silt and clay than LW2 for instance (Figure 11). Overall, the intrasite variability is smaller than between-site variability with the LW, LW2 (Figure 12), and MT samples having the most within-site variability (Table 2).

The Ross Sea piston cores containing till were sub-sampled at approximately 50 cm intervals. All of the Ross Sea samples have high amounts of clay and silt with variable amounts of sand (Table 2) and show consistent spatial variation in relation to

travel distance (Figures 9, 13, 14, and 15). For example, compared to the Ross Sea tills, the northern Byrd Glacier samples (BN, BR, CJ, and HB) have a higher percentage of sand (Figure 13). The LW, LW2 and MT samples show a higher amount of sand compared to the western Ross Sea samples.

5.1.1. Statistical Analysis of Particle-size Data

In order to objectively interpret such a large data set and compare the Byrd Glacier particle-size data with those from the Ross Sea, a suite of statistical procedures was performed on the data, including cluster analysis (CA), principal component analysis (PCA), and discriminate analysis (DA).

Cluster analysis (CA) was performed on the complete data set using PAST 1.7 (Figure 14). Four groups (1 – 4) and 2 subgroups (A and B) were clustered and labeled accordingly. CA was also performed on a Ross Sea subset of the data in Appendix B in order to discern any differences among the samples within the western and central Ross Sea (Figure 15). Two groups were recognized that lack any clear distinction between western and central Ross Sea.

The CA delineated four groups at a similarity distance of around 5.5. Group 1 are samples from the Ross Sea and several LW and LW2 samples. Subgroups A and B separate group 1 into more centrally located Ross Sea samples with most of the LW and LW2 samples (subgroup A) and more westerly located Ross Sea samples with one LW2 sample (subgroup B). Group 2 consists of all of all the MT samples and LW-A1 and LW2-B. Groups 3 and 4 consist of the northern Byrd Glacier samples.

PCA was also performed using Aable 2.1 on the complete data set in order to determine the patterns of covariation within the particle-size range data, how well particle size data differentiate samples into the groups, and to test the validity of the cluster analysis. DA was also performed using SYSTAT 8.0 and PAST 1.7 on the main data set to test the validity of the cluster analysis groupings.

CA was also performed solely on the Ross Sea till data (Figure 15). The CA shows two groups at a similarity distance of around 3, which are labeled 1 and 2. Both of these groups match the groupings found in the first CA even without the addition of the Byrd Glacier samples. Forward stepwise DA was also performed on the two Ross Sea groups (Appendix G-5). The selected *F*-to-remove variables included medium silt (6.51), very fine sand (2.56), and medium sand (4.82). Both normal and Jackknifed classification methods classified groups 1 and 2 with 100% accuracy.

A PCA was performed in order to confirm the uniqueness of these clusters along the first and second principal components. A clear distinction can be seen between the samples collected along the northern side of the Byrd Glacier and those from the southern Byrd Glacier and Ross Sea (Figure 16). All four CA groups show good separation in the PCA graph. The CA and PCA highlight the dissimilarity in particle-sizes from the northern Byrd Glacier samples from those to the south. The analyses also show that some of the LW and LW2 samples have similar particle-size distributions as the Ross Sea samples.

The loadings from the first principal component of the PCA (Figure 17) indicate that the medium sand (mSAND) size fraction has the highest Eigen vector. But the

overall composition of the first principal component is more likely the Clay+Silt/Sand ratio. The very fine to medium grained sand/coarse sand ratio is the main contributor to principal component 2, while the fine clay is the main contributor to the third principal component. The first principal component accounts for 79.2% of the cumulative variance, while the second and third account for 11.9% and 3.8% respectively.

Complete and forward stepwise DA was performed on all four groups from the CA (Figure 18a) and the subgroups A and B (Figure 18b) using Systat 8. Groups 1 through 4 from the complete CA were grouped with 100% accuracy using normal classification and 92% using Jackknifed classification with one sample from group 2 falling into group 1 (Appendix G-1). Figure 17a shows good separation between the groups with groups 1 and 2 having a possible slight overlap.

The *F*-to-remove value (Appendix G-1) for each variable relates the importance of the variables included in the model. For the complete DA of the groups 1 through 4, the largest *F*-to-remove absolute values were for coarse silt (47.58), medium silt (34.14), fine silt (12.12), fine sand (11.29), and medium sand (10.84).

Forward stepwise DA of groups 1 through 4 (Appendix G-2) were grouped with 100% accuracy using normal classification and 97% using Jackknifed with one sample from group 2 falling into group 3. The forward stepwise DA selected medium clay with a *F*-to-remove value of 25.9 and also very fine silt (9.94), coarse silt (12.46), coarse sand (5.28), and very coarse sand (4.12).

DA using PAST 1.7 was performed on the two subgroups A and B (Figure 17b), which includes several the Lonewolf Nunatak with the Ross Sea samples, shows excellent separation between the two groups with 100% accuracy. The largest absolute values of the discriminant functions for subgroups and B are for fine silt (-14.43), medium silt (14.47), and coarse silt (-14.46).

Backward and forward stepwise DA was also performed on subgroups A and B using SYSTAT 8.0. Versus complete DA and forward stepwise DA, backward stepwise DA all variables are entered regardless of their *F*-to-enter values. With each step SYSTAT removes one single variable having the lowest *F*-to-remove value that passes the Remove limit of the *F* statistic. Forward stepwise DA, variables are entered in the model and *F*-to-enter values are reported along with *F*-to-remove values with forced variables. At each step, SYSTAT enters the variables with the highest *F*-to-enter value that passes the Enter limit of the *F* statistic. Both of these techniques can produce different sets of predictor variables.

The forward stepwise DA for subgroups A and B (Appendix G-3) selected only fine silt and very coarse sand with *F*-to-remove values of 41.13 and 3.21 respectively. The forward stepwise DA classified the two subgroups with 100% accuracy using normal classification and 96% using Jackknifed classification with one of subgroup B falling into subgroup A.

For subgroups A and B, the backward stepwise selected the medium clay variable with an *F*-to-remove value of 11.71, coarse clay (13.90), very fine silt (27.89), medium silt (3.66), coarse silt (19.36), and medium sand (10.70). The backward

stepwise DA classified the two subgroups with 100% accuracy using normal classification and 96% using Jackknifed classification with one of the samples from subgroup A falling into B (Appendix G-4).

5.2. Byrd Glacier Pebble and Sand Petrography Data

For each site ~300 pebbles were collected to classify the major rock types and determine their relative abundances at each sample site. This data can be compared to known local geology and help determine what extraneous material is being transported to each site. The pebble data can also be compared to the sand petrography data. The average pebble count data (Table 5) for the samples collected from the Byrd Glacier show a wide diversity of rock types (Figure 19).

The bedrock at sites BN and BR are mapped as Beacon Supergroup and both sites have a large proportion of the pebbles are coarse mafic igneous rocks, 87.6% for BN and 81.4% for BR. BN has a minor amount of fine-grained mafic igneous rocks. Sandstone pebbles are also present at both sites with 7.3% at BN and 18.6% at BR, and a minor (2.7%) amount of metamorphic quartzite (*Mq*) at BN.

The Lonewolf Nunataks are also mapped as Beacon Supergroup (Figure 6), however both Lonewolf sites have a wider variety of rock types present in their pebble populations than BN and BR. At LW only 34% of pebbles were mafic igneous (*Icm +Ifm*) and sandstone (*Ss*) as was found at BN and BR. The remaining pebbles were *Ici*, *Mg*, and *Sw*. At LW2, 56% were mafic igneous (*Icm+Ifm*) and sandstone (*Ss*), and the rest were *Sw*, *Mg*, and *Sq* but lacked *Ici*. Many pebbles from the Lonewolf sites show faceting and striations, which are consistent with glacial erosion at or near the

bed. The pebble compositions contain components of the mapped bedrock of this area, but the pebble compositions as a whole are inconsistent with derivation from the Beacon Supergroup. The *Sw* pebbles found at the LW and LW2 could be from the base of the Beacon but not enough data is available to make such a conclusion.

The composition of the sand sized fraction among the Byrd Glacier samples varies widely. The BN and BR sites have a high percentage of mafic lithic fragments (Figure 20b), which reflects the pebble compositions of both sites. Although the outcrops adjacent to the LW and LW2 sites are also mapped as Beacon Supergroup, the sand fraction is dominated by polymict (59%-LW, 39%-LW2) but also includes quartz (17%-LW, 35%-LW) and smaller amounts of mafic, intermediate, and felsic igneous fragments (Figure 20a) which is similar to the pebble count data.

A significant amount of coal fragments were also observed under a dissecting microscope in loose sand grains from LW and LW2 samples using the 0.5 – 2mm sand fraction as well as as the < 0.5 mm fraction. These fragments are likely pieces from coal measures located in the Victoria Group (Beacon Supergroup, Figure 7) (Bernet and Gaupp 2005). One single piece of crystalline graphite was also observed in LW-A.

Downstream of the BN and BR sites, the area is mapped as Granite Harbour Intrusives (Grindely and Laird, 1969) (Figure 6). Sites CJ and HB from this area have large populations of metamorphic gneiss (*Mg*) and schist (*Ms*) (Table 5) consistent with Borg (1989). Intermediate and/or felsic coarse-grained igneous pebbles are present at both sites as well (37% at CJ). No intermediate or mafic

igneous rocks were found at HB while CJ has a small population (8%) of coarse and fine-grained mafic igneous pebbles. Although none is mapped upstream, a 2% population of sedimentary wacke (*Sw*) pebbles was also found at CJ which may be from the base of the Beacon Supergroup as with the LW and LW2 sites.

Sand petrography data of the CJ site shows a high percentage of intermediate and felsic igneous lithic fragments (~38%), feldspar (~20%), and smaller amounts (6% – 16%) of quartz, metamorphic, and mafic igneous lithic fragments. The HB site is located downstream of CJ and contains a high amount of intermediate and felsic igneous fragments (52.5%) with smaller amounts of feldspar, quartz, and metamorphic lithic fragments. HB also contains less lithic fragments overall than CJ which is located upstream from HB. Observations of loose sand grains (0.5 – 2mm) from both CJ and HB under a dissecting microscope also show a significant population of flat crystals of graphite (plates 14 and 15).

Downstream from the Lonewolf Nunataks on the south side of the Byrd Glacier, the bedrock is mapped as Shackleton limestone (Figure 6). The MT site is almost solely composed of sedimentary limestone (*Sl*) with a minor percentage of marble (*Mm*). A few pebbles of *Icm* and *Sv* were found as well (Table 5). An wider and informal pebble survey of the area found several gneiss, schist, and granite pebbles.

Within the sand-sized fraction, the MT site has a fairly even distribution of polymict and limestone+marble fragments with an average of 47.4% polymict grains and 44% limestone+marble. MT also contains and average of 4.7% silt/sandstone

grains and 1.3% metamorphic grains. The matrix of the polymicts found at the MT site has a high amount of carbonate indicated by their reaction with HCL.

5.3. Ross Sea Sand Petrography Data

The Ross Sea samples show variability in regards to geography and to depth. When looking at the spatial variability, the cores collected more toward the western Ross Sea show greater amounts of extrusive igneous lithic fragments and opaque mineral fragments.

The petrography data from three Ross Sea piston cores also show a distinct pattern with depth. Some depths have a wide variety of grains while other depths are > 87% of one lithology (polymict) (Figure 21). For instance, in core NBP-01-02 (Figure 9) the 50 – 52 cm and 150 – 152 cm intervals have a variety of sand-sized grains that include quartz, feldspar, metamorphic, intermediate, and felsic igneous lithic fragments. A high amount (~10% – 15%) of extrusive igneous grains are present in both samples, however the 150 – 152 cm interval shows a much higher percentage of mafic igneous grains than the 50 – 52 cm interval. In contrast, the 111 – 116 cm interval is dominated by polymict. This interval contains > 90% polymict while the lower interval contains < 9%, and the upper interval contains ~38%.

The ELT32-20 and ELT32-21 piston cores show a similar pattern (Table 6), Figure 21). In ELT32-20, the upper (64 – 68 cm) interval contains ~68% polymict with quartz, feldspar, metamorphic, intermediate, felsic, and mafic igneous fragments ranging from ~4% – 7.5%. There are also trace amounts (0.17%) of limestone/marble, and extrusive igneous grains (0.17%) in this interval. The change toward a dominant

polymict population can be seen in the 132 – 134 cm interval. This interval contains > 96% polymict, a minor amount (~1%) of feldspar, and a trace amount (0.14%) of extrusive igneous grains (Table 6).

The ELT32-21 piston core is located in the central Ross Sea (Figure 9). The uppermost interval (54 – 58 cm) contains significant populations (~10% – 16%) of quartz, feldspar, metamorphic, intermediate, and felsic igneous fragments. This interval contains a trace percentage (0.80%) of limestone/marble, and extrusive igneous grains (0.23%) as well. The largest percentage (~33%) of its overall sand population is polymict. The 104 – 108 cm interval is similar with a greater percentage of polymict and a fairly even reduction of all other grains. The 154 – 160 cm again shows a change in composition with a dominant polymict population of ~ 87%. The interval also contains minor percentages of intermediate, felsic, and metamorphic grains ranging from ~2% – 4.5% respectively.

The ELT27-14 piston core (Figure 9) includes four intervals (47 – 50 cm, 63 – 66 cm, 105 – 109 cm, and 164 – 170cm) and three intervals (47 – 50 cm, 63 – 66 cm, and 164 – 170 cm) are dominated by polymict grains (Table 6). ELT27-14's other petrographic categories are similar as well with populations of metamorphic (~8.5%), intermediate+felsic igneous (4 – 6.5%), mafic igneous (2 – 3%), feldspar (~5.5%), and quartz grains (~10%) present. Both intervals have extrusive igneous grains with SAL1635 having the greatest at 1.6% and also 0.16% limestone/marble. SAL1634 lacks limestone/marble and contains only 0.28% extrusive grains.

The 105 – 109 cm interval (SAL1636) changes in composition with an increase in quartz grains to 19% and a slight drop in polymict grains to 56%. SAL1636 also shows a minor gain in mafic igneous grains to 5%. SAL1636 has no limestone/marble or extrusive grains but contains similar amounts of metamorphic (8%), intermediate +felsic (5.5%), and a slight decrease in feldspar grains (3%) compared to the other intervals. Overall, the ELT27-14 core is rather uniform in nature and doesn't show much change or great variability in the sand content.

Sample NBP94-07-39 (100 – 102cm) SAL283 is located in the central Ross Sea. This sample contains ~92% polymict with 2.8% quartz and contains single grains of plagioclase, k-spar, and a metamorphic fragment. No other depth intervals from this core were point counted.

Using a dissecting microscope, several Ross Sea samples were found to contain fragments of coal similar to those found in the LW and LW2 samples. These included ELT32-21(SAL1640, SAL1641, and SAL1642), ELT27-14(SAL1637), and NBP94-01-02(SAL1634). SAL1642 had the largest amount of coal fragments of all the Ross Sea samples.

5.3.1. Ross Sea polymict fragments

Several differing populations seem to be present among the polymict grains. Sample NBP94-0-02(SAL1633) which contains > 90% polymict grains, has two populations (plate 4). One of these contains clasts of mostly quartz, feldspar, and unknown opaque grains. The other population has a more rounded and zoned appearance with a lighter colored zone encapsulating a darker inner zone. Some

fragments contain clasts of quartz, feldspar, or volcanic fragments within the center and covered in zoned matrix (plates 5 and 6).

Viewed under a dissecting microscope, it is clear that the polymict fragments are indeed well-rounded balls of tillite with a light colored outer shell normally encapsulating a mineral or lithic grain. In a study of the Ricker Hills Tillite (Figure 1), Baroni and Fasano (2006) describe "rolling-ball" structures or nodules that are "very well rounded and have a core stone with a diameter significantly smaller than the nodule size. The external part consists of fine material that surrounds the core stone in concentric layers or skin…" These observations are consistent with those made of certain polymict grains found NBP94-01-02.

Core ELT27-14 contains what look to be three populations of polymict fragments. The first has smaller clasts of what looks to be quartz and other darker but unrecognizable grains with a very light brown matrix under plane light. The matrix shows heavy extinction when seen through cross-polar light. This population also has several instances where grains contain veins that appear to be composed of opal (plate 7). It is possible that this population is a diatomite due to the nature of its matrix.

The second population has a much darker matrix under plane light with larger euhedral clasts of quartz, possibly feldspar, and other dark grains. The third population and least in quantity, are more rounded and zoned fragments with mineral or lithic fragment cores. Some of these polymicts look to have a polymict center or core that is surrounded by a different and more fine outer shell of matrix.

Sample ELT32-20(SAL1639) also contains two to three populations of polymict fragments. The first population is similar to that of ELT27-14 with a very light brown

matrix shows nearly complete extinction in cross-polar light (plates 7 and 8). The major difference between the two cores is that the SAL1639 light brown population contains what looks to be almost perfectly round "polymict-like nodules" that are surrounded by matrix. The second population looks much like the zoned population in ELT27-14 with dark matrix and obvious zoning only they seem to be much more abundant in SAL1639. The third population is also similar those found in ELT27-14 with a dark, non-zoned matrix. One polymict fragment seemed to contain a core of the first light brown polymict surrounded by the much darker polymict material.

Core ELT32-21 also contains at least two populations of polymict fragments similar to both ELT27-14 and ELT32-20. ELT32-21(SAL1640 and SAL1641) polymict population is dominated by a light brown polymict with very small quartz clasts surrounded by light-brown matrix that is extinct under cross-polar light (plates 7). There seems to be veins that run through some of these polymict fragments as well that can be seen in plate 7. Veins were also seen in polymict fragments in samples SAL1635 and SAL1638. These lighter colored polymicts have distinct zoning with a darker zone surrounding a lighter inner core. This is also slight evidence of microfossils present in one or two of these lighter colored polymicts. A smaller population of polymict with a dark matrix (under plane light) with larger clasts of quartz, feldspar, and other darker grains is also present but in lesser amounts than the previously mention population.

ELT32-21(SAL1642) contains a dominant total sand population of polymict (> 90%). However it is the polymict with the dark matrix and larger clasts that makes up the majority of the total polymict fragments. The lighter matrix polymict is also

present, but it is not as abundant.

Polymict fragments were also found at the Lonewolf Nunatak sites. These fragments were similar to the population with the dark matrix found in the Ross Sea samples. However those found at LW and LW2 had a lighter colored matrix and the clasts were larger on average (plates 10 and 11). No polymict fragments matching the light brown population found in the Ross Sea samples were found. There were however several rounded fragments with large clasts making up the core (plates 12 and 13). These were similar to those found in SAL1633.

5.4. Statistical Analysis of Point Count Data

Cluster analysis (CA) using PAST 1.7 was performed on the averaged point count data in Table 6. Any categories with an average overall total among the samples of < 1% were excluded from the statistical analyses. These categories included muscovite, chlorite, iron ore, and unknown/other. To reduce the effects of identification errors and to simplify the interpretation of the analyses, several categories were combined into one. These included k-spar and plagioclase, intermediate igneous and felsic igneous, and limestone, marble, and calcite. Discriminant analysis (DA) and principal component analysis (PCA) were also performed on the data in order to confirm the CA results.

The CA distinguishes four groups (Figure 22) at a similarity distance of around 10. Group 1 contains CJ and HB from the northern Byrd Glacier. Group 2 contains LW2, all three intervals from ELT32-13, and two intervals from NBP94-01-02, which are both located in the western Ross Sea. Group 2 also includes all intervals of NBP95-01-11 and NBP95-01-17 and one interval from ELT32-21, all which are from

the west central Ross Sea. Group three contains LW, all four intervals from ELT27-14, both intervals of ELT32-20, two intervals from ELT32-32, two intervals from ELT32-21, and the single sample from NBP-07-39. Group 4 contains BN and BR from the northern head of Byrd Glacier. Due to high amounts of limestone and marble, MT did not fall into any group below the chosen similarity value. Subgroups A, B, C, and D from groups 2 and 3 are also shown in Figure 22.

Complete and forward stepwise DA was performed on subgroups A, B, C, and D in order to validate the CA (Figure 23). The complete DA (Appendix H) classified the subgroups with 100% accuracy using normal classification and 96% with Jackknifed classification. One sample from subgroup C fell into subgroup D. The largest *F*-to-remove values for the complete DA were polymict (425.17), quartz (320.6), and metamorphics (193.71). (Other variables scored high as well and are given in Appendix H).

The forward stepwise DA (Appendix H-2) also classified the subgroups with 100% using normal and 96% using Jackknifed classification. The *F*-to-remove values of the selected variables include opaques (17.79), polymict (13.91), extrusive igneous (7.49), silt and sandstone (4.20), mafic igneous (3.01), and intermediate and felsic igneous (2.94).

PCA was also performed on subgroups A – D of the CA (Appendix I). Figure 24 shows a graph of the first and second principal components. The loadings (Figure 25) show polymict and extrusive igneous fragments to be the largest contributor to the overall variance. The first principal component (polymict) accounts 91.65% of the variance and the second (extrusive igneous) accounts for 4.17%. The PCA loadings

are similar to the *F*-to-remove values of the forward stepwise DA. Therefore it is likely that the forward stepwise DA is a better statistical technique than complete DA for this data set due to the fact that the two different statistical analyses give similar output.

5.5. Detrital zircon U/Pb age data

5.5.1. Byrd Glacier

A total of 1009 zircon grains were analyzed, of which 914 were found to be concordant to nearly concordant (Figure 10). The BN sample contains 91 grains of which 91% have a U/Th ratio of < 9.5 and are therefore considered to be of igneous origin (Figure 26). Accounting for error, 57% of the total zircon grain ages for BN lie between 508 – 655 Ma. Within this range 46% of the total zircon ages lie between 560 – 655 Ma, ages typically thought of as pre-Ross Orogeny, which are reflected in the sample's maximum peak probability at 588 Ma. However there is also a minor peak at 537 Ma which is almost unresolvable from the 588 Ma peak. For the rest of the significant zircon ages, 18% of the total zircon ages lie between 803 – 1118 Ma with significant probability peaks at 850, 912, and 1010 Ma. Other minor peaks include 1062, 1357, 1506, 2255, 2432, 2570, and 3346 Ma. A single 256±4 Ma grain was also found at the BN site. Of the minor population of grains with U/Th of > 9.5 U/Th, 63% range from 545 – 648 Ma, with the rest having ages of 692±36, 929±38, and 1324±62 Ma.

The BR sample includes 95 concordant grains, out of which 99% have U/Th < 9.5. The only grain with > 9.5 U/Th is 535±35 Ma. Forty-three percent of the BR

grains range from 505 – 653 Ma. Within this range, three large probability peaks are present at 534, 556, and 590 Ma. Thirty-eight percent of the total zircon ages range from 661 – 1322 Ma with significant probability peaks at 688, 814, 947, 1147, and 1258 Ma. The remaining data show minor probability peaks at 1473, 1760, 1847, 1998, 2241, 2366, 2455, 2643, 2709, 2853, and 3180 Ma.

The CJ sample includes 77 concordant grains with 88% containing < 9.5 U/Th. Of the total zircon ages, 88% of the data ranges from 460 – 674 Ma with a maximum probability peak of 532 Ma. Eight percent of the data ranges from 967 – 1305 Ma with minor probability peaks at 1047, 1167, and 1280 Ma. Three younger grains with ages of 240±3, 315±27, and 325±15 are also present. Of the grains with > 9.5 U/Th, 86% range from 460 – 575 Ma, excluding one other grain at 1046±50 Ma.

The HB sample has 84 concordant grains with 98% containing < 9.5 U/Th. Of the total, 87% range from 490 – 588 Ma with a maximum probability of 530 Ma. Of the remaining data, minor probability peaks include 482, 650, 1135, 1265, and 1940 Ma. The two grains with > 9.5 U/Th have ages of 526±10 and 557±10 Ma.

LW contains a total of 90 concordant grains of which 96% have < 9.5 U/Th. Forty-seven percent of the total zircon ages for LW range from 528 – 650 Ma with a maximum probability peak of 597 Ma and a significant peak at 576 Ma. Twenty-two percent of the remaining data ranges from 878 – 1309 Ma with significant probability peaks of 937, 1040, and 1115 Ma. The other significant probability peaks within LW are 1615, and 2718 Ma with remaining minor peaks of 702, 904, 1852, 1953, 2172, 2305, 2424, 3111 Ma including a single 376±10 Ma grain. The ages of LW grains with

> 9.5 U/Th include 591±12, 708±23, 1553±35, and 2719±35 Ma.

The LW2 U/Pb ages have been combined into one plot in Figure 26. A total of 211 concordant grains are plotted. Of the 211 grains, 43% lie between 515 – 655 Ma. Within this range 34% of the total zircon ages lie between 550 – 655 Ma with a maximum probability peak at 579 Ma. Another 21% of the total zircon ages for LW2 range between 863 – 1350 Ma with significant probability peaks at 974 and 1100 Ma and minor peaks at 737, 1484 and 1590 Ma. Another significant peak lies at 2729 Ma with 6% of the total zircon age data ranging between 2659 – 2838 Ma.

For the LW2 site, zircons were dated for all three sub-samples, to test intra-site variability. LW2-A contains a total of 68 concordant grains out of which 94% have U/Th ratios < 9.5. The > 9.5 U/Th grains have ages of 552±15, 563±13, 2501±24, and 3022±48 Ma. Thirty-seven percent of the total ages for LW2-A (Figure 27) lie between 515 – 615 Ma with a maximum probability peak of 565 Ma. A significant peak is also present at 597 Ma. Eighteen percent of the ages lie in the 695 – 1253 Ma with significant probability peaks at 717 and 895 Ma with a minor peak and 1208 Ma. Another 12% of the zircon ages lie in the range of 1427 – 1638 Ma with a significant probability peak at 1480 Ma. Another 9% of the zircon age data range from 2659 – 2818 Ma with a significant probability peak at 2690 Ma. Other less significant peaks within the LW2-A probability plot include: 498, 1564, 1920, 2240, 2508, 2734, 2995, 3325, and 3545 Ma.

The zircon age data for sub-sample LW2-B contains 87 concordant grains out of which 95% have < 9.5 U/Th. The ages of grains with > 9.5 U/Th are 563±9, 605±7, 627

±14, and 1283±51 Ma. Forty percent of the zircon age data for LW2-B ranges between 530 – 640 Ma with the maximum probability peak at 564 Ma, and a significant peak at 610 Ma. Around 29% of the zircon data ranges range from 860 – 1350 Ma, with a significant probability peaks at 967 and 1094 Ma and a minor peak at around 1280 Ma. Other minor peaks for LW2-B include 730, 796, 840, 1594, 1728, 1841, 1918, 2067, 2249, 2403, 2726, 2818, 2960, 3040, and 3404 Ma.

Sub-sample LW2-C contains 56 concordant grains out of which 96% have, 9.5 U/Th. The ages of grains containing > 9.5 U/Th include 537±8, 589±16, and 2478±51 Ma. Fifty-two percent of the total grains range from 529 – 645 Ma with the maximum probability peak at 583 Ma. Another 27% of the zircon age data ranges from 913 – 1658 Ma with peaks at 1004 and 1098 Ma, and minor peaks at 1248 and 1628 Ma. One other minor peaks for LW2-C are 1994, 2158, 2497, 2730, 2869, and 3300 Ma.

The MT sample only contained a total of 12 concordant zircon grains with three of these grain having errors > 100 Ma. Despite the lack of data, this sample does contain very small populations of Ross to Pan-African (520 – 590 Ma), Early Proterozoic (1669 – 1838 Ma), and Late Archean (2720 – 2876 Ma) ages (Appendix C).

5.5.2. Central and Western Ross Sea

Most of the central and western Ross Sea samples (Figure 28) in this study show a dominant population of Ross to Pan-African detrital zircon ages. Sample NBP94-01-02 (111 – 116 cm) SAL1633 contains a total of 48 concordant grains with 96% having < 9.5 U/Th. Out of the total zircon ages 46% range from 474 – 663 Ma

with a maximum probability peak at 547 Ma with significant peaks at 491 and 598 Ma. A significant peak of 718 Ma is also present. Seventeen percent of the data ranges from 951 – 1224 Ma with a significant probability peak of 1045 and 1080 Ma and minor peaks of 944 and 1200 Ma. Other minor peaks include 1304, 1495, 1664, 2030, 2185, 2459, and 2678 Ma; three younger grains yielded ages of 252±4, 334±14, and 335±15 Ma grains. There are two grains with ages of 556±9 and 1055±37 Ma with > 9.5 U/Th.

Sample ELT32-20 (132 – 137 cm) SAL1639 contains 40 concordant grains of which 97% have < 9.5 U/Th, with a single 651±41 Ma grain having U/Th > 9.5. Of the total zircon ages 50% range from 506 – 644 Ma with a maximum probability plot of 516 Ma and significant peaks of 564 and 608 Ma. The older ages (> 644 Ma) for this sample yield minor peaks of 695, 889, 1051, 1140, 1283, 1672, 1731, 1933, 2288, and 2697 Ma. The younger (< 485 Ma) data consist of several grains with ages of 126±4, 147±3, 169±4, 201±5, 216±4, 250±6, and 300±11 Ma.

Sample ELT27-14 (105 – 109 cm) SAL1636 has 42 concordant grains with 100% of the grains with < 9.5 U/Th. Fifty-seven percent of the total zircon ages range from 474 – 636 Ma with a maximum probability peak of 553 Ma and significant peaks of 490, 523, and 599 Ma. The other significant peak for this sample is 1005 Ma with minor peaks of 687, 839, 1149, 1371, 1833, 2432, 2737, and 3372 Ma.

The ELT32-21 (104 – 108 cm) SAL1641 sample contains 94 concordant grains of which 96% have < 9.5 U/Th. Four grains with > 9.5 U/Th have dates of 557±9, 563

±9, 936±19, and 986±16 Ma. Of the total zircon ages, 65% range from 464 – 654 Ma with a maximum probability peak of 519 Ma and significant peaks of 490, 562, and 592 Ma. Twenty-eight percent of the total zircon data ranges from 675 – 1269 with a significant peak at 1059 Ma, and minor peaks at 702, 728, 783, 885, 960, 990, 1200, 1637, 1849, 2472, and 2658 Ma. Four grains of 232±7, 254±7, 319±9, and 354±10 Ma are also present within this sample.

Sample NBP94-07-39 (90 – 92 cm) SAL282 only contains 23 concordant zircon grains. Of these grains, 48% range from 98 – 213 Ma with 38% raging from 98 – 121 Ma with a maximum probability peak of 102 Ma. Thirteen percent of the ages range from 525 – 570 and 22% range from 608 – 707 Ma. The remaining data (22%) ranges from 743 – 1109 Ma. This is the only sample in the entire data set lacking any ages > 1200 Ma.

5.5.3. Kolmogorov-Smirnoff (K-S) test of concordant detrital zircon U/Pb ages

The K-S test was performed on the detrital zircon ages from the Byrd Glacier and Ross Sea samples in order to determine any similarities among the zircon population from both areas. The K-S test is a statistical method that compares two distributions of data in order to determine any significant differences. The method tests the null hypothesis that the two distributions are the same and originate from the same parent population. The K-S test itself actually determines, to a certain level of confidence, that the two populations are not the same. This makes it possible to disprove that two samples have the same distribution but the K-S cannot determine if two populations are truly the same (Guynn, 2006). The K-S test uses cumulative

distribution functions (CDF) by comparing the maximum probability difference or rather the maximum vertical difference between the curves of the CDF's (Figure 29).

Table 7 displays the results of the K-S test for the total zircon ages for the Byrd Glacier and Ross Sea samples and Table 8 displays K-S test results for only the 440 – 655 Ma zircon ages. There are three separate matrices within the Table. The first displays P-values of a K-S that accounts for error while the second does not. The third matrix uses the "Monte-Carlo" method, which generates 1000 random ages for each zircon analysis based on the input age and its uncertainty using the standard deviation of the input uncertainty. This creates a synthetic age distribution that accounts for uncertainty in the original measured zircon. The output of the Monte-Carlo gives the P-values of the 1000 simulations and the standard deviation of the 1000 calculated P-values (Guynn, 2006)

The P-value equals the probability that the observed difference (D_{obv}) in the CDF's could be due to random error. A smaller P-value expresses a smaller likelihood that the D_{obv} is due to random error and that the D_{obv} is due to the data distributions not being the same. All P-values < 0.05 reject the null hypothesis that the distributions are the same.

In the first matrix, cells highlighted in yellow indicate P-values > 0.05 and an inability to reject the null hypothesis. In the second matrix, red cells indicate a different conclusion for the second K-S test, which doesn't account for error. An example would be during the first K-S test accounting for error, sample A and B

passed the test, but during the second K-S test excluding error, sample A and B failed the test and the P-value was < 0.05. In the third "Monte-Carlo" matrix, blue cells indicate the P-value defined by the standard deviation (95% confidence level) overlaps the 0.05 P-value (Figure 30). This indicates that during the simulations that a certain percentage of the 1000 synthetic distributions passed and failed at the 95% confidence level (Guynn, 2006).

A. Byrd Glacier

In Table 7, the K-S test results are shown for the total concordant U/Pb isotope data. Beginning with inter-Byrd Glacier comparisons, the first matrix using error shows positive test results between sites BN and BR (0.607), LW (0.145), LW2-B (0.056), and LW2-C (0.517). BR shows positive test results with BN (0.607), LW (0.262), LW2-B (0.225), and LW2-C (0.684). CJ and HB only show positive test results with one another with a P-value of 0.167. LW tested positive with BN (0.145), BR (0.262), LW2-A (0.306), LW2-B (0.835), and LW2-C (0.968). LW2-A tested positive with LW (0.306), LW2-B (0.229), and LW2-C (0.381). LW2-B shows positive test results with BN (0.056), BR (0.225), LW (0.835), LW2-A (0.229), and LW2-C (0.467). LW2-C shows positive test results with BN (0.517), BR (0.684), LW (0.968), LW2-A (0.381), and LW2-B (0.467).

In the second K-S matrix, which doesn't account for error, we find several red cells indicating opposite results than those of the first test. These include BN and LW2-B with a P-value of 0.014, which is less than the required 0.05 P-value therefore rejecting the null hypothesis. The only other is CJ and HB with a P-value of (0.004).

The third "Monte-Carlo" matrix shows blue cells for several inter-Byrd Glacier samples as well. These include BN vs. LW (0.087) and LW2-B (0.030), BR vs. LW2-B (0.135), LW2-B vs. LW2-C (0.258), and CJ vs. HB (0.061). The blue cells indicate that of the 1000 synthetically generated ages, a certain percentage passed the test and the rest did not. Of these highlighted cells, those with P-values > 0.05, had more than 50% of the synthetic runs pass the test and vice versa for those with > 0.05. Of the highlighted cells of inter-Byrd Glacier comparisons, each has a P-value ≥ 0.05 except for LW2-B vs. LW2-C (0.030).

B. Ross Sea

Comparing the Ross Sea samples with one another, the first K-S matrix shows positive results between all samples except SAL282. For SAL282, the K-S test rejects the null hypothesis that the distributions are the same for all Ross Sea samples except for SAL1639 (0.102). The P-values between the other Ross Sea samples range from 0.105 for SAL1636 and SAL1641 to 0.998 for SAL1633 and SAL1636.

The second matrix discounting error displays only one red cell. It includes SAL1636 and SAL1641 (0.038). For these comparisons, the second K-S test rejects the null hypothesis whereas the first test does not. The same cell is highlighted in the Monte-Carlo K-S test. The P-values are 0.063 for SAL1636 and SAL1641. Both are > 0.05 showing more than 50% of the simulations passed the test.

C. Byrd Glacier vs. Ross Sea

Comparing Byrd Glacier and Ross Sea detrital zircon U/Pb ages using the K-S test makes it possible to identify similarities in the age distributions between the two areas. Beginning with the northern side of the Byrd Glacier, the first K-S test shows positive test results with several Ross Sea samples. BN shows positive results with SAL1633 (0.168) and SAL1636 (0.529). BR shows positive test results SAL1633 (0.645), SAL1636 (0.708), and SAL1639 (0.055). CJ has positive test results with only one Ross Sea sample with a P-value of 0.100 for SAL1639. HB has no positive test results with any of the Ross Sea cores.

The second K-S test shows opposite results for three cells of the northern side of the Byrd Glacier compared to the Ross Sea cores. These include BN vs. SAL1633 (0.016), BR vs. SAL1639 (0.008) and CJ vs. SAL1639 (0.022).

The Monte-Carlo results for these samples highlight several cells. For BN these include SAL1633 (0.089) and SAL1636 (0.272) and for CJ, SAL1639 (0.041). Only one of these have P-values have < 0.05 with CJ vs. SAL1639 (0.041) indicating that more than 50% of the simulations of these sample comparisons failed the test.

For the Byrd Glacier samples from the Lonewolf Nunataks, several cells show positive test result for the first K-S test using error. LW has positive results with SAL1633 (0.054) and SAL1636 (0.069). LW2-A tests positive with SAL1636 (0.099), and LW2-B and LW2-C show positive results with both SAL1633 (0.085 for B, 0.234 for C) and SAL1636 (0.245 for B, 0.511 for C). The second K-S test highlights LW

vs. SAL1633 (0.008) and SAL1636 (0.032), and LW2-B and LW2-C vs. SAL1633 (0.009 for B, 0.045 for C).

The Monte-Carlo results display blue cells for SAL1633 and SAL1636 vs. all of the Lonewolf samples except LW2-A. Two of these results (LW vs. SAL1633 and LW2-B) are < 0.05 and therefore < 50% of the simulations failed to pass the test.

5.5.4. K-S test of the 440 – 655 Ma detrital zircon U/Pb data

A. Byrd Glacier samples

A K-S test was performed on the Byrd Glacier and Ross Sea U/Pb age data focusing on the 440 – 655 Ma age range (Table 8). This age range covers the Ross Orogen and Pan-African orogenic events. Comparing the Byrd Glacier samples to one another, the K-S test relates positive test results with most of the samples. CJ and HB have no positive results with any of the other Byrd Glacier samples. CJ and HB do however test positive with one another with a P-value of 0.199.

The second matrix displays three red cells. These are BN vs. BR (0.017), LW vs. BR (0.008), and CJ vs. HB (0.007). The Monte-Carlo results display blue cells for BN vs. BR (0.081), BR vs. LW (0.008), LW2-A (0.478), LW2-B (0.157), and LW-C (0.192); and LW vs. LW2-A (0.277), LW2-B (0.450), and LW2-C (0.491).

B. Ross Sea samples

Comparing the Ross Sea samples to one another, the K-S test displays positive results for all samples P-values of 0.076 to 1.000. SAL282 was not included because it lacked 20 grains within this age range. The second K-S test displays opposite results

for SAL1641 vs. SAL1633 (0.008), SAL1636 (0.021), and SAL1639 (0.024). The Monte-Carlo results show blue cells for SAL1641 vs. SAL1633 (0.116), SAL1636 (0.042), and SAL1639 (0.095).

C. Byrd Glacier vs. Ross Sea samples

Comparing the Byrd Glacier and Ross Sea samples to each other there are positive results for the first K-S test for many of the samples. BR and BN are positive for all Ross Sea samples except SAL1641. CJ tests positive for all the Ross Sea samples while HB is only positive with SAL1633. LW2-A, LW2-B, and LW2-C are positive with all the Ross Sea samples except SAL1641 and LW is only positive with SAL1636 (0.075) and SAL1639 (0.080).

The second K-S test shows opposite results, marked in red, for all of the first BN K-S test results (SAL1633, SAL1636, and SAL1639). Others include CJ vs. SAL1636 (0.008); HB vs. SAL1633 (0.019); LW vs. SAL1636 (0.006) and SAL1639 (0.016). LW2-A vs. SAL1633 (0.020); LW2-B vs. SAL1633 (0.007) and SAL1639 (0.040); and LW2-C vs. SAL1633 (0.008), SAL1636 (0.025), and SAL1639 (0.032).

The Monte-Carlo results display blue cells for BN vs. SAL1633 (0.025), SAL1636 (0.082), and SAL1639 (0.078); CJ vs. SAL1633 (0.143), SAL1636 (0.031), and SAL1639 (0.075); HB vs. SAL1633 (0.027); LW vs. SAL1636 (0.031) and SAL1639 (0.036); LW2-B vs. SAL1633 (0.058), SAL1636 (0.174), and SAL1639 (0.135); and LW2-C vs. SAL1633 (0.057), SAL1636 (0.157), and SAL1639 (0.147).

6. Potential provenance of detrital zircons

6.1. Cretaceous to Permian

Figure 31 shows the cumulative data set of all detrital zircon U/Pb ages collected from the Byrd Glacier and Ross Sea. Within the data set, 13 significant groups of ages (Table 9) were identified based on groups defined by the DZ Age Pick program from the Arizona LaserChron Laboratory (Appendix D) and the main data set in Appendix C. These groups either represent populations of zircon age-groups that correlate between the Byrd Glacier and the central and western Ross Sea samples or are simply a significant group found within the data set.

The significant age groups in Appendix D include error as a probability distribution and therefore the total number within each significant age group can only be considered as the potential total. Due to larger age errors in some grains it is possible that some may fall into two groups, which needs to be taken into account when considering the size of these 13 age groups.

The younger (< 235 Ma) zircon ages are exclusively found in the Ross Sea samples (Figure 31b). Samples NBP04-07-39(SAL282) and ELT32-20(SAL1639) contain all of the ages < 235 Ma and both of these samples contain > 85% polymict fragments in their sand fraction. The K-S test also shows a positive result between SAL282 and SAL1639, which is the only positive test result for SAL282.

The majority of grains between 235 and 360 Ma are also derived from the Ross Sea with only a few grains coming from the Byrd Glacier (BN and CJ). Samples

ELT32-21(SAL1641) and NBP94-01-02(SAL1633) both contain several zircon grains ranging from 231±7 – 354±10 Ma. SAL1633 contains > 85% polymict fragments, while SAL1641 contains ~50%. Both test positive with one another using the K-S test.

Even though these four samples show similar sand contents, the absence of 99 – 216 Ma detrital zircons suggests that the provenance of SAL282 and SAL1639 is at least in part distinct from SAL1641 and SAL1633. However this posses a difficult spacial problem in that SAL1641 is located between SAL282 and SAL1639.

One potential source for these ages of zircon grains is Marie Byrd Land in West Antarctica (Figure 1). Siddoway et al. (2004) dated zircon grains from mylonitic gneiss from the eastern Ross Sea with ages of 97 – 102 Ma that correlate to the Byrd Coast Granites of Marie Byrd Land. Mukasa and Dalziel (2000) also reported detrital zircon ages of 96±1 – 124±1 Ma from A and I-type granites and migmities from the Pine Island Bay and Rupert-Hobbs coast area of West Antarctica. SAL282 has 5 zircon ranging from 100±2 – 107±3 Ma which correlate well to zircon ages from A-type syenites and quartz syenites along the Ruppert and Hobbs coast of western Marie Byrd Land that range in age from 98.4±0.8 – 102±1 Ma.

Reconstructive ice-flow lines (Denton and Hughes, 2000; 2002) show it to be improbable that these Cretaceous zircon grains found in NBP94-07-39 are from the areas mentioned above. However, knowing that rocks of these ages are found in outcrops along the margins of West Antarctica makes it a potential source area. What bedrock lies underneath the WAIS isn't known, but inference of similar bedrock ages as those found in the Ford Ranges and the Ruppert and Hobbs coast underneath the

WAIS isn't out of the question. Similarly aged bedrock could potentially be eroded and transported by West Antarctic ice steams into the Ross embayment.

The Carboniferous to Permian grains found in samples ELT32-21(SAL1641), ELT32-20(SAL1639), and NBP94-01-02(SAL1633) have several potential source areas, which includes the Ford Ranges of Marie Byrd Land, the Walgreen Coast, and the Kohler Ranges (Pankhurst et al., 1998; Mukasa and Dalziel, 2000). These Cretaceous to Permian zircons correlate to the Rangitata (Suggate, 1978) and Tuhua Orogenies (Carter et al., 1974) of New Zealand, and the Hunter-Bowen Orogeny of Australia (Holcombe et al., 1997) (Figure 31).

Another potential source for these younger grains could be the Robertson Bay, Bowers, and Wilson Terranes of northern Victoria Land (Figure 33). Lisker (2002) summarizes previously collected fission-track ages of apatites from the Outback Shoulder and Rennick Graben, and Admiralty Block of Northern Victoria Land (Figure 33) which range in age from ~40 – 350 Ma (Fitzgerald and Gleadow, 1988; Arne et al., 1993; Lisker, 1996; and Schafer, 1998). Yet based on it's geographic location and reconstructive ice-flow lines (Denton and Hughes, 2000; 2002), it is difficult to assume that northern Victoria Land is a likely source area for these zircon grains.

One other possibility of provenance could be the Byrd Glacier itself. The CJ sample site has three zircon grains ranging in age from ~239 – 325 Ma. This range is very similar to that found in sample NBP94-01-02(SAL1633) which also contains 3 grains ranging in age from ~252 – 335 Ma. It is possible that SAL1633 is receiving a

mixture of material from Byrd Glacier and areas of Victoria Land. Whether or not these Carboniferous to Permian aged grains come from the Byrd Glacier's CJ area or Victoria Land is uncertain.

Polymict fragments found in NBP94-01-02(SAL1633) have a potential correlation to the polymict fragments found in the Ricker Hills Tillite (Baroni and Fasano, 2006), therefore it is possible that the younger detrital zircon grains (~252 – 335 Ma) may be derived from the Rennick Graben due to its close proximity to the Ricker Hills. Only 3 grains < 350 Ma are present in SAL1633, so the percentage of these grains in relation to the overall population is minimal.

The remaining younger detrital zircon grains (235 – 360 Ma) found with the other Ross Sea samples may also derive from the northern Victoria Land region but geography and reconstructive ice-flow paths (Denton and Hughes, 2000; 2002) make this questionable. The presence of similarly aged zircon grains in Marie Byrd Land also makes this area a possibility, but also unlikely due to this core's geographic location.

ELT32-20(SAL1639) and ELT32-21(SAL1641) also contain Carboniferous to Early Cretaceous aged grains. SAL1639's zircon grains are relatively younger and slightly more abundant than SAL1633 with an age range of ~126 – 299 Ma while SAL1641 has zircon ages that more closely match those of SAL1633 with a range of ~231 – 354 Ma. Overall for ages < 400 Ma, SAL1641 correlates best with SAL1633 and SAL1639 correlates more with NBP94-07-39(SAL282).

At this time it can not be determined that these Ross Sea core samples represent the same time horizon. Therefore the complexity that these Late Paleozoic and Mesozoic zircon grains imply for ice-flow patterns suggests that U/Pb detrital zircon ages need to be analyzed from a series of depths from Ross Sea cores, which may yield more complex provenance patters as a function of time at individual sites in the Ross Sea.

6.2. Late Neoproterozoic – Late Ordovician

The accepted age range of the Ross Orogeny is ~465 – 550 Ma (Goodge, 2002. The frequency diagram shows a large portion of 560 – 650 Ma zircon ages. Figure 33 is modified from Federico et al. (2006) and shows the zircon age groups from 450 – 650 Ma. This graph shows the correlation of the zircon groups 1 – 3 (488 – 523, 530 – 545, and 553 – 570 Ma) with magmatic, sedimentological, and tectonic events in the northern Victoria Land (NVI). Sample distributions of these age groups can be seen in Figure 33.

There is a high correlation with the groups 1 – 3 with syn- and postkinematic magmatism in NVI. We can also see that there is a large group (12 grains) of metamorphic (> 9.5 U/Th) grains that cluster around 550 Ma with several other metamorphic grains of Cambrian age with one grain at 478±17 Ma. The ages from 478 – 502 Ma correlate with eclogite-facies metamorphism found in the Lanterman Range.

Group 4 (583 – 610 Ma) does not correlate with any other events in this graph. Group 4 is found in the Byrd Glacier samples BN, BR, LW, and LW2. Group 4 is also present in NBP94-01-02, ELT32-20, and ELT27-14.

Group 1 (488 – 523 Ma) is mostly found in the Ross Sea samples, with only a very small percentage found in LW2 and HB with a higher percentage found in CJ (Figure 34). In Figure 31 the total number of grains of this age range look to be about equal. However the potential percentage of each sample's population is represented in Figure 34 while the Figure 31 shows the frequency of total grains. Therefore the data indicates that most of the zircons of this age group are not being transported from the Byrd Glacier to the western Ross Sea, but from some other source. Correlations of this age group can be found in southern Victoria Land in the Dry Valleys region with a major pulse of calc-alkaline plutonism occurring at 505±2 Ma and another pulse of adakitic plutonism around 490 Ma (Cox et al., 2000).

Another probable source of this group of ages is the Starshot formation (formally Douglas Fm.) which outcrops at the mouth of the southern margin of the Byrd Glacier (Goodge et al., 2004). Dominant U/Pb zircon ages of ~520 Ma, with ages as young as 506±6, were reported from samples of the Douglas conglomerate with a dominant population of ~520 Ma grains in the Starshot Formation as well (Goodge et al., 2004). ELT32-21(SAL1641) had two dominant groups of grains at 488 and 518 Ma (Appendix D). Boulders of conglomerate were seen at the LW2 site and may have been derived from the Starshot.

Zircon ages for group 2 (530 – 545 Ma) are common in Byrd Glacier samples BN, BR, CJ, and HB. For sites CJ and HB, group 2 is the single dominant age population (Figures 26 and 34). Stump et al. (2006), reported mean zircon ages of 531 ±5 and 545.7±3.2 Ma from bedrock on the northern side of Byrd Glacier adjacent to Ramseier Glacier. This age group appears distinctly in NBP94-01-02(SAL1633)

Zircon ages for group 3 (553 – 570 Ma) are present in Byrd Glacier samples BR, LW, LW2-A, and LW2-B (Figures 26 and 27). The Ross Sea samples with group 3 are ELT32-20, ELT27-14, and ELT32-21 (Figure 34). Group 3 is the largest population in both ELT32-20 and ELT27-14.

Zircon ages for group 4 (583 – 610 Ma) are found in BN, BR, LW, and LW2 from the Byrd Glacier. Ross Sea samples NPB94-01-02(SAL1633), ELT32-20 (SAL1639), and ELT27-14(SAL1636) also contain group 4. This age group dominates BN, BR, LW, and LW2. It is evident that a large component of zircons of this age are being transported into and through the Byrd Glacier from a source, likely located underneath the ice sheet, since no zircon grains of this age range have been dated in the proximity of the Byrd Glacier. Most zircon ages dated in this area range from 530 – 570 Ma. Goodge et al., (2004) dated zircons derived from sandstones from the Pensacola Mountains (Figure 1) and have zircon age peaks of 600 and 610 Ma, which they interpreted as early development of the Ross belt or early Pan-African detritus from the southern area of the East African orogen.

If these ages from group 4 in the Byrd Glacier do not represent early development of the Ross belt, they may be related to early subduction of the

hypothesized "Beardmore microcontinent" (Stump et al., 2006). This group of grains may also be related to major Gondwanan accretion that peaked from 650 – 520 Ma (Meert, 2003; Collins and Pisarevsky, 2005). The assembly of western Gondwana peaked at ~620 Ma with the East African Orogeny and the closure of the Mozambique suture (Meert, 2003). This suture extends into East Antarctica and Dronning Maud Land (Jacobs et al., 1998), and passes through the Prince Charles Mountains and Prydz Bay (Boger et al., 2001; Meert, 2003). U/Pb zircon data from central Dronning Maud Land ~600 Ma was dated from charnockite and anorthsite emplacement with ages of 590 – 550 Ma representing high-grade tectonism and magmatism (Mikhalsky et al., 1997; Jacobs et al., 1998).

A small percentage of zircon grains in the data set fall in the age range of 687 – 730 (group 5). U/Pb zircon ages of 695 Ma were found in clastic deposits of the Dick Formation (now Starshot Formation) from Cape Selbourne of the Byrd Group (Goodge et al., 2004). Therefore it is likely that these zircon ages found in the central Ross Sea (ELT32-21) are from this source. This age group is also found in small quantities in the LW2 samples and BR. We also find a portion of group 5 in the NBP94-01-02(SAL1633) sample.

6.3. Middle Proterozoic – Archean

There is a small population of zircons ranging in age from 800 – 850 Ma (Group 6). This group is only found at sites from the Byrd Glacier (BN, BR, and LW2) with only 1 grain found within the Ross Sea (ELT27-14). Zircons of ~850 Ma in age were also found in the Dick Formation (now Starshot Fm.) of the Byrd Group by Goodge

et al. (2004), but the zircons found at sites BN and BR are likely not derived from the Starshot due to their northern location along the Byrd Glacier. Therefore the grains from BN and BR may be recycled from Beacon Supergroup siliciclastics or from original source rocks underneath the ice sheet.

The remaining percentage of zircon age groups (7–13) comprise < 50% of most samples. There are good correlations with the Dick Formation from the Goodge et al. (2004) study with several of these age groups including 885 – 1006, 1027 – 1080, 1094 – 1149, 1232 – 1283, 1439 – 1493, and 1821 – 1909 Ma.

Group 11 (1439 – 1493) has an age range that is more indicative of A-type granite ages found in Laurentian rocks in what is now North America (Anderson, 1983; Anderson and Bender, 1989; van Schmus et al., 1993). A granite clast collected by Goodge et al., (2007) from the Nimrod Glacier area has a U/Pb age of ~1440 Ma. Detrital zircons of this age range have been found in the Nimrod area (Goodge et al., 2002; 2004) but until the discovery of the granitic clast at the head of the Nimrod Glacier (Goodge et al., 2007), no basement sources of these ages has been found (Goodge et al., 2006). It is probable that ~1.4 Ma granite is present underneath the EAIS due to detrital zircon and granitic clast evidence found by Goodge et al., (2002; 2004; 2007) and this study. If so, this has implication on supercontinental reconstructions that place both Laurentia and Antarctica in Rodinia during the Middle to Late Proterozoic (Moores, 1991).

Group 13 (2678 – 2737 Ma) is not found in the Dick Formation at Cape Selbourne, and there are not correlations with any of the samples from the Nimrod

and Starshot Glacier areas from the Goodge et al. (2004) study. The only correlation for this group of zircon ages is located in Stillwell Hills of the Rayner complex, with ages only from Rb/Sr (Halpin et al., 2005).

The age groups > 800 Ma correlate with several U/Pb and Rb/Sr ages in the Rayner complex (Figure 1) from the Stillwell Hills, Oygarden Group, and Rippon Point (Figures 35 and 36). While it impossible to attribute the zircon ages form this study to the Rayner Complex, this suggests that the Rayner complex (Figure 1) may extend into the center of the East Antarctic Craton and may form parts of the basement of the Gambertsev Mountain belt.

The zircon age group 13 is prevalent in the sample from the Lonewolf Nunataks and is present in very small numbers in the BN and BR sample sites. This age group is also found in every Ross Sea sample site except NBP94-07-39(SAL282), making it a possible tracer for this study. Group 13 ranges in age from 2678 – 2737 and may correlate with zircon ages related to the Insel Orogeny ~2650 Ma (Grikurov, 1982).

7. Discussion

Mapped geology of the TAM shows that the Byrd Glacier crosses four distinct groups of bedrock that include the Byrd Group, Granite Harbour Intrusives, Beacon Supergroup, and Ferrar Group (Grindely and Laird, 1969; Barrett, 1972, 1991; Collinson and Pennington, 1986). These bedrocks types are generally reflected in the pebble and petrographic data collected from moraines along the Byrd Glacier; samples from the Lonewolf Nunataks show the most compositional variation from the mapped rock types.

7.1. The Lonewolf Nunataks

The Lonewolf Nunatak sites (LW and LW2) show a wide variety of pebbles, sand mineralogy/lithology, and detrital zircon U/Pb ages that cannot solely be attributed to the locally-mapped bedrock (Figures 19, 20, and 26). This, in addition to a particle-size signature similar to Ross Sea till (Figures 12, 13, and 14), suggests that glacial till is being transported to the Lonewolf Nunataks via subglacial processes and exposed by ablation (plates 1, 2, and 3).

The pebble data from the Byrd Glacier (Figures 6 and 19) shows that local material is being deposited at several sites in addition to material that is inconsistent with derivation from the mapped bedrock. For instance, both sites from the Lonewolf Nunataks have substantial amounts of quartzite, felsic to intermediate igneous pebbles, and several metamorphic pebbles. The sand petrography data of the Lonewolf Nunataks is also consistent with the pebble data in that there are lithic grains present which are inconsistent with the Beacon Group (Table 6). Other sites have pebbles

and sand-sized lithic fragments that are inconsistent with the mapped geology. These include MT, BN, BR, and CJ.

However, within many of the LW and LW2 grains, the polymict lithic fragments contained cores of well-rounded to very well-rounded quartz and possibly feldspar grains surrounded by a fine-grained matrix. It is possible that these well-rounded grains are derived from disaggregated Beacon sandstones, or are remnants of Granite Harbor Intrusives. The interpretation of these grains has implications on not only the provenance of the Lonewolf till, but potentially transport processes and distance of material being eroded by the EAIS and Byrd Glacier. Geochronological analysis of observed zircon grains encased within these rounded quartz grains may provide enough data to determine provenance, while SEM analysis of the surficial properties of these quartz grains may assist in determining the extent to which these grains have interacted with the glacial bed.

It is clear from the particle-size analysis, sand petrography, and U/Pb detrital zircon age data that the till found around the Lonewolf Nunataks is not completely homogenous. Variability in all three data sets between the LW and LW2 sites indicate similarity but not homogeneity. This is certainly true when comparing the LW and LW2 sites to one another which were collected several kilometers apart, but can also be seen with the LW2 sub-samples which were taken at an estimated maximum of 100 meters from one another.

When comparing the zircon data to one another, all the Lonewolf Nunatak samples (LW2/LW) pass the K-S test using this statistical analysis, which makes it

impossible to reject the null hypothesis that all three sub-samples are the same and originate from the same parent population. This is likely due to the majority of grains from the Lonewolf samples sites ranging from ~515 – 615 Ma. The high percentages of these Ross to Pan-African ages make the differences in the older zircon grain populations less relevant to the statistical analysis.

The U/Pb detrital zircon data from the Lonewolf Nunataks show a group of zircon grains that range in age from ~583 – 610 Ma (Appendix C and D). LW and the three LW2 samples (A, B, and C) have maximum probability peaks of 597, 579, 564, and 583 Ma respectively. LW2-A and B also have significant probability peaks of 597 and 610 respectively. These older ages (590 – 610 Ma) have not been described in the Byrd Glacier area before and may represent either early development of the Ross Belt or early subduction of the hypothesized Beardmore microcontinent. These zircons may also be related to the late Pan-African closure of the Mozambique suture located underneath the EAIS. These Pan-African zircon grains could also be coming from the local sandstones of the Beacon Supergroup but until the geochronology of these units is determined, it cannot be further constrained. Geochronological data from the well-rounded quartz grains found in the Lonewolf samples may also provide information that may shed light upon this question as well.

The detrital zircon data also shows a significant population of Grenville-aged (~950 – 1267) grains. Phillips et al., (2005) described dominant zircon ages of 1140 and 1040 Ma in garnet-bearing quartzite from Mount Maguire of the Sodruzhestvo Series located in the southern Prince Charles Mountains (Figure 1). Other age groups

from two other localities in the Sodruzhestvo Group include 1170 and 1020 Ma for one locale, and a range of 970 – 1130 Ma for the other. These age groups are also found within the LW (1027 and 1101 Ma), LW2-B (1076), and LW2-C (1080) including BN (1048) and BR (1138).

Older groups of zircon are also found in the Lonewolf Nunatak samples that correlate with samples from the Ruker Complex and possibly the Rayner, Napier and Rauer Complexes as well. One group in particular includes ages of 2694 – 2714 Ma (Appendix D), which can be found in both Byrd Glacier and Ross Sea samples.

While it is impossible that these grains are coming directly from the exposed and mapped Ruker, Rayner, Napier, or Rauer Complexes, it is possible that these complexes continue underneath the ice sheet and extend beneath the drainage of the Byrd Glacier. These zircons may also come from siliciclastic sedimentary basins underneath the EAIS or are likely a combination of both. Either way it is likely that common-aged material located underneath the EAIS is contributing to zircon grain populations on both sides of the East Antarctic craton.

The LW2 sub-samples' U/Pb detrital zircon data show definite intra-site variability. Gehrels et al. (2006) suggeted sampling 100 grains for detrital zircon analysis in order to identify each of the main age groups present within a representative sample. It is possible that when collecting detrital zircon age data from glacial material, more than 100 grains need to be collected per representative sample. Although the LW and LW2 samples ranged from 56–90 concordant grains (Figure 30, it can still be concluded that important and viable information was obtained from the

limited data sets. By observing the intra-site variability of LW2, more grains may need to be analyzed to develop a more robust dataset.

7.2. The Bates Nunataks and the Britannia Range sample sites

Sample sites BN and BR have a particle-size signature indicative of local derivation as indicated by dominance of the sand-size fraction. The particle-size cluster analysis in Figure 14 shows all the BN samples and sample BR-A clustering together into group 4. However their sand petrography data show small amounts of metamorphic lithic fragments that are inconsistent with the mapped Beacon Supergroup. Both sites show similar pebble counts, with BN having a small amount of quartzite and BR having a greater amount of sandstone.

BN has the higher (about double) clay and silt content (Table 2) when compared to BR, which suggests that BN might be receiving some minor amounts of glacial material from underneath the EAIS. The particle-size differences between BN and BR are more evident in Appendix B with BN and BR-A having higher amounts of coarse and very coarse sand and smaller amounts of fine and medium sized sand than the other BR samples. This data in conjunction with the headward location of the BN makes it plausible that BN is indeed receiving material from underneath the EAIS.

The U/Pb detrital zircon data shows a large population of 586 and 588 Ma for BN and BR (Figure 26 and Appendix D). These ages may also be related to early development of the Ross belt or be from Pan-African orogenic events as was mentioned for the Lonewolf Nunataks. The dominant zircon population of the BN and BR sites are similar to an age group found in LW2-C (583 Ma). Older (596–608

Ma) zircon groups are found in LW, LW2-A, and LW2-B. If these zircons are related to Ross belt development, it is possible there is a transition from older to younger plutons emplaced underneath the ice along the central and northern TAM moving toward Victoria Land.

7.3. Crazy Jim and Horney Bluff sample sites

Both of the CJ and HB sites have very similar sand petrography data with both having particle size distributions indicative of local derivation. CJ's sand and pebble fractions contain a small population of mafic material, which suggests that either an unmapped unit of Ferrar Group rocks is located close to the site, or material from upstream is being transported and deposited at the CJ site. No mafic material was found at HB.

The total pebble count and point count data from both CJ and HB show clear differences. Metamorphic pebbles dominate the pebble counts for both sites with significant populations of intermediate and felsic igneous pebbles also present (Figure 19). The sand petrography data is dominated by intermediate and felsic igneous lithic fragments with lesser amounts of metamorphic grains (Table 6). This may be a result of faster comminution of the metamorphic rock than the more quartz-rich and harder igneous rock. It is also possible that when looking at this size fraction (0.5 - 2.0 mm), metamorphic grains are less able to be recognized.

CJ and HB are both mapped as Granite Harbour Intrusive (Grindley and Laird, 1969). Borg et al., (1989) named the Horney Formation after finding amphibolite-grade schist and gneiss. The pebble content of both sites show a dominance of gneiss

and schist with lesser but still significant amounts of felsic and intermediate igneous pebbles. This suggests bedrock of metamorphic basement intruded by less voluminous or less exposed plutons of Granite Harbour Intrusives.

The geochronology of these two sites show identical maximum probability peak of 533. This suggests earlier plutonic emplacement of granitoid material in this large area of the Byrd Glacier with crystallization zircon around 533 Ma. Both sites however have differing Grenville-aged zircons (Figure 26). CJ's only other zircon group is 1039 Ma (Appendix D), while HB has two groups of 1112 and 1248 Ma. The presence of graphite crystals in the sand fraction indicates a potential metamorphosed sedimentary protolith. If one assumes that these the majority of these zircons are coming from a more local source, the geography of the two sites in relation to the zircon ages suggests a general southern tilting stratigraphy with possible older meta-sedimentary units (HB: 1112 and 1248 Ma) located close to the HB site, which are overlain by younger meta-sedimentary units (CJ: 1039) with both areas being intruded by 533 Ma granitoid plutons. Toward the head of the Byrd Glacier, the basement located along the northern side is overlain by the Carboniferous to Triassic sediments and Jurassic mafic igneous intrusions of the Beacon Supergroup (BN and BR). The limited data in this study certainly cannot prove such a hypothesis but it is a tesTable one nonetheless and makes it obvious that further mapping needs to be done in this area.

7.4. Mount Tuatara site

The MT site contains > 95% limestone/marble in the pebble count. The sand petrography however shows a large percentage of polymict grains (Table 6). This and the particle-size data showing high amounts of clay and silt suggests rapid comminution of the limestone bedrock into fine particles which likely comprise the matrix of the polymicts found here. The presence of zircon grains and minor amounts of metamorphic grains in the sand fraction suggest transportation of material from other locales.

MT has a group of 6 grains with an average age of 1788 Ma (Appendix C). This age is not found, in significant amounts, within any of the other Byrd Glacier samples. Goodge et al., (2004) found zircon ages from ~1720 – 1730 Ma within the Miller Range of the TAM and 1770 within sandstone and 1780 within Goldie Formation conglomerate along the Prince Ann Glacier (Nimrod Glacier area). It is possible that the 1788 Ma grains found at the MT site correlate with those found by Goodge et al., (2004) in the Nimrod Glacier area.

7.5. The Ross Sea sample sites

Particle-size analysis shows that the cores located down the centerline of the central and western Ross Sea (ELT32-21, NBP95-01-17) have a higher sand signature. Other than this observation, no consistent pattern can be seen in the Ross Sea particle size data using this limited data set.

The forward stepwise DA of the Ross Sea particle size data suggests the dominant factors of discrimination are medium silt, very-fine sand, and medium sand (Appendix G-5). When looking at the particle size distribution in Table 2 and Appendix B, all the samples from NBP95-01-17 and NBP95-01-11(SAL537) have greater amounts of sand and a reduction in silt and clay compared to the other Ross Sea samples.

A time horizon seems to exist within cores NBP94-01-02, ELT32-20, and ELT32-21 (Figure 9). The sand petrography shows, at a certain interval within each core, that the sand fraction becomes dominated by polymict (Figure 21). These intervals include samples NBP94-01-02(SAL1633), ELT32-20(SAL1639), and ELT32-21(SAL1642). Sample NBP04-07-39(SAL282), located in the central Ross Sea, is also dominated by polymict.

There seems to be multiple populations of polymict present in all of the western and central Ross Sea cores except possibly NBP94-07-39. These populations have very different characteristics, therefore making it possible to easily differentiate them in thin section and under a dissecting microscope. One polymict population found in core NBP94-01-02 is similar in appearance to a certain component in tillites from the Ricker Hills in Victoria Land (Figure 1) (Boroni and Fasano, 2006).

Detrital zircon data taken from NBP04-07-39(SAL282) shows a significant population of Cretaceous grains (~100 – 139 Ma) that may correlate with rocks from Marie Byrd Land in West Antarctica (Mukasa and Dalziel, 2000; Siddoway, et al., 2004). A few very Late Triassic to very Early Jurassic grains (~201 – 208 Ma) are

present as well that may also correlate to rocks in Marie Byrd Land or possibly northern Victoria Land (Lisker, 2002). ELT32-20(SAL1639) also contains several grains ranging from Early Cretaceous to Pennsylvanian.

NBP94-01-02(SAL1633) and ELT32-21(SAL1641) have small populations of Early Mississippian to Permian zircon grains that may correlate with ages found in Marie Byrd Land, northern Victoria Land or possibly the Byrd Glacier's CJ site. Due to the location of the NBP94-01-02 core, the Byrd Glacier is the more probable origin. However, such a small population of Late Paleozoic grains at the CJ site increases the uncertainty of this correlation with SAL1633.

A large population of Cambrian to Ordovician (~488 – 523 Ma) grains is present within most of the Ross Sea samples that does not correlate significantly with any populations from the Byrd Glacier (Figure 34, Appendix D). While zircon grains of this age are found in samples from the Byrd Glacier (LW, BR, CJ, and HB), a large percentage of this age group in samples such as ELT32-21, and ELT32-20 make it unlikely that the Byrd Glacier is the only source for such aged grains. A possible provenance of this population could be from granites associated with the Dry Valley granitoids (Cox et al., 2000) or from recycled grains from the Douglas Formation found within the Nimrod Glacier area (Goodge et al., 2004).

Although the detrital zircon populations do not show consistent variability within the Ross Sea, the sand petrography data shows a pattern of separation between the western and central Ross Sea samples (Table 6). Discriminant analysis and principle

component analysis shows the main factors of discrimination are extrusive igneous lithic fragments, polymict, and opaque mineral fragments (Appendix H and I).

By looking at the detrital zircon and sand petrography data it is apparent that, for most of the Ross Sea samples, the Byrd Glacier cannot be determined as the sole source of sediment in these cores. We can observe changes in the amounts of material being deposited in the cores by observing the differences in the sand petrography of each interval. Evidence from the younger (Mesozoic and Paleozoic) detrital zircon ages and sand petrography show that SAL1641 and possibly SAL282 are receiving material from multiple sources. One source may very well be Marie Byrd Land but due to the Late Paleozoic ages found at the CJ sample site, the Byrd Glacier cannot be ruled out as a potential source for SAL1641.

Extrusive igneous material from southern Victoria Land is the likely source for the extrusive lithics found in the Ross Sea samples with the largest population found in core NBP94-01-02 but present in all except core NBP94-07-39. The Permian and younger zircon grains found in the Ross Sea samples likely come from either West Antarctica or possibly an unknown source in the southern TAM. Similar ages are also found in Northern Victoria Land, but due to its location, it is an unlikely source area.

By looking at the sand petrography data and detrital zircon data of the Ross Sea cores several questions arise:

1. Do the depth intervals with the dominant polymict sand populations correlate or represent the same time horizon?

2. Are these areas of the Ross Sea receiving material from Victoria Land, Marie Byrd Land, or the Byrd Glacier?

3. What properties of this polymict-dominated Ross Sea till makes it structurally or geochemically different from till located stratigraphically above and below?

4. Does this till represent warm-based glacial deposition as mentioned by Baroni and Fasano (2006) when describing the Ricker Hills Tilite in Northern Victoria Land?

5. Is it possible to positively correlate these polymict-dominated depth intervals to one another and therefore consider them to have been deposited at the same point in time?

6. If the Cretaceous zircon grains in NBP94-07-39(SAL282) originate in Marie Byrd Land, and therefore all or portions of the till itself, and this till has properties considered related to warm-based glacial deposition, might this horizon represent significant ice-stream activity from the WAIS during a certain point in time?

7. Are there potentially more of these polymict-dominated horizons within the stratigraphic column of the Ross Sea till?

8. Conclusions

The original question on the ability to trace material from the Byrd Glacier into the Ross Sea can be positively answered using both sand petrography and U/Pb detrital zircon age dating. Statistical analysis of the sand petrography data shows a convincing correlation between ELT27-14 and LW (Figures 22 and 24). The detrital zircon data also shows a statistical correlation between ELT27-14(SAL1636) and LW and LW2 using the K-S test (Table 7). As additional evidence for a correlation, when combining all of the Lonewolf Nunatak detrital zircon data together, the K-S test shows a positive correlation with only ELT27-14(SAL1636) (Table 7). This, in addition to the similar sand petrography data, makes a strong case for a positive tracing of material from the head of the Byrd Glacier into the Ross Sea over a distance of 500 kilometers. Positive correlation also exists between ELT32-20(SAL1638) and LW using sand petrography (Figures 22 and 24). Detrital zircon data were not collected for sample SAL1638 but was for SAL1639, which shows no correlation to any Byrd Glacier samples using the K-S test.

Further investigation into the polymict populations show there to be differing populations within the Ross Sea cores. The light brown polymict fragments found in many of the Ross Sea cores including ELT27-14(SAL1636) are not found in any of the Byrd Glacier samples including those from the Lonewolf Nunataks. Yet there are similarities to the polymict fragments with darker matrix in ELT27-14(SAL1636) and those found in LW and LW2. Therefore it is likely that there is a positive correlation

of sand petrography between LW and samples from ELT27-14. However the lighter colored polymict is likely coming from another source.

The presence of coal fragments in all three intervals of ELT32-21 (SAL1640, SAL1641, and SAL1642) as well as ELT27-14(SAL1637) and NBP94-01-02 (SAL1634) are potential correlative with coal fragments found in the Lonewolf Nunatak sand fraction. Coal measures are common in other glacial areas of the TAM making it impossible to conclude that these Ross Sea coal fragments are definitely from the Byrd Glacier. The combination of the additional petrographic and U/Pb isotopic data from these sites makes this evidence more supportive.

Regarding the two ice sheet models proposed by Stuiver et al. (1981) and Licht and Fastook (1998) (Figure 2), the data from this study suggests both models may be considered valid but not during the same time period. With the positive correlation of material from the Byrd Glacier and core ELT27-14 and sample ELT32-20(SAL1638) it can be concluded that the Byrd Glacier dominated the input of ice and material into the western Ross Sea during the LGM. This conclusion is consistent with flow-lines of the Licht and Fastook (1998) model.

If indeed the polymict-dominated ELT32-20(SAL1639) interval can be attributed to a source other than the Byrd Glacier, which the data from this study suggests, then it can be concluded that during the time when this material was deposited, the Byrd Glacier was not the dominant input of ice and material to the western Ross Sea. However, this does not validate the Stuiver et al. (1981) model because positive correlation of material from West Antarctica must be found for these

Ross Sea samples. From this study, only one sample (NBP94-07-39) seems to fit this criterion but this hypothesis can not be proven without further research. Therefore from the limited finding of this study, a new two-fold model can be proposed.

Evidence from core ELT32-20 suggests a possible influx of material occurred into the Ross embayment from both West and East Antarctic sources with possible convergence in the central Ross Sea. The Ross Embayment may have experienced ice-flow regime changes of both the East and West Antarctic Ice Sheets that resulted in deposition of glacial till that supports both models put forth by Stuvier et al. (1981), and Licht and Fastook (1998). These two models may have just operated at different times and under different physical conditions during the entire cycle of the LGM. Further study of Ross Sea and Antarctic tills may provide additional evidence that prove or disprove the hypotheses put forth in this study.

Table 1: Latitude, longitude, and sampling information for Byrd Glacier and Ross Sea samples

Sample ID	Latitude	Longitude	Sampling depths (cm)	Water depth (m)
Byrd Glacier				
LW - Lonewolf Nunataks	-81.300	153.167	NA	NA
LW2 - Lonewolf Nunataks	-81.341	152.679	NA	NA
MT - Mount Tuatara	-80.478	158.670	NA	NA
BN - Bates Nunataks	-80.262	153.653	NA	NA
BR - Britannia Range	-80.386	155.333	NA	NA
CJ - Crazy Jim	-80.402	157.134	NA	NA
HB - Horney Bluff	-80.209	159.143	NA	NA
Ross Sea				
NBP94-01-02	-76.284	169.704	111-126	679
ELT27-14	-77.8	177.333	47-50, 63-66, 105-109, 164-170	722
ELT32-20	-77.585	174.918	64-69, 132-137	728
ELT32-21	-77.933	178.013	54-58, 104-108, 154-160	680
NBP95-07-39	-77.9200	-178	52-54, 90-92	694
ELT32-13	-74.96	172.157	49-51, 100-102, 149-151	537
NBP95-01-17	-77.452	179.05	48-50, 100-102, 153-155	732
NBP95-01-11	-76.45	-179.087	48-50, 100-102	659

Table 2. Average particle size distributions of Byrd Glacier and Ross Sea till samples

Sample ID	Clay(%)	Silt(%)	Sand(%)	Clay(%)	Silt(%)	Sand(%)	Gravel(%)
Byrd Glacier							
LW - Lonewolf Nunataks							
LW-A1 (SAL1577)	22.28	25.15	52.57	11.52	13.01	27.18	48.30
LW-A2 (SAL1578)	20.47	32.98	46.56	8.34	13.43	18.96	59.27
LW-B (SAL1579)	13.84	45.10	41.06	12.91	42.06	38.29	6.75
LW (avg.)	**18.86**	**34.41**	**46.73**	**10.92**	**22.83**	**28.14**	**38.10**
S.dev.	4.4	10.1	5.8	2.3	16.7	9.7	27.7
S.error	2.57	5.80	3.32	1.35	9.61	5.60	15.99
LW2 - Lonewolf Nunataks							
LW2-A (SAL1580)	32.63	39.93	27.44	24.17	29.58	20.32	25.92
LW2-B (SAL1581)	30.46	35.66	33.89	25.43	29.78	28.30	16.49
LW2-C (SAL1582)	16.83	52.36	30.82	15.46	48.11	28.32	8.10
LW2-D (SAL1583)	32.47	41.68	25.86	30.56	39.23	24.34	5.88
LW2 (avg.)	**28.10**	**42.40**	**29.50**	**23.82**	**39.04**	**26.99**	**10.16**
S.dev.	7.6	7.1	3.6	6.3	8.9	3.8	9.1
S.error	3.79	3.55	1.79	3.14	4.43	1.91	4.56
MT - Mount Tuatara							
MT-A (SAL1590)	30.14	20.86	49.01	19.50	13.49	31.71	35.30
MT-B (SAL1591)	23.57	26.60	49.82	14.11	15.92	29.82	40.15
MT-C (SAL1592)	40.54	28.22	31.24	29.14	20.28	22.46	28.12
MT (avg.)	**31.42**	**25.23**	**43.36**	**20.92**	**16.57**	**28.00**	**34.52**
S.dev.	8.6	3.9	10.5	7.6	3.4	4.9	6.0
S.error	4.94	2.23	6.06	4.40	1.99	2.82	3.49
BN - Bates Nunataks							
BN-A (SAL1574)	3.88	16.43	79.69	3.12	13.19	63.96	19.73
BN-B (SAL1575)	3.98	18.52	77.49	3.16	14.70	61.52	20.61
BN-C (SAL1576)	3.49	14.69	81.82	1.97	8.28	46.13	43.62
BN (avg.)	**3.79**	**16.55**	**79.67**	**2.75**	**12.06**	**57.20**	**27.99**
S.dev.	0.3	1.9	2.2	0.7	3.4	9.7	13.5
S.error	0.15	1.11	1.25	0.39	1.94	5.58	7.82
BR - Britannia Range							
BR-A (SAL1571)	2.11	6.85	91.04	0.77	2.70	61.36	35.16
BR-B (SAL1572)	1.19	4.17	94.64	0.99	1.93	45.84	51.24
BR-C (SAL1573)	2.03	3.95	94.02	3.12	13.19	63.96	19.73
BR (avg.)	**1.77**	**4.99**	**93.23**	**1.63**	**5.94**	**57.05**	**35.38**
S.dev.	0.5	1.6	1.9	1.3	6.3	9.8	15.8
S.error	0.29	0.93	1.11	0.75	3.63	5.66	9.10
CJ - Crazy Jim							
CJ-Bulk (SAL1617)	0.29	11.59	88.13	0.23	9.31	70.79	19.68
CJ-C (SAL1618)	0.36	11.48	88.17	0.20	6.51	49.98	43.32
CJ (avg.)	**0.32**	**11.53**	**88.15**	**0.14**	**5.27**	**40.25**	**21.00**
S.dev.	0.0	0.1	0.0	0.0	2.0	14.7	16.7
S.error	0.03	0.06	0.02	0.01	1.40	10.41	11.82

Table 2 (cont.) Average particle size distributions of Byrd Glacier and Ross Sea piston cores

Sample ID	Clay(%)	Silt(%)	Sand(%)	Clay(%)	Silt(%)	Sand(%)	Gravel(%)
HB - Horney Bluff							
HB-B (SAL1588)	0.15	7.95	91.91	0.05	2.81	32.46	64.68
HB-C (SAL1589)	0.44	12.84	86.72	0.15	4.37	29.50	65.99
HB (avg.)	**0.29**	**10.39**	**89.31**	**0.07**	**2.39**	**20.65**	**43.55**
S.dev.	0.2	3.5	3.7	0.1	1.1	2.1	0.9
S.error	0.15	2.45	2.59	0.05	0.78	1.48	0.65
Between Site S.dev.	**13.7**	**13.7**	**26.4**				
Between Site S.error	**5.18**	**5.20**	**9.96**				
Ross Sea - (western)							
NBP94-01-02							
111-116cm (SAL1633)	34.67	48.41	16.92	33.54	46.82	16.36	3.28
150-152cm (SAL374) Lederer, 2003	36.13	42.96	20.91				
S.dev.	1.0	3.9	2.8				
S.error	0.73	2.72	2.00				
ELT32-13 (Lederer, 2003)							
49-51cm (SAL406)	33.88	49.37	16.75				
100-102cm (SAL407)	31.62	50.19	18.19				
149-151cm (SAL408)	33.11	48.89	17.99				
S.dev.	1.1	0.7	0.8				
S.error	0.81	0.46	0.55				
Ross Sea - (central)							
ELT32-20							
64-66cm (SAL1638)	29.67	51.72	18.61	27.18	47.38	17.05	8.39
132-137cm (SAL1639)	30.82	51.27	17.90	24.13	40.14	14.01	21.72
S.dev.	0.8	0.3	0.5	2.2	5.1	2.1	9.4
S.error	0.58	0.22	0.35	1.53	3.62	1.52	6.66
ELT27-14							
47-50cm (SAL1634)	34.35	54.25	11.41	33.35	52.67	11.07	2.90
105-109cm (SAL1636)	35.12	53.43	11.45	32.38	49.27	10.56	7.79
164-170 (SAL1637)	34.53	55.66	9.81	28.15	45.37	8.00	18.48
S.dev.	0.4	1.1	0.9	2.8	3.7	1.6	8.0
S.error	0.23	0.65	0.54	1.60	2.11	0.95	4.60
ELT32-21							
54-58cm (SAL1640)	32.97	45.47	21.57	30.76	42.42	20.12	6.70
104-108cm (SAL1641)	31.72	41.64	26.65	29.34	38.52	24.65	7.49
154-160cm (SAL1642)	32.35	46.38	21.28	30.61	43.88	20.13	5.38
S.dev.	0.6	2.5	3.0	0.8	2.8	2.6	1.1
S.error	0.36	1.45	1.74	0.45	1.60	1.51	0.62
NBP95-01-11 (Lederer, 2003)							
48-50cm (SAL537)	34.75	37.13	28.12				
100-102cm (SAL538)	31.35	57.30	11.32				
S.dev.	2.4	14.3	11.9				
S.error	1.39	8.23	6.86				

Table 2 (cont.) Average particle size distributions of Byrd Glacier and Ross Sea piston cores

Sample ID	Clay(%)	Silt(%)	Sand(%)	Clay(%)	Silt(%)	Sand(%)	Gravel(%)
NBP95-01-17 (Lederer, 2003)							
48-50cm (SAL540)	25.04	33.49	41.47				
100-102cm (SAL543)	29.01	40.22	30.68				
153-155cm (SAL534)	25.04	39.16	35.80				
S.dev.	2.3	3.6	5.4				
S.error	1.32	2.09	3.12				
NBP95-07-39 (Lederer, 2003)							
90-92cm (SAL282)	42.99	55.17	1.89				

Table 3. Lithic fragment categories and mineral criteria used to classify each as such. Lithic fragments all met the Indiana method definition of a rock fragment.

Category	Lithic-Fragment Classification Mineral Criteria
Sedimentary Lithic Fragments	
silt/sandstone	grains with distinct boundaries possibly contain some matrix sand- and/or silt-sized components
mudstone	contain silt and clay-sized particles difficult to determine exact composition
claystone	no discernable grain boundaries
polymict	lithic fragment consists of unknown clasts surrounded by fine-grained matrix may or may not be true lithic fragment but just clumps of till
Intrusive igneous fragments	large crystals and obvious boundaries
Felsic	quartz + k-spar ± plagioclase, biotite, hornblende, muscovite
Intermediate	± quartz + >50% plagioclase + minor K-spar ± hornblende, biotite, clinopyroxene
Mafic	>50% plagioclase + ortho/clinopyroxene, ± olivine, iron oxide
Extrusive igneous fragments	± large crystals with matrix of smaller elongate angular crystals
basalt ± andesite ± rhyolite	multiple zoned and/or twinned plagioclase ± fibrous glass ± opaque minerals ± volcanic glass ± clinopyroxene
Metamorphic Fragments	
Quartzite	intergrowth of quartz crystals
Marble	twinned calcite
Schist	grains exhibit fabric

Table 4. Average point count % differerences with Lederer 2003 data from Byrd Glacier and Ross Sea samples.

Sample ID	qtz	pyr	kspar	plag	cal	oli	musc	biot	chlor	iron ore	opaq	unknown other	gwacke	silt/s. s.	mudst clayst	maf	int	fel	marble l. s.	meta	ext	*n*
SAL406 (2007)	42.0	1.0	16.0	17.0	0.0	0.0	0.0	1.0	0.0	0.0	9.0	1.0	83.0	18.0	3.0	8.0	16.0	46.0	0.0	24.0	76.0	365.0
SAL406 (2003)	88.0	7.0	1.0	10.0	0.0	0.0	0.0	0.0	0.0	0.0	8.0	4.0	40.0	0.0	14.0	32.0	0.0	18.0	0.0	4.0	42.0	268.0
st.dev.	32.5	4.2	10.6	4.9	0.0	0.0	0.0	0.7	0.0	0.0	0.7	2.1	30.4	12.7	7.8	17.0	11.3	19.8	0.0	14.1	24.0	68.6
st.error	23.0	3.0	7.5	3.5	0.0	0.0	0.0	0.5	0.0	0.0	0.5	1.5	21.5	9.0	5.5	12.0	8.0	14.0	0.0	10.0	17.0	48.5
% Difference (variable)	52.3	85.7	93.8	41.2	0.0	0.0	0.0	100.0	0.0	0.0	11.1	75.0	51.8	100.0	78.6	75.0	0.0	60.9	0.0	83.3	44.7	26.6
% Difference (total)	46.0	6.0	15.0	7.0	0.0	0.0	0.0	1.0	0.0	0.0	1.0	3.0	43.0	18.0	11.0	24.0	16.0	28.0	0.0	20.0	34.0	
SAL407 (2007)	46.0	0.0	9.0	24.0	0.0	0.0	0.0	1.0	0.0	0.0	10.0	1.3	47.0	6.0	1.0	4.0	3.0	26.0	0.0	17.0	23.0	226.0
SAL407 (2003)	85.0	7.0	6.0	6.0	0.0	1.0	0.0	1.0	0.0	0.0	7.0	7.0	24.0	3.0	11.0	17.0	0.0	23.0	0.0	3.0	12.0	213.0
st.dev.	27.6	4.9	2.1	12.7	0.0	0.7	0.0	0.0	0.0	0.0	2.1	4.0	16.3	2.1	7.1	9.2	2.1	2.1	0.0	9.9	7.8	9.2
st.error	19.5	3.5	1.5	9.0	0.0	0.5	0.0	0.0	0.0	0.0	1.5	2.9	11.5	1.5	5.0	6.5	1.5	1.5	0.0	7.0	5.5	6.5
% Difference (variable)	45.9	100.0	33.3	75.0	0.0	100.0	0.0	0.0	0.0	0.0	30.0	81.4	48.9	50.0	90.9	76.5	100.0	11.5	0.0	82.4	47.8	5.8
% Difference (total)	39.0	7.0	3.0	18.0	0.0	1.0	0.0	0.0	0.0	0.0	3.0	5.7	23.0	3.0	10.0	13.0	3.0	3.0	0.0	14.0	11.0	
SAL408 (2007)	21.0	0.0	6.0	9.0	0.0	0.0	0.0	0.0	0.0	0.0	3.0	0.0	15.0	7.0	1.0	4.0	8.0	17.0	0.0	13.0	21.0	125.0
SAL408 (2003)	53.0	0.0	1.0	8.0	0.0	0.0	0.0	0.0	0.0	0.0	2.0	4.0	0.0	0.0	10.0	11.0	0.0	17.0	4.0	0.0	11.0	121.0
st.dev.	22.6	0.0	3.5	0.7	0.0	0.0	0.0	0.0	0.0	0.0	0.7	2.8	10.6	4.9	6.4	4.9	5.7	0.0	2.8	9.2	7.1	2.8
st.error	16.0	0.0	2.5	0.5	0.0	0.0	0.0	0.0	0.0	0.0	0.5	2.0	7.5	3.5	4.5	3.5	4.0	0.0	2.0	6.5	5.0	2.0
% Difference (variable)	60.4	100.0	83.3	11.1	0.0	0.0	0.0	0.0	0.0	0.0	33.3	100.0	100.0	100.0	90.0	63.6	100.0	0.0	100.0	100.0	47.6	3.2
% Difference (total)	32.0	0.0	5.0	1.0	0.0	0.0	0.0	0.0	0.0	0.0	1.0	4.0	15.0	7.0	9.0	7.0	8.0	0.0	4.0	13.0	10.0	4.0
SAL283 (2007)	2.8	0.0	0.7	0.7	0.0	0.0	0.0	0.0	0.0	0.0	1.4	0.7	92.3	0.7	0.0	0.0	0.0	0.0	0.0	0.7	0.0	142.0
SAL283 (2003)	5.5	0.0	0.0	0.0	0.0	0.0	0.0	0.0	0.0	0.0	0.0	0.0	88.6	0.0	4.0	0.0	0.0	1.0	0.0	0.5	0.5	201.0
st.dev.	1.9	0.0	0.5	0.5	0.0	0.0	0.0	0.0	0.0	0.0	1.0	0.5	2.6	0.5	2.8	0.0	0.0	0.7	0.0	0.1	0.4	41.7
st.error	1.3	0.0	0.4	0.4	0.0	0.0	0.0	0.0	0.0	0.0	0.7	0.4	1.8	0.4	2.0	0.0	0.0	0.5	0.0	0.1	0.3	29.5
% Difference (variable)	48.8	0.0	100.0	100.0	0.0	0.0	0.0	0.0	0.0	0.0	100.0	100.0	4.0	100.0	100.0	100.0	100.0	100.0	100.0	28.6	100.0	29.4
% Difference (total)	2.7	0.0	0.7	0.7	0.0	0.0	0.0	0.0	0.0	0.0	1.4	0.7	3.7	0.7	4.0	0.0	0.0	1.0	0.0	0.2	0.5	59.0

Table 4 (cont.) Average point count % differerences with Lederer 2003 data from Byrd Glacier and Ross Sea samples.

Sample ID	qtz	pyr	kspar	plag	cal	oli	musc	biot	chlor	iron ore	opaq	unknown other	gwacke	silt/s. s.	mudst clayst	maf	int	fel	marble l. s.	meta	ext	n
SAL374 (2007)	19.2	0.0	5.3	7.3	0.0	0.0	0.0	0.7	0.0	0.0	5.3	1.3	9.3	2.0	2.6	9.3	4.6	7.9	0.0	13.9	11.3	151.0
SAL374 (2003)	36.7	3.3	1.3	7.3	0.0	2.7	0.0	0.0	0.0	0.0	5.3	0.7	5.3	0.0	0.4	9.0	0.0	10.0	0.0	1.3	15.3	150.0
st.dev.	**12.4**	**2.3**	**2.8**	**0.0**	**0.0**	**1.9**	**0.0**	**0.5**	**0.0**	**0.0**	**0.0**	**0.4**	**2.8**	**1.4**	**1.6**	**0.2**	**3.3**	**1.5**	**0.0**	**8.9**	**2.9**	**0.7**
st.error	**8.7**	**1.7**	**2.0**	**0.0**	**0.0**	**1.4**	**0.0**	**0.3**	**0.0**	**0.0**	**0.0**	**0.3**	**2.0**	**1.0**	**1.1**	**0.1**	**2.3**	**1.0**	**0.0**	**6.3**	**2.0**	**0.5**
% Difference (variable)	47.7	100.0	75.5	0.2	0.0	100.0	0.0	100.0	0.0	0.0	0.0	46.2	42.8	100.0	84.9	2.9	100.0	20.5	0.0	90.6	26.4	0.7
% Difference (total)	**17.5**	**3.3**	**4.0**	**0.0**	**0.0**	**2.7**	**0.0**	**0.7**	**0.0**	**0.0**	**0.0**	**0.6**	**4.0**	**2.0**	**2.2**	**0.3**	**4.6**	**2.1**	**0.0**	**12.6**	**4.0**	
SAL537 (2007)	17.3	1.3	7.2	6.5	0.0	0.0	0.0	0.0	0.0	0.0	1.3	1.0	30.1	3.6	1.0	0.3	10.1	7.8	0.0	12.1	0.3	306.0
SAL537 (2003)	56.8	1.5	2.0	3.0	0.5	0.0	0.0	0.2	0.2	0.0	0.7	0.5	15.2	0.2	2.0	2.2	0.7	10.0	0.7	1.2	1.2	405.0
st.dev.	**27.9**	**0.1**	**3.7**	**2.5**	**0.4**	**0.0**	**0.0**	**0.1**	**0.1**	**0.0**	**0.4**	**0.3**	**10.5**	**2.4**	**0.7**	**1.3**	**6.7**	**1.5**	**0.5**	**7.7**	**0.6**	**70.0**
st.error	**19.7**	**0.1**	**2.6**	**1.8**	**0.3**	**0.0**	**0.0**	**0.1**	**0.1**	**0.0**	**0.3**	**0.2**	**7.4**	**1.7**	**0.5**	**0.9**	**4.7**	**1.1**	**0.4**	**5.5**	**0.4**	**49.5**
% Difference (variable)	69.5	12.9	72.2	54.1	100.0	0.0	0.0	100.0	75.5	75.5	46.5	49.0	49.4	94.4	51.0	85.1	93.1	21.6	100.0	90.1	75.5	24.4
% Difference (total)	**39.5**	**0.2**	**5,2**	**3.5**	**0.5**	**0.0**	**0.0**	**0.2**	**0.2**	**0.0**	**0.6**	**-0.5**	**14.9**	**3.4**	**1.0**	**1.9**	**9.4**	**2.2**	**0.7**	**10.9**	**0.9**	
SAL534 (2007)	20.7	0.3	5.2	5.8	0.0	0.0	0.0	0.3	0.0	0.0	0.3	0.3	22.4	5.5	0.3	1.2	5.0	20.7	0.9	11.1	0.0	343.0
SAL534 (2003)	44.1	4.1	1.6	3.4	2.8	0.0	0.0	0.0	0.0	0.0	1.0	0.6	20.9	0.6	2.2	3.1	1.0	7.8	2.8	1.9	1.6	320.0
st.dev.	**16.5**	**2.7**	**2.6**	**1.7**	**2.0**	**0.0**	**0.0**	**0.2**	**0.0**	**0.0**	**0.5**	**0.2**	**1.1**	**3.5**	**1.3**	**1.4**	**2.8**	**9.1**	**1.4**	**6.5**	**1.1**	**16.3**
st.error	**11.7**	**1.9**	**1.8**	**1.2**	**1.4**	**0.0**	**0.0**	**0.1**	**0.0**	**0.0**	**0.4**	**0.2**	**0.8**	**2.5**	**1.0**	**1.0**	**2.0**	**6.4**	**1.0**	**4.6**	**0.8**	**11.5**
% Difference (variable)	53.1	92.9	69.5	41.7	100.0	0.0	0.0	100.0	0.0	0.0	70.8	50.0	6.9	89.2	86.7	50.0	79.8	62.3	50.0	82.9	72.2	6.7
% Difference (total)	**23.4**	**3.8**	**3.6**	**2.4**	**2.8**	**0.0**	**0.0**	**0.3**	**0.0**	**0.0**	**0.7**	**0.3**	**1.5**	**4.9**	**1.9**	**1.9**	**4.0**	**12.9**	**1.9**	**9.2**	**1.6**	
SAL538 (2007)	18.6	0.2	4.7	12.1	0.0	0.0	0.0	0.0	0.0	0.0	0.4	0.9	32.2	2.0	0.7	0.7	6.7	11.2	0.0	8.0	1.6	447.0
SAL538 (2003)	44.4	6.1	1.9	3.5	0.8	0.0	0.3	0.0	0.0	0.0	0.5	0.5	27.0	1.0	0.5	4.3	0.3	4.8	0.5	3.0	1.3	374.0
st.dev.	**18.3**	**4.2**	**2.0**	**6.1**	**0.6**	**0.0**	**0.2**	**0.0**	**0.0**	**0.0**	**0.0**	**0.3**	**3.7**	**0.7**	**0.1**	**2.6**	**4.5**	**4.5**	**0.4**	**3.6**	**0.2**	**51.6**
st.error	**12.9**	**2.9**	**1.4**	**4.3**	**0.4**	**0.0**	**0.2**	**0.0**	**0.0**	**0.0**	**0.0**	**0.2**	**2.6**	**0.5**	**0.1**	**1.8**	**3.2**	**3.2**	**0.3**	**2.5**	**0.1**	**36.5**
% Difference (variable)	58.2	96.3	59.6	71.0	100.0	0.0	100.0	0.0	0.0	0.0	10.5	44.4	16.2	50.3	25.5	84.4	95.5	57.1	100.0	62.6	17.0	16.3
% Difference (total)	**25.8**	**5.9**	**2.8**	**8.6**	**0.8**	**0.0**	**0.3**	**0.0**	**0.0**	**0.0**	**0.1**	**0.4**	**5.2**	**1.0**	**0.2**	**3.6**	**6.4**	**6.4**	**0.5**	**5.0**	**0.3**	

Table 4 (cont.) Average point count % differerences with Lederer 2003 data from Byrd Glacier and Ross Sea samples.

Sample ID	qtz	pyr	kspar	plag	cal	oli	musc	biot	chlor	iron ore	opaq	unknow n other	pmict	silt/s. s.	mudst clayst	maf	int	fel	marble l. s.	meta	ext	n
SAL540 (2007)	25.0	0.8	3.3	4.9	0.0	0.0	0.0	0.0	0.0	0.0	0.8	0.3	23.4	1.1	1.4	0.0	4.9	19.0	1.4	13.1	0.5	364.0
SAL540 (2003)	49.3	1.6	1.6	2.7	0.0	0.0	0.0	0.3	0.3	0.0	0.5	0.3	20.8	0.2	3.7	1.1	1.3	12.0	0.3	2.7	0.5	375.0
st.dev.	17.2	0.5	1.2	1.6	0.0	0.0	0.0	0.2	0.2	0.0	0.2	0.0	1.8	0.6	1.6	0.8	2.6	4.9	0.8	7.4	0.0	7.8
st.error	12.2	0.4	0.8	1.1	0.0	0.0	0.0	0.2	0.2	0.0	0.2	0.0	1.3	0.4	1.2	0.6	1.8	3.5	0.5	5.2	0.0	5.5
% Difference (variable)	49.3	48.5	51.5	16.2	0.0	0.0	0.0	100.0	100.0	0.0	39.3	0.0	10.9	81.8	62.9	100.0	73.7	36.7	78.2	79.5	0.0	73.7
% Difference (total)	24.3	0.8	1.7	2.2	0.0	0.0	0.0	0.3	0.3	0.0	-0.3	0.0	2.6	0.9	2.3	1.1	3.6	7.0	1.1	10.4	0.0	
SAL543 (2007)	14.7	0.0	6.4	4.4	0.2	0.0	0.0	0.7	0.0	0.0	0.7	0.5	30.1	2.7	0.5	0.5	6.1	17.6	0.7	13.7	0.5	409.0
SAL543 (2003)	49.7	1.9	1.9	1.9	0.6	0.0	0.6	0.6	0.0	0.0	0.6	0.3	20.4	0.3	1.2	2.5	1.2	9.9	2.8	3.7	0.0	324.0
st.dev.	24.8	1.3	3.2	1.8	0.3	0.0	0.4	0.1	0.0	0.0	0.1	0.1	6.8	1.7	0.5	1.4	3.5	5.4	1.5	7.0	0.3	60.1
st.error	17.5	1.0	2.2	1.3	0.2	0.0	0.3	0.1	0.0	0.0	0.1	0.1	4.8	1.2	0.4	1.0	2.5	3.9	1.0	5.0	0.2	42.5
% Difference (variable)	70.5	100.0	70.1	56.8	59.3	100.0	100.0	18.2	0.0	0.0	18.2	40.0	32.2	88.8	59.3	80.4	80.4	43.8	73.8	72.9	100.0	20.8
% Difference (total)	35.0	1.9	4.5	-2.5	0.4	0.0	0.6	0.1	0.0	0.0	0.1	0.2	9.7	2.4	0.7	2.0	4.9	7.7	2.1	10.0	0.5	
Average *st.dev.* for all samples	20.2	2.0	3.2	3.3	0.3	0.3	0.1	0.2	0.0	0.0	0.6	1.1	8.7	3.1	3.0	3.9	4.2	5.0	0.7	7.4	4.4	32.9
Average *st.error* for all samples	14.3	1.4	2.3	2.3	0.2	0.2	0.0	0.1	0.0	0.0	0.4	0.8	6.1	2.2	2.1	2.7	3.0	3.5	0.5	5.3	3.1	23.3
Average % difference (per variable)	55.6	73.6	70.9	46.7	35.9	30.0	20.0	51.8	17.5	7.5	36.0	58.6	36.3	85.5	73.0	71.8	82.3	41.4	60.2	77.3	53.1	20.8
Average % total difference (total)	28.5	2.9	4.0	4.1	0.4	0.4	0.1	0.3	0.1	0.0	0.8	1.4	12.3	4.3	4.2	5.5	6.0	7.0	1.0	10.5	6.3	

Table 5. Clast Percentage Data from Sample Sites at Byrd Glacier, Anatarctica

	Igneous				Metamorphic				Sedimentary						
Site	**Icf**	**Ici**	**Icm**	**Ifm**	**Mg**	**Ms**	**Mq**	**Mm**	**Ss**	**Sc**	**Sw**	**Sch**	**Sl**	**Other**	***n***
BN-A	0.0	0.0	80.8	0.0	0.0	0.0	8.2	0.0	11.0	0.0	0.0	0.0	0.0	0.0	73
BN-B	0.0	0.0	90.1	5.3	0.0	0.0	0.0	0.0	4.6	0.0	0.0	0.0	0.0	0.0	131
BN-C	0.0	0.0	91.9	1.8	0.0	0.0	0.0	0.0	6.3	0.0	0.0	0.0	0.0	0.0	110
BN	**0.0**	**0.0**	**87.6**	**2.4**	**0.0**	**0.0**	**2.7**	**0.0**	**7.3**	**0.0**	**0.0**	**0.0**	**0.0**	**0.0**	**314**
S.dev.	0.0	0.0	5.9	2.7	0.0	0.0	4.7	0.0	3.3	0.0	0.0	0.0	0.0	0.0	29.4
S.error	0.00	0.00	3.43	1.57	0.00	0.00	2.74	0.00	1.90	0.00	0.00	0.00	0.00	0.00	16.95
BR-A	0.0	0.0	84.4	0.0	0.0	0.0	0.0	0.0	15.6	0.0	0.0	0.0	0.0	0.0	90
BR-B	0.0	0.0	84.2	0.0	0.0	0.0	0.0	0.0	15.8	0.0	0.0	0.0	0.0	0.0	114
BR-C	0.0	0.0	75.5	0.0	0.0	0.0	0.0	0.0	24.5	0.0	0.0	0.0	0.0	0.0	106
BR	**0.0**	**0.0**	**81.4**	**0.0**	**0.0**	**0.0**	**0.0**	**0.0**	**18.6**	**0.0**	**0.0**	**0.0**	**0.0**	**0.0**	**310**
S.dev.	0.0	0.0	5.1	0.0	0.0	0.0	0.0	0.0	5.1	0.0	0.0	0.0	0.0	0.0	12.2
S.error	0.00	0.00	2.95	0.00	0.00	0.00	0.00	0.00	2.95	0.00	0.00	0.00	0.00	0.00	7.06
CJ-A	20.5	22.3	3.6	7.1	32.1	14.3	0.0	0.0	0.0	0.0	0.0	0.0	0.0	0.0	112
CJ-B	24.1	10.8	0.0	0.0	45.8	14.5	0.0	0.0	1.2	0.0	0.0	0.0	0.0	3.6	83
CJ-C	22.5	10.2	6.1	7.1	36.7	15.3	0.0	0.0	0.0	0.0	2.0	0.0	0.0	0.0	98
CJ	**22.4**	**14.5**	**3.2**	**4.8**	**38.2**	**14.7**	**0.0**	**0.0**	**0.4**	**0.0**	**0.7**	**0.0**	**0.0**	**1.2**	**293**
S.dev.	1.8	6.8	3.1	4.1	6.9	0.5	0.0	0.0	0.7	0.0	1.2	0.0	0.0	2.1	14.5
S.error	1.03	3.94	1.77	2.38	4.01	0.32	0.00	0.00	0.40	0.00	0.68	0.00	0.00	1.20	8.37
HB-A	8.8	0.0	0.0	0.0	43.2	48.0	0.0	0.0	0.0	0.0	0.0	0.0	0.0	0.0	125
HB-B	19.1	0.0	0.0	0.0	25.8	55.1	0.0	0.0	0.0	0.0	0.0	0.0	0.0	0.0	89
HB-C	5.0	0.0	0.0	0.0	48.0	47.0	0.0	0.0	0.0	0.0	0.0	0.0	0.0	0.0	100
HB	**11.0**	**0.0**	**0.0**	**0.0**	**39.0**	**50.0**	**0.0**	**0.0**	**0.0**	**0.0**	**0.0**	**0.0**	**0.0**	**0.0**	**314**
S.dev.	7.3	0.0	0.0	0.0	11.7	4.4	0.0	0.0	0.0	0.0	0.0	0.0	0.0	0.0	18.4
S.error	4.21	0.00	0.00	0.00	6.73	2.54	0.00	0.00	0.00	0.00	0.00	0.00	0.00	0.00	10.65
LW-A	0.9	20.3	48.3	9.3	8.5	4.2	1.7	0.0	1.7	0.0	5.1	0.0	0.0	0.0	118
LW-B	2.3	28.7	3.5	0.0	5.8	0.0	8.1	0.0	5.8	0.0	46.0	0.0	0.0	0.0	87
LW	**1.6**	**24.5**	**25.9**	**4.7**	**7.1**	**2.1**	**4.9**	**0.0**	**3.7**	**0.0**	**25.5**	**0.0**	**0.0**	**0.0**	**205**
S.dev.	1.7	14.8	27.0	5.4	1.4	2.1	4.2	0.0	3.0	0.0	25.2	0.0	0.0	0.0	55.2
S.error	1.19	10.45	19.06	3.80	0.97	1.51	3.00	0.00	2.09	0.00	17.83	0.00	0.00	0.00	39.07
LW2-A	0.8	0.0	38.1	8.2	4.5	0.0	13.4	0.0	8.2	0.0	25.4	0.0	1.5	0.0	134
LW2-B	1.9	0.0	41.7	2.8	5.6	0.9	13.0	0.0	4.6	0.0	28.7	0.9	0.0	0.0	108
LW-2-C	5.1	0.0	58.1	0.0	5.1	3.4	16.2	0.0	6.0	0.0	6.0	0.0	0.0	0.0	117
LW2	**2.6**	**0.0**	**46.0**	**3.7**	**5.1**	**1.5**	**14.2**	**0.0**	**6.3**	**0.0**	**20.0**	**0.3**	**0.5**	**0.0**	**359**
S.dev.	2.3	0.0	10.7	4.2	0.5	1.8	1.8	0.0	1.8	0.0	12.3	0.5	0.9	0.0	13.2
S.error	1.32	0.00	6.17	2.41	0.31	1.02	1.02	0.00	1.04	0.00	7.08	0.31	0.50	0.00	7.62
MT-A	0.0	0.0	0.9	0.0	0.0	0.0	0.0	2.8	0.0	0.0	0.0	0.0	96.2	0.0	106
MT-B	0.0	0.0	0.0	0.0	0.0	0.0	0.0	0.0	0.0	0.0	0.0	0.0	100.0	0.0	124
MT-C	0.0	0.0	0.0	0.0	0.0	0.0	0.0	1.0	1.0	0.0	0.0	0.0	97.9	0.0	97
MT	**0.0**	**0.0**	**0.3**	**0.0**	**0.0**	**0.0**	**0.0**	**1.3**	**0.3**	**0.0**	**0.0**	**0.0**	**98.1**	**0.0**	**327**
S.dev.	0.0	0.0	0.5	0.0	0.0	0.0	0.0	1.4	0.6	0.0	0.0	0.0	1.9	0.0	13.7
S.error	0.00	0.00	0.31	0.00	0.00	0.00	0.00	0.83	0.34	0.00	0.00	0.00	1.09	0.00	7.94

KEY

Icf = Course Grained Felsic	**Mg** = Gneiss	**Ss** = Sandstone
Ici = Coarse Grained Intermediate	**Ms** = Schist	**Sc** = Conglomerate
Icm = Coarse Grained Mafic	**Mq** = Quartzite	**Sw** = Wacke
Ifm = Fine Grained Mafic	**Mm** = Marble	**Sch** = Chert
		Sl = Limestone

Table 6. Average point count data from Byrd Glacier and Ross Sea samples.

Sample ID	qtz	pyr	kspar	plag	cal	oli	musc	biot	chlor	iron ore	opaq	unknown other	pmict	silt/s. s.	mudst clayst	maf	int	fel	marble l. s.	meta	ext	*n*
Byrd Glacier																						
BN-A	1.4	0.9	0.5	0.9	0.0	0.0	0.0	0.0	0.0	0.0	0.0	0.5	0.0	0.0	0.0	93.9	1.9	0.0	0.0	0.0	0.0	213
BN-B	0.9	0.0	1.8	0.5	0.0	0.0	0.0	0.0	0.0	0.0	0.2	0.9	0.0	0.0	0.0	95.7	0.0	0.0	0.0	0.0	0.0	439
BN-C	0.5	4.3	0.5	0.5	0.0	0.0	0.0	0.0	0.0	0.0	0.0	0.3	0.0	0.0	0.0	93.5	0.3	0.0	0.0	0.0	0.0	369
BN Avg	**1.0**	**1.8**	**0.9**	**0.6**	**0.0**	**0.0**	**0.0**	**0.0**	**0.0**	**0.0**	**0.1**	**0.6**	**0.0**	**0.0**	**0.0**	**94.4**	**0.7**	**0.0**	**0.0**	**0.0**	**0.0**	**1021**
												0.0							0.0	0.0		
BR-A	0.9	0.9	0.0	0.3	0.0	0.0	0.0	0.0	0.0	0.0	0.0	0.0	0.0	1.2	0.0	93.9	0.0	0.0	0.0	2.8	0.0	327
BR-B	4.2	0.0	0.0	1.8	0.0	0.0	0.0	0.0	0.0	0.0	0.0	0.0	0.0	4.2	0.6	75.6	0.0	0.0	0.0	13.7	0.0	168
BR-C	0.0	0.7	0.0	0.7	0.0	0.0	0.0	0.0	0.7	0.0	0.0	2.2	2.2	2.2	0.0	89.6	0.0	0.7	0.0	0.7	0.0	135
BR Avg.	**1.7**	**0.6**	**0.0**	**0.9**	**0.0**	**0.0**	**0.0**	**0.0**	**0.2**	**0.0**	**0.0**	**0.7**	**0.7**	**2.5**	**0.2**	**86.4**	**0.0**	**0.2**	**0.0**	**5.7**	**0.0**	**630**
												0.0										
CJ-B	24.9	1.0	14.2	8.4	0.0	0.0	0.0	2.9	0.0	0.0	0.3	2.1	0.3	0.0	0.0	9.7	8.9	24.1	0.0	3.1	0.0	381
CJ-C	9.6	0.5	10.6	7.3	0.0	0.0	0.0	2.3	0.0	0.0	0.3	3.0	0.0	0.0	0.0	4.5	18.1	27.0	0.0	16.6	0.3	397
CJ Avg.	**17.3**	**0.8**	**12.4**	**7.9**	**0.0**	**0.0**	**0.0**	**2.6**	**0.0**	**0.0**	**0.3**	**2.6**	**0.1**	**0.0**	**0.0**	**7.1**	**13.5**	**25.5**	**0.0**	**9.9**	**0.1**	**778**
												0.0							0.0	0.0		
HB-B	11.3	0.0	4.8	11.9	0.0	0.0	0.0	4.8	0.0	0.0	0.0	3.0	0.0	0.0	0.0	0.6	29.2	23.2	0.0	11.3	0.0	168
HB-C	7.1	0.0	4.7	16.6	0.0	0.0	0.0	6.6	0.0	0.0	0.0	1.4	0.0	0.0	0.0	0.0	29.9	20.9	0.0	12.8	0.0	211
HB Avg.	**9.2**	**0.0**	**4.8**	**14.2**	**0.0**	**0.0**	**0.0**	**5.7**	**0.0**	**0.0**	**0.0**	**2.2**	**0.0**	**0.0**	**0.0**	**0.3**	**29.5**	**22.0**	**0.0**	**12.1**	**0.0**	**379**
												0.0							0.0	0.0		
LW-A1	24.1	0.5	2.4	1.0	0.0	0.0	0.0	0.0	0.0	0.0	0.3	1.1	53.5	4.3	0.0	4.3	1.0	4.0	0.0	3.5	0.0	626
LW-A2	13.7	0.0	2.0	2.0	0.0	0.0	0.0	0.0	0.0	0.0	0.0	0.0	43.1	0.0	0.0	17.0	1.3	11.8	0.0	9.2	0.0	153
LW-B	14.4	0.5	0.5	0.3	0.0	0.0	0.0	0.0	0.0	0.0	0.2	0.3	78.2	1.0	0.3	0.5	0.2	2.3	0.2	0.8	0.0	859
LW Avg.	**17.4**	**0.3**	**1.6**	**1.1**	**0.0**	**0.0**	**0.0**	**0.0**	**0.0**	**0.0**	**0.2**	**0.5**	**58.3**	**1.8**	**0.1**	**7.3**	**0.8**	**6.0**	**0.1**	**4.5**	**0.0**	**1638**
												0.0							0.0	0.0		
LW2-A	32.5	0.8	1.3	0.7	0.0	0.0	0.0	0.0	0.0	0.0	0.1	0.4	34.5	1.8	0.1	17.5	0.9	6.0	0.1	3.4	0.0	853
LW2-B	32.5	1.9	1.4	0.8	0.0	0.0	0.0	0.0	0.0	0.0	0.3	0.5	44.5	1.6	0.0	3.3	1.4	9.3	0.0	2.5	0.0	366
LW2-C	19.6	0.9	2.2	0.4	0.0	0.0	0.0	0.0	0.0	0.0	0.9	0.4	52.0	2.7	0.0	4.0	0.4	10.7	0.9	4.4	0.4	225
LW2-D	28.1	1.9	2.9	0.3	0.3	0.0	0.0	0.0	0.0	0.0	0.5	0.3	50.8	2.7	0.0	1.3	0.5	8.8	0.3	1.3	0.0	374
LW2 Avg.	**28.2**	**1.4**	**2.0**	**0.6**	**0.1**	**0.0**	**0.0**	**0.0**	**0.0**	**0.0**	**0.5**	**0.4**	**45.5**	**2.2**	**0.0**	**6.5**	**0.8**	**8.7**	**0.3**	**2.9**	**0.1**	**1818**
MT-A	0.00	0.00	0.00	0.00	0.00	0.00	0.00	0.00	0.00	0.00	0.00	0.00	54.22	6.93	0.90	0.00	0.00	0.30	36.14	1.51	0	278
MT-B	0.00	0.00	0.00	0.00	0.00	0.00	0.00	0.00	0.00	0.00	0.00	0.00	15.41	5.02	0.00	0.00	0.00	0.00	77.78	1.79	0	279
MT-C	0.00	0.00	0.00	0.00	0.00	0.00	0.00	0.00	0.00	0.00	0.00	0.00	72.67	6.69	0.87	0.00	0.00	0.00	18.02	1.74	0	344
MT Avg.	**0.0**	**0.0**	**0.0**	**0.0**	**0.0**	**0.0**	**0.0**	**0.0**	**0.0**	**0.0**	**0.0**	**0.0**	**35.6**	**4.7**	**0.4**	**0.0**	**0.0**	**0.1**	**33.0**	**1.3**	**0.0**	**901**

Table 6 cont. Average point count data from Byrd Glacier and Ross Sea.

Sample ID	qtz	pyr	kspar	plag	cal	oli	musc	biot	chlor	iron ore	opaq	unknow n other	pmict	silt/s. s.	mudst clayst	maf	int	fel	marble l. s.	meta	ext	n
Ross Sea																						
NPB94-01-02 (50-52cm) SAL372	13.5	0.3	8.3	4.0	0.0	0.3	0.0	0.0	0.0	0.0	2.0	1.3	37.3	1.0	0.7	1.7	4.0	5.6	0.0	10.2	10.0	**303**
NBP94-01-02 (111-116cm) SAL1633	1.7	0.2	0.6	0.1	0.0	0.0	0.0	0.0	0.0	0.0	0.3	0.0	90.9	0.8	0.2	0.9	0.7	0.9	0.0	1.6	1.2	**903**
NPB94-01-02 (150-152cm) SAL374	19.2	0.0	5.3	7.3	0.0	0.0	0.0	0.7	0.0	0.0	5.3	1.3	9.3	2.0	2.6	9.3	4.6	7.9	0.0	13.9	11.3	**151**
ELT27-14 (47-50cm) SAL1634	9.4	0.6	3.1	2.0	0.0	0.0	0.0	0.0	0.0	0.0	0.0	0.6	65.3	1.1	0.3	2.0	2.8	3.7	0.3	8.5	0.3	**352**
ELT27-14 (63-66)cm SAL1635	10.3	0.2	1.4	4.2	0.0	0.0	0.0	0.0	0.0	0.0	0.3	0.0	65.5	0.3	0.5	3.1	1.6	2.6	0.2	8.2	1.6	**621**
ELT27-14 (105-109cm) SAL1636	18.9	0.6	1.7	0.9	0.0	0.0	0.0	0.0	0.0	0.0	0.3	0.3	55.9	1.7	1.4	4.9	0.0	5.4	0.0	8.0	0.0	**349**
ELT27-14 (164-170cm) SAL1637	9.9	0.0	3.3	1.7	0.0	0.0	0.0	0.0	0.0	0.0	0.3	0.2	67.1	0.3	0.2	2.1	1.2	5.3	0.7	7.7	0.7	**605**
ELT32-20 (64-69cm) SAL1638	5.8	0.4	2.4	2.4	0.0	0.0	0.0	0.0	0.0	0.0	0.0	0.2	61.0	1.8	0.6	7.2	3.6	5.2	0.2	8.9	0.2	**497**
ELT32-20 (132-134cm) SAL1639	0.0	0.0	0.6	0.3	0.0	0.0	0.0	0.0	0.0	0.0	0.1	0.1	96.7	0.3	0.0	0.5	0.5	0.3	0.0	0.4	0.2	**1188**
ELT32-21 (54-58cm) SAL1640	15.2	0.1	4.8	5.4	0.1	0.0	0.0	0.0	0.0	0.0	0.3	0.6	33.0	6.1	1.2	1.7	4.3	9.5	0.8	16.6	0.3	**1090**
ELT32-21 (104-108cm) SAL1641	14.2	0.1	3.3	2.6	0.0	0.0	0.0	0.0	0.0	0.0	0.0	0.0	50.7	3.7	2.2	2.2	2.5	5.6	0.3	12.1	0.4	**957**
ELT32-21 (154-160cm) SAL1642	2.1	0.0	1.1	0.6	0.0	0.0	0.0	0.0	0.0	0.0	0.2	0.2	87.4	1.3	0.2	0.2	0.6	1.6	0.0	4.6	0.0	**1238**
NPB94-07-39 (100-102cm) SAL282	2.8	0.0	0.7	0.7	0.0	0.0	0.0	0.0	0.0	0.0	1.4	0.7	92.3	0.7	0.0	0.0	0.0	0.0	0.0	0.7	0.0	**142**

Table 7. K-S test of detrital zircon U/Pb ages for Byrd Glacier and Ross Sea samples. Analysis run on: Friday, May 4, 2007 @ 12:03:30 PM. Version: 1.0.

K-S P-values using error in the CDF

	SAL1633												
SAL1636	0.998	SAL1636											
SAL1639	0.532	0.433	SAL1639										
SAL1641	0.406	0.105	0.567	SAL1641									
SAL282	0.006	0.007	0.102	0.002	SAL282								
BN	0.168	0.529	0.008	0.000	0.002	BN							
BR	0.645	0.708	0.055	0.004	0.002	0.607	BR						
CJ	0.000	0.001	0.100	0.003	0.002	0.000	0.000	CJ					
HB	0.000	0.000	0.006	0.000	0.002	0.000	0.000	0.167	HB				
LW	0.054	0.165	0.002	0.000	0.0005	0.145	0.262	0.000	0.000	LW			
LW2-A	0.013	0.099	0.008	0.000	0.0008	0.006	0.005	0.000	0.000	0.306	LW2-A		
LW2-B	0.085	0.243	0.003	0.000	0.0009	0.056	0.225	0.000	0.000	0.835	0.229	LW2-B	
LW2-C	0.234	0.511	0.018	0.001	0.0035	0.517	0.684	0.000	0.000	0.968	0.381	0.467	LW-C
All-Lwolf	0.033	0.148	0.001	0.000	0.000	0.014	0.034	0.000	0.000	1.000	0.426	0.936	0.871

D-values using error in the CDF

n													
48	SAL1633												
42	0.082	SAL1636											
40	0.173	0.193	SAL1639										
94	0.158	0.225	0.148	SAL1641									
23	0.435	0.435	0.319	0.432	SAL282								
90	0.198	0.151	0.313	0.336	0.438	BN							
95	0.131	0.130	0.252	0.259	0.435	0.112	BR						
77	0.377	0.379	0.238	0.278	0.435	0.522	0.491	CJ					
84	0.450	0.473	0.326	0.354	0.435	0.624	0.578	0.176	HB				
90	0.240	0.209	0.356	0.360	0.474	0.170	0.148	0.580	0.682	LW			
68	0.299	0.240	0.331	0.392	0.476	0.271	0.276	0.544	0.641	0.156	LW2-A		
87	0.226	0.193	0.341	0.359	0.461	0.200	0.155	0.563	0.663	0.093	0.168	LW2-B	
56	0.204	0.168	0.319	0.339	0.441	0.138	0.121	0.539	0.641	0.084	0.164	0.145	LW-C
301	0.221	0.186	0.336	0.348	0.455	0.185	0.166	0.558	0.660	0.042	0.116	0.064	0.086

K-S P-values for no error

	SAL1633												
SAL1636	0.937	SAL1636											
SAL1639	0.347	0.133	SAL1639										
SAL1641	0.078	0.038	0.521	SAL1641									
SAL282	0.006	0.007	0.076	0.002	SAL282								
BN	0.016	0.177	0.001	0.000	0.000	BN							
BR	0.283	0.468	0.008	0.001	0.002	0.455	BR						
CJ	0.000	0.000	0.022	0.000	0.002	0.000	0.000	CJ					
HB	0.000	0.000	0.002	0.000	0.002	0.000	0.000	0.004	HB				
LW	0.008	0.032	0.000	0.000	0.000	0.062	0.094	0.000	0.000	LW			
LW2-A	0.008	0.060	0.002	0.000	0.0003	0.004	0.004	0.000	0.000	0.276	LW2-A		
LW2-B	0.009	0.126	0.001	0.000	0.0002	0.014	0.078	0.000	0.000	0.225	0.200	LW2-B	
LW2-C	0.045	0.100	0.001	0.000	0.0009	0.308	0.484	0.000	0.000	0.227	0.275	0.178	LW-C
All-Lwolf	0.002	0.028	0.000	0.000	0.000	0.004	0.016	0.000	0.000	0.959	0.388	0.491	0.333

D-values for no error

n													
48	SAL1633												
42	0.113	SAL1636											
40	0.200	0.257	SAL1639										
94	0.226	0.261	0.154	SAL1641									
23	0.435	0.435	0.335	0.435	SAL282								
90	0.277	0.205	0.367	0.382	0.489	BN							
95	0.175	0.157	0.314	0.288	0.435	0.125	BR						
77	0.435	0.429	0.293	0.339	0.435	0.552	0.526	CJ					
84	0.461	0.524	0.361	0.389	0.435	0.688	0.623	0.279	HB				
90	0.297	0.268	0.403	0.383	0.521	0.195	0.182	0.627	0.733	LW			
68	0.313	0.260	0.366	0.404	0.506	0.283	0.279	0.571	0.697	0.160	LW2-A		
87	0.295	0.221	0.389	0.394	0.510	0.236	0.189	0.598	0.705	0.157	0.174	LW2-B	
56	0.271	0.250	0.400	0.376	0.486	0.164	0.141	0.615	0.726	0.177	0.180	0.188	LW-C
301	0.288	0.239	0.377	0.377	0.507	0.206	0.180	0.590	0.703	0.060	0.120	0.100	0.136

Average K-S P-values using Monte-Carlo

	SAL1633												
SAL1636	0.873	SAL1636											
SAL1639	0.304	0.215	SAL1639										
SAL1641	0.207	0.063	0.525	SAL1641									
SAL282	0.006	0.007	0.076	0.002	SAL282								
BN	0.089	0.272	0.003	0.000	0.001	BN							
BR	0.347	0.412	0.014	0.001	0.002	0.380	BR						
CJ	0.000	0.000	0.041	0.001	0.002	0.000	0.000	CJ					
HB	0.000	0.000	0.003	0.000	0.002	0.000	0.000	0.061	HB				
LW	0.026	0.080	0.001	0.000	0.0003	0.087	0.173	0.000	0.000	LW			
LW2-A	0.008	0.058	0.002	0.000	0.0005	0.004	0.003	0.000	0.000	0.232	LW2-A		
LW2-B	0.037	0.082	0.001	0.000	0.0004	0.030	0.135	0.000	0.000	0.569	0.189	LW2-B	
LW2-C	0.113	0.285	0.006	0.000	0.0015	0.346	0.444	0.000	0.000	0.625	0.249	0.258	LW-C
All-Lwolf	0.013	0.062	0.000	0.000	0.000	0.006	0.017	0.000	0.000	0.861	0.313	0.678	0.482

Two std devs. of P-values using Monte-Carlo

n													
48	SAL1633												
42	0.268	SAL1636											
40	0.204	0.218	SAL1639										
94	0.236	0.083	0.058	SAL1641									
23	0.000	0.001	0.024	0.000	SAL282								
90	0.142	0.321	0.008	0.000	0.001	BN							
95	0.284	0.261	0.018	0.003	0.001	0.238	BR						
77	0.000	0.000	0.069	0.003	0.000	0.000	0.000	CJ					
84	0.000	0.000	0.007	0.000	0.000	0.000	0.000	0.141	HB				
90	0.048	0.120	0.002	0.000	0.001	0.063	0.117	0.000	0.000	LW			
68	0.006	0.036	0.003	0.000	0.000	0.003	0.002	0.000	0.000	0.105	LW2-A		
87	0.055	0.091	0.002	0.000	0.001	0.033	0.132	0.000	0.000	0.396	0.072	LW2-B	
56	0.155	0.335	0.012	0.001	0.002	0.186	0.207	0.000	0.000	0.496	0.131	0.263	LW-C
301	0.022	0.092	0.001	0.000	0.000	0.006	0.012	0.000	0.000	0.222	0.116	0.381	0.391

Table 8. K-S test of detrital zircon U/Pb ages for Byrd Glacier and Ross Sea samples from 440 - 655 Ma. Analysis run on: Friday, May 4, 2007 @ 12:03:30 PM. Versio

K-S P-values using error in the CDF

	SAL1633											
SAL1636	1.000	SAL1636										
SAL1639	1.000	1.000	SAL1639									
SAL1641	0.210	0.076	0.221	SAL1641								
BN	0.055	0.213	0.185	0.000	BN							
BR	0.969	1.000	1.000	0.015	0.177	BR						
CJ	0.425	0.070	0.249	0.845	0.000	0.015	CJ					
HB	0.060	0.006	0.014	0.047	0.000	0.000	0.199	HB				
LW	0.018	0.075	0.080	0.000	1.000	0.069	0.000	0.000	LW			
LW2-A	0.397	0.863	0.724	0.002	0.962	0.861	0.001	0.000	0.706	LW2-A		
LW2-B	0.133	0.462	0.319	0.000	1.000	0.354	0.000	0.000	0.965	1.000	LW2-B	
LW2-C	0.127	0.343	0.359	0.000	1.000	0.441	0.000	0.000	0.964	0.997	0.999	LW-C

D-values using error in the CDF

n

	SAL1633											
SAL1636	0.098	SAL1636										
SAL1639	0.067	0.064	SAL1639									
SAL1641	0.263	0.307	0.264	SAL1641								
BN	0.336	0.258	0.277	0.508	BN							
BR	0.127	0.081	0.066	0.315	0.225	BR						
CJ	0.213	0.305	0.252	0.112	0.529	0.305	CJ					
HB	0.316	0.393	0.382	0.243	0.647	0.441	0.183	HB				
LW	0.399	0.323	0.334	0.544	0.066	0.280	0.584	0.713	LW			
LW2-A	0.255	0.167	0.199	0.437	0.119	0.147	0.450	0.560	0.173	LW2-A		
LW2-B	0.312	0.223	0.260	0.512	0.061	0.210	0.510	0.616	0.114	0.083	LW2-B	
LW2-C	0.325	0.254	0.260	0.489	0.065	0.205	0.509	0.641	0.120	0.106	0.093	LW-C

K-S P-values for no error

	SAL1633											
SAL1636	0.654	SAL1636										
SAL1639	0.772	0.891	SAL1639									
SAL1641	0.015	0.019	0.024	SAL1641								
BN	0.001	0.032	0.029	0.000	BN							
BR	0.456	0.758	0.717	0.001	0.017	BR						
CJ	0.103	0.008	0.111	0.210	0.000	0.002	CJ					
HB	0.019	0.001	0.002	0.000	0.000	0.000	0.007	HB				
LW	0.001	0.006	0.016	0.000	0.752	0.008	0.000	0.000	LW			
LW2-A	0.020	0.368	0.205	0.000	0.646	0.261	0.000	0.000	0.117	LW2-A		
LW2-B	0.007	0.203	0.040	0.000	0.574	0.077	0.000	0.000	0.345	0.794	LW2-B	
LW2-C	0.008	0.025	0.032	0.000	0.465	0.158	0.000	0.000	0.104	0.198	0.538	LW-C

D-values for no error

n

	SAL1633											
SAL1636	0.212	SAL1636										
SAL1639	0.198	0.169	SAL1639									
SAL1641	0.387	0.367	0.373	SAL1641								
BN	0.498	0.350	0.371	0.587	BN							
BR	0.220	0.168	0.182	0.391	0.316	BR						
CJ	0.296	0.391	0.297	0.193	0.608	0.368	CJ					
HB	0.365	0.464	0.450	0.382	0.750	0.513	0.287	HB				
LW	0.509	0.433	0.409	0.589	0.140	0.360	0.626	0.792	LW			
LW2-A	0.430	0.255	0.306	0.497	0.175	0.247	0.544	0.682	0.294	LW2-A		
LW2-B	0.452	0.280	0.381	0.589	0.171	0.289	0.589	0.719	0.214	0.166	LW2-B	
LW2-C	0.462	0.400	0.403	0.556	0.195	0.267	0.600	0.759	0.290	0.285	0.200	LW-C

Average K-S P-values using Monte-Carlo

	SAL1633											
SAL1636	0.746	SAL1636										
SAL1639	0.783	0.843	SAL1639									
SAL1641	0.116	0.042	0.095	SAL1641								
BN	0.025	0.082	0.078	0.000	BN							
BR	0.558	0.787	0.757	0.008	0.081	BR						
CJ	0.143	0.033	0.075	0.471	0.000	0.004	CJ					
HB	0.027	0.002	0.008	0.015	0.000	0.000	0.094	HB				
LW	0.009	0.031	0.036	0.000	0.615	0.033	0.000	0.000	LW			
LW2-A	0.190	0.440	0.360	0.001	0.498	0.478	0.001	0.000	0.277	LW2-A		
LW2-B	0.058	0.174	0.135	0.000	0.664	0.157	0.000	0.000	0.450	0.645	LW2-B	
LW2-C	0.057	0.157	0.147	0.000	0.687	0.192	0.000	0.000	0.491	0.618	0.642	LW-C

Two std devs. of P-values using Monte-Carlo

n

	SAL1633											
SAL1636	0.461	SAL1636										
SAL1639	0.394	0.323	SAL1639									
SAL1641	0.244	0.086	0.183	SAL1641								
BN	0.072	0.159	0.170	0.000	BN							
BR	0.505	0.402	0.415	0.024	0.160	BR						
CJ	0.253	0.079	0.150	0.411	0.000	0.016	CJ					
HB	0.068	0.008	0.027	0.030	0.000	0.000	0.182	HB				
LW	0.030	0.079	0.095	0.000	0.516	0.084	0.000	0.000	LW			
LW2-A	0.353	0.490	0.454	0.004	0.547	0.500	0.003	0.000	0.441	LW2-A		
LW2-B	0.140	0.270	0.242	0.000	0.490	0.251	0.000	0.000	0.500	0.487	LW2-B	
LW2-C	0.137	0.275	0.260	0.000	0.507	0.295	0.000	0.000	0.554	0.541	0.496	LW-C

Table 9. Zircon U-Pb age groups.

Group #	Age (Ma)	BN (%)	BR	CJ	HB	LW	LW2-ALL	LW2-A	LW2-B	LW2-C	SAL1633	SAL1639	SAL1636	SAL1641	SAL282
1	488-523		3.2	10.4	3.6		1.5	1.5			8.3	22.5	9.5	39.4	
2	530-545	12.1	16.8	55.8	60.7						27.1				13.0
3	553-570		24.2			31.1	16.6	22.1	23.0			30.0	26.2	11.7	
4	583-610	42.9	26.3			30.0	26.5	22.1	20.7	41.1	18.8	22.5	19.1	0.0	
5	687-730		4.2				1.4	4.4			8.3		0.0	6.4	
6	800-850	7.7	6.3				2.4		5.7						
7	885-1006	13.2	11.6			7.8	11.9	5.9	16.1	12.5	6.3		9.5	6.4	
8	1027-1080	6.6		6.5		11.1	10.0		16.1	12.5	12.5			8.5	13.0
9	1094-1149		6.3		7.1	14.4							7.1		
	1185-1194						1.9	5.9			6.3			3.2	
10	1232-1283		3.2				5.2		8.0	7.1					
	1333-1333	5.5													
11	1439-1493	5.5	3.2				6.2	11.8		8.9					
12	1580-1638					7.8	3.8		4.6	7.1				3.2	
	1821-1909					4.4	1.4	4.4					7.1		
	1941-2054						3.3	5.9	3.4						
	2234-2238	4.4					1.4	4.4							
	2449-2552	3.3					1.4	4.4							
13	2678-2737	1.1	1.1			5.6	5.7	7.4	4.6	5.4	2.1	5.0	4.8	1.1	
	2981-2981						1.4	4.4							

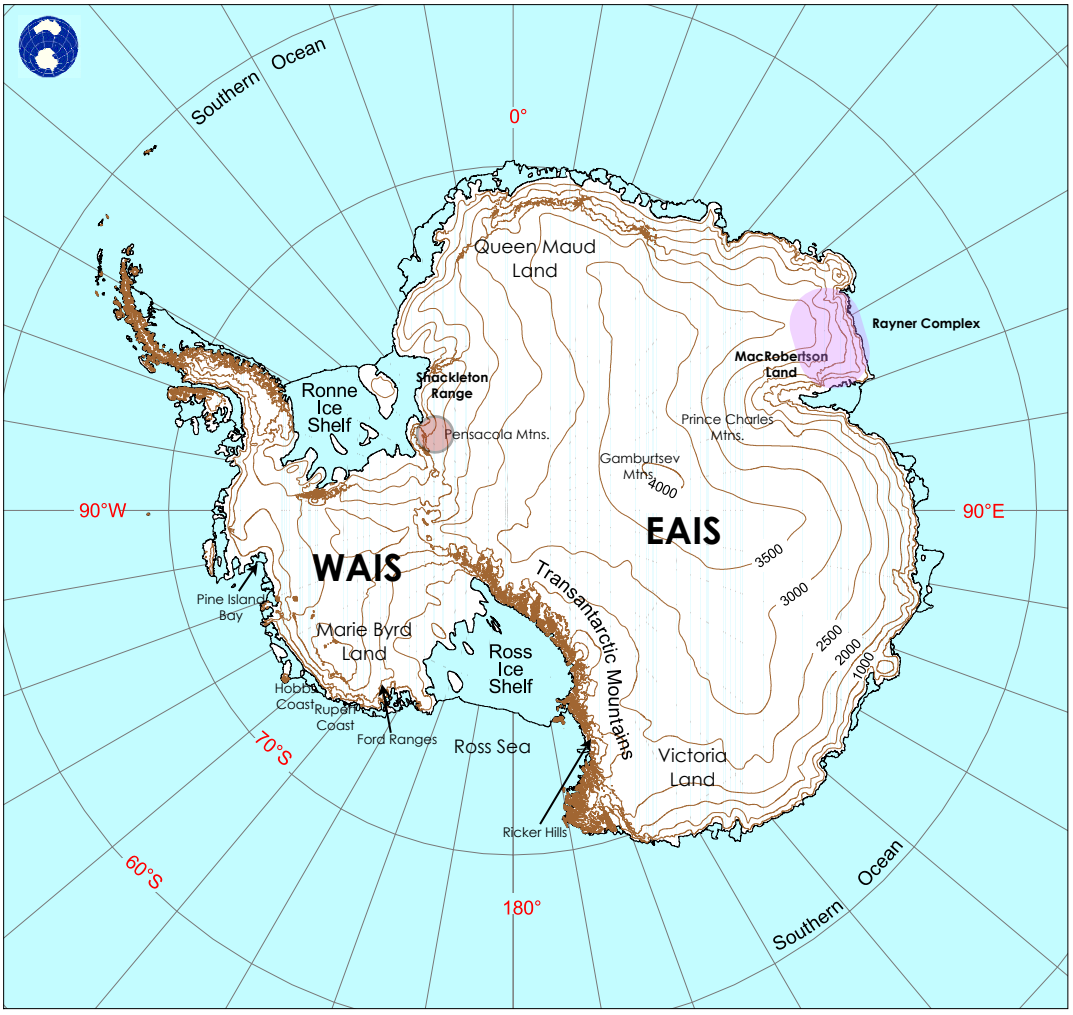

Projection: Polar Stereographic
True Scale at 71°S

Figure 1: Map of Antarctica showing the East and West Antarctic ice sheets and the Transantarctic Mountains. Contour interval is 500 m. EAIS = East Antarctic Ice Sheet; WAIS = West Antarctic Ice Sheet. (Australian Antarctic Data Centre, 2000)

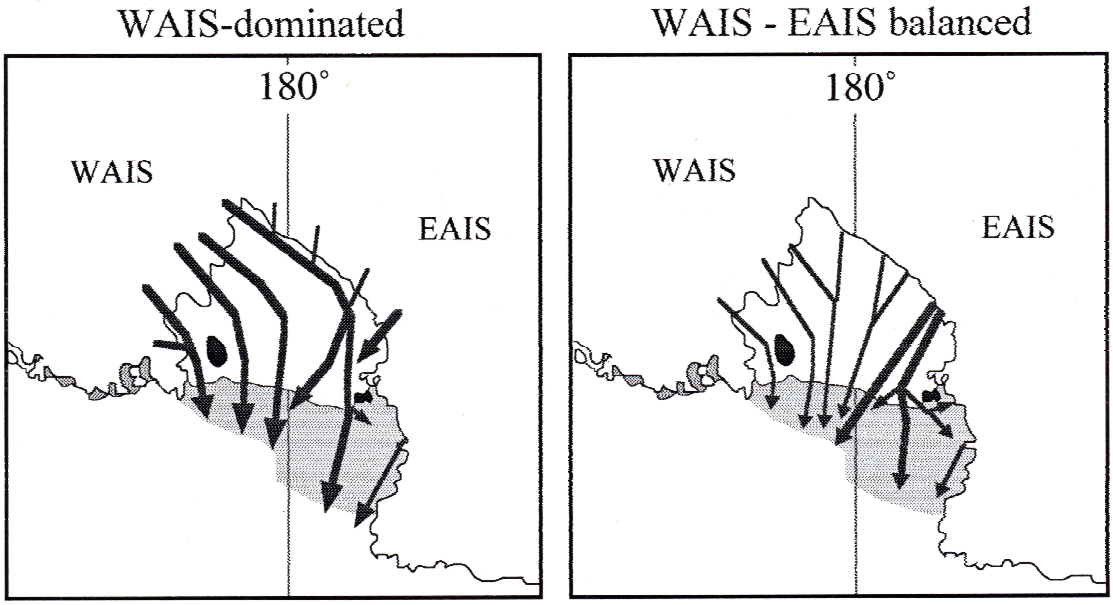

Figure 2: Paleo ice-flow models of Stuiver et al. (1981) and Licht and Fastook (1998). Wide lines indicate higher ice velocity. (From Licht et al. 2005)

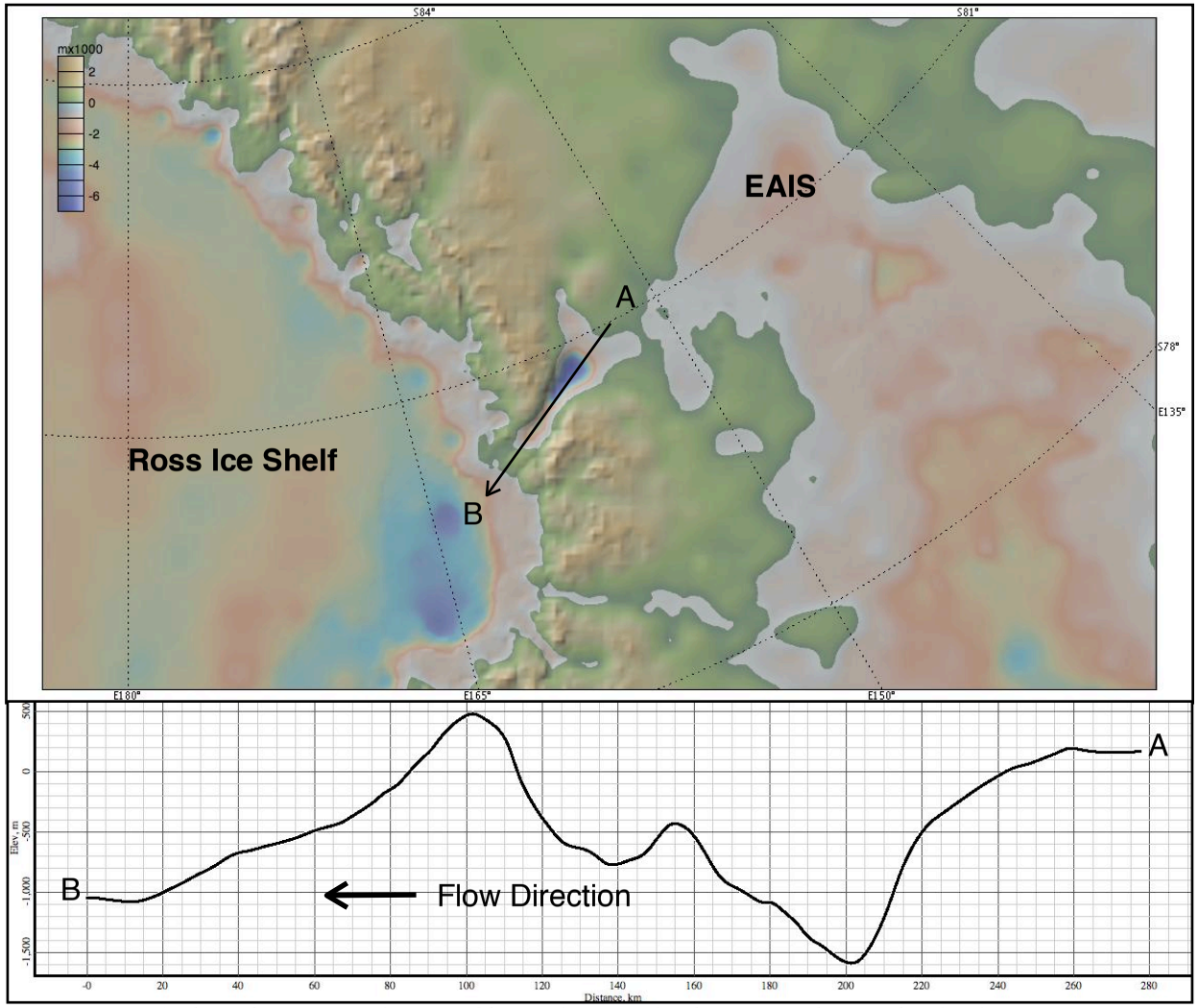

Figure 3: Subglacial topographic profile of the Byrd Glacier. Color scale shading is in1000 meter increments. (Geomapp app.)

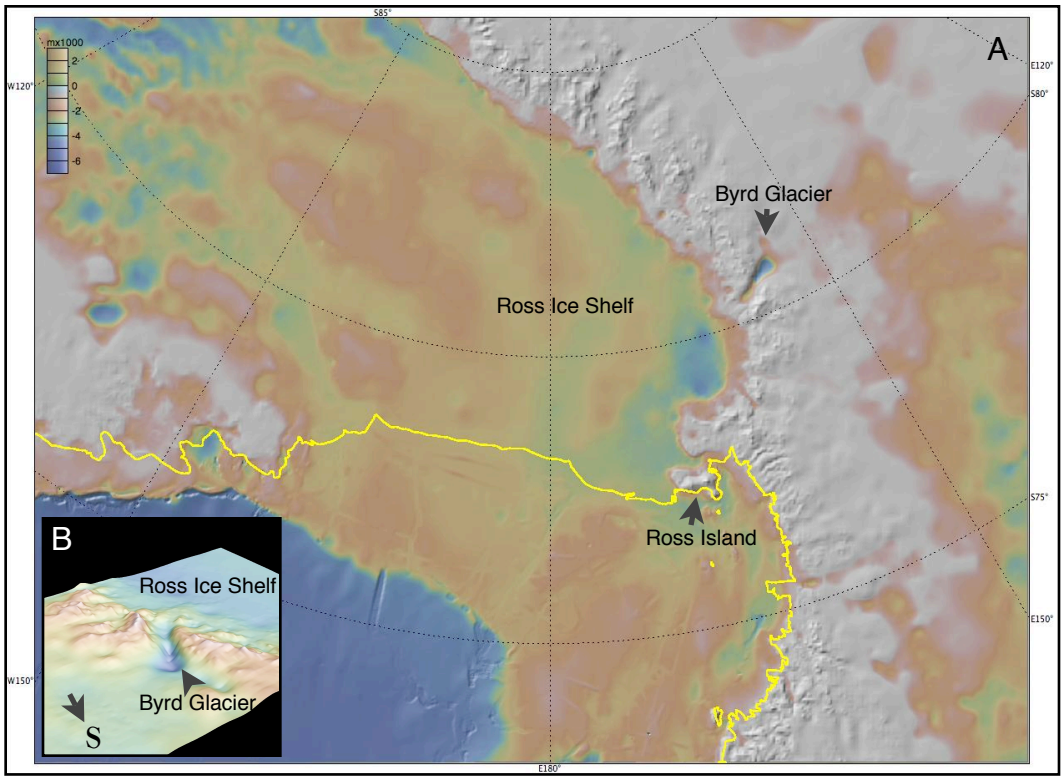

Figure 4: A = Map of Ross Sea Bathymetry. Color scale shading is in1000 meter increments. B = Three dimensional subglacial topographic map of Byrd Glacier. 4X vertical exaggeration. (Geomap app)

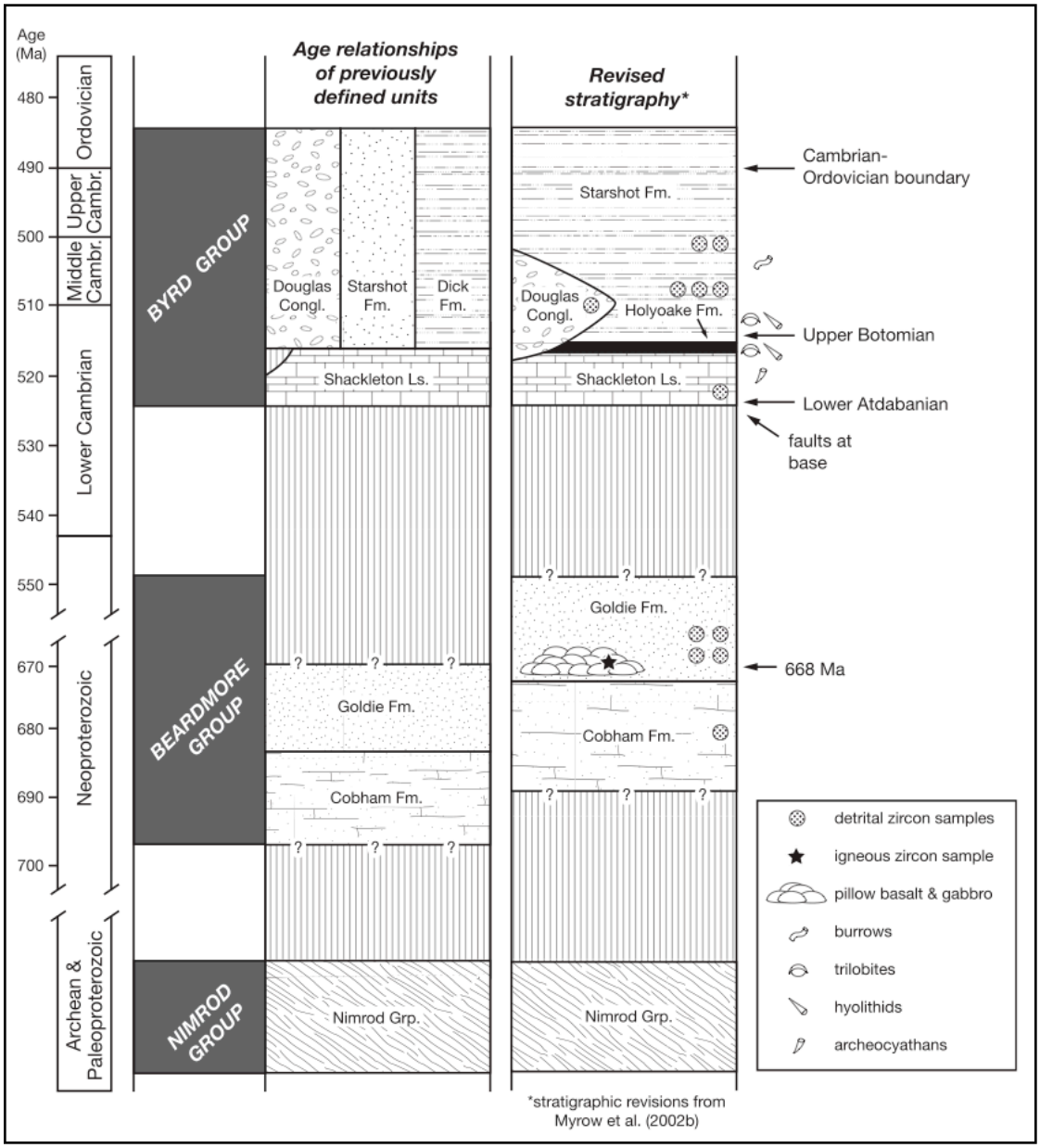

Figure 5: Stratigraphic column of Neoproterozoic and lower Paleozoic sedimentary units in the TAM. (from Goodge, 2004, and Myrow, 2002)

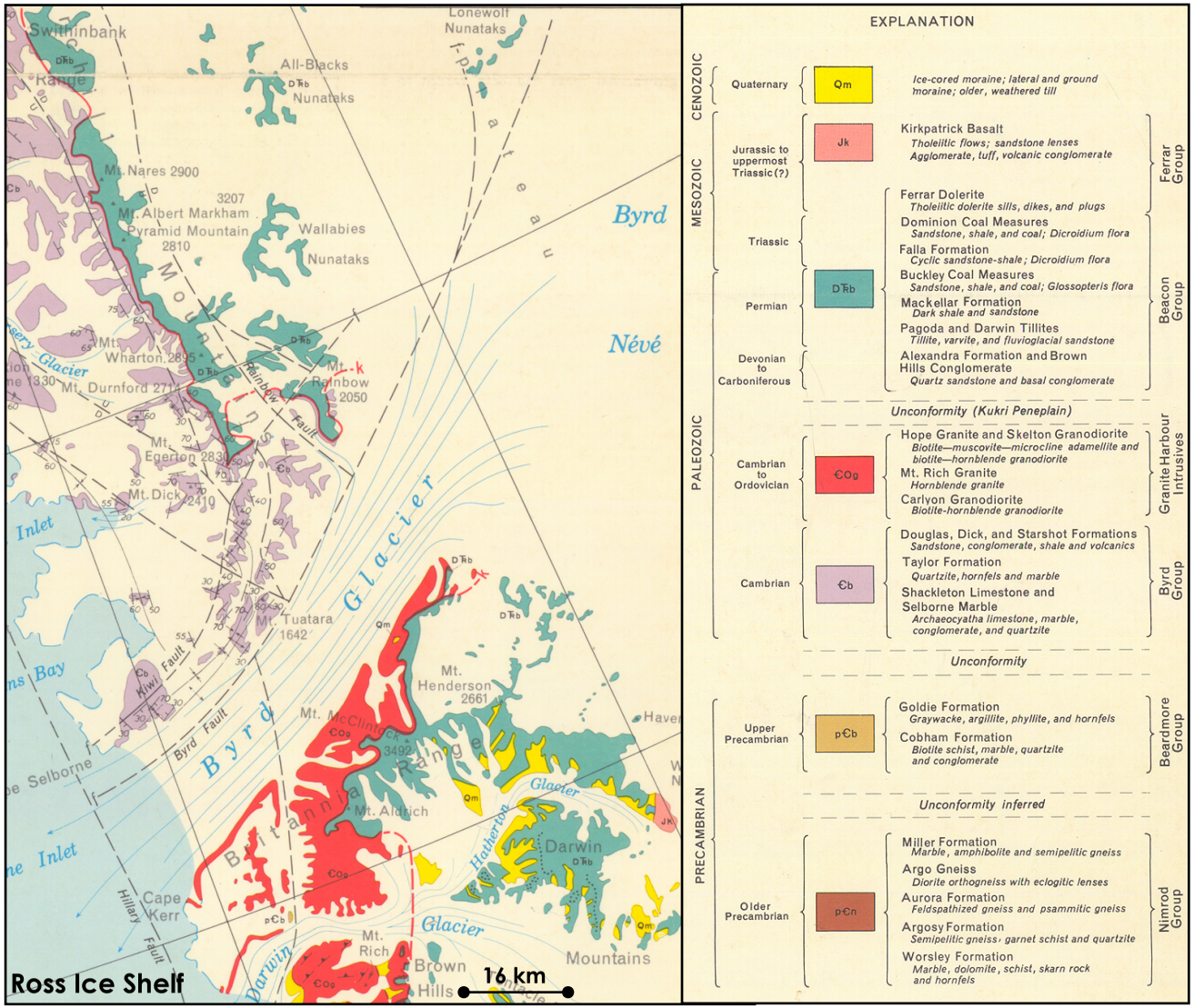

Figure 6: Geologic map of the Byrd Glacier area. (from Grindley and Laird, 1969)

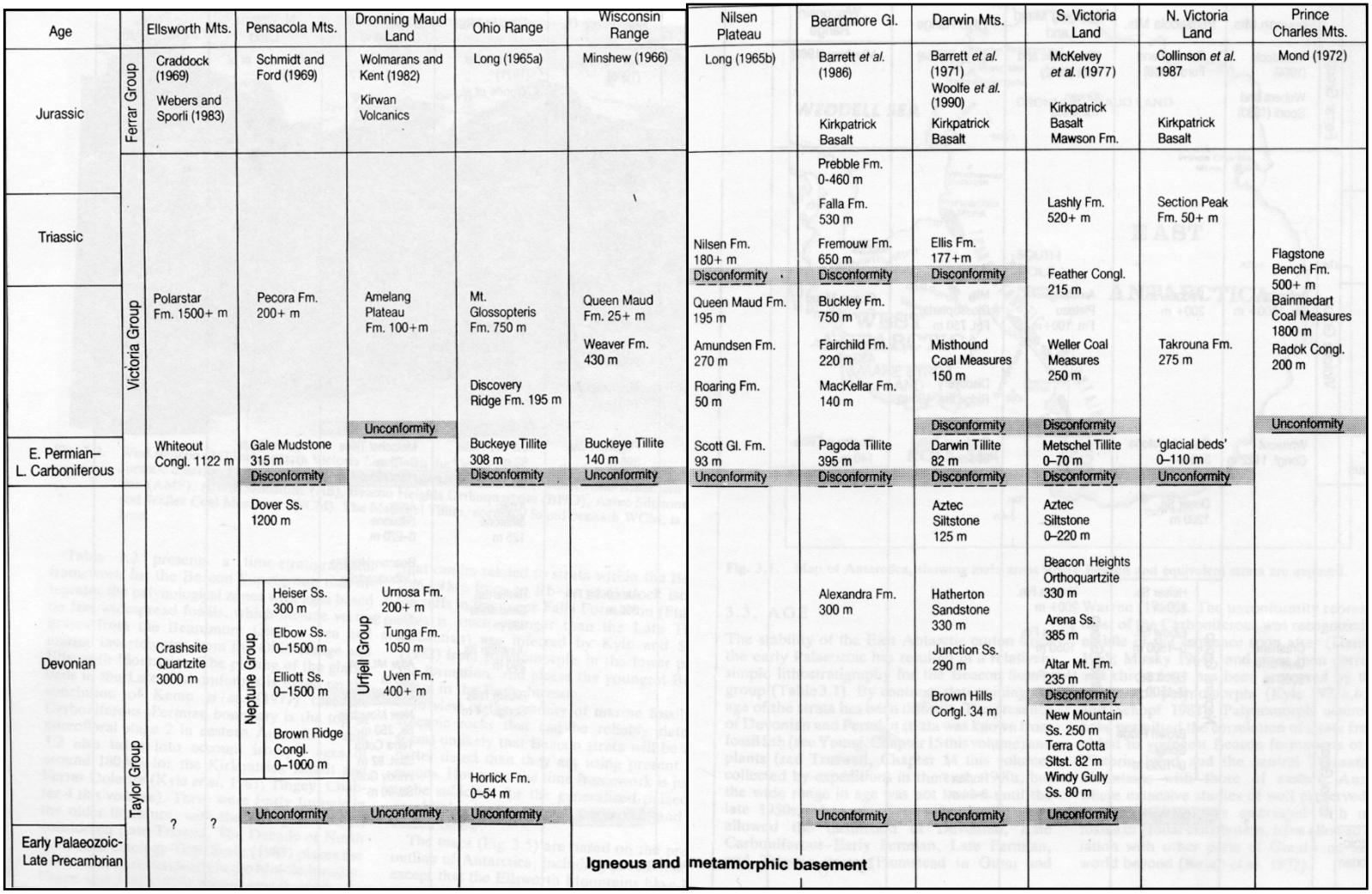

Figure 7: Formations of Beacon Supergroup and Ferrar Group including equivalent strata in the Ellsworth Mountains (from Barret, 1991)

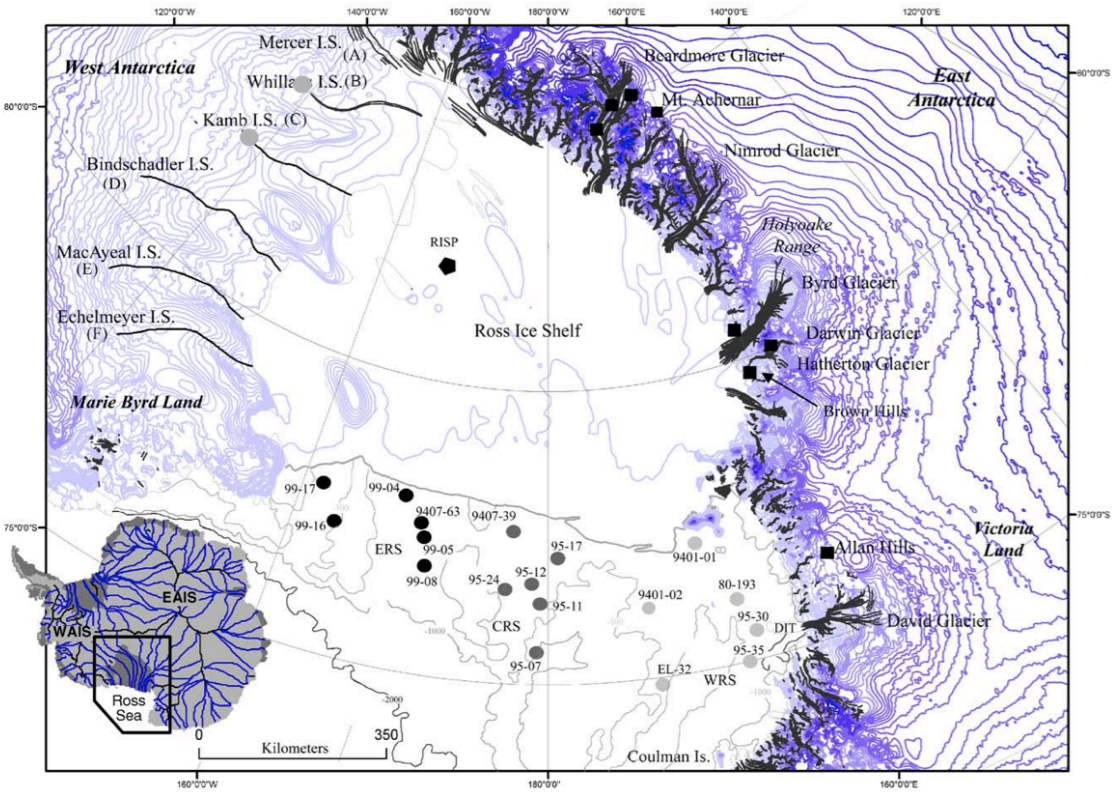

Figure 8: Map from Licht et al., (2005) showing Ross Sea sample site locations. Black squares show EA terrestrial till sample and grey dots show location of WA sub-ice stream samples.

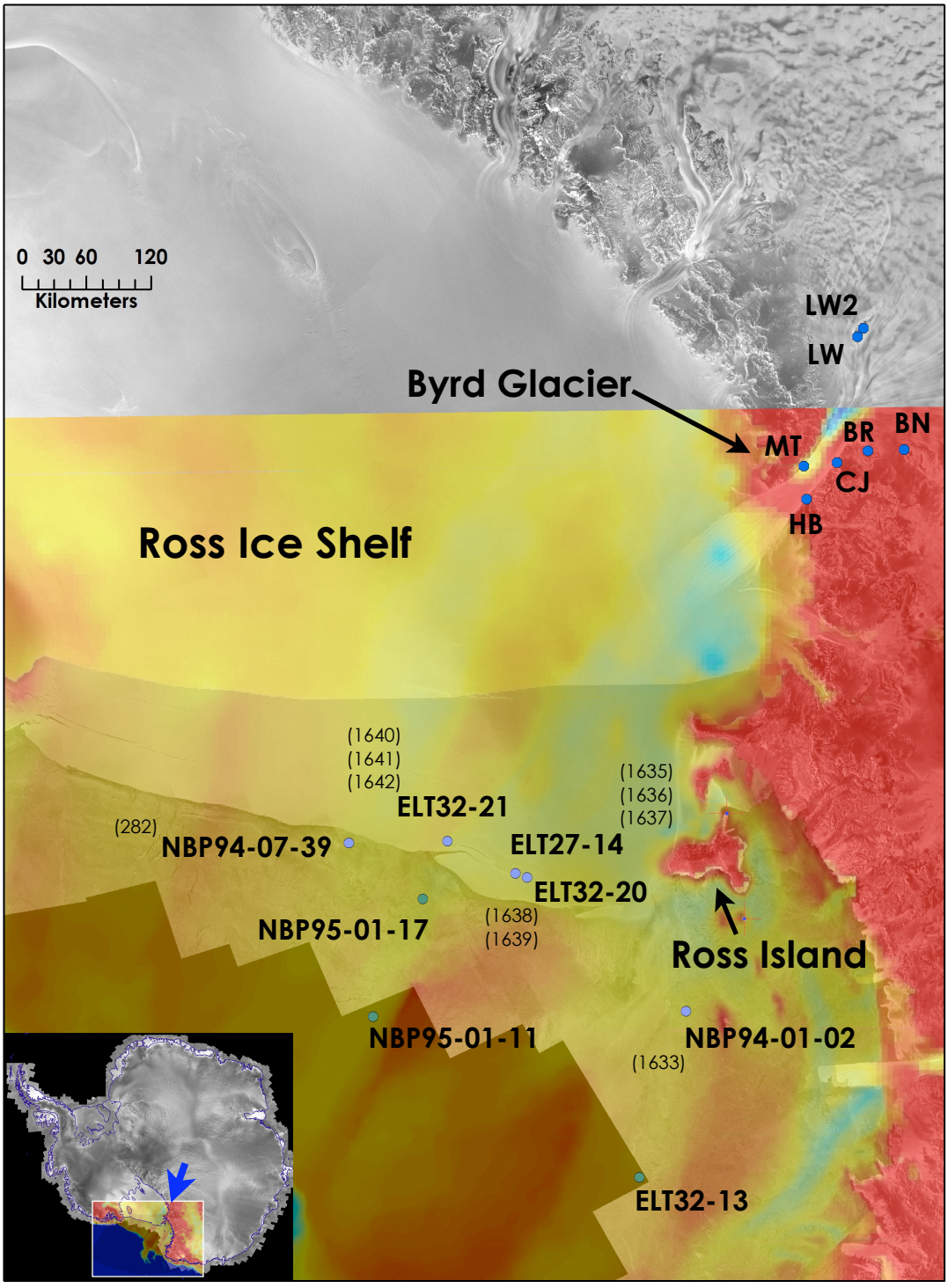

Figure 9: RadarSat image of Ross embayment overlain by Ross Sea bathymetry map (Davey, 2004). Sample sites along Byrd Glacier shown in blue and Ross Sea piston core are shown in purple.

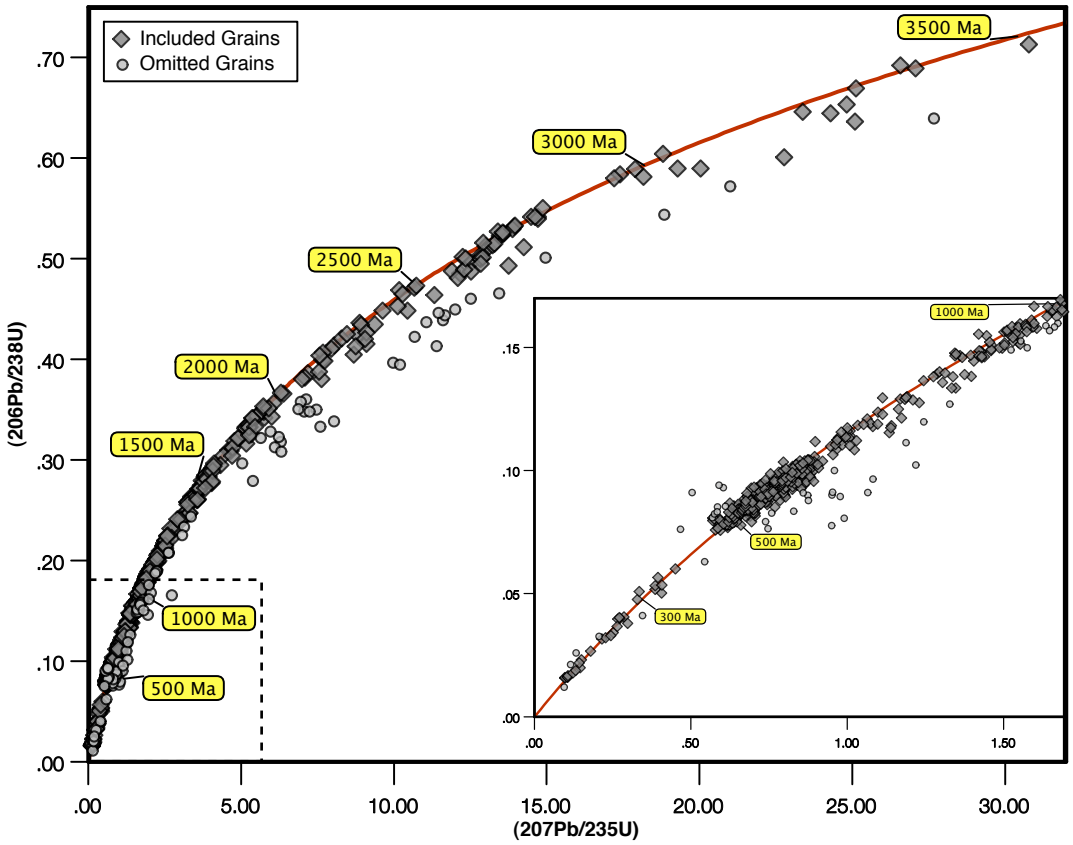

Figure 10: Concordia plot of all zircon grains from the Byrd Glacier and the Ross Sea. For analysis of the zircon age data, all discordant grains were removed from the original total data set. For all grains with $^{206}Pb/^{238}U$ ages < 1000 Ma, the difference between the $^{206}Pb/^{238}U$ apparent age vs. the $^{207}Pb/^{235}U$ apparent age (Appendix C) was used with a rejection threshold of ≥10%. For all grains with $^{206}Pb/^{207}Pb$ ages > 1000 Ma, the difference between the $^{206}Pb/^{238}U$ vs. the $^{206}Pb/^{207}Pb$ was used for rejection.

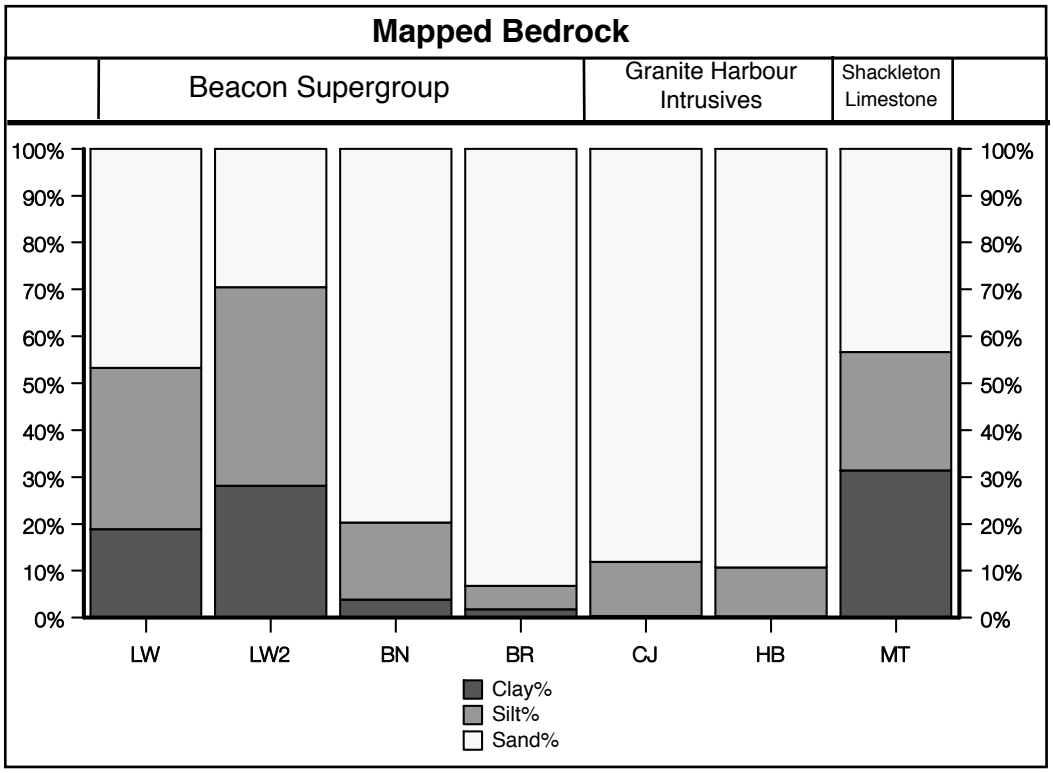

Figure 11: Average particle size distributions of samples from the margins of the Byrd Glacier with mapped bedrock types.

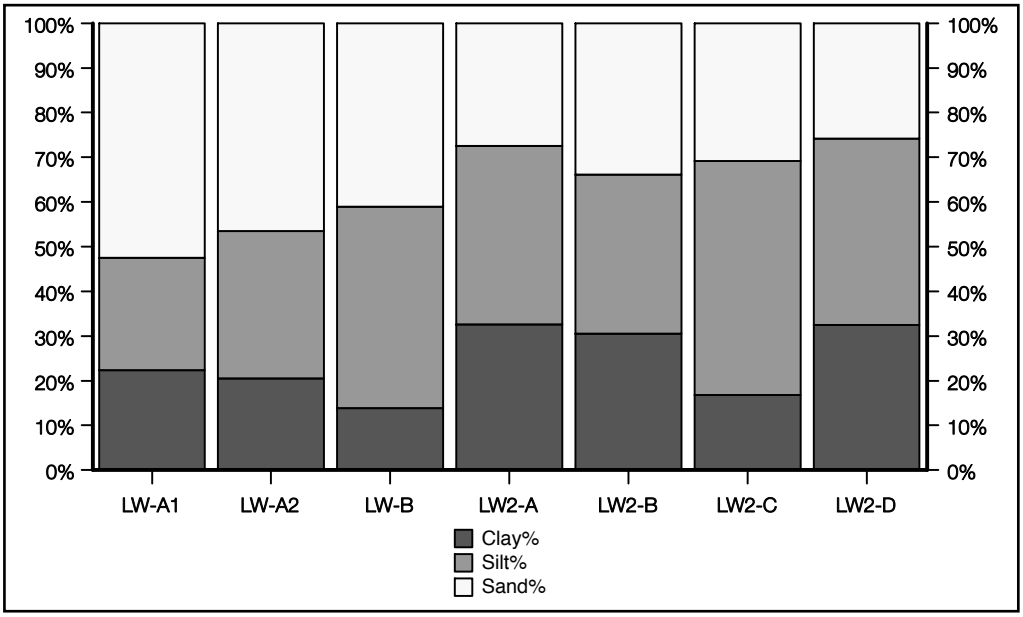

Figure 12: Particle size distributions of samples from the Lonewolf Nunataks (LW and LW2 sites).

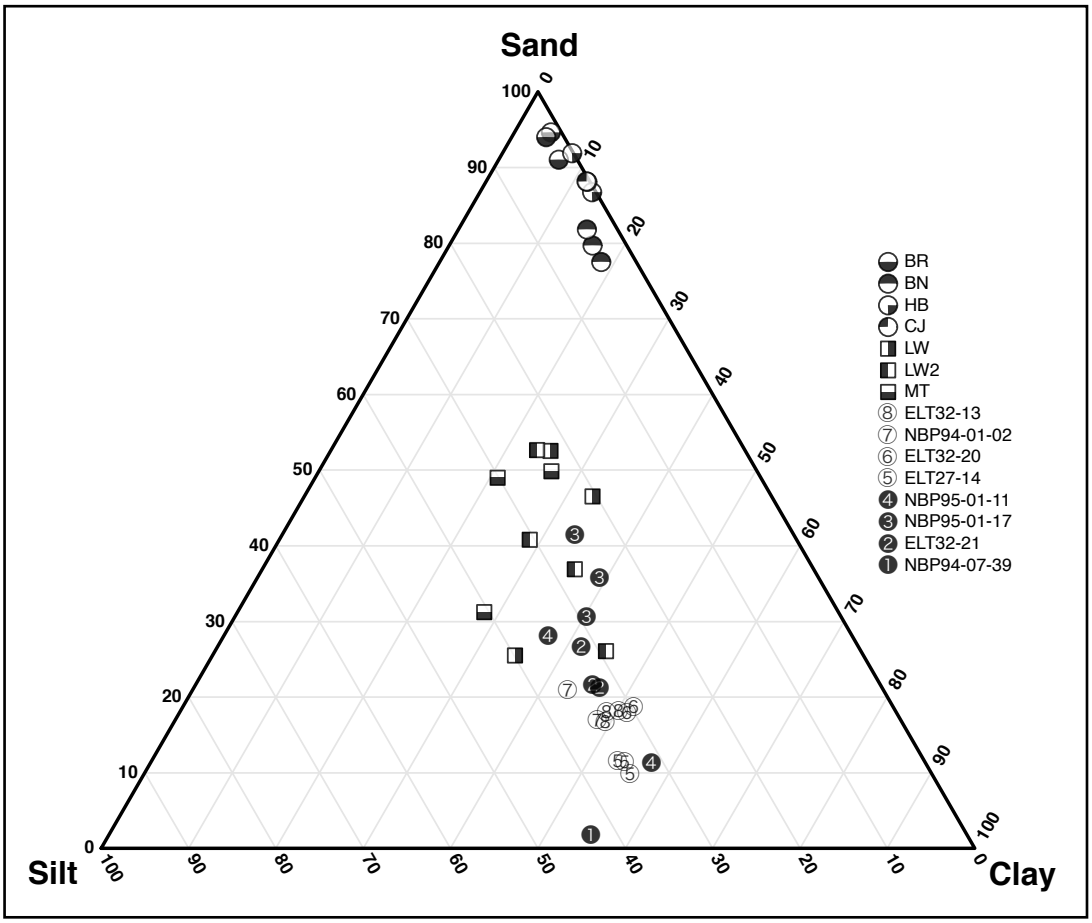

Figure 13: Ternary diagram of Sand, Silt and Clay percent for Byrd Glacier and Ross Sea samples. Data from Lederer, 2003 are included for samples from NBP94-07-39, ELT32-13, and NBP95-01-11 cores. The Byrd Glacier samples are represented by the non-numbered round symbols (northern margin) and squares (southern margin). The Ross Sea samples are represented by numbered circular symbols subdivided by white (western Ross Sea) and black (central Ross Sea). The numbers represent position within the Ross Sea with ELT32-13 (#8) being located furthest west and NBP-07-39 (#1) being located more in the central Ross Sea.

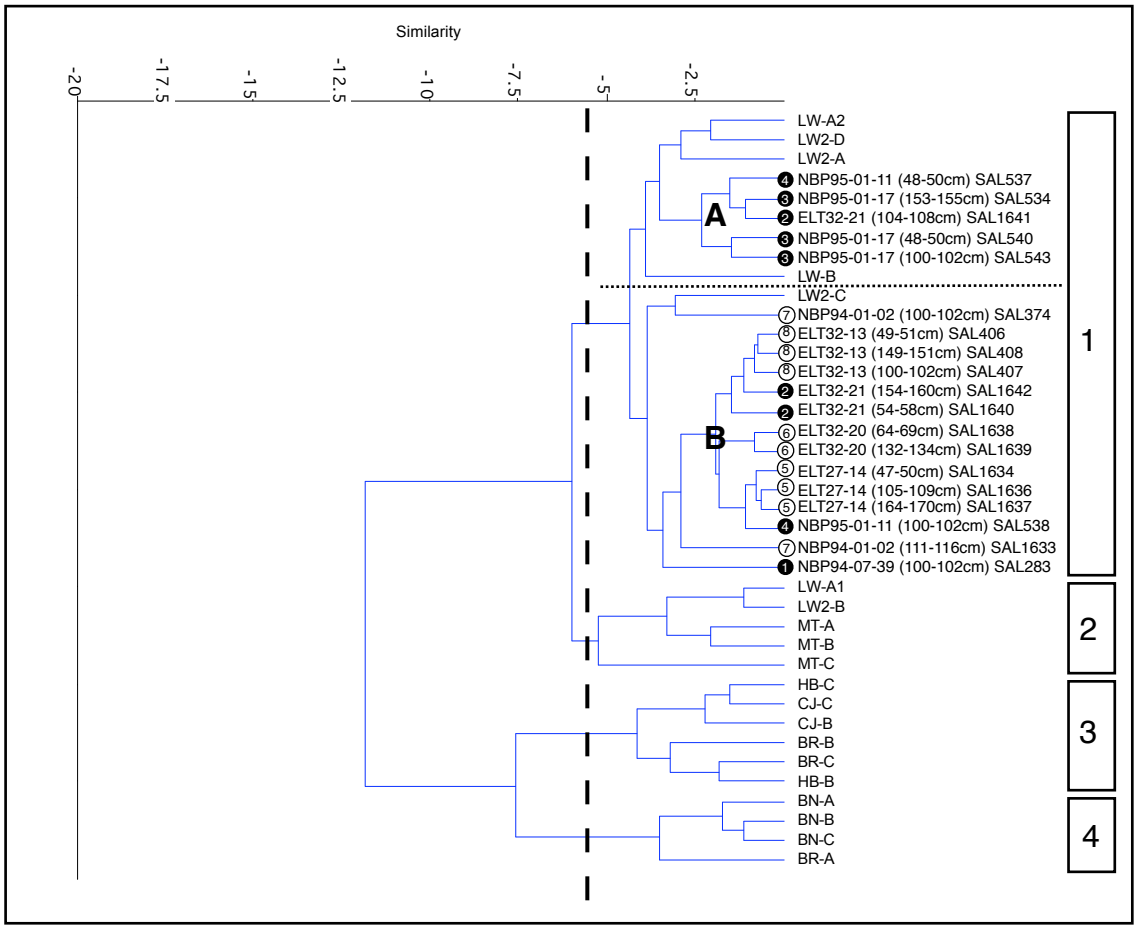

Figure 14: Results of cluster analysis on the particle size data of the Byrd Glacier and Ross Sea. Data from Lederer, 2003 are included for samples from cores NBP94-07-39, ELT32-13, NBP95-01-17, and NBP95-01-11.

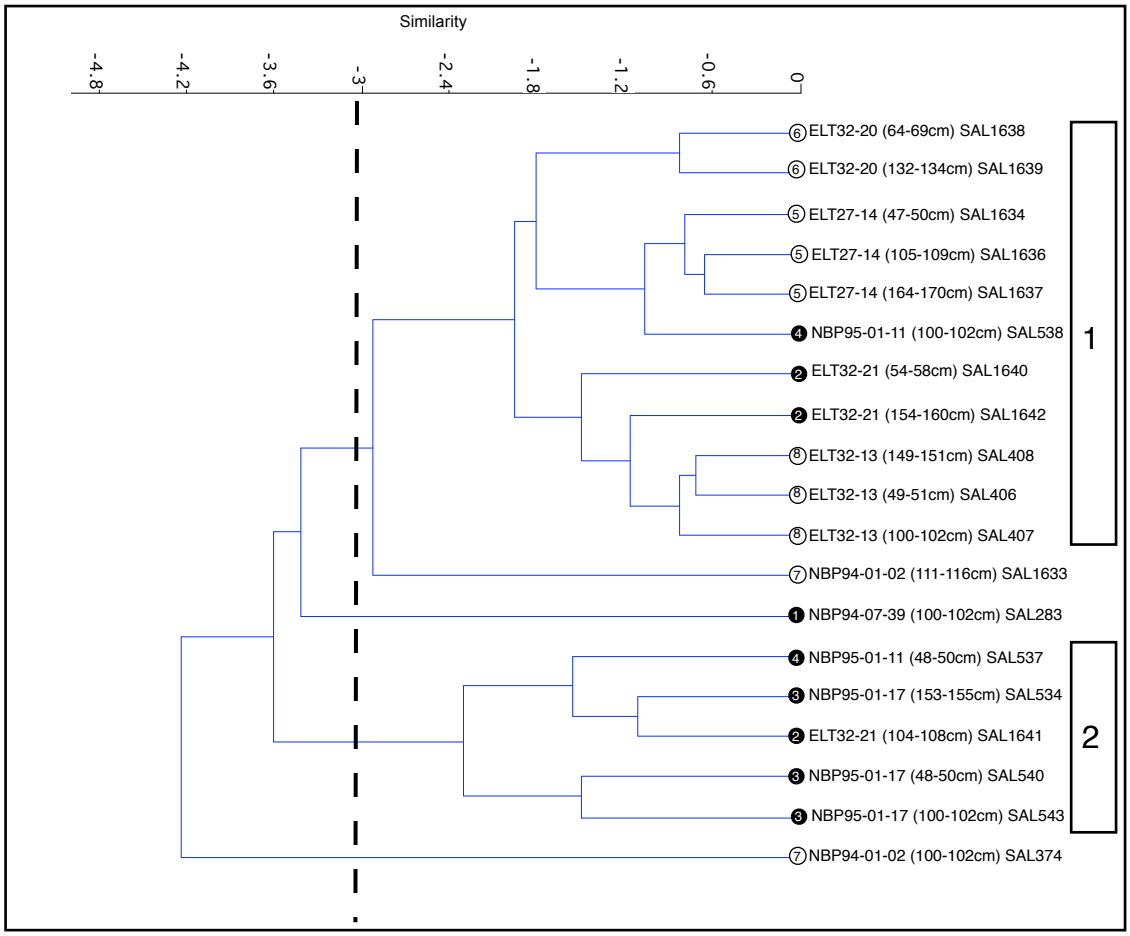

Figure 15: Results of cluster analysis on the particle size data from the Ross Sea. Data from Lederer, 2003 are included for samples from NBP94-07-39, ELT32-13, NBP95-01-17, and NBP95-01-11 cores.

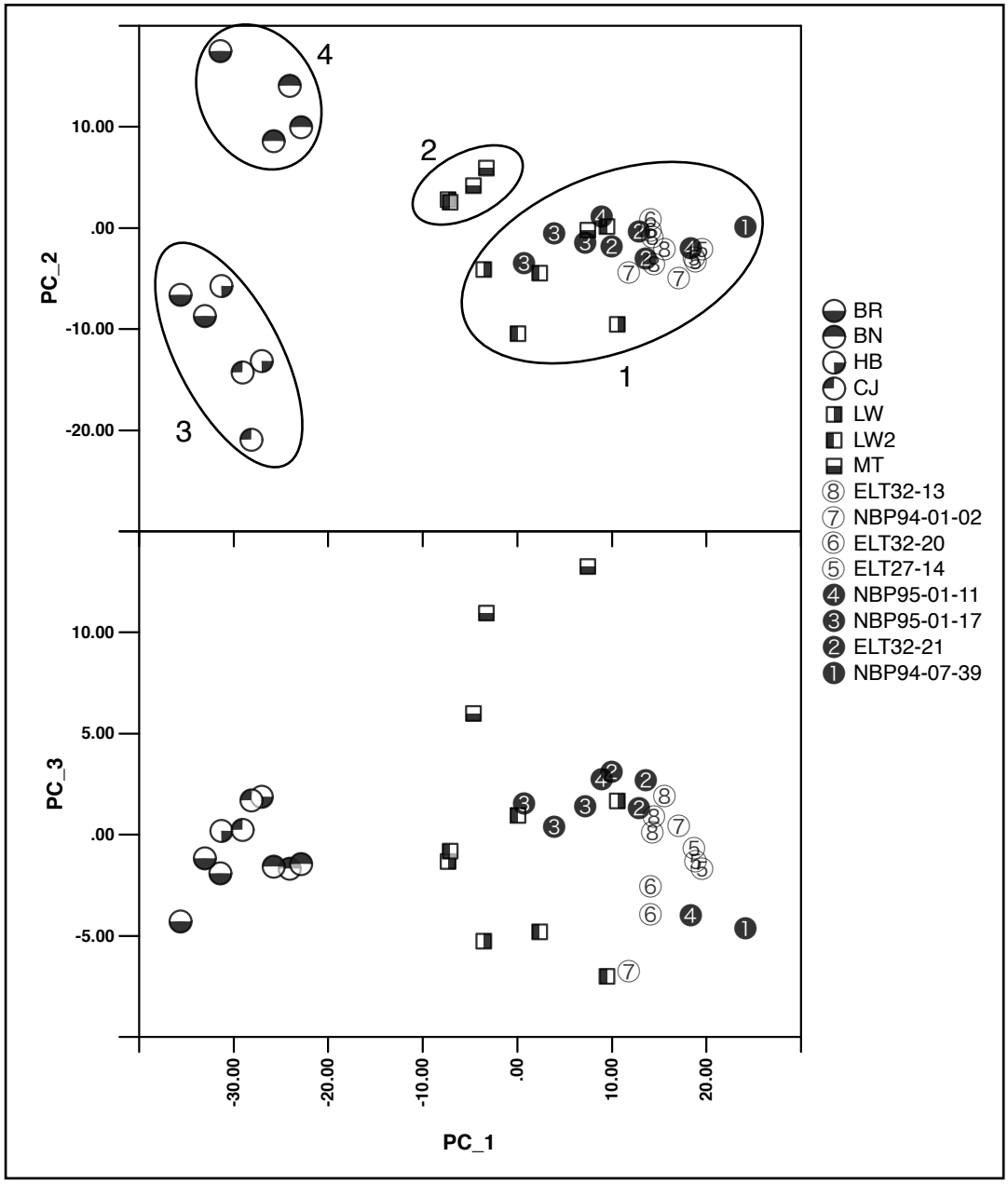

Figure 16: Results of principle component analysis on the particle size data from the Byrd Glacier and Ross Sea. Data from Lederer, 2003 are included for samples from NBP94-07-39, ELT32-13, NBP95-01-17, and NBP95-01-11 cores. Ellipses were placed in the graph to highlight the four groups and are not statistically significant.

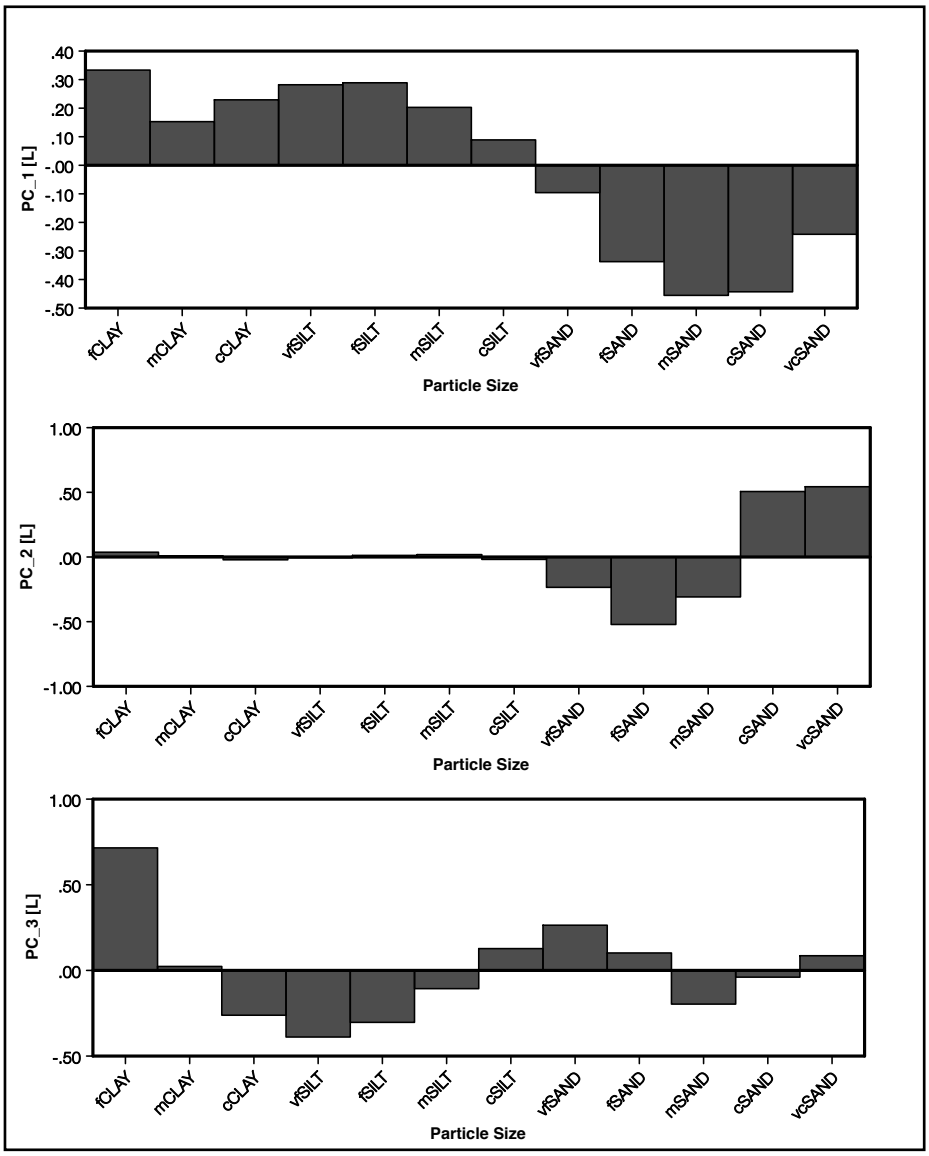

Figure 17: Loadings [L] of principle component analysis on the raw particle size data from the Byrd Glacier and Ross Sea. Data from Lederer, 2003 are included.

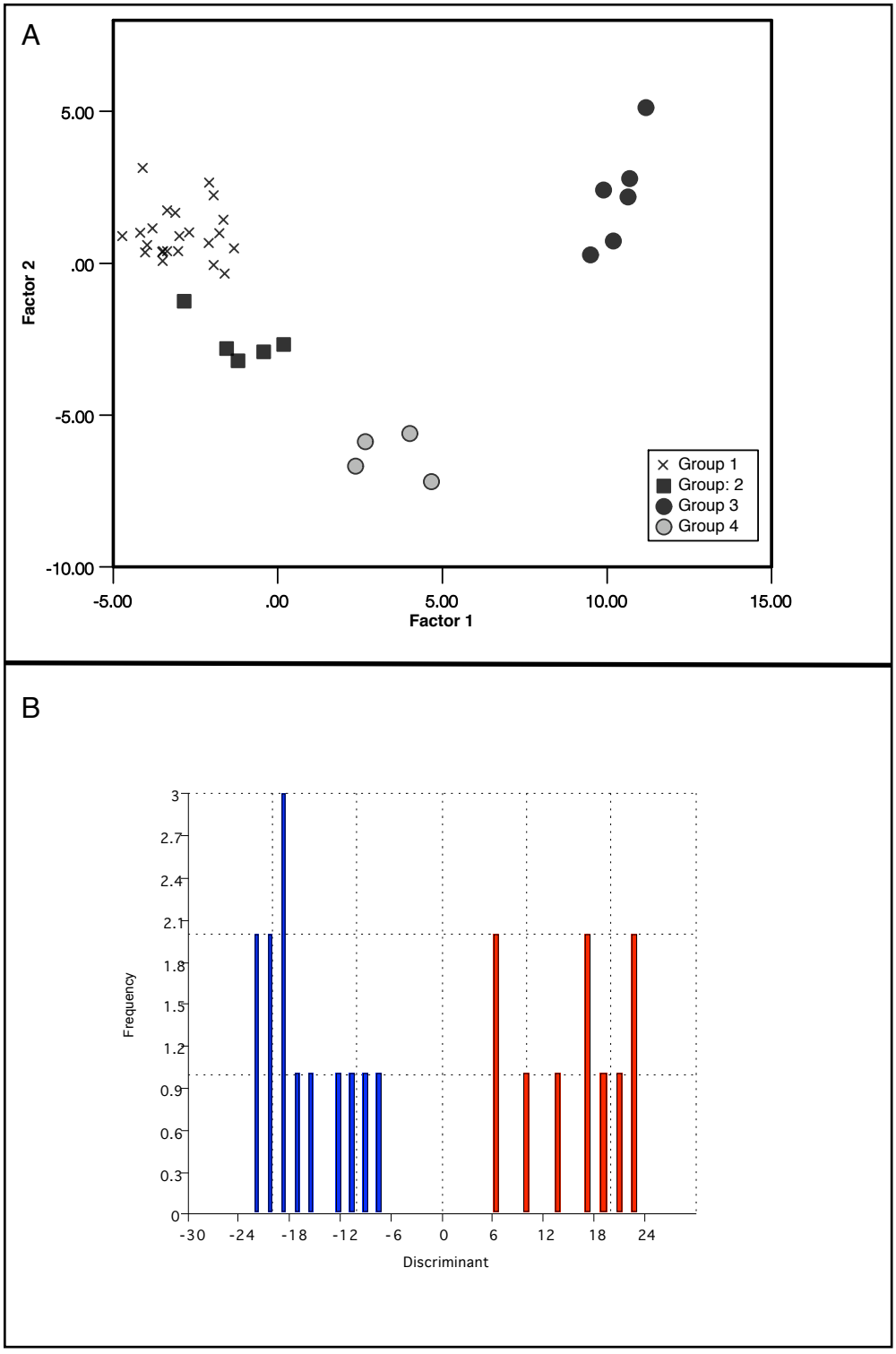

Figure 18: Graph A are the results of complete discriminant analysis (DA) for groups 1 through 4 of the cluster analysis (Figure 14). Graph B is the DA of subgroups A (blue) and B (red). 17a was performed using SYSTAT 8 and 17b was performed using PAST 1.7.

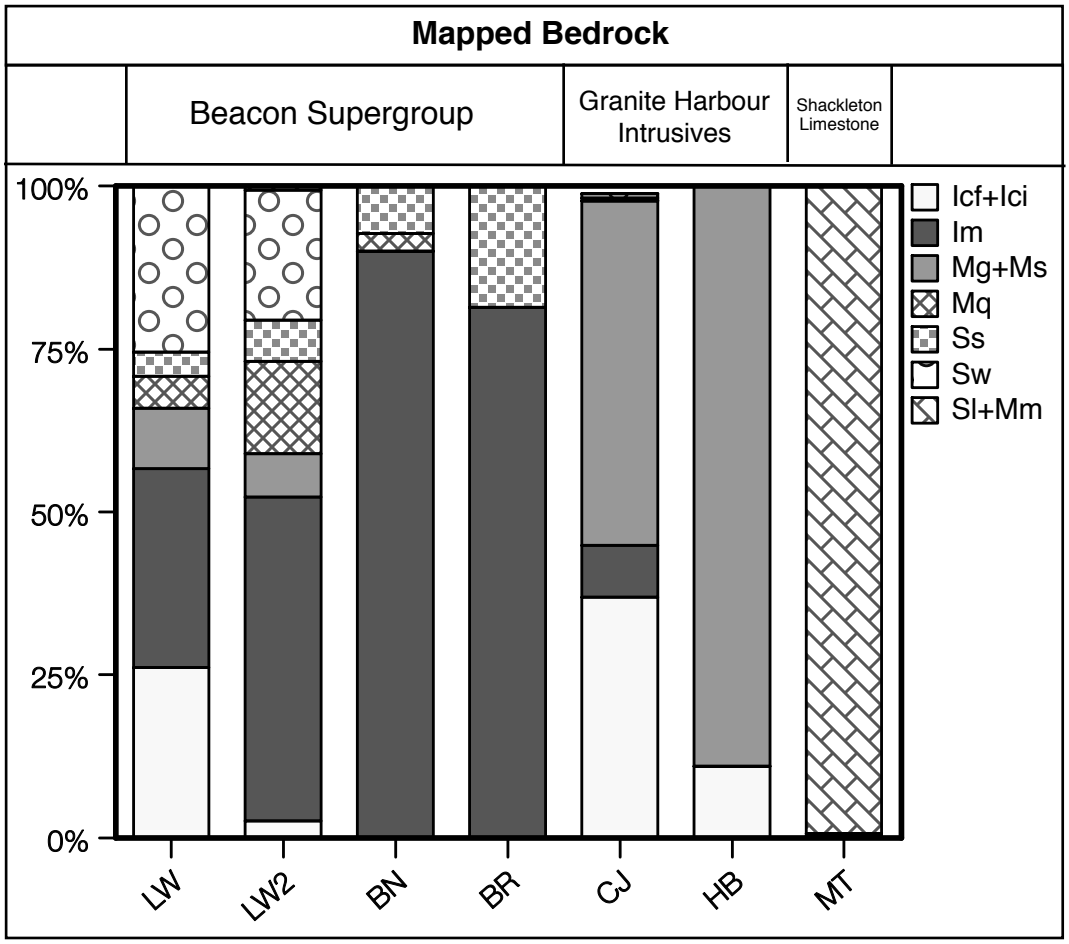

Figure 19: Average pebble count data from the Byrd Glacier. See Table 3 for pebble nomenclature.

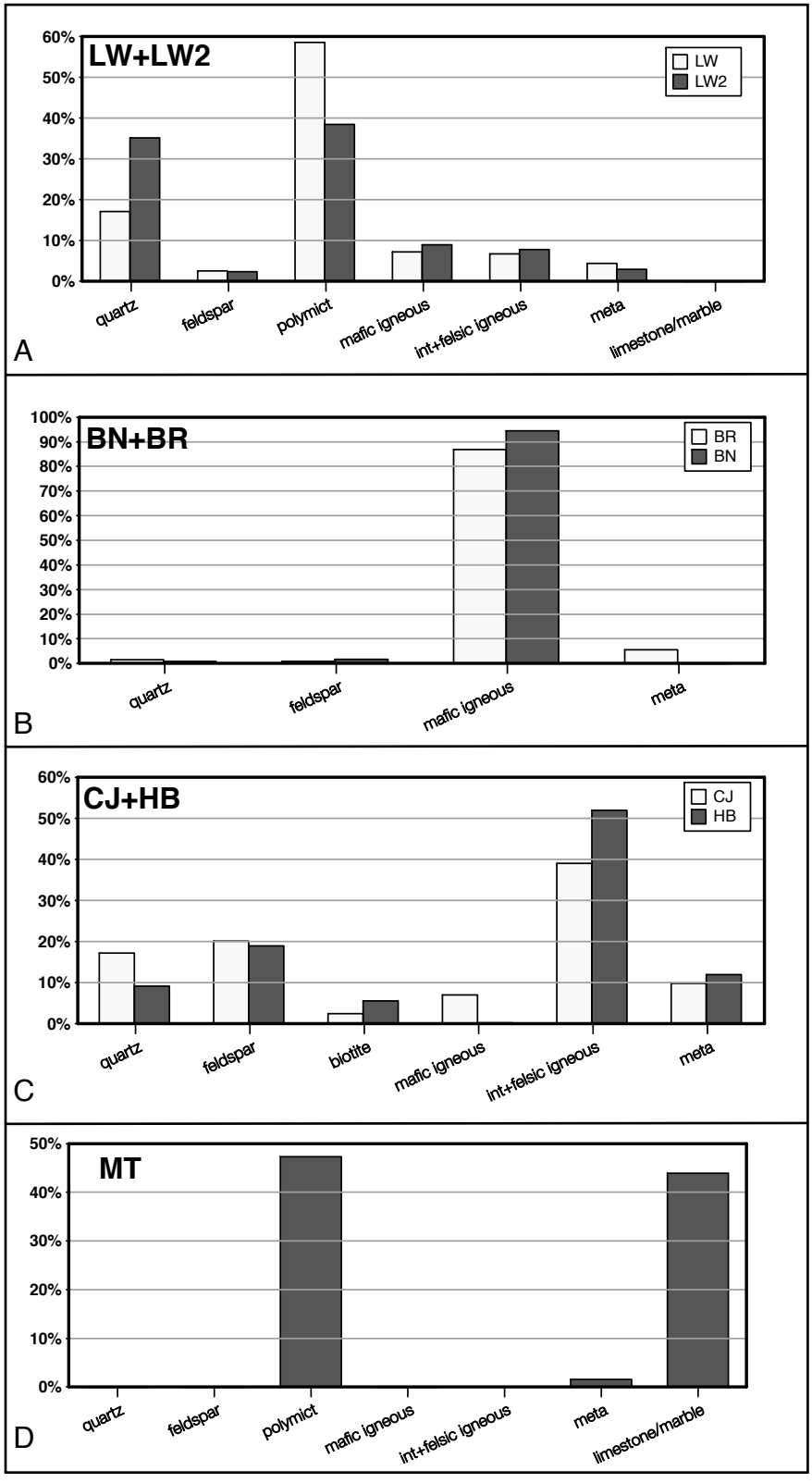

Figure 20: Average point count data from the Byrd Glacier.

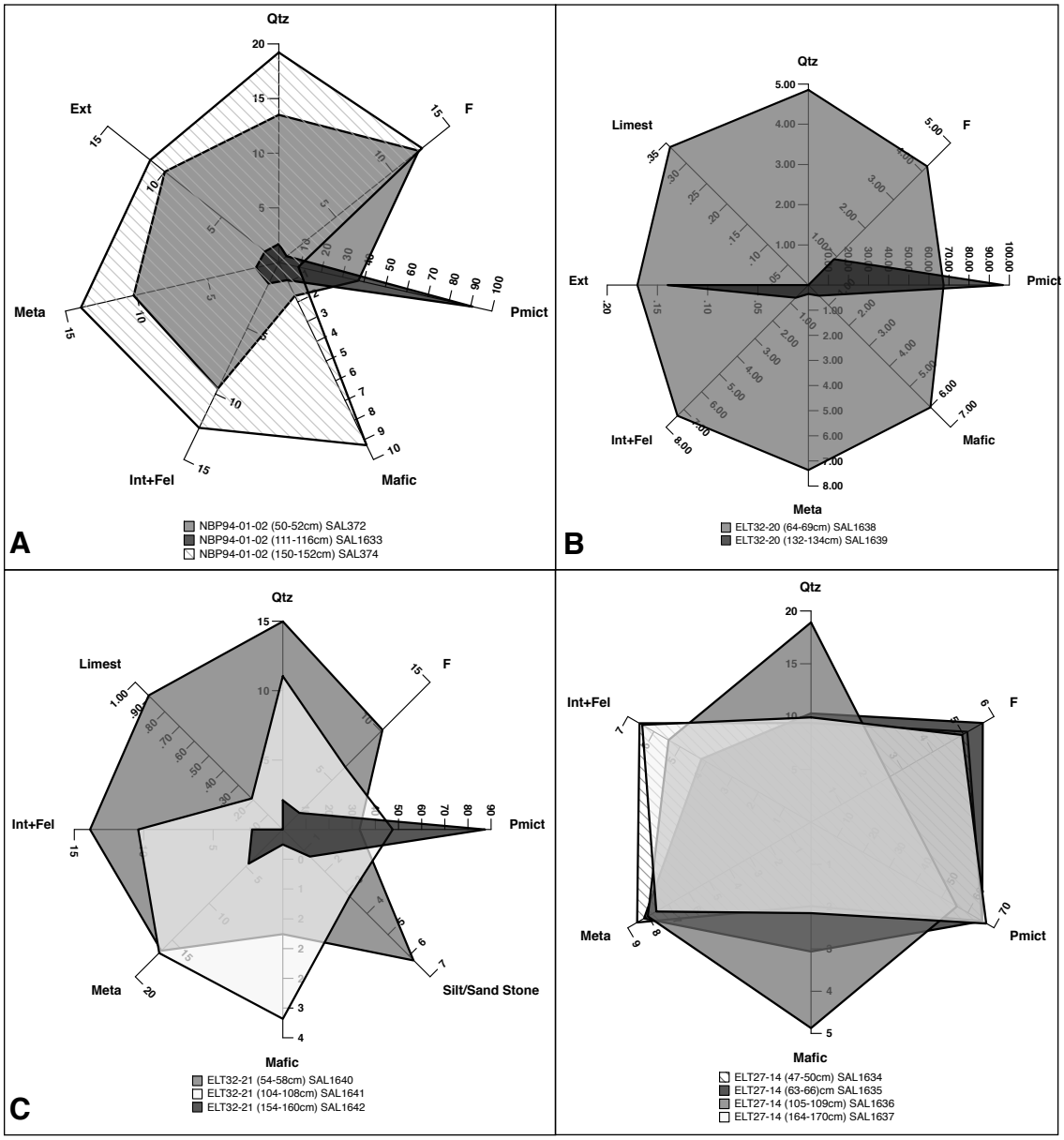

Figure 21. Spider diagrams of the sand composition of three Ross Sea piston cores. A. NBP94-01-02; B. ELT32-20; C. ELT32-21. These three piston cores show a transition in the petrography of the sand sized fraction. At intervals in three of the cores, the sand content changes from a relatively diverse mixture of mineral and lithic fragments to dominantly polymict fragments. All petrographic categories ≥5% are included with the exception of limestone and extrusive igneous fragments, which in some samples were < 5%. These were included due to provenance implications. (refer to Table 5 for abbreviations)

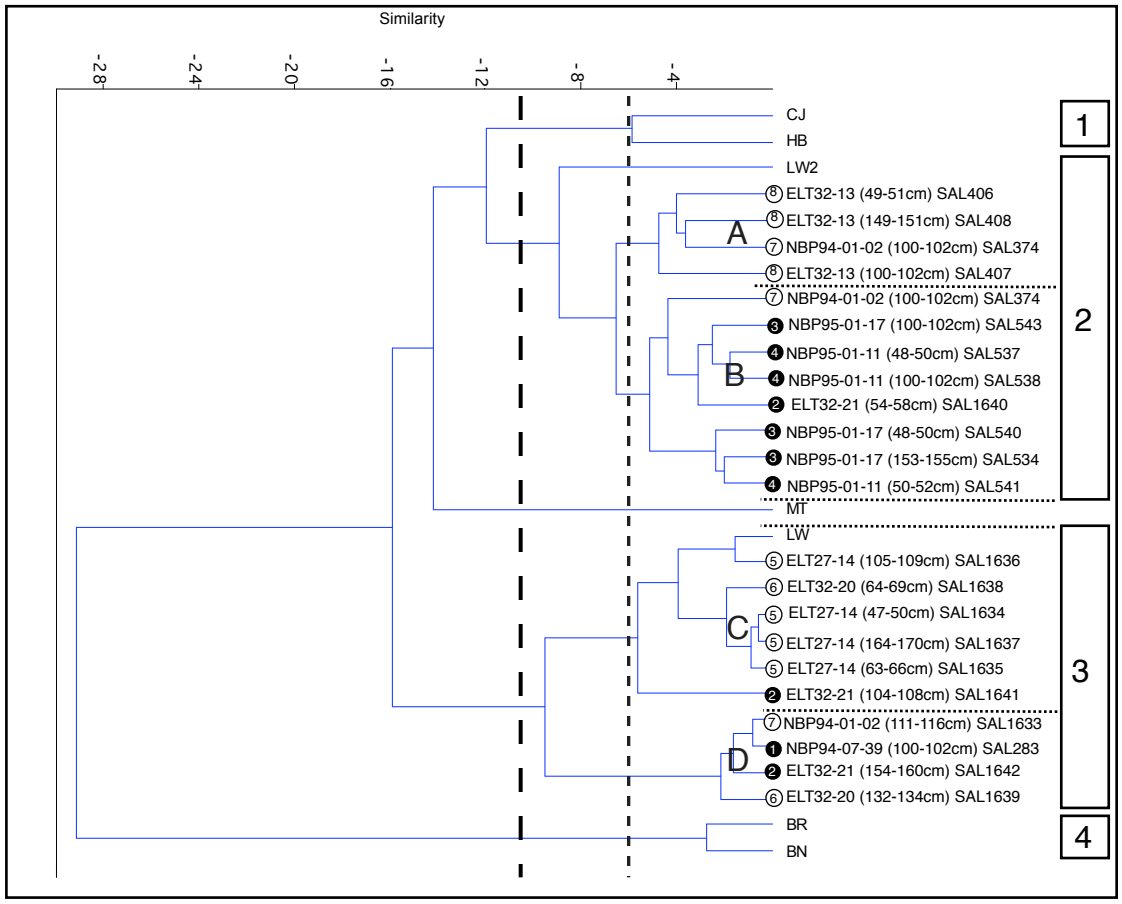

Figure 22: Results of cluster analysis on average(%) point count data of the Byrd Glacier and Ross Sea. Data from Lederer, 2003 are included for samples from cores NBP94-07-39, ELT32-13, NBP95-01-17, and NBP95-01-11.

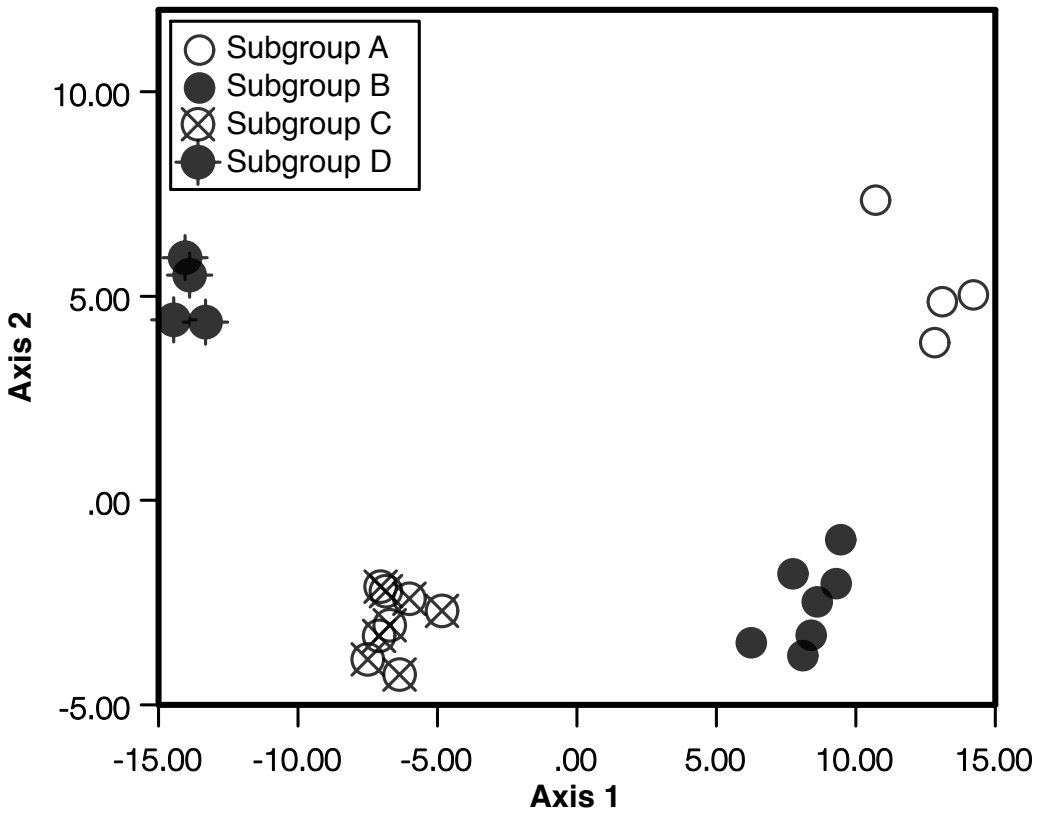

Figure 23: Discriminant analysis of subgroups A, B, C, and D from the cluster analysis in Figure 22.

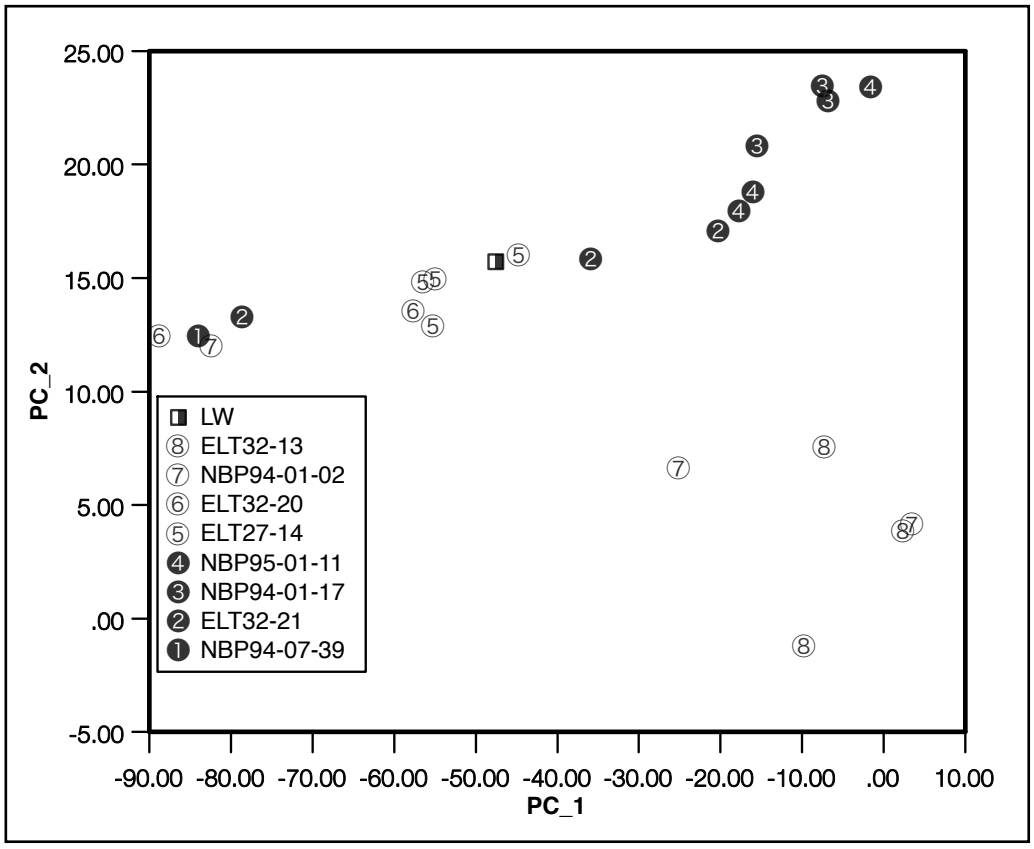

Figure 24: First and second principle components of point count CA subgroups A, B, C, and D.

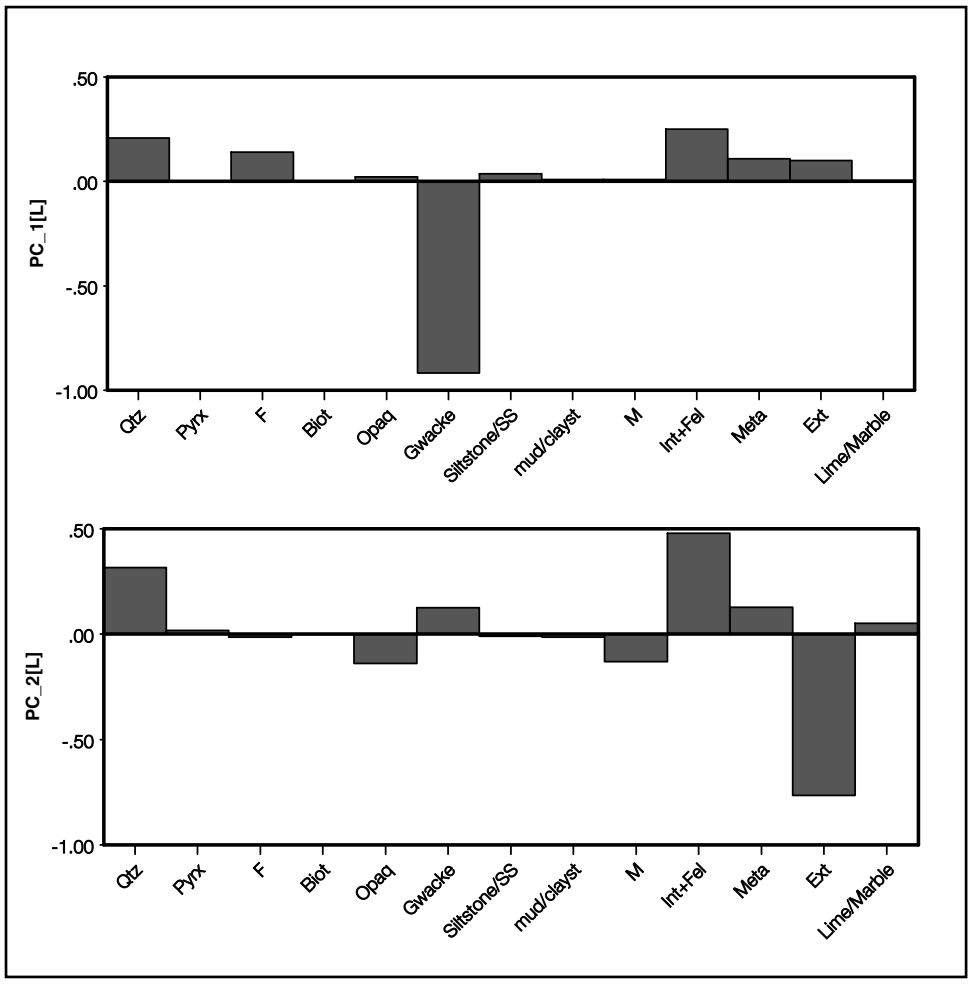

Figure 25: First and second principal component loadings [L] of point count PCA. Polymict is the major contributor to PC-1 and extrusive igneous is the major contributor to PC-2.

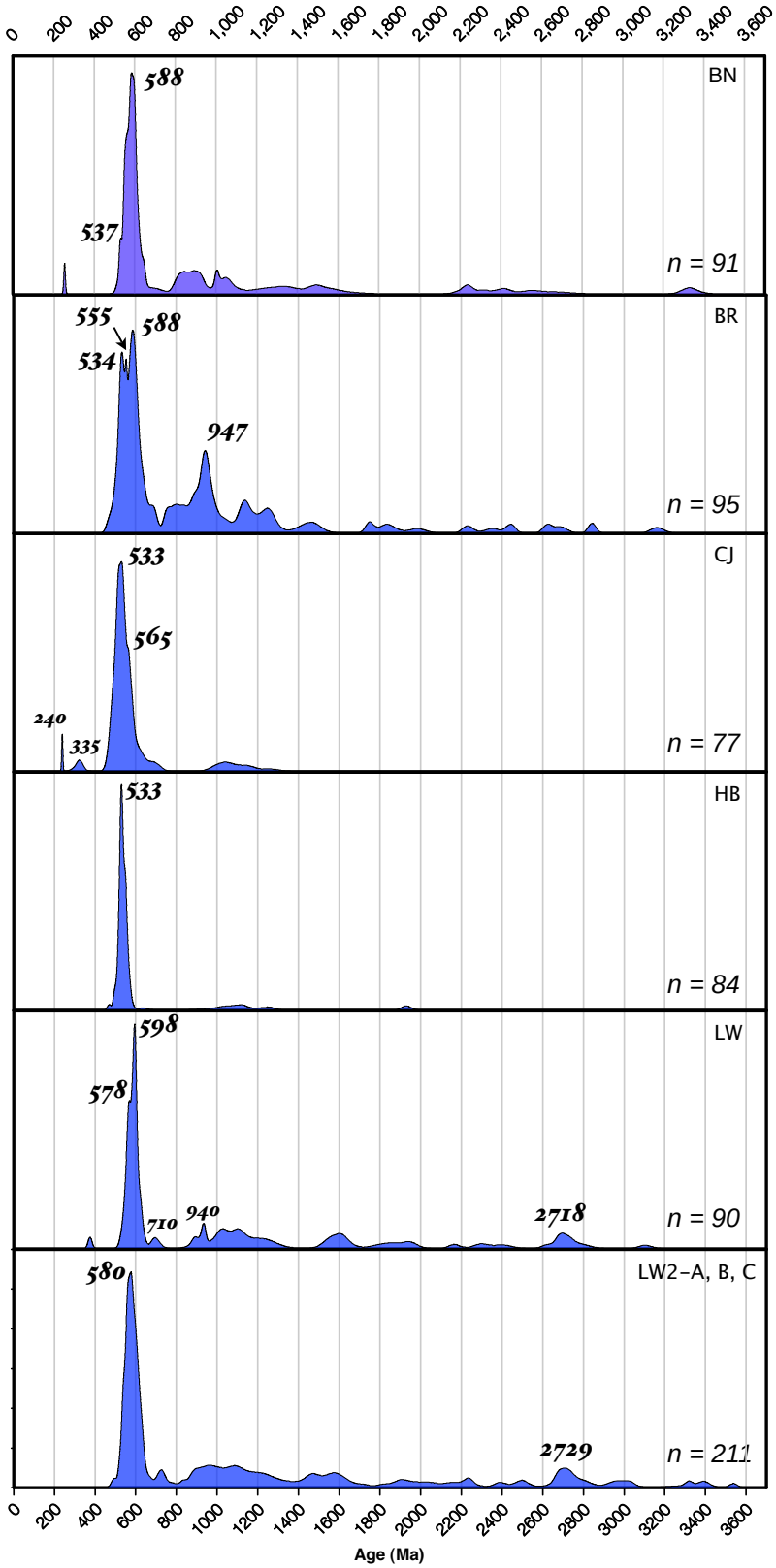

Figure 26: Probability plots of detrital zircon U/Pb ages from the Byrd Glacier.

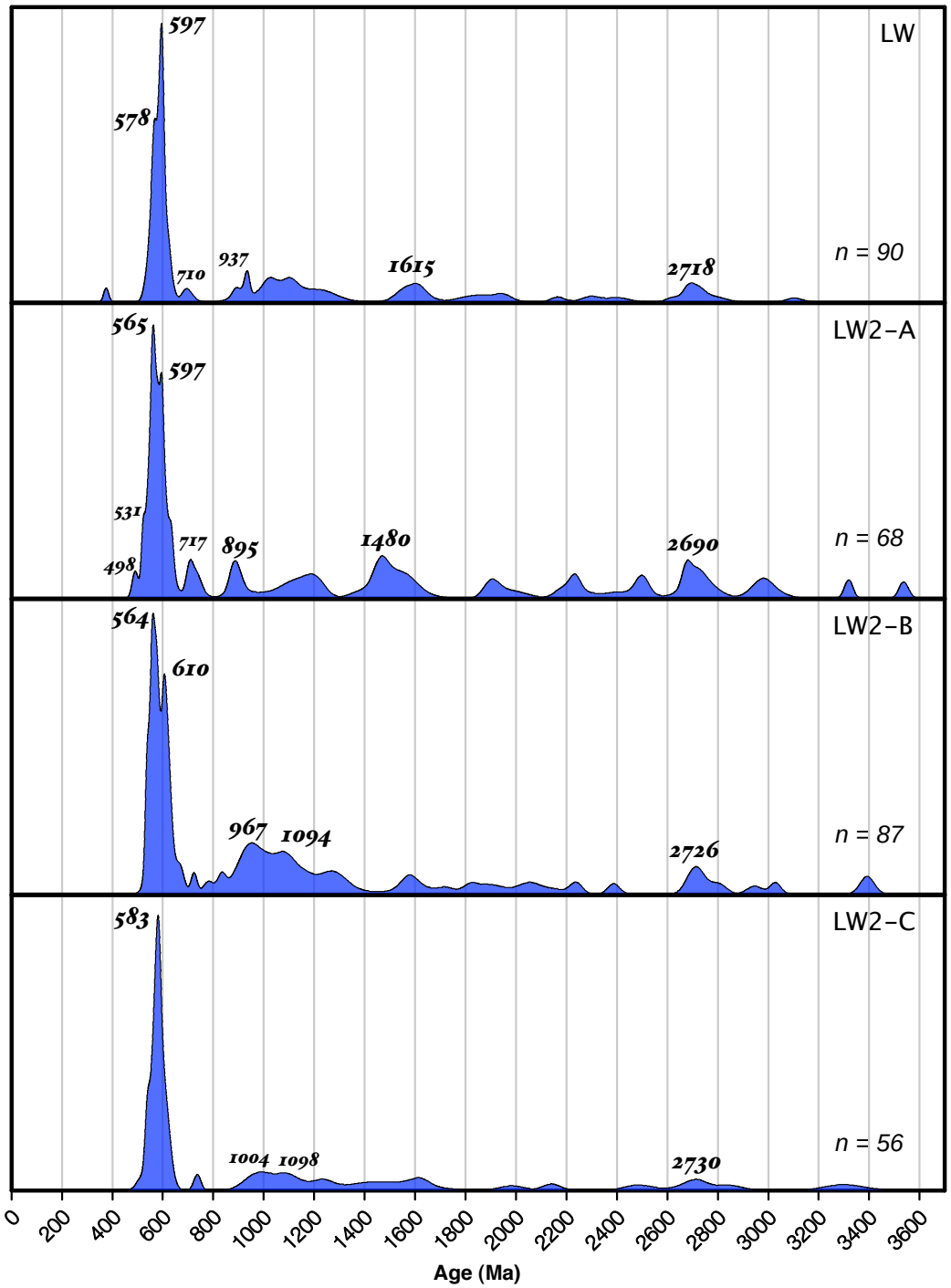

Figure 27: Probability plots of detrital zircon U/Pb ages from the sites LW and LW2, Byrd Glacier.

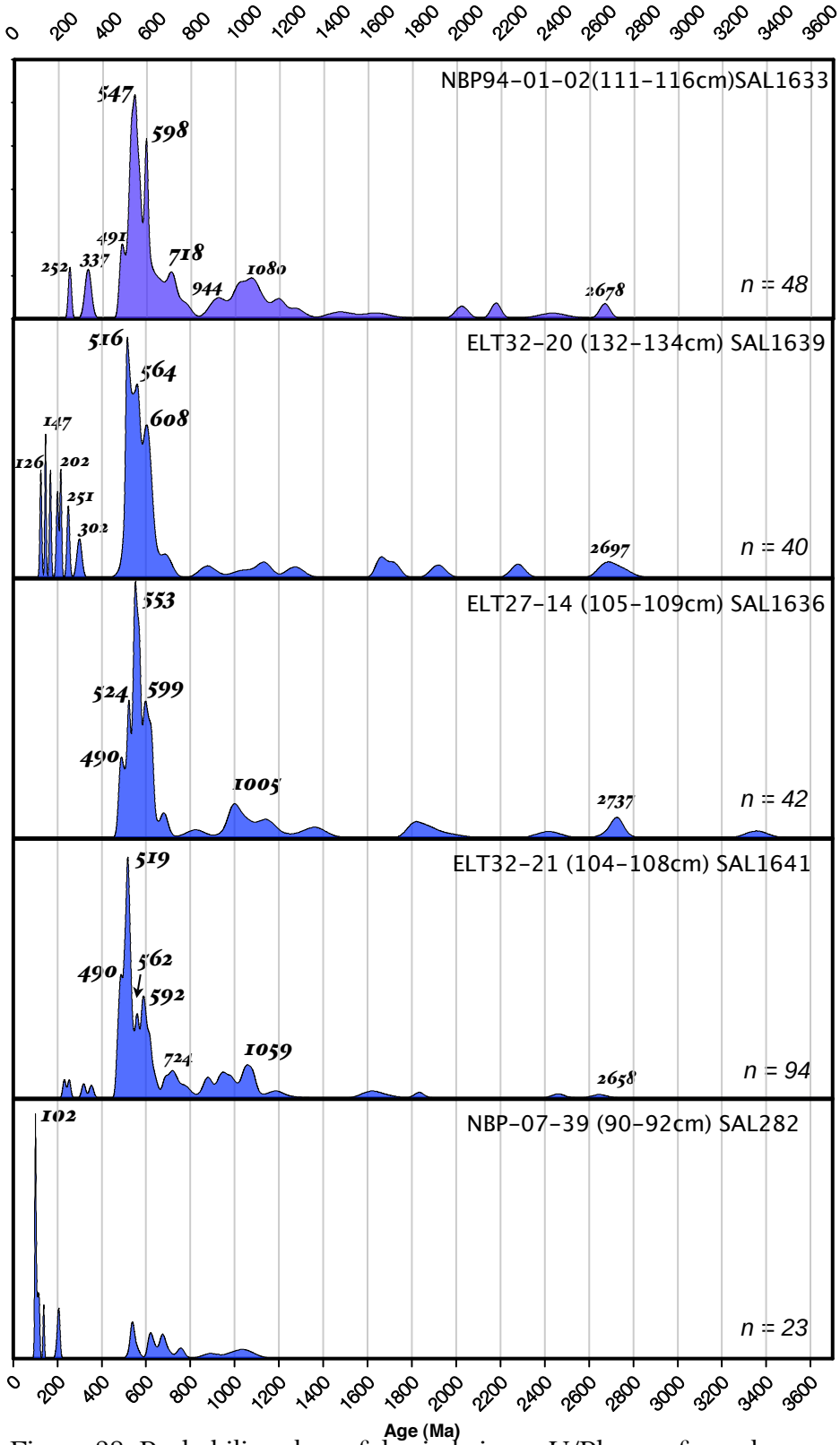

Figure 28: Probability plots of detrital zircon U/Pb ages from the central/western Ross Sea.

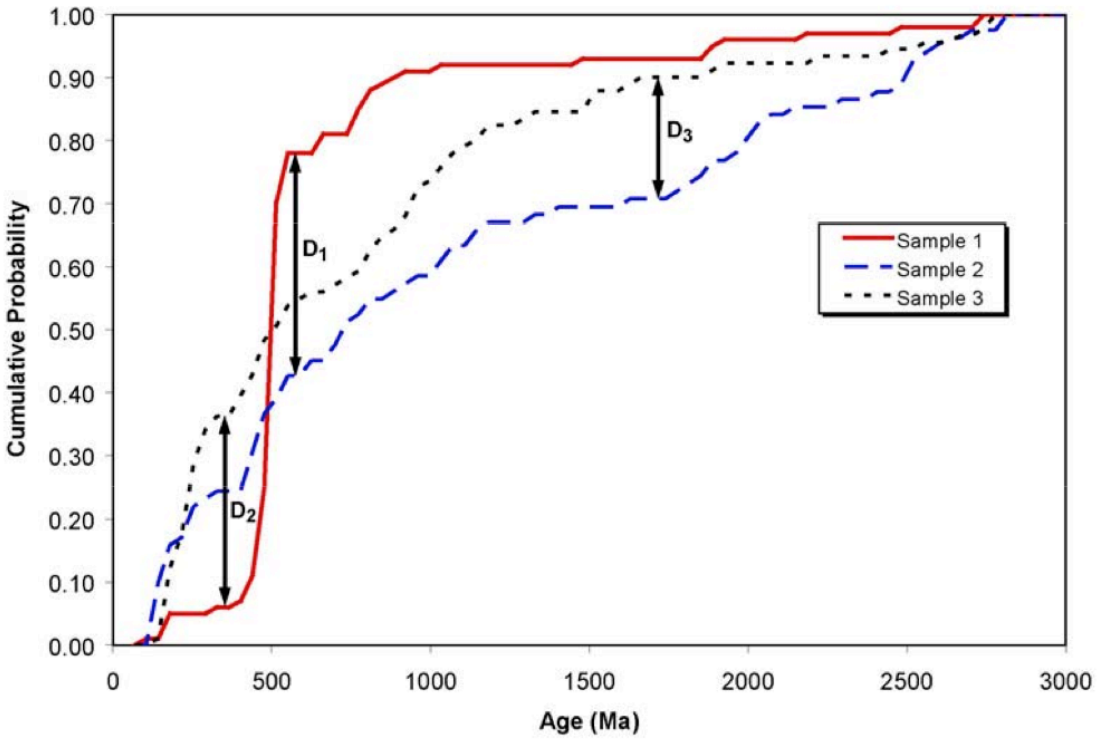

Figure 29: Example of cumulative distance functions (CDF). D = maximum difference between CDF's. (from Guynn, 2006)

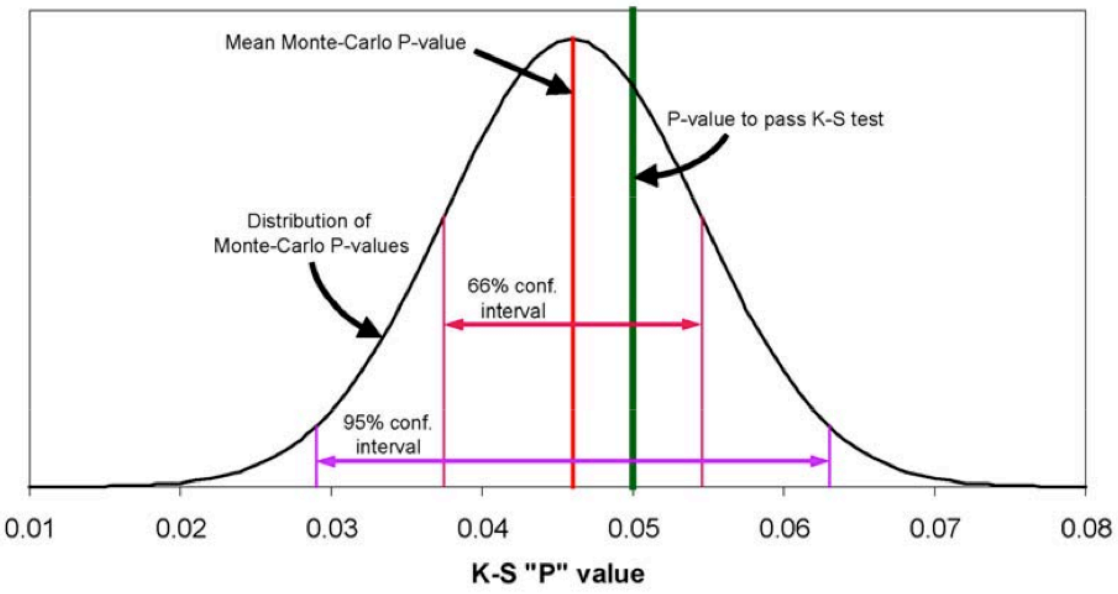

Figure 30: Example of P-value distribution from a Monte-Carlo simulation with comparison to the 95% confidence P-value of 0.05. (from Guynn, 2006)

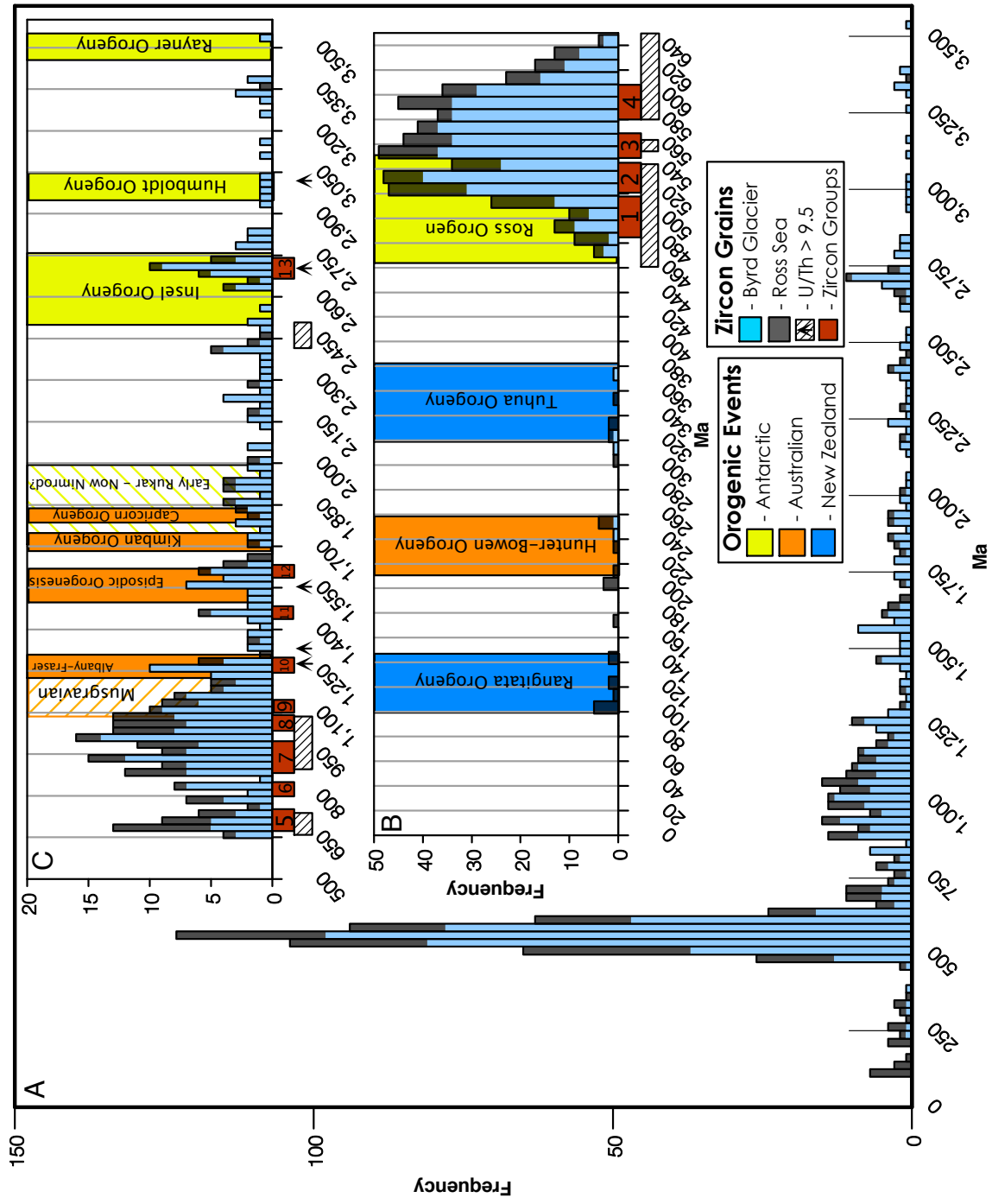
A
B
C
Frequency
Ma
Zircon Grains
- Byrd Glacier
- Ross Sea
- U/Th > 9.5
- Zircon Groups
Orogenic Events
- Antarctic
- Australian
- New Zealand
Ross Orogen
Tuhua Orogen
Hunter–Bowen Orogeny
Rangitata Orogeny
Raynerian Orogeny
Humboldt Orogeny
Inset Orogeny
Early Ruker – Now Nimrod?
Kimban Orogeny
Capricorn Orogeny
Episodic Orogenesis
Albany–Fraser
Musgravian

Figure 31: Cumulative frequency diagram of entire detrital zircon U/Pb isotope data set from the Byrd Glacier and Ross Sea(A). B includes age data from 0 - 640 Ma while C includes age data from 650 - 3600 Ma. Within the frequency diagrams, blue equals data collected from the Byrd Glacier, while black is from the Ross Sea. Orogenic events from Antarctica, Australia, and New Zealand are highlighted. Significant age groups of zircon grains are shown in red. Age ranges of grains inferred to be metamorphic (> 9.5 U/Th) are also shown.

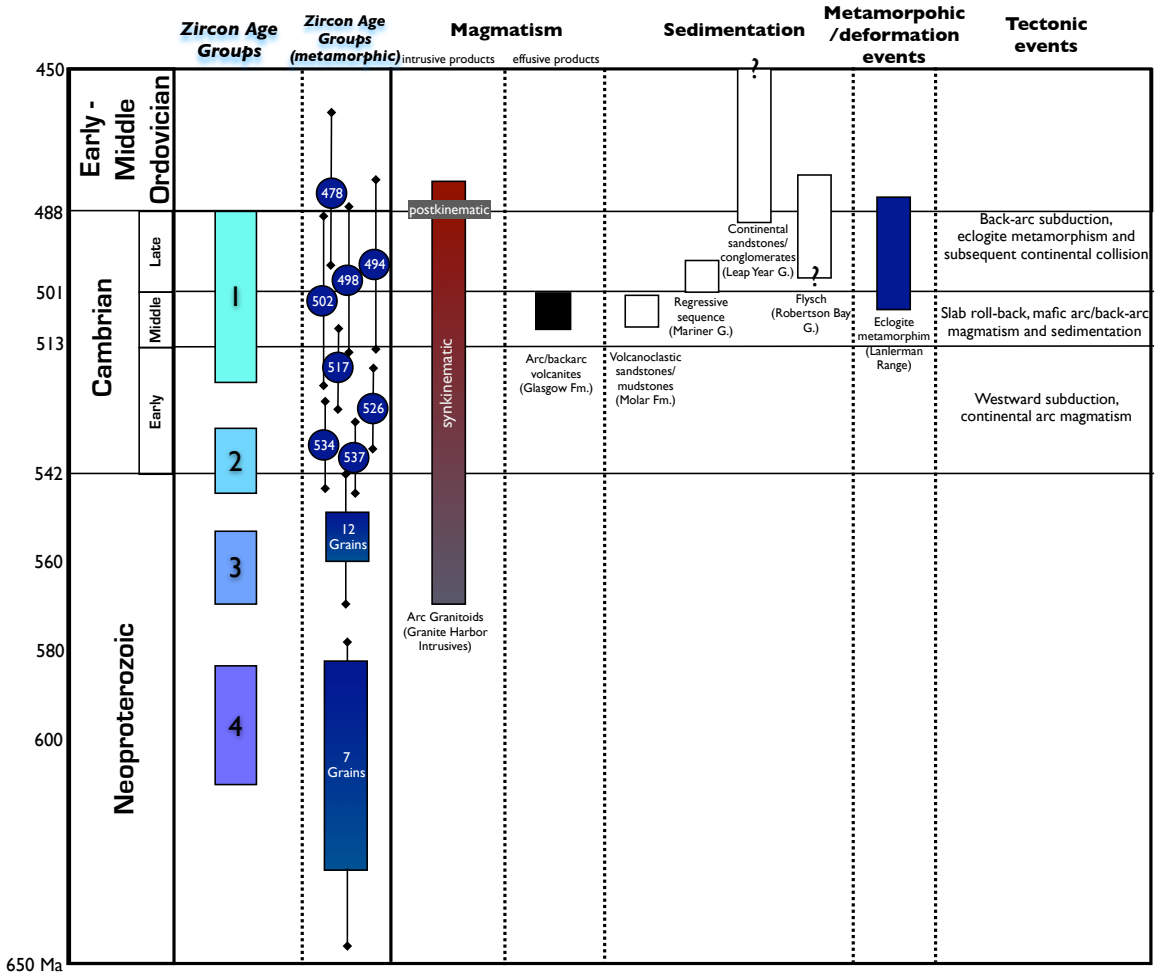

Figure 32: Zircon age groups (450 - 650 Ma) with magmatic, sedimentological, and tectonic events of northern Victoria Land (modified from Federico et al., 2006).

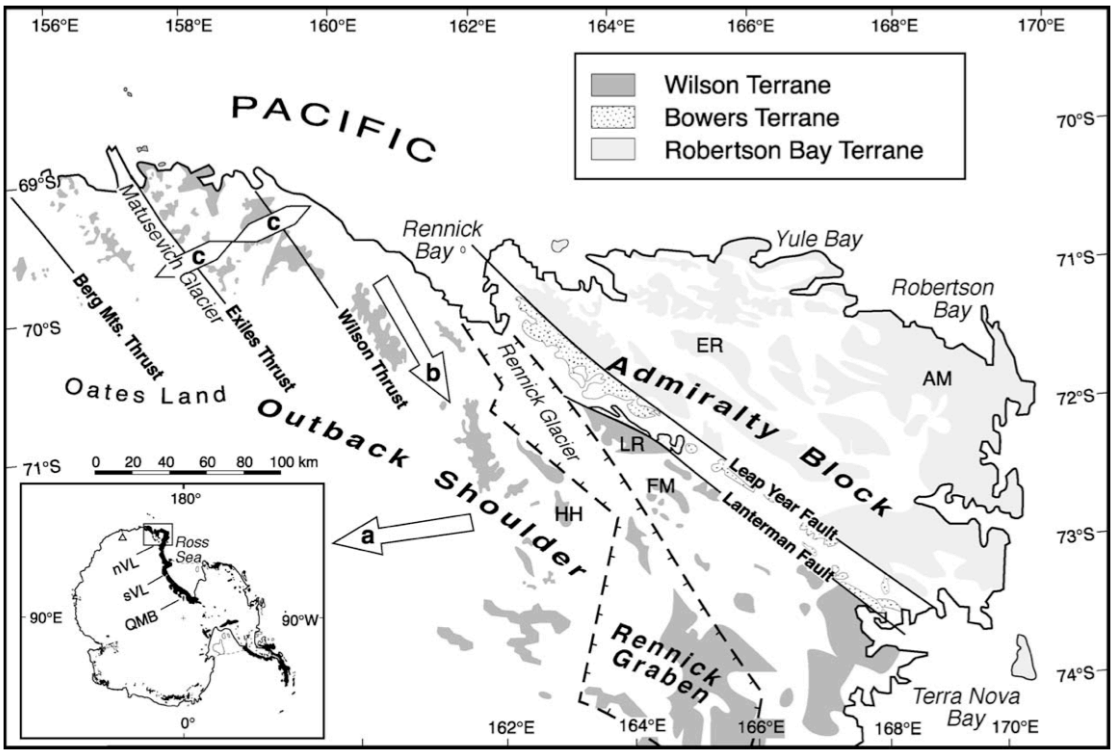

Figure 33: Northern Victoria Land with basement complexes. (from Lisker, 2002).

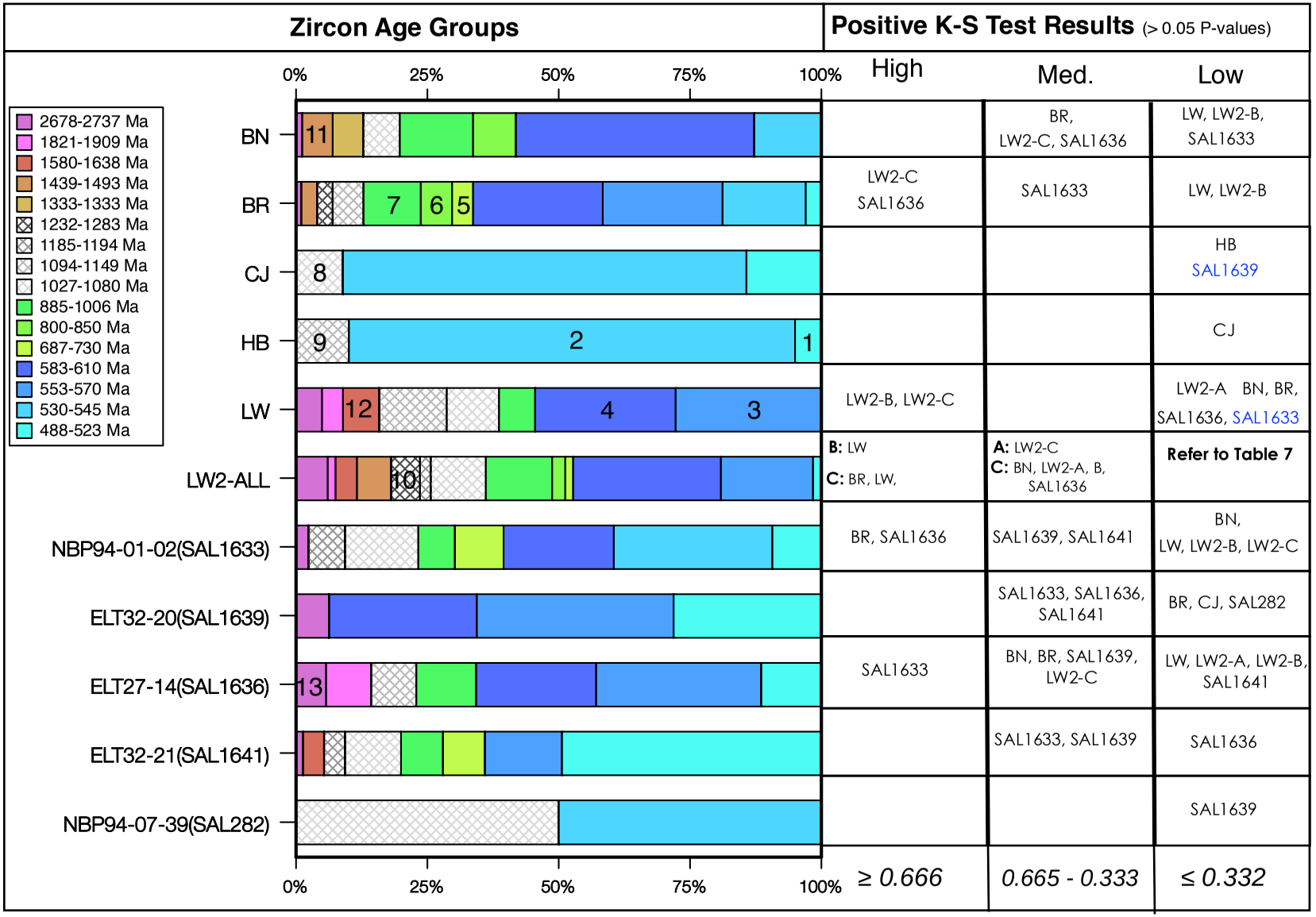
Zircon Age Groups
Positive K-S Test Results (> 0.05 P-values)
0%
25%
50%
75%
100%
2678-2737 Ma
1821-1909 Ma
1580-1638 Ma
1439-1493 Ma
1333-1333 Ma
1232-1283 Ma
1185-1194 Ma
1094-1149 Ma
1027-1080 Ma
885-1006 Ma
800-850 Ma
687-730 Ma
583-610 Ma
553-570 Ma
530-545 Ma
488-523 Ma
BN
BR
CJ
HB
LW
LW2-ALL
NBP94-01-02(SAL1633)
ELT32-20(SAL1639)
ELT27-14(SAL1636)
ELT32-21(SAL1641)
NBP94-07-39(SAL282)
11
7
6
5
8
9
2
1
12
4
3
10
13
High
Med.
Low
BR, LW2-C, SAL1636
LW, LW2-B, SAL1633
LW2-C SAL1636
SAL1633
LW, LW2-B
HB SAL1639
CJ
LW2-B, LW2-C
LW2-A BN, BR, SAL1636, SAL1633
B: LW
C: BR, LW,
A: LW2-C
C: BN, LW2-A, B, SAL1636
Refer to Table 7
BR, SAL1636
SAL1639, SAL1641
BN, LW, LW2-B, LW2-C
SAL1633, SAL1636, SAL1641
BR, CJ, SAL282
SAL1633
BN, BR, SAL1639, LW2-C
LW, LW2-A, LW2-B, SAL1641
SAL1633, SAL1639
SAL1636
SAL1639
≥ 0.666
0.665 - 0.333
≤ 0.332

Figure 34: Graph of zircon age groups Byrd Glacier and Ross Sea samples along with positive K-S test results. Age groups were selected using the DZ age pick program (Appendix D) and the raw data from Appendix C. Only with samples containing a similar number of grains can the P-values be compared and degree of similarity be inferred. Samples with differing number of grains and P-values > 0.05 have passed the K-S test but the differences in P-values are irrelevant. Samples highlighted above in blue are also highlighted in the Monte-Carlo simulation in Table 7. These blue samples above failed the K-S test discounting error and failed > 50% of the Monte-Carlo simulations. Therefore these positive sample comparisons using the K-S test accounting for error must be considered inconclusive due to measurement uncertainties.

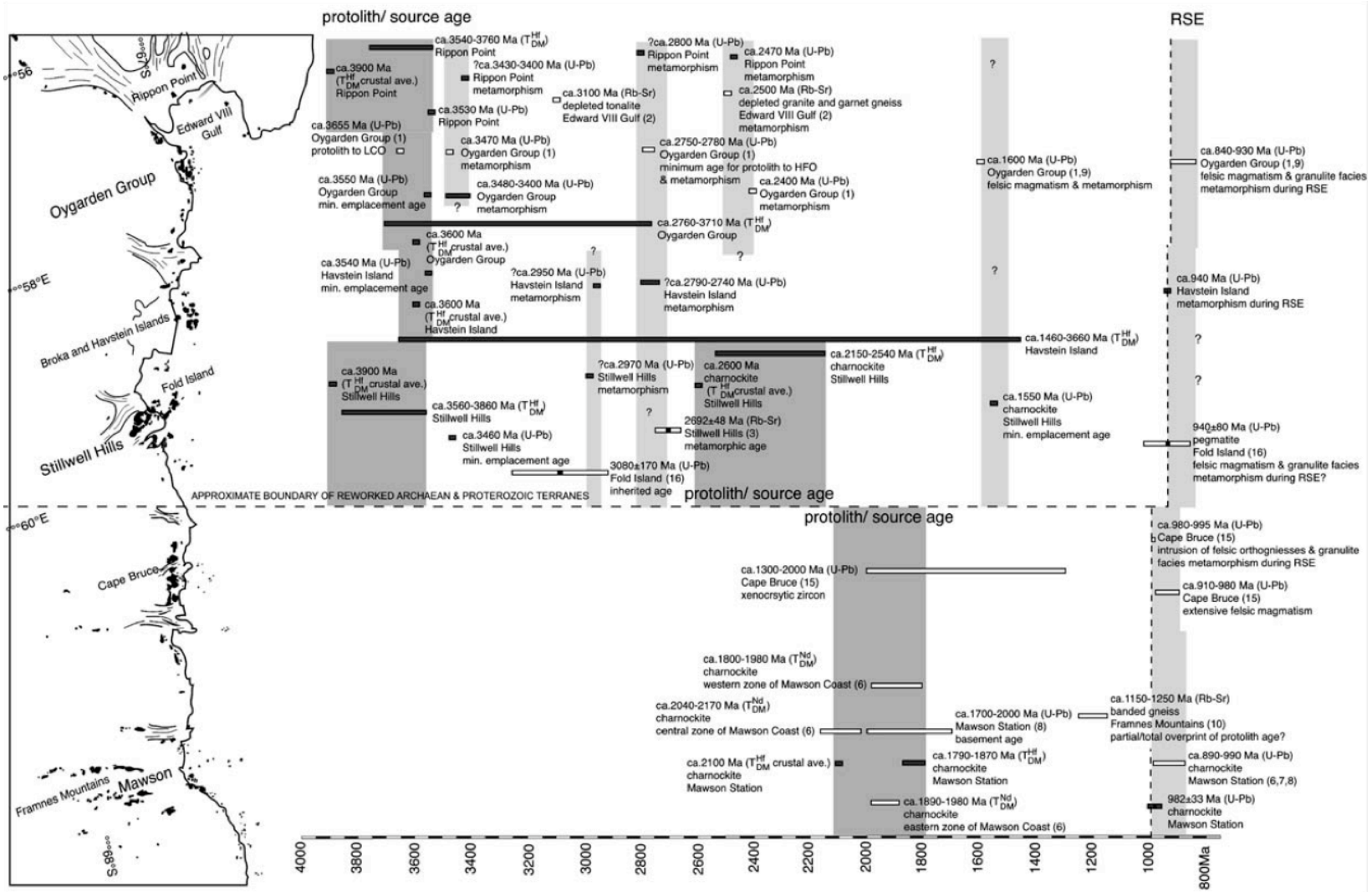

Figure 35: Graph of previous geochronology of Rayner Complex. (from Halpin et al., 2005)

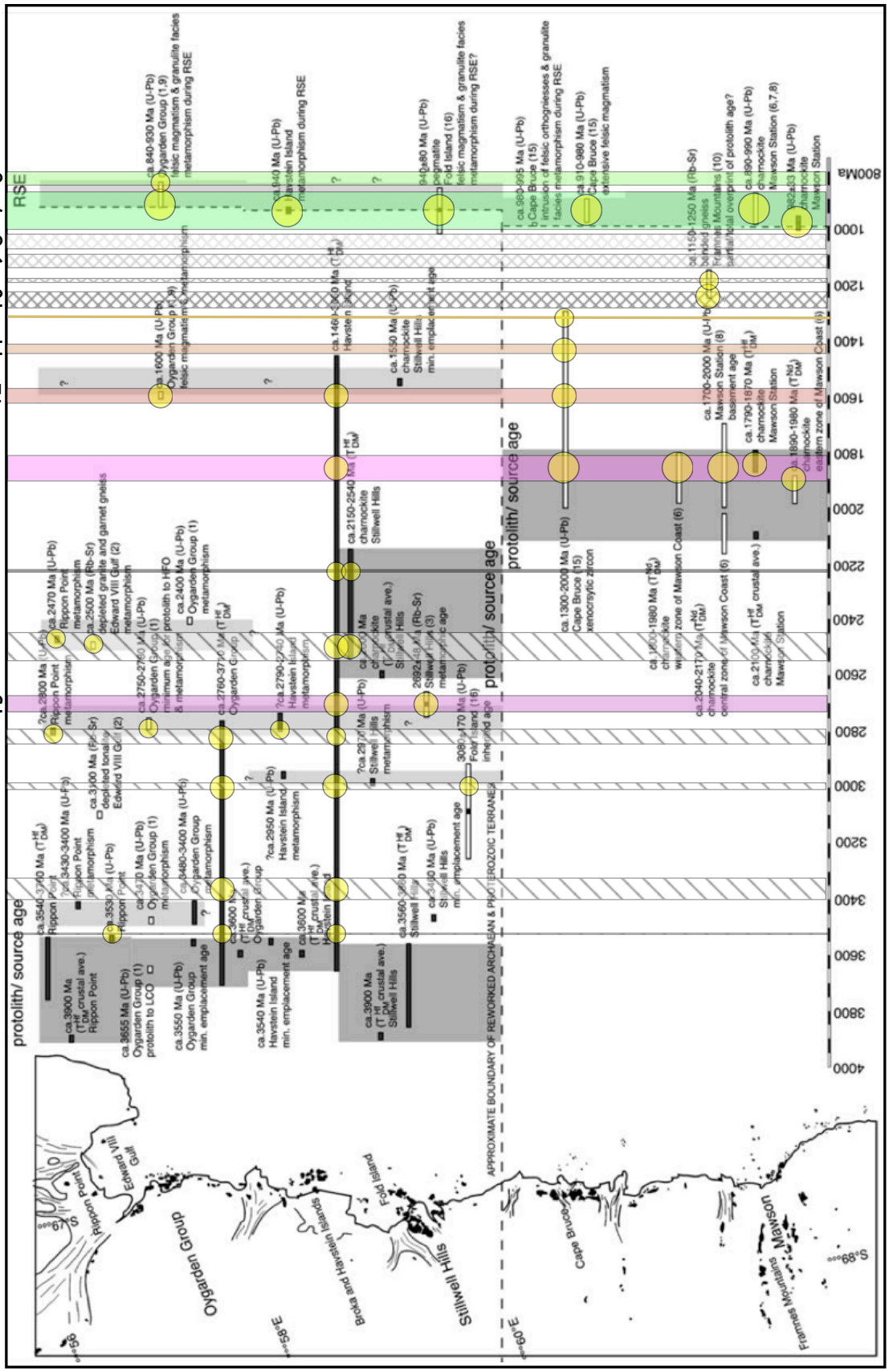
protolith/ source age
protolith/ source age
protolith/ source age
APPROXIMATE BOUNDARY OF REWORKED ARCHAEAN & PROTEROZOIC TERRANES
RSE
800Ma
1000
1200
1400
1600
1800
2000
2200
2400
2600
2800
3000
3200
3400
3600
3800
4000
Oygarden Group
Stillwell Hills
Cape Bruce
Framnes Mountains
Mawson
Rippon Point
Edward VIII Gulf
Haystein Island
Broka and Haystein Islands
Fold Island
67°S
58°E
60°E
89°E

Figure 36: Correlations of U/Pb zircon age groups from the Byrd Glacier and Ross Sea to the Rayner Complex. Major age groups are colored and labeled at the top of the Figure. Colors correlate with the key in Figure 34. Less significant age groups are stripped. Yellow circles indicate a correlation with a known age from the Rayner Complex. Light grey areas indicate the extent of the Rayner Structural Episode as infered from previously collected data. Blue arrows highlight correlation with Oygarden Group and Red arrows indicate correlation with Stillwell Hills. (modified from Halpin et al., 2005)

Appendix A. **ISET field rock classification scheme**

Byrd Nimrod Site # _____

Site name _____ Date _____

Square (circle one): A B C

Latitude _____ Longitude _____

UTM _____

	shape				roundness				
Igneous	B	R	D	S	A	SA	SR	R	Other Igneous:
Coarse-grained									
felsic									
intermediate									
mafic									
Fine-grained									
felsic									
intermediate									
mafic									
Metamorphic									Other Metamorphic:
gneiss									
augen									
garnet									
schist									
phyllite/slate									
quartzite									
marble									
Sedimentary									Other Sedimentary:
mudstone									
sandstone									
conglomerate									
wacke									
chert									
limestone									
bioclastic									

Unknown _____

Appendix B. Particle size distribution of Byrd Glacier and Ross Sea piston cores (% by volume)

Sample Site	fCLAY	mCLAY	cCLAY	vfSILT	fSILT	mSILT	cSILT	vfSAND	fSAND	mSAND	cSAND	vcSAND
BN-A	0.32	1.54	2.03	2.66	3.39	4.46	5.9	7.33	9.04	14.99	27.67	20.65
BN-B	0.39	1.65	1.95	2.72	3.77	5.03	7	9.3	10.02	15.38	26.57	16.23
BN-C	0.32	1.44	1.73	2.23	2.81	3.68	5.96	9.24	11.14	18.31	27.76	15.37
BR-A	0.17	0.84	1.1	1.31	1.4	1.73	2.4	4.19	10.35	19.34	31.61	25.53
BR-B	0.02	0.45	0.73	0.88	0.82	0.98	1.49	5.8	21.38	34.63	24.47	8.33
BR-C	0.16	0.81	1.05	1.02	0.75	0.89	1.29	9.54	25.92	27.77	20.93	9.85
CJ-Bu	0	0	0.29	0.68	1.44	2.92	6.55	17.31	29.56	26.87	11.79	2.6
CJ-C	0	0	0.36	0.79	1.63	3.04	6.02	14.34	25.32	27.02	16.38	5.12
HB-B	0	0	0.15	0.47	0.97	2	4.51	11.89	22.06	25.62	20.78	11.55
HB-C	0	0	0.44	0.86	1.7	3.3	6.99	16.33	25.39	22.96	14.8	7.25
LW-A2	5.5	5.31	9.66	11.01	9.17	6.53	6.26	7.36	10.52	14.1	8.84	5.73
LW-B	14.98	9.59	15.29	12.96	8.07	6.26	7.34	8.17	11.15	6.11	0.06	0
LW-A1	8.16	5.67	8.47	8.49	6.66	4.81	5.19	7.02	8.67	12.32	16.85	7.71
LW2-A#1	11.91	8.07	10.55	8.9	6.95	5.83	7.01	9.07	11.83	15.03	4.83	0.03
LW2-B	8.01	6.44	9.31	8.18	5.7	4.45	5.27	6.55	9.61	11.97	14.33	10.17
LW2-C	8.81	6.68	13.66	16.59	13.22	8.32	6.61	5.75	4.27	5.62	6.85	3.57
LW2-D	8.29	6.53	12.49	13.35	9.51	6.57	6.32	7.02	9.16	10.45	8.22	2.06
MT-A	19.35	5.8	4.97	4.75	5.09	5.09	5.93	6.96	7.9	8.21	13.58	12.34
MT-B	13.39	5.06	5.12	5.5	6.26	6.74	8.1	8.22	7.98	9.21	14.14	10.3
MT-C	25.68	7.81	7.06	7.02	7.21	6.51	7.48	7.32	6.1	6.55	7.49	3.8
ELT32-13 (49-51cm) SAL406	16.32	7.28	10.29	12.41	13.63	12.44	10.89	7.57	3.37	2.58	2.54	0.69
ELT32-13 (100-102cm) SAL407	14.57	6.86	10.17	12.57	13.93	12.93	10.76	6.58	3.17	3.15	3.37	1.92
ELT32-13 (149-151cm) SAL408	15.61	7.2	10.3	12.53	13.58	12.35	10.46	6.7	4.72	4.18	1.93	0.46
NBP94-01-02 (111-116cm) SAL1633	13.4	8.19	13.07	14.67	13.63	9.85	10.24	12.58	4.34	0	0	0
NBP94-01-02 (150-152cm) SAL374	13.65	7.93	14.56	17.46	14.21	7.53	3.76	1.01	5.74	10.76	2.24	1.16
ELT32-20 (64-69cm) SAL1638	13.03	6.92	9.72	13.38	16.21	13.65	8.49	4.74	3.22	2.97	3.89	3.81
ELT32-20 (132-134cm) SAL1639	12.14	7.81	10.86	13.91	16.02	13.17	8.16	4.78	3.25	3.64	4.41	1.81
ELT27-14 (47-50cm) SAL1634	15.17	7.98	11.2	14.26	16.74	13.96	9.29	5.92	3.97	1.52	0.01	0
ELT27-14 (105-109cm) SAL1636	16.99	7.61	10.51	14.11	17.03	13.85	8.45	4.81	3.18	3.17	0.29	0
ELT27-14 (164-170cm) SAL1637	15.84	7.74	10.96	14.62	17.33	14.37	9.32	5.09	2.15	2.12	0.46	0
NBP95-01-11 (48-50cm) SAL537	16.68	7.21	10.86	12.18	10.29	7.81	6.85	5.55	6.04	4.31	6.71	5.51
NBP95-01-11 (100-102cm) SAL538	13.8	6.51	11.04	15.61	17.73	14.68	9.28	4.26	3.17	2.3	1.52	0.07
NBP95-01-17 (48-50cm) SAL540	10.78	5.91	8.35	9.69	8.59	7.19	8.01	9.49	10.87	8.17	7.89	5.06
NBP95-01-17 (100-102cm) SAL543	11.13	5.64	8.27	10.23	10.79	9.47	8.67	8.2	7.53	6.47	8.39	5.22
NBP95-01-17 (153-155cm) SAL534	13.87	6.16	9.08	11.08	11.36	9.57	8.2	7.4	7.08	5.75	6.56	3.87
ELT32-21 (54-58cm) SAL1640	16.52	6.83	9.61	12.9	14.23	10.42	7.91	6.77	4.1	3.33	5.96	1.43
ELT32-21 (104-108cm) SAL1641	16.72	6.4	8.59	11.29	12.43	9.78	8.15	7.16	6.03	5.48	4.62	3.36
ELT32-21 (154-160cm) SAL1642	16.67	6.59	9.09	12.22	13.89	11.03	9.25	7.98	5.48	3.5	1.95	2.35
NBP94-07-39 (100-102cm) SAL283	16.76	10.17	16.05	18.17	17.65	12.58	6.71	1.75	0.12	0	0	0

Appendix C. U-Pb (zircon) geochronologic analyses by Laser-Ablation Multicollector ICP Mass Spectrometery

			Isotopic ratios					Apparent ages (Ma)							
U	206Pb	U/Th	207Pb*		206Pb*		error	206Pb*		207Pb*		206Pb*		Best	
(ppm)	204Pb		235U	(%)	238U	(%)	corr.	238U	±(Ma)	235U	±(Ma)	207Pb*	±(Ma)	age	±(Ma)
SAL282															
319.6	677	1	0.09732	6.90	0.01564	2.24	0.32	100.1	2.2	94	6	-49	159	**100**	**2**
635.8	2162	0	0.10612	4.48	0.01594	2.36	0.53	101.9	2.4	102	4	114	90	**102**	**2**
171	400	0	0.09725	10.89	0.01590	3.02	0.28	101.7	3.0	94	10	-91	257	**102**	**3**
198.6	736	0	0.10548	10.37	0.01601	3.76	0.36	102.4	3.8	102	10	89	229	**102**	**4**
260	758	0	0.10684	10.28	0.01665	2.50	0.24	106.5	2.6	103	10	25	240	**106**	**3**
423.6	881	0	0.12251	15.49	0.01767	2.53	0.16	112.9	2.8	117	17	208	356	**113**	**3**
513.3	1807	1	0.13210	6.56	0.01870	2.21	0.34	119.4	2.6	126	8	252	142	**119**	**3**
252.2	1056	1	0.14337	5.51	0.02183	2.37	0.43	139.2	3.3	136	7	81	118	**139**	**3**
682.3	3946	1	0.22792	6.05	0.03200	3.75	0.62	203.1	7.5	208	11	270	109	**203**	**7**
370.8	3060	1	0.24387	4.29	0.03285	2.22	0.52	208.3	4.6	222	9	365	83	**208**	**5**
114	1455	0	0.69753	2.91	0.08697	1.51	0.52	537.6	7.8	537	12	536	54	**538**	**8**
72.48	1088	1	0.67620	5.16	0.08758	3.08	0.60	541.2	16.0	524	21	452	92	**541**	**16**
1154	5931	1	0.72522	4.03	0.08941	3.37	0.84	552.1	17.8	554	17	561	48	**552**	**18**
751.5	1483	5	0.80387	6.59	0.10069	1.64	0.25	618.5	9.7	599	30	526	140	**618**	**10**
326.1	3694	2	0.85894	2.54	0.10294	2.10	0.83	631.6	12.6	630	12	622	31	**632**	**13**
171.3	3508	1	1.00839	8.13	0.11017	6.21	0.76	673.7	39.7	708	41	818	110	**674**	**40**
133.9	2541	1	0.96275	4.41	0.11047	1.84	0.42	675.5	11.8	685	22	715	85	**675**	**12**
136	3321	1	0.96810	4.67	0.11231	3.25	0.69	686.1	21.1	687	23	692	72	**686**	**21**
158.5	3430	1	1.16400	3.18	0.12496	2.20	0.69	759.1	15.8	784	17	855	48	**759**	**16**
180.9	983	1	1.34839	5.97	0.14730	4.24	0.71	885.8	35.1	867	35	819	88	**886**	**35**
163	3900	1	1.68143	3.95	0.16938	3.34	0.85	1008.7	31.2	1002	25	986	43	**986**	**43**
421.1	11603	1	1.75666	3.83	0.17273	3.31	0.86	1027.1	31.4	1030	25	1035	39	**1035**	**39**
310.6	8828	1	1.87741	2.63	0.18169	1.59	0.60	1076.2	15.8	1073	17	1067	42	**1067**	**42**
SAL1633															
273.3	2568	1	0.27369	4.67	0.03992	2.79	0.60	252.3	6.9	246	10	182	87	**252**	**7**
152.8	1600	2	0.38583	6.45	0.05316	4.34	0.67	333.9	14.1	331	18	313	109	**334**	**14**
223.6	3081	2	0.40774	5.38	0.05336	4.45	0.83	335.1	14.5	347	16	429	68	**335**	**15**
437	6750	1	0.61510	4.10	0.07794	2.23	0.54	483.8	10.4	487	16	501	76	**484**	**10**
74.7	1268	1	0.60038	7.34	0.07904	2.61	0.36	490.4	12.3	477	28	416	153	**490**	**12**
167.1	2600	1	0.63668	5.31	0.08272	3.42	0.64	512.3	16.9	500	21	445	90	**512**	**17**
318.7	5374	4	0.68163	3.43	0.08491	3.04	0.89	525.3	15.3	528	14	538	35	**525**	**15**
137.8	2906	2	0.66722	3.81	0.08535	2.08	0.55	528.0	10.5	519	15	480	71	**528**	**11**
135.8	830	2	0.63790	8.24	0.08562	1.59	0.19	529.6	8.1	501	33	373	182	**530**	**8**
154.1	2523	1	0.65112	7.50	0.08619	4.21	0.56	532.9	21.5	509	30	404	139	**533**	**22**
296.7	4822	1	0.68643	4.09	0.08720	2.44	0.60	538.9	12.6	531	17	495	73	**539**	**13**
748.8	10404	3	0.71508	3.67	0.08826	3.50	0.95	545.2	18.3	548	16	558	24	**545**	**18**
166.8	2629	1	0.71281	2.47	0.08842	1.38	0.56	546.2	7.2	546	10	547	45	**546**	**7**
380.7	6911	2	0.72560	4.82	0.08936	4.43	0.92	551.8	23.4	554	21	563	41	**552**	**23**
441.4	1193	2	0.68058	6.70	0.08944	2.83	0.42	552.2	15.0	527	28	420	136	**552**	**15**
749.7	13322	8	0.72386	2.28	0.09009	1.77	0.77	556.1	9.4	553	10	540	32	**556**	**9**
317	3821	1	0.72933	6.10	0.09025	5.27	0.86	557.0	28.1	556	26	553	67	**557**	**28**
69.8	1263	2	0.70754	5.87	0.09058	2.78	0.47	559.0	14.9	543	25	478	114	**559**	**15**
494.8	9452	1	0.75633	3.15	0.09248	1.54	0.49	570.2	8.4	572	14	579	60	**570**	**8**
46.28	1052	0	0.73819	8.59	0.09603	3.37	0.39	591.1	19.0	561	37	442	176	**591**	**19**
46.94	1021	1	0.79074	6.46	0.09694	1.70	0.26	596.4	9.7	592	29	573	136	**596**	**10**
395.3	9684	2	0.82563	4.08	0.09696	1.80	0.44	596.5	10.3	611	19	666	79	**597**	**10**
647.2	12182	2	0.79733	2.63	0.09743	1.00	0.38	599.3	5.7	595	12	580	53	**599**	**6**
146.1	1644	1	0.82102	8.68	0.09954	2.85	0.33	611.7	16.6	609	40	597	178	**612**	**17**
173	4163	3	0.86443	5.47	0.10388	4.35	0.80	637.1	26.4	633	26	616	71	**637**	**26**
408.3	7845	4	0.84896	4.98	0.10393	4.03	0.81	637.4	24.5	624	23	576	64	**637**	**24**
273.6	6454	4	0.98372	5.06	0.11032	3.87	0.77	674.6	24.8	696	25	764	69	**675**	**25**
343.5	8644	3	1.00689	7.68	0.11325	6.63	0.86	691.6	43.5	707	39	758	82	**692**	**44**
285.3	3651	1	1.00116	4.60	0.11730	2.49	0.54	715.0	16.9	704	23	671	83	**715**	**17**
585	13338	4	1.13948	4.84	0.11735	4.17	0.86	715.3	28.2	772	26	941	51	**715**	**28**
350.1	8793	3	1.23060	5.96	0.12753	3.65	0.61	773.7	26.6	815	33	928	97	**774**	**27**
118.4	4241	1	1.55344	5.37	0.15133	4.05	0.75	908.4	34.3	952	33	1054	71	**908**	**34**
103.9	1261	1	1.42020	8.47	0.15537	4.57	0.54	931.0	39.6	897	50	816	149	**931**	**40**
263.8	4830	1	1.72655	4.20	0.17283	3.47	0.82	1027.7	32.9	1018	27	999	48	**999**	**48**

			Isotopic ratios					Apparent ages (Ma)							
U	206Pb	U/Th	207Pb*		206Pb*		error	206Pb*		207Pb*		206Pb*		Best age	
(ppm)	204Pb		235U	(%)	238U	(%)	corr.	238U	±(Ma)	235U	±(Ma)	207Pb*	±(Ma)		±(Ma)
SAL1633															
265.5	8111	1	1.74278	1.91	0.17311	1.52	0.80	1029.2	14.5	1024	12	1014	23	**1014**	**23**
910.6	21909	8	1.85078	2.96	0.18010	2.26	0.76	1067.5	22.2	1064	20	1056	39	**1056**	**39**
265.6	9438	1	1.90888	3.18	0.18391	2.85	0.90	1088.3	28.6	1084	21	1076	28	**1076**	**28**
165	3667	1	1.96609	3.86	0.18935	2.30	0.60	1117.9	23.6	1104	26	1077	62	**1077**	**62**
85.02	2948	1	1.98854	3.38	0.19004	2.70	0.80	1121.6	27.8	1112	23	1092	41	**1092**	**41**
180.5	7672	1	2.12932	4.61	0.19856	3.80	0.82	1167.6	40.6	1158	32	1141	52	**1141**	**52**
245.1	10038	2	2.18382	2.33	0.19792	1.92	0.83	1164.1	20.5	1176	16	1198	26	**1198**	**26**
81.74	7050	1	2.58444	3.41	0.22517	2.84	0.83	1309.2	33.6	1296	25	1275	37	**1275**	**37**
100	4668	1	3.24401	3.63	0.25590	2.11	0.58	1468.9	27.7	1468	28	1466	56	**1466**	**56**
274	9042	2	4.10970	4.74	0.29641	3.17	0.67	1673.5	46.7	1656	39	1634	66	**1634**	**66**
123.8	8605	1	6.30015	4.66	0.36698	4.37	0.94	2015.2	75.6	2018	41	2022	29	**2022**	**29**
96.07	3856	1	7.57427	3.50	0.40382	3.24	0.93	2186.6	60.1	2182	31	2177	23	**2177**	**23**
64.16	4136	1	10.18300	4.51	0.46900	2.15	0.48	2479.2	44.3	2452	42	2429	67	**2429**	**67**
380.9	8594	1	12.92778	4.48	0.51618	4.24	0.95	2683.0	93.0	2674	42	2668	24	**2668**	**24**
SAL1636															
139.9	976	1	0.20457	11.51	0.03288	3.51	0.31	208.5	7.2	189	20	-49	267	**209**	**7**
346.6	7746	1	0.62203	4.21	0.07809	1.95	0.46	484.7	9.1	491	16	521	82	**485**	**9**
92.92	1671	1	0.59324	7.33	0.07972	2.74	0.37	494.4	13.0	473	28	370	153	**494**	**13**
118.8	2356	1	0.67442	6.37	0.08135	3.68	0.58	504.2	17.8	523	26	608	113	**504**	**18**
140	2353	1	0.63940	5.87	0.08319	3.33	0.57	515.2	16.5	502	23	442	107	**515**	**17**
372.1	7519	6	0.67984	2.07	0.08443	1.17	0.57	522.5	5.9	527	9	545	37	**523**	**6**
127.9	2390	1	0.65427	4.47	0.08447	2.27	0.51	522.7	11.4	511	18	459	85	**523**	**11**
26.93	570	2	0.58241	16.46	0.08544	3.83	0.23	528.5	19.4	466	62	169	376	**528**	**19**
218.2	778	1	0.60789	13.28	0.08569	4.52	0.34	530.0	23.0	482	51	261	288	**530**	**23**
171.8	3174	3	0.69956	4.12	0.08809	2.40	0.58	544.2	12.5	539	17	514	74	**544**	**13**
504.8	11385	1	0.72494	4.42	0.08870	2.54	0.57	547.8	13.3	554	19	577	79	**548**	**13**
674.6	9311	4	0.71660	2.39	0.08892	1.16	0.49	549.2	6.1	549	10	547	46	**549**	**6**
311.7	6088	1	0.71903	3.36	0.08953	1.80	0.54	552.7	9.5	550	14	539	62	**553**	**10**
294.2	4325	2	0.72909	2.61	0.09017	1.69	0.65	556.5	9.0	556	11	554	43	**557**	**9**
69.38	1401	2	0.67954	8.51	0.09067	2.90	0.34	559.5	15.6	526	35	386	180	**560**	**16**
426.5	10319	2	0.74429	3.81	0.09127	1.98	0.52	563.0	10.7	565	17	572	71	**563**	**11**
1030	2871	2	0.72047	4.61	0.09135	2.11	0.46	563.5	11.4	551	20	499	90	**564**	**11**
93.16	2377	2	0.74608	5.79	0.09172	2.45	0.42	565.7	13.3	566	25	567	114	**566**	**13**
384.5	7391	6	0.74332	3.33	0.09291	1.04	0.31	572.7	5.7	564	14	531	69	**573**	**6**
172.9	684	2	0.70240	11.06	0.09326	3.94	0.36	574.8	21.7	540	46	397	232	**575**	**22**
157.5	2835	1	0.76543	4.79	0.09659	2.47	0.51	594.4	14.0	577	21	510	90	**594**	**14**
253.8	4021	3	0.77373	3.40	0.09670	1.48	0.43	595.0	8.4	582	15	531	67	**595**	**8**
81.16	1868	1	0.77459	7.02	0.09761	3.27	0.47	600.4	18.7	582	31	513	137	**600**	**19**
87.05	1048	1	0.78184	6.90	0.09925	1.65	0.24	610.0	9.6	587	31	497	148	**610**	**10**
125.3	2305	0	0.79511	5.48	0.10004	2.39	0.44	614.7	14.0	594	25	516	108	**615**	**14**
176.6	4507	1	0.82542	4.68	0.10162	2.78	0.60	623.9	16.6	611	21	564	82	**624**	**17**
230.5	5298	1	0.83669	2.83	0.10238	1.37	0.48	628.3	8.2	617	13	577	54	**628**	**8**
467.3	626	2	0.79653	18.60	0.10343	8.04	0.43	634.5	48.6	595	84	447	375	**634**	**49**
62.45	1179	0	0.89766	8.77	0.11170	2.60	0.30	682.6	16.8	650	42	540	183	**683**	**17**
357.8	7630	1	1.24400	6.18	0.13643	5.74	0.93	824.5	44.4	821	35	810	48	**824**	**44**
140.1	4171	3	1.64153	7.40	0.16663	5.21	0.70	993.5	48.0	986	47	970	107	**994**	**48**
38.92	1943	4	1.59782	5.85	0.16665	2.34	0.40	993.6	21.5	969	37	915	110	**994**	**22**
178.9	5257	2	1.80724	2.53	0.17779	1.53	0.60	1054.9	14.9	1048	17	1034	41	**1034**	**41**
231.8	11064	2	1.77171	2.87	0.17400	1.83	0.64	1034.1	17.5	1035	19	1037	45	**1037**	**45**
185.4	8296	2	2.09597	5.45	0.19594	5.06	0.93	1153.5	53.4	1147	38	1136	41	**1136**	**41**
258.5	10348	3	2.02580	3.52	0.18794	2.86	0.81	1110.2	29.2	1124	24	1151	41	**1151**	**41**
530.3	10508	6	1.75995	11.82	0.15178	9.62	0.81	910.9	81.7	1031	77	1295	134	**1295**	**134**
65.65	1891	2	2.50164	6.97	0.21479	5.08	0.73	1254.3	57.9	1273	51	1303	93	**1303**	**93**
85.59	2929	2	2.90071	4.16	0.24117	3.42	0.82	1392.8	42.8	1382	31	1366	46	**1366**	**46**
65.47	6144	1	4.89459	3.45	0.32176	2.98	0.86	1798.3	46.8	1801	29	1805	32	**1805**	**32**
275.1	19533	3	5.36445	4.69	0.34150	4.09	0.87	1893.9	67.1	1879	40	1863	42	**1863**	**42**
175.2	5298	1	5.44516	10.71	0.33289	9.85	0.92	1852.4	158.6	1892	92	1936	75	**1936**	**75**
160.3	8631	2	7.20012	3.40	0.34949	1.62	0.48	1932.2	27.1	2137	30	2339	51	**2339**	**51**
408.5	24942	4	9.05904	4.33	0.42022	2.90	0.67	2261.5	55.3	2344	40	2417	55	**2417**	**55**
47.01	4564	1	11.43305	3.21	0.44740	2.71	0.84	2383.7	54.0	2559	30	2701	29	**2701**	**29**
104	8129	2	10.16715	4.67	0.39636	4.22	0.90	2152.2	77.3	2450	43	2707	33	**2707**	**33**

			Isotopic ratios					Apparent ages (Ma)							
U	206Pb	U/Th	207Pb*		206Pb*		error	206Pb*		207Pb*		206Pb*		Best age	
(ppm)	204Pb		235U	(%)	238U	(%)	corr.	238U	±(Ma)	235U	±(Ma)	207Pb*	±(Ma)		±(Ma)
SAL1636															
118	9566	1	12.91306	3.44	0.50153	1.82	0.53	2620.4	39.2	2673	32	2714	48	**2714**	**48**
52.5	6706	1	12.85774	2.61	0.49533	2.07	0.79	2593.7	44.1	2669	25	2727	26	**2727**	**26**
427.6	33558	6	26.61358	4.42	0.69249	3.00	0.68	3392.1	79.2	3369	43	3356	51	**3356**	**51**
62.08	8416	1	27.66133	3.75	0.64085	2.73	0.73	3192.4	68.9	3407	37	3536	40	**3536**	**40**
SAL1639															
367.7	1860	1	0.14623	4.26	0.01980	3.01	0.71	126.4	3.8	139	6	353	68	**126**	**4**
125	622	1	0.11347	24.92	0.02143	6.02	0.24	136.7	8.1	109	26	-457	646	**137**	**8**
1159	2364	1	0.15050	5.27	0.02302	2.06	0.39	146.7	3.0	142	7	70	115	**147**	**3**
428.6	2256	2	0.17944	5.02	0.02661	2.33	0.46	169.3	3.9	168	8	144	104	**169**	**4**
846.8	5313	2	0.21622	3.57	0.03159	2.52	0.71	200.5	5.0	199	6	178	59	**201**	**5**
272.9	1821	1	0.25168	3.74	0.03414	2.05	0.55	216.4	4.4	228	8	349	71	**216**	**4**
245.2	1830	1	0.26705	7.26	0.03961	2.53	0.35	250.4	6.2	240	16	143	160	**250**	**6**
486.7	3668	1	0.32892	5.64	0.04756	3.74	0.66	299.6	11.0	289	14	202	98	**300**	**11**
208.1	1935	2	0.62872	7.94	0.08271	5.49	0.69	512.3	27.0	495	31	417	128	**512**	**27**
531.3	7335	2	0.66200	4.27	0.08289	1.00	0.23	513.4	4.9	516	17	527	91	**513**	**5**
137.6	555	1	0.58216	15.48	0.08352	3.13	0.20	517.1	15.5	466	58	220	352	**517**	**16**
266.1	5025	2	0.65082	4.36	0.08410	1.49	0.34	520.5	7.4	509	17	457	91	**521**	**7**
132.7	3116	3	0.65749	4.95	0.08412	2.99	0.61	520.7	15.0	513	20	479	87	**521**	**15**
86.06	1703	1	0.69594	4.29	0.08415	3.04	0.71	520.8	15.2	536	18	603	65	**521**	**15**
217.7	3333	1	0.69670	11.51	0.08591	3.11	0.27	531.3	15.9	537	48	560	242	**531**	**16**
45.98	887	1	0.62462	12.81	0.08678	4.23	0.33	536.5	21.7	493	50	294	277	**536**	**22**
215.7	4235	2	0.69703	3.69	0.08738	2.66	0.72	540.0	13.8	537	15	524	56	**540**	**14**
632.3	4792	2	0.69046	4.98	0.08760	3.74	0.75	541.3	19.4	533	21	498	72	**541**	**19**
180.1	4319	3	0.75134	3.00	0.08947	2.60	0.87	552.4	13.8	569	13	636	32	**552**	**14**
478.4	7693	2	0.74251	3.45	0.09071	2.33	0.68	559.7	12.5	564	15	581	55	**560**	**13**
10.43	294	2	0.50162	36.48	0.09140	5.77	0.16	563.8	31.2	413	124	-364	959	**564**	**31**
110.8	3015	1	0.75348	5.85	0.09148	3.37	0.58	564.3	18.2	570	26	594	104	**564**	**18**
935	13717	3	0.74718	3.47	0.09195	1.57	0.45	567.1	8.5	567	15	565	67	**567**	**9**
174.3	2227	1	0.73680	6.14	0.09237	4.56	0.74	569.5	24.9	561	26	524	90	**570**	**25**
14.27	385	1	0.60154	23.38	0.09328	3.80	0.16	574.9	20.9	478	89	38	558	**575**	**21**
197.6	350	2	0.58778	28.42	0.09437	3.41	0.12	581.3	18.9	469	107	-46	698	**581**	**19**
61.13	1368	2	0.78968	5.44	0.09563	2.81	0.52	588.8	15.8	591	24	600	101	**589**	**16**
278.8	3340	1	0.79614	4.92	0.09709	2.72	0.55	597.3	15.5	595	22	584	89	**597**	**16**
535.5	13078	3	0.81188	4.51	0.09783	4.20	0.93	601.7	24.1	604	21	610	35	**602**	**24**
180.7	4677	1	0.81682	4.41	0.09927	3.14	0.71	610.1	18.3	606	20	592	67	**610**	**18**
478.3	8479	2	0.84755	5.22	0.09945	2.97	0.57	611.2	17.3	623	24	667	92	**611**	**17**
360.1	6300	1	0.82768	3.44	0.10055	2.71	0.79	617.6	16.0	612	16	593	46	**618**	**16**
383.9	10069	3	0.82630	4.74	0.10089	4.05	0.86	619.6	23.9	612	22	582	53	**620**	**24**
408.2	8564	12	0.95483	12.65	0.10635	6.68	0.53	651.5	41.4	681	63	778	227	**652**	**41**
98	2218	2	0.99620	4.78	0.11364	3.97	0.83	693.8	26.1	702	24	728	56	**694**	**26**
297.2	6425	4	1.36724	5.31	0.14587	4.53	0.85	877.8	37.2	875	31	868	57	**878**	**37**
228.5	5205	1	1.87615	5.25	0.18367	4.46	0.85	1087.0	44.6	1073	35	1044	56	**1044**	**56**
200.6	4694	1	2.00092	4.48	0.18706	4.17	0.93	1105.4	42.4	1116	30	1136	32	**1136**	**32**
119.1	4275	1	2.57083	4.52	0.22426	4.02	0.89	1304.4	47.5	1292	33	1273	40	**1273**	**40**
646.4	7821	1	4.06024	5.34	0.28906	5.19	0.97	1636.8	75.1	1646	44	1659	23	**1659**	**23**
199.3	11268	3	4.03758	3.92	0.27831	3.60	0.92	1582.8	50.5	1642	32	1718	29	**1718**	**29**
253.2	12410	2	5.26327	2.87	0.32461	2.14	0.75	1812.2	33.8	1863	25	1920	34	**1920**	**34**
109.2	7872	1	5.92042	3.11	0.32954	2.45	0.79	1836.2	39.2	1964	27	2102	34	**2102**	**34**
143	13381	1	8.46118	3.08	0.42518	2.45	0.79	2283.9	47.0	2282	28	2280	32	**2280**	**32**
289.7	8072	1	12.30280	6.89	0.48956	6.53	0.95	2568.8	138.4	2628	65	2674	36	**2674**	**36**
151.6	17280	1	13.96903	7.29	0.53338	6.72	0.92	2755.7	150.7	2748	69	2742	47	**2742**	**47**
SAL1641															
62.1	177	2	0.13026	33.02	0.02616	6.07	0.18	166.5	10.0	124	39	-622	906	**166**	**10**
338.3	2033	2	0.26449	4.07	0.03663	3.03	0.75	231.9	6.9	238	9	301	62	**232**	**7**
379.3	898	2	0.27157	5.74	0.04021	2.64	0.46	254.1	6.6	244	12	147	120	**254**	**7**
221.2	875	1	0.33568	10.70	0.05079	2.89	0.27	319.3	9.0	294	27	96	245	**319**	**9**
122.7	852	1	0.39480	8.14	0.05649	3.01	0.37	354.2	10.4	338	23	227	175	**354**	**10**
565.4	3685	1	0.57863	4.11	0.07582	1.47	0.36	471.1	6.7	464	15	426	86	**471**	**7**
211.2	286	1	0.46399	24.52	0.07640	4.01	0.16	474.6	18.4	387	79	-108	603	**475**	**18**
1176	9665	1	0.58647	2.50	0.07651	1.64	0.66	475.3	7.5	469	9	436	42	**475**	**8**

			Isotopic ratios					Apparent ages (Ma)							
U	206Pb	U/Th	207Pb*		206Pb*		error	206Pb*		207Pb*		206Pb*		Best age	
(ppm)	204Pb		235U	(%)	238U	(%)	corr.	238U	±(Ma)	235U	±(Ma)	207Pb*	±(Ma)		±(Ma)
SAL1641															
945.7	8665	1	0.61753	2.85	0.07762	2.01	0.70	481.9	9.3	488	11	518	44	**482**	**9**
219.4	3246	1	0.62342	2.70	0.07775	1.88	0.70	482.7	8.7	492	11	536	42	**483**	**9**
241.9	3094	1	0.61541	3.27	0.07791	1.56	0.48	483.7	7.2	487	13	503	63	**484**	**7**
760.4	7560	1	0.60485	3.92	0.07817	2.54	0.65	485.2	11.9	480	15	457	66	**485**	**12**
159.9	2469	2	0.63360	5.06	0.07855	1.46	0.29	487.5	6.8	498	20	549	106	**487**	**7**
386.9	4883	3	0.61998	2.17	0.07915	1.77	0.82	491.0	8.4	490	8	484	28	**491**	**8**
1094	6741	4	0.63798	2.86	0.08011	1.98	0.69	496.8	9.5	501	11	521	45	**497**	**9**
427.1	4501	3	0.64054	2.76	0.08051	2.21	0.80	499.2	10.6	503	11	518	36	**499**	**11**
107.5	1503	2	0.62376	4.52	0.08073	2.68	0.59	500.5	12.9	492	18	454	81	**500**	**13**
617	10551	4	0.63535	1.72	0.08125	1.08	0.63	503.6	5.2	499	7	480	30	**504**	**5**
141.9	1710	1	0.63004	5.95	0.08212	3.73	0.63	508.8	18.2	496	23	438	103	**509**	**18**
239.7	2844	2	0.65986	3.44	0.08227	1.93	0.56	509.6	9.5	515	14	536	62	**510**	**9**
282.6	3904	1	0.65251	3.10	0.08237	2.10	0.68	510.3	10.3	510	12	509	50	**510**	**10**
92.23	1208	1	0.65133	4.83	0.08277	2.75	0.57	512.7	13.5	509	19	494	88	**513**	**14**
510.2	5846	2	0.66162	1.57	0.08283	1.00	0.64	513.0	4.9	516	6	527	27	**513**	**5**
48.34	647	2	0.62064	8.59	0.08301	2.82	0.33	514.0	14.0	490	33	381	183	**514**	**14**
127.5	1924	2	0.66506	4.18	0.08354	2.77	0.66	517.2	13.8	518	17	520	69	**517**	**14**
105	1662	1	0.68342	4.93	0.08355	2.80	0.57	517.3	13.9	529	20	579	88	**517**	**14**
479	7478	2	0.67348	1.79	0.08362	1.05	0.59	517.7	5.2	523	7	545	32	**518**	**5**
290.8	2695	2	0.67782	3.98	0.08384	2.60	0.65	519.0	13.0	525	16	553	66	**519**	**13**
292.2	4212	7	0.67405	3.71	0.08386	2.35	0.63	519.1	11.7	523	15	541	63	**519**	**12**
347	6613	2	0.70046	3.08	0.08396	1.88	0.61	519.7	9.4	539	13	622	53	**520**	**9**
359.3	3954	1	0.66530	2.00	0.08402	1.26	0.63	520.1	6.3	518	8	508	34	**520**	**6**
147.6	1711	3	0.68294	3.72	0.08405	1.89	0.51	520.3	9.4	529	15	565	70	**520**	**9**
853	1024	1	0.63205	7.53	0.08461	1.76	0.23	523.6	8.8	497	30	378	165	**524**	**9**
355	3861	2	0.69515	3.69	0.08472	1.90	0.52	524.3	9.6	536	15	586	69	**524**	**10**
197.9	2654	1	0.66967	2.84	0.08485	1.63	0.57	525.0	8.2	521	12	501	51	**525**	**8**
226	2585	2	0.67619	3.75	0.08533	1.77	0.47	527.9	9.0	524	15	510	73	**528**	**9**
561.3	5134	4	0.71757	3.85	0.08578	2.25	0.59	530.5	11.5	549	16	628	67	**531**	**11**
289.5	4885	2	0.72365	2.90	0.08630	2.32	0.80	533.6	11.9	553	12	633	38	**534**	**12**
403.1	1879	2	0.67509	5.04	0.08652	3.58	0.71	534.9	18.4	524	21	476	78	**535**	**18**
476.4	2139	2	0.69276	5.97	0.08792	5.18	0.87	543.2	27.0	534	25	497	65	**543**	**27**
172.7	3252	2	0.73936	3.35	0.08858	2.72	0.81	547.1	14.3	562	14	623	42	**547**	**14**
278.6	3621	1	0.74977	5.07	0.08939	2.73	0.54	551.9	14.4	568	22	633	92	**552**	**14**
1081	19931	58	0.74685	2.95	0.09029	1.65	0.56	557.3	8.8	566	13	603	53	**557**	**9**
152.2	2468	1	0.74127	2.56	0.09042	1.78	0.69	558.0	9.5	563	11	584	40	**558**	**9**
226.1	4502	18	0.76411	2.68	0.09131	1.63	0.61	563.3	8.8	576	12	628	46	**563**	**9**
344.9	6281	2	0.75830	2.19	0.09160	1.27	0.58	565.0	6.9	573	10	605	39	**565**	**7**
155.8	2103	0	0.76938	2.51	0.09484	1.35	0.54	584.1	7.5	579	11	561	46	**584**	**8**
390.8	1927	2	0.79271	6.91	0.09490	2.33	0.34	584.4	13.0	593	31	624	140	**584**	**13**
214	3053	0	0.77412	3.41	0.09544	1.80	0.53	587.7	10.1	582	15	561	63	**588**	**10**
271.6	3155	2	0.80869	4.03	0.09562	2.88	0.72	588.7	16.2	602	18	651	60	**589**	**16**
364.7	4810	5	0.76671	4.54	0.09572	1.97	0.43	589.3	11.1	578	20	533	90	**589**	**11**
114.7	2502	2	0.79211	6.83	0.09576	1.97	0.29	589.5	11.1	592	31	603	142	**590**	**11**
416.7	6141	2	0.80433	2.63	0.09712	2.03	0.77	597.5	11.6	599	12	606	36	**598**	**12**
436.2	8028	2	0.81920	4.56	0.09732	1.96	0.43	598.7	11.2	608	21	641	88	**599**	**11**
55.2	1077	1	0.85567	7.11	0.09837	3.31	0.47	604.9	19.1	628	33	711	134	**605**	**19**
24.85	502	2	0.75532	10.85	0.09871	4.85	0.45	606.8	28.1	571	47	432	217	**607**	**28**
396	5364	2	0.83845	2.51	0.09882	2.17	0.86	607.5	12.6	618	12	658	27	**607**	**13**
938.7	12607	7	0.82467	4.38	0.09916	3.04	0.70	609.5	17.7	611	20	615	68	**609**	**18**
99.28	2012	2	0.85628	3.44	0.10083	1.27	0.37	619.3	7.5	628	16	660	69	**619**	**7**
140.5	2234	3	0.84907	3.48	0.10202	2.65	0.76	626.3	15.8	624	16	616	49	**626**	**16**
78.26	1534	2	0.88258	4.64	0.10406	3.57	0.77	638.2	21.7	642	22	657	64	**638**	**22**
756.3	13995	2	0.87434	3.00	0.10421	2.47	0.82	639.0	15.0	638	14	634	37	**639**	**15**
533.1	2759	3	0.96625	5.06	0.11233	1.65	0.33	686.3	10.7	687	25	687	102	**686**	**11**
91.25	705	1	0.98114	4.28	0.11560	2.87	0.67	705.2	19.2	694	22	659	68	**705**	**19**
697.7	10218	3	1.03381	4.60	0.11831	2.85	0.62	720.9	19.4	721	24	721	77	**721**	**19**
173.1	4145	2	1.05272	3.31	0.11872	2.61	0.79	723.2	17.9	730	17	752	43	**723**	**18**
194.9	3783	2	1.09786	4.47	0.11880	3.86	0.86	723.7	26.4	752	24	838	47	**724**	**26**
382.4	1599	4	1.11351	4.78	0.12286	3.91	0.82	747.0	27.5	760	26	798	58	**747**	**28**
203.1	5351	6	1.21028	3.74	0.12867	2.92	0.78	780.3	21.4	805	21	875	48	**780**	**21**

			Isotopic ratios					Apparent ages (Ma)							
U	206Pb	U/Th	207Pb*		206Pb*		error	206Pb*		207Pb*		206Pb*		Best age	
(ppm)	204Pb		235U	(%)	238U	(%)	corr.	238U	±(Ma)	235U	±(Ma)	207Pb*	±(Ma)		±(Ma)
SAL1641															
947.8	6422	0	1.18874	7.05	0.12965	5.11	0.73	785.8	37.8	795	39	822	101	**786**	**38**
262.3	3429	2	1.42997	3.43	0.14582	2.39	0.70	877.5	19.6	902	21	961	50	**877**	**20**
77	1864	4	1.42993	4.35	0.14629	2.11	0.49	880.1	17.4	902	26	954	78	**880**	**17**
831.3	1012	3	1.34532	4.74	0.14661	3.45	0.73	881.9	28.4	866	28	824	68	**882**	**28**
318	2365	4	1.45580	6.18	0.15214	5.76	0.93	913.0	49.0	912	37	911	46	**913**	**49**
755.4	13889	17	1.57409	3.90	0.15634	2.12	0.54	936.4	18.5	960	24	1015	66	**936**	**19**
242.7	4593	2	1.57414	3.44	0.15800	2.27	0.66	945.7	20.0	960	21	993	53	**946**	**20**
110	2966	2	1.70766	4.37	0.15886	2.33	0.53	950.4	20.6	1011	28	1146	73	**950**	**21**
424.6	10705	2	1.67056	4.21	0.16241	3.15	0.75	970.2	28.4	997	27	1058	56	**970**	**28**
482.5	11136	10	1.68627	3.45	0.16533	1.73	0.50	986.3	15.9	1003	22	1041	60	**986**	**16**
316.9	5465	6	1.71307	4.91	0.16556	2.86	0.58	987.6	26.2	1013	31	1070	80	**988**	**26**
222.5	5300	7	1.78965	3.14	0.17246	2.28	0.73	1025.7	21.6	1042	20	1075	43	**1026**	**22**
250.9	2579	1	1.80049	4.06	0.17698	1.53	0.38	1050.5	14.8	1046	26	1036	76	**1050**	**15**
341.6	11376	3	1.81368	4.02	0.17768	1.86	0.46	1054.3	18.0	1050	26	1042	72	**1054**	**18**
248.7	4790	2	1.82992	3.75	0.17839	2.98	0.80	1058.2	29.1	1056	25	1052	46	**1058**	**29**
321	9374	2	1.86317	2.78	0.17912	2.25	0.81	1062.2	22.0	1068	18	1080	33	**1062**	**22**
832.1	21429	1	1.91608	2.82	0.18268	1.45	0.51	1081.6	14.4	1087	19	1097	48	**1082**	**14**
191.8	6563	2	1.89315	2.35	0.18312	1.94	0.83	1084.0	19.4	1079	16	1068	26	**1084**	**19**
308.6	5906	2	2.00892	4.17	0.18985	2.18	0.52	1120.6	22.4	1119	28	1115	71	**1115**	**71**
192.7	3998	1	2.24947	1.88	0.20504	1.00	0.53	1202.3	11.0	1197	13	1186	31	**1186**	**31**
146.4	4596	2	2.23111	3.61	0.20143	1.56	0.43	1183.0	16.9	1191	25	1205	64	**1205**	**64**
149.2	5539	2	3.55935	2.98	0.26041	2.13	0.71	1491.9	28.3	1541	24	1608	39	**1608**	**39**
121.9	4762	2	4.08691	3.49	0.29420	2.03	0.58	1662.5	29.7	1652	28	1638	53	**1638**	**53**
852.4	4535	4	3.82040	9.55	0.27242	8.80	0.92	1553.1	121.5	1597	77	1656	69	**1656**	**69**
332.8	17917	2	4.70626	2.30	0.30437	1.92	0.83	1712.9	28.9	1768	19	1834	23	**1834**	**23**
308.1	18614	2	10.29276	2.34	0.46527	1.46	0.62	2462.8	29.9	2461	22	2460	31	**2460**	**31**
686.8	6808	2	12.36327	6.52	0.50054	6.12	0.94	2616.1	131.7	2632	61	2645	37	**2645**	**37**
419.9	17365	1	18.82551	2.18	0.54527	1.49	0.68	2805.5	33.8	3033	21	3187	25	**3187**	**25**
225	16028	2	20.98609	4.26	0.57344	3.82	0.90	2921.9	89.8	3138	41	3279	29	**3279**	**29**
BN															
177.9	1749	2	0.28631	6.35	0.04043	1.41	0.22	255.5	3.5	256	14	257	142	**256**	**4**
92.69	1400	2	0.65987	5.31	0.08504	2.83	0.53	526.1	14.3	515	21	463	100	**526**	**14**
290.6	5606	3	0.70374	4.03	0.08546	1.04	0.26	528.6	5.3	541	17	594	84	**529**	**5**
22.24	664	0	0.68714	9.48	0.08860	3.94	0.42	547.3	20.7	531	39	462	191	**547**	**21**
158.6	3258	1	0.72720	3.86	0.08898	2.52	0.65	549.5	13.3	555	17	577	64	**550**	**13**
418.1	7031	12	0.74032	2.71	0.08898	1.02	0.38	549.5	5.4	563	12	616	54	**550**	**5**
74.16	1497	1	0.71071	5.02	0.08932	4.13	0.82	551.5	21.8	545	21	519	63	**552**	**22**
62.91	1329	1	0.72394	5.44	0.09012	4.08	0.75	556.3	21.7	553	23	540	79	**556**	**22**
231.2	4470	3	0.72335	4.39	0.09021	3.16	0.72	556.8	16.8	553	19	536	67	**557**	**17**
364.6	6961	2	0.74807	4.00	0.09061	1.86	0.46	559.2	10.0	567	17	599	77	**559**	**10**
816.6	12149	3	0.73664	2.93	0.09066	1.98	0.68	559.5	10.6	560	13	564	47	**559**	**11**
114.4	2768	1	0.73755	3.60	0.09078	1.73	0.48	560.1	9.3	561	15	564	69	**560**	**9**
1062	19837	18	0.72481	5.12	0.09078	2.28	0.45	560.2	12.2	554	22	526	101	**560**	**12**
276.1	7033	4	0.78221	3.97	0.09118	2.23	0.56	562.5	12.0	587	18	682	70	**563**	**12**
73.15	1451	0	0.74432	3.68	0.09194	3.51	0.95	567.0	19.1	565	16	556	24	**567**	**19**
290.3	4777	3	0.75709	5.05	0.09211	2.12	0.42	568.0	11.5	572	22	590	99	**568**	**12**
118.3	3416	2	0.80087	5.77	0.09221	2.31	0.40	568.6	12.6	597	26	708	113	**569**	**13**
128.4	3047	2	0.75151	4.42	0.09236	3.28	0.74	569.5	17.9	569	19	568	65	**569**	**18**
82.85	2680	6	0.74372	6.33	0.09260	3.62	0.57	570.9	19.8	565	27	539	114	**571**	**20**
47.61	1434	1	0.71096	8.07	0.09275	4.57	0.57	571.8	25.0	545	34	436	148	**572**	**25**
216.5	4627	4	0.73465	5.93	0.09281	2.36	0.40	572.1	12.9	559	25	507	120	**572**	**13**
82.1	1501	1	0.72812	6.07	0.09328	3.76	0.62	574.9	20.7	555	26	477	105	**575**	**21**
145.3	3050	1	0.79448	6.99	0.09375	4.09	0.58	577.7	22.6	594	31	656	122	**578**	**23**
78.65	2027	1	0.78190	5.13	0.09401	3.41	0.66	579.2	18.9	587	23	615	83	**579**	**19**
145.6	3281	1	0.79157	2.57	0.09434	1.07	0.42	581.1	5.9	592	12	634	50	**581**	**6**
284.8	6466	16	0.77547	2.13	0.09462	1.03	0.48	582.8	5.7	583	9	583	40	**583**	**6**
450.4	12712	1	0.79991	4.35	0.09502	2.09	0.48	585.1	11.7	597	20	641	82	**585**	**12**
301.1	6129	8	0.77571	3.50	0.09504	1.64	0.47	585.3	9.2	583	16	574	67	**585**	**9**
109.2	2903	1	0.81002	11.54	0.09537	2.07	0.18	587.2	11.6	602	52	660	244	**587**	**12**
788.5	22514	5	0.78538	3.71	0.09568	1.74	0.47	589.0	9.8	589	17	587	71	**589**	**10**
111.1	2008	0	0.76839	4.21	0.09568	2.81	0.67	589.1	15.8	579	19	539	69	**589**	**16**

			Isotopic ratios					Apparent ages (Ma)							
U	206Pb	U/Th	207Pb*		206Pb*		error	206Pb*		207Pb*		206Pb*		Best age	
(ppm)	204Pb		235U	(%)	238U	(%)	corr.	238U	±(Ma)	235U	±(Ma)	207Pb*	±(Ma)		±(Ma)
BN															
596.7	11961	3	0.79307	3.72	0.09617	2.48	0.67	591.9	14.0	593	17	597	60	**592**	**14**
296	8883	7	0.78950	2.78	0.09627	1.57	0.56	592.5	8.9	591	12	585	50	**593**	**9**
605.4	13865	2	0.81714	4.63	0.09642	2.27	0.49	593.4	12.8	606	21	656	87	**593**	**13**
360.2	7490	1	0.80865	4.50	0.09647	1.17	0.26	593.7	6.7	602	20	632	94	**594**	**7**
33.69	860	2	0.82844	7.45	0.09651	5.34	0.72	593.9	30.3	613	34	683	111	**594**	**30**
184.3	3416	1	0.81407	3.56	0.09689	2.19	0.61	596.2	12.4	605	16	637	61	**596**	**12**
79.43	2402	4	0.82615	4.28	0.09697	2.70	0.63	596.6	15.4	611	20	667	71	**597**	**15**
20.84	1928	0	0.78134	9.33	0.09760	6.80	0.73	600.3	39.0	586	42	532	140	**600**	**39**
400.5	7043	1	0.83080	2.93	0.09766	1.67	0.57	600.7	9.6	614	13	664	51	**601**	**10**
818.7	16426	3	0.80327	2.54	0.09775	1.27	0.50	601.2	7.3	599	12	589	48	**601**	**7**
201.9	4638	2	0.80849	3.66	0.09802	1.10	0.30	602.8	6.3	602	17	597	76	**603**	**6**
392.2	2708	4	0.82363	3.93	0.09868	2.45	0.62	606.7	14.2	610	18	623	66	**607**	**14**
127.7	2896	2	0.80369	3.94	0.09879	2.92	0.74	607.3	16.9	599	18	567	58	**607**	**17**
102.8	2458	1	0.88227	4.46	0.09882	1.83	0.41	607.5	10.6	642	21	766	86	**608**	**11**
267	5370	1	0.83097	4.92	0.09902	2.79	0.57	608.6	16.2	614	23	635	87	**609**	**16**
73.82	1544	2	0.78920	8.16	0.09905	6.50	0.80	608.8	37.8	591	37	522	108	**609**	**38**
73.17	1801	2	0.89008	4.93	0.09958	2.35	0.48	611.9	13.7	646	24	769	91	**612**	**14**
272.4	4581	14	0.86550	5.96	0.09974	4.23	0.71	612.9	24.7	633	28	706	89	**613**	**25**
281.5	4154	1	0.82334	4.05	0.09999	2.68	0.66	614.3	15.7	610	19	594	66	**614**	**16**
278.3	5352	3	0.87228	3.61	0.10175	2.02	0.56	624.7	12.0	637	17	680	64	**625**	**12**
640.5	9035	33	0.88675	3.29	0.10253	3.10	0.94	629.2	18.6	645	16	699	24	**629**	**19**
435.9	6910	3	0.89594	2.35	0.10563	1.32	0.56	647.3	8.1	650	11	657	42	**647**	**8**
481.1	5925	13	0.97250	6.32	0.11333	5.51	0.87	692.1	36.1	690	32	682	66	**692**	**36**
329.3	9636	2	1.08212	10.48	0.11781	8.45	0.81	718.0	57.4	745	55	826	129	**718**	**57**
122.1	3176	2	1.34679	4.13	0.13352	2.36	0.57	807.9	17.9	866	24	1018	69	**808**	**18**
48.23	1352	1	1.33873	5.31	0.13814	3.93	0.74	834.2	30.8	863	31	937	73	**834**	**31**
289.3	3102	2	1.39700	10.23	0.13826	3.45	0.34	834.8	27.0	888	61	1022	195	**835**	**27**
336.5	8054	3	1.28708	3.69	0.13927	3.19	0.86	840.5	25.1	840	21	839	39	**841**	**25**
433.9	12467	4	1.29517	4.94	0.14011	2.60	0.53	845.3	20.6	844	28	839	88	**845**	**21**
209.6	5950	2	1.36045	3.38	0.14664	2.55	0.75	882.1	21.0	872	20	847	46	**882**	**21**
174.8	5018	2	1.34411	6.28	0.14763	2.57	0.41	887.7	21.3	865	37	807	120	**888**	**21**
185	4865	1	1.46081	4.55	0.15101	2.73	0.60	906.6	23.1	914	27	933	75	**907**	**23**
94.2	3917	3	1.54729	7.47	0.15193	4.47	0.60	911.8	38.0	949	46	1038	121	**912**	**38**
188.8	7332	3	1.53679	4.06	0.15461	2.14	0.53	926.7	18.4	945	25	989	70	**927**	**18**
389.2	9264	10	1.55168	5.38	0.15501	3.19	0.59	929.0	27.6	951	33	1003	88	**929**	**28**
306.4	11196	3	1.72119	3.90	0.16752	2.72	0.70	998.4	25.2	1016	25	1056	56	**998**	**25**
115.7	8059	5	1.73558	4.83	0.16876	1.00	0.21	1005.3	9.3	1022	31	1057	95	**1005**	**9**
228.2	7300	2	1.72144	3.87	0.17229	2.13	0.55	1024.7	20.2	1017	25	999	66	**1025**	**20**
38.58	1164	1	1.80188	4.47	0.17718	3.12	0.70	1051.5	30.3	1046	29	1035	65	**1052**	**30**
142.1	6210	1	1.84174	3.19	0.17798	1.93	0.60	1055.9	18.8	1060	21	1070	51	**1056**	**19**
767.8	31814	2	1.88419	4.64	0.18363	3.10	0.67	1086.8	31.0	1076	31	1053	70	**1087**	**31**
307.3	1741	1	1.97835	7.92	0.18244	2.99	0.38	1080.3	29.8	1108	53	1163	146	**1163**	**146**
237	11026	1	2.19819	4.41	0.20120	3.12	0.71	1181.7	33.7	1180	31	1178	62	**1178**	**62**
274.2	7369	1	2.52550	3.33	0.21979	1.19	0.36	1280.8	13.9	1279	24	1277	61	**1277**	**61**
185.8	5867	2	2.48738	3.53	0.21564	1.23	0.35	1258.8	14.1	1268	26	1285	65	**1285**	**65**
328.9	3545	8	1.98593	10.16	0.16907	9.54	0.94	1007.0	89.0	1111	69	1320	67	**1320**	**67**
141.4	4553	13	2.45631	3.98	0.20867	2.37	0.60	1221.7	26.4	1259	29	1324	62	**1324**	**62**
277.2	7731	3	2.79058	2.89	0.23206	1.96	0.68	1345.3	23.8	1353	22	1365	41	**1365**	**41**
110.5	5552	2	2.59332	6.76	0.20896	4.43	0.66	1223.3	49.3	1299	50	1426	98	**1426**	**98**
205.2	10080	2	3.25624	4.55	0.25835	3.64	0.80	1481.4	48.1	1471	35	1455	52	**1455**	**52**
57.15	5400	2	3.08758	3.15	0.24179	2.55	0.81	1396.0	32.0	1430	24	1480	35	**1480**	**35**
147.3	8135	1	3.42189	2.73	0.26400	1.93	0.71	1510.3	26.0	1509	21	1508	36	**1508**	**36**
130	6152	1	3.80241	3.70	0.28356	3.02	0.82	1609.3	43.0	1593	30	1572	40	**1572**	**40**
429.8	23485	1	4.03735	3.99	0.29158	1.03	0.26	1649.4	15.0	1642	32	1632	72	**1632**	**72**
258.7	7578	2	2.67798	6.02	0.16675	5.36	0.89	994.2	49.4	1322	45	1903	49	**1903**	**49**
360.4	22828	3	7.65967	4.95	0.39960	4.42	0.89	2167.2	81.3	2192	45	2215	39	**2215**	**39**
169	15928	1	8.04431	2.51	0.41388	2.16	0.86	2232.7	40.7	2236	23	2239	22	**2239**	**22**
151.9	10928	3	6.24669	5.51	0.31930	3.40	0.62	1786.3	53.0	2011	48	2250	75	**2250**	**75**
243.3	14183	1	7.02273	3.67	0.34946	2.29	0.62	1932.0	38.2	2114	33	2297	49	**2297**	**49**
396	38552	7	8.87722	3.17	0.43633	1.70	0.54	2334.2	33.3	2325	29	2318	46	**2318**	**46**

			Isotopic ratios					Apparent ages (Ma)							
U	206Pb	U/Th	207Pb*		206Pb*		error	206Pb*		207Pb*		206Pb*		Best age	
(ppm)	204Pb		235U	(%)	238U	(%)	corr.	238U	±(Ma)	235U	±(Ma)	207Pb*	±(Ma)		±(Ma)
BN															
123.1	9864	2	9.37953	2.38	0.43496	1.54	0.65	2328.0	30.2	2376	22	2417	31	**2417**	**31**
211	9645	2	7.54738	4.96	0.33424	3.26	0.66	1858.9	52.6	2179	45	2495	63	**2495**	**63**
253.8	23382	4	10.44902	3.95	0.44839	2.62	0.66	2388.1	52.3	2475	37	2548	49	**2548**	**49**
93.49	8569	2	12.17916	5.17	0.48540	3.02	0.58	2550.8	63.6	2618	49	2671	70	**2671**	**70**
107.3	9421	1	24.31645	2.81	0.64496	1.76	0.63	3208.5	44.4	3281	27	3326	34	**3326**	**34**
174	19786	1	24.84320	3.52	0.65388	1.91	0.54	3243.3	48.6	3302	34	3338	46	**3338**	**46**
BR															
63.46	1248	1	0.61762	4.92	0.07685	3.84	0.78	477.3	17.7	488	19	540	67	**477**	**18**
220.2	4418	1	0.63860	4.93	0.07890	4.14	0.84	489.5	19.5	501	20	556	58	**490**	**20**
195.9	4279	1	0.68975	3.49	0.08144	2.39	0.68	504.7	11.6	533	14	654	55	**505**	**12**
269.6	4963	1	0.68273	3.44	0.08382	2.75	0.80	518.9	13.7	528	14	570	45	**519**	**14**
335.2	6269	1	0.67755	4.70	0.08465	3.55	0.76	523.8	17.9	525	19	532	67	**524**	**18**
275.8	5373	1	0.68661	1.88	0.08478	1.53	0.81	524.6	7.7	531	8	557	24	**525**	**8**
192.8	3039	0	0.67606	4.37	0.08489	3.92	0.90	525.3	19.8	524	18	521	43	**525**	**20**
1025	16278	2	0.68010	3.16	0.08507	2.99	0.95	526.3	15.1	527	13	529	23	**526**	**15**
291.8	7037	1	0.71340	3.00	0.08618	2.15	0.72	532.9	11.0	547	13	605	45	**533**	**11**
287.5	6411	2	0.71197	2.23	0.08621	1.78	0.80	533.1	9.1	546	9	600	29	**533**	**9**
91.39	2024	1	0.71876	5.83	0.08623	3.11	0.53	533.2	15.9	550	25	620	107	**533**	**16**
1272	11376	76	0.69191	3.11	0.08651	2.59	0.83	534.9	13.3	534	13	530	38	**535**	**13**
284.5	1471	0	0.71189	9.76	0.08705	4.04	0.41	538.1	20.9	546	41	579	193	**538**	**21**
85.59	1798	0	0.71992	4.70	0.08774	3.37	0.72	542.2	17.5	551	20	586	71	**542**	**18**
342	5438	1	0.70776	2.47	0.08789	1.82	0.74	543.1	9.5	543	10	545	37	**543**	**9**
215.8	2813	1	0.71428	4.58	0.08919	3.24	0.71	550.7	17.1	547	19	533	71	**551**	**17**
376.5	7864	1	0.72694	4.34	0.08967	3.26	0.75	553.6	17.3	555	19	560	62	**554**	**17**
50.21	605	1	0.79373	28.25	0.08977	4.72	0.17	554.2	25.0	593	128	746	600	**554**	**25**
362.5	8012	3	0.73696	1.60	0.08991	1.00	0.63	555.0	5.3	561	7	583	27	**555**	**5**
349.7	3546	1	0.75928	5.31	0.09224	3.77	0.71	568.8	20.5	574	23	593	81	**569**	**21**
175	3786	1	0.75147	3.96	0.09247	3.23	0.81	570.1	17.6	569	17	565	50	**570**	**18**
340.1	6774	2	0.77139	3.13	0.09260	2.55	0.81	570.9	13.9	581	14	619	39	**571**	**14**
627.4	6037	1	0.75453	3.15	0.09283	2.91	0.92	572.2	15.9	571	14	565	26	**572**	**16**
359.8	4293	4	0.73623	4.15	0.09300	2.35	0.57	573.3	12.9	560	18	507	75	**573**	**13**
57.9	1269	2	0.75879	5.82	0.09326	3.41	0.59	574.8	18.7	573	26	567	103	**575**	**19**
325.8	4778	2	0.78238	3.14	0.09418	2.82	0.90	580.2	15.6	587	14	612	30	**580**	**16**
133.7	3150	1	0.80192	2.49	0.09423	1.92	0.77	580.5	10.7	598	11	664	34	**581**	**11**
956	31460	2	0.79073	2.79	0.09470	2.58	0.93	583.3	14.4	592	12	623	23	**583**	**14**
279.1	6560	4	0.76020	5.17	0.09490	4.46	0.86	584.5	24.9	574	23	533	57	**584**	**25**
268	3967	1	0.77862	3.24	0.09581	2.66	0.82	589.8	15.0	585	14	565	40	**590**	**15**
125.2	2818	0	0.80156	2.21	0.09617	1.91	0.86	591.9	10.8	598	10	620	24	**592**	**11**
137	3607	1	0.81238	3.64	0.09687	2.93	0.81	596.0	16.7	604	17	633	46	**596**	**17**
76.18	1704	1	0.88376	5.68	0.09713	3.05	0.54	597.6	17.4	643	27	806	100	**598**	**17**
129	2754	1	0.80601	3.23	0.09753	2.05	0.63	599.9	11.8	600	15	601	54	**600**	**12**
260.3	4623	0	0.80103	3.41	0.09799	2.96	0.87	602.6	17.0	597	15	578	37	**603**	**17**
204.1	3971	1	0.81536	6.05	0.09811	2.72	0.45	603.3	15.7	605	28	613	117	**603**	**16**
784.4	13664	0	0.81966	3.07	0.09831	2.52	0.82	604.5	14.6	608	14	620	38	**604**	**15**
463.4	6117	2	0.81913	2.98	0.09860	2.66	0.89	606.2	15.4	608	14	613	29	**606**	**15**
83.32	1971	1	0.84897	6.25	0.09933	5.54	0.89	610.5	32.3	624	29	674	62	**610**	**32**
90.17	2503	1	0.85027	5.25	0.09972	3.40	0.65	612.8	19.9	625	25	668	86	**613**	**20**
104	2687	0	0.88059	4.94	0.10143	3.42	0.69	622.8	20.3	641	23	707	76	**623**	**20**
712.7	10633	8	0.86204	3.50	0.10208	2.93	0.84	626.6	17.5	631	16	648	41	**627**	**17**
185.9	4403	1	0.86600	4.71	0.10298	4.28	0.91	631.8	25.7	633	22	639	42	**632**	**26**
64.81	1500	1	0.87487	3.83	0.10442	2.13	0.56	640.3	13.0	638	18	631	69	**640**	**13**
200.3	3769	1	0.96560	3.75	0.10847	2.96	0.79	663.9	18.7	686	19	760	48	**664**	**19**
195.9	6329	1	0.97385	4.07	0.11130	2.88	0.71	680.3	18.6	690	20	724	61	**680**	**19**
604.1	8938	3	1.00992	3.64	0.11405	2.21	0.61	696.2	14.6	709	19	749	61	**696**	**15**
854.8	21719	5	1.09902	3.29	0.12369	2.11	0.64	751.8	15.0	753	17	756	53	**752**	**15**
142.7	4414	0	1.17017	5.37	0.12899	5.01	0.93	782.1	36.9	787	29	800	40	**782**	**37**
153	1213	1	1.11351	6.02	0.12947	3.36	0.56	784.8	24.8	760	32	687	107	**785**	**25**
117.4	2579	1	1.19169	3.82	0.13002	3.24	0.85	788.0	24.0	797	21	821	42	**788**	**24**
289.9	5417	1	1.30521	4.01	0.13571	3.66	0.91	820.3	28.2	848	23	921	34	**820**	**28**
242.1	8718	2	1.37586	4.97	0.13897	4.13	0.83	838.8	32.5	879	29	980	57	**839**	**32**
684.8	20487	2	1.31252	3.30	0.13953	2.74	0.83	842.0	21.7	851	19	875	38	**842**	**22**

			Isotopic ratios					Apparent ages (Ma)							
U	206Pb	U/Th	207Pb*		206Pb*		error	206Pb*		207Pb*		206Pb*		Best age	
(ppm)	204Pb		235U	(%)	238U	(%)	corr.	238U	±(Ma)	235U	±(Ma)	207Pb*	±(Ma)		±(Ma)
BR															
313.9	8841	1	1.40451	3.70	0.14440	2.65	0.72	869.5	21.6	891	22	944	53	**870**	**22**
87.31	2632	1	1.42910	3.14	0.14800	2.08	0.66	889.7	17.3	901	19	929	48	**890**	**17**
656.8	27746	3	1.49630	3.37	0.14967	2.33	0.69	899.1	19.5	929	21	1000	49	**899**	**20**
76.01	2812	1	1.52968	5.12	0.15240	3.02	0.59	914.4	25.8	942	31	1008	84	**914**	**26**
102.8	3049	1	1.44614	4.34	0.15478	2.56	0.59	927.7	22.1	908	26	861	73	**928**	**22**
372.2	1883	7	1.51707	5.29	0.15634	1.63	0.31	936.4	14.2	937	32	939	103	**936**	**14**
261.8	6461	1	1.60604	2.78	0.15773	2.52	0.91	944.1	22.2	973	17	1037	24	**944**	**22**
355.3	15260	1	1.54225	3.10	0.15811	2.66	0.86	946.3	23.4	947	19	950	33	**946**	**23**
345.2	12578	2	1.59199	4.22	0.15825	3.68	0.87	947.0	32.4	967	26	1013	42	**947**	**32**
273.5	8915	9	1.59566	3.69	0.15836	3.37	0.92	947.7	29.7	969	23	1016	30	**948**	**30**
57.41	2356	1	1.56789	3.41	0.15870	2.05	0.60	949.5	18.1	958	21	976	56	**950**	**18**
228.6	8638	1	1.55267	2.46	0.15966	2.01	0.82	954.9	17.8	952	15	944	29	**955**	**18**
610.5	17952	2	1.58970	3.70	0.16111	3.29	0.89	963.0	29.4	966	23	974	35	**963**	**29**
79.41	3353	1	1.66161	2.47	0.16543	2.15	0.87	986.9	19.7	994	16	1010	25	**987**	**20**
288	8305	1	1.68741	4.78	0.16797	4.46	0.93	1000.9	41.4	1004	30	1010	35	**1001**	**41**
610.6	9904	6	1.76187	3.80	0.17359	2.88	0.76	1031.9	27.4	1032	25	1031	50	**1032**	**27**
546.7	21685	2	1.90138	5.64	0.18109	4.49	0.80	1072.9	44.4	1082	38	1099	68	**1073**	**44**
327.7	9371	1	1.98513	2.78	0.18584	2.57	0.92	1098.8	25.9	1110	19	1133	21	**1133**	**21**
142.7	4782	1	2.07894	4.24	0.19397	4.01	0.95	1142.8	42.0	1142	29	1140	27	**1140**	**27**
232.3	9037	6	2.08099	4.05	0.19393	3.35	0.83	1142.6	35.1	1143	28	1142	45	**1142**	**45**
338.5	8887	6	2.07008	4.24	0.19276	3.86	0.91	1136.3	40.2	1139	29	1144	35	**1144**	**35**
264.1	8323	3	2.01586	4.83	0.18643	4.31	0.89	1102.0	43.7	1121	33	1158	43	**1158**	**43**
248.1	7776	1	2.23703	3.37	0.20229	3.06	0.91	1187.6	33.2	1193	24	1202	28	**1202**	**28**
374.7	13478	1	2.35965	1.67	0.20828	1.00	0.60	1219.7	11.1	1230	12	1249	26	**1249**	**26**
254.3	5131	1	2.50146	4.30	0.21970	4.00	0.93	1280.3	46.4	1272	31	1259	31	**1259**	**31**
238.1	11161	2	2.47786	3.07	0.21737	2.47	0.80	1268.0	28.4	1266	22	1262	36	**1262**	**36**
211.9	8375	1	2.41475	5.59	0.21115	4.86	0.87	1235.0	54.6	1247	40	1268	54	**1268**	**54**
60.18	1265	1	2.19551	5.01	0.19095	4.53	0.90	1126.5	46.9	1180	35	1278	42	**1278**	**42**
468.3	15645	2	2.91249	3.90	0.23615	3.08	0.79	1366.7	37.9	1385	29	1414	46	**1414**	**46**
169.7	1883	1	3.12393	4.63	0.24577	4.19	0.90	1416.6	53.3	1439	36	1471	37	**1471**	**37**
64.93	2957	1	3.36096	3.47	0.26360	1.78	0.51	1508.3	23.9	1495	27	1477	56	**1477**	**56**
310.8	3040	3	4.56949	5.03	0.30969	4.91	0.98	1739.2	74.8	1744	42	1749	20	**1749**	**20**
166.8	7614	1	5.14433	4.31	0.33286	2.90	0.67	1852.2	46.7	1843	37	1834	58	**1834**	**58**
145.8	9824	1	5.13132	2.45	0.33166	1.44	0.59	1846.4	23.2	1841	21	1836	36	**1836**	**36**
339.7	15573	1	5.75860	4.01	0.34235	3.13	0.78	1898.0	51.5	1940	35	1986	44	**1986**	**44**
123.1	7909	1	5.33597	5.72	0.28038	2.81	0.49	1593.3	39.7	1875	49	2203	87	**2203**	**87**
241.7	13237	1	7.94549	5.37	0.41055	5.15	0.96	2217.4	96.6	2225	49	2232	27	**2232**	**27**
295.2	9160	1	7.08594	4.46	0.36169	4.18	0.94	1990.2	71.5	2122	40	2253	27	**2253**	**27**
190.7	23714	2	8.80841	4.03	0.42421	3.17	0.79	2279.6	60.9	2318	37	2353	43	**2353**	**43**
323.9	21392	2	9.10797	3.97	0.41548	3.73	0.94	2239.9	70.6	2349	36	2445	23	**2445**	**23**
214.3	11080	1	7.99572	5.64	0.33991	5.25	0.93	1886.2	85.8	2231	51	2564	35	**2564**	**35**
193.5	21259	1	11.90056	3.24	0.48788	2.89	0.89	2561.5	61.1	2597	30	2624	24	**2624**	**24**
273.3	21137	1	13.01959	4.28	0.51273	3.82	0.89	2668.3	83.5	2681	40	2691	32	**2691**	**32**
97.85	9011	1	14.26175	1.94	0.51161	1.50	0.77	2663.5	32.7	2767	18	2844	20	**2844**	**20**
564.7	42034	1	20.06523	3.20	0.59016	2.34	0.73	2990.1	55.9	3095	31	3163	35	**3163**	**35**
CJ															
413.3	2344	2	0.29800	2.66	0.03789	1.45	0.54	239.7	3.4	265	6	493	49	**240**	**3**
2584	1410	1	0.40694	15.75	0.05015	8.86	0.56	315.4	27.3	347	46	562	285	**315**	**27**
2148	791	2	0.38653	6.70	0.05173	4.71	0.70	325.1	14.9	332	19	379	107	**325**	**15**
86.98	121	1	0.74427	5.74	0.07669	2.69	0.47	476.3	12.3	565	25	940	104	**476**	**12**
56.18	143	13	0.59070	8.84	0.07697	3.82	0.43	478.0	17.6	471	33	439	178	**478**	**18**
49.87	168	2	0.59014	4.58	0.07753	3.36	0.73	481.4	15.6	471	17	420	70	**481**	**16**
120.6	137	2	0.66014	5.55	0.07778	3.57	0.64	482.8	16.6	515	22	659	91	**483**	**17**
317.2	423	2	0.69400	7.23	0.07917	2.71	0.37	491.2	12.8	535	30	727	142	**491**	**13**
83.25	116	1	0.58750	7.80	0.07943	3.71	0.48	492.7	17.6	469	29	356	155	**493**	**18**
226.3	134	18	0.56969	13.48	0.07965	4.60	0.34	494.0	21.9	458	50	280	291	**494**	**22**
128.8	254	2	0.59281	7.50	0.08023	2.71	0.36	497.5	13.0	473	28	354	158	**497**	**13**
43.78	427	17	0.57507	10.72	0.08033	3.57	0.33	498.1	17.1	461	40	282	232	**498**	**17**
64.45	382	4	0.57003	16.12	0.08070	5.40	0.34	500.3	26.0	458	59	251	351	**500**	**26**
54.63	96	20	0.62495	8.34	0.08111	4.78	0.57	502.7	23.1	493	33	448	152	**503**	**23**

			Isotopic ratios					Apparent ages (Ma)							
U	206Pb	U/Th	207Pb*		206Pb*		error	206Pb*		207Pb*		206Pb*		Best age	
(ppm)	204Pb		235U	(%)	238U	(%)	corr.	238U	±(Ma)	235U	±(Ma)	207Pb*	±(Ma)		±(Ma)
CJ															
120.3	272	3	0.56657	15.96	0.08119	4.58	0.29	503.2	22.2	456	59	223	355	**503**	**22**
109.4	180	2	0.63038	5.80	0.08143	4.28	0.74	504.6	20.8	496	23	458	87	**505**	**21**
184.4	2798	1	0.70596	5.54	0.08158	3.79	0.68	505.5	18.4	542	23	700	86	**506**	**18**
65.19	378	0	0.65713	8.17	0.08201	5.03	0.62	508.1	24.6	513	33	534	141	**508**	**25**
168.4	229	0	0.66148	4.17	0.08227	1.88	0.45	509.7	9.2	516	17	542	81	**510**	**9**
118.1	153	2	0.70276	6.09	0.08248	2.08	0.34	510.9	10.2	540	26	667	123	**511**	**10**
111.4	645	3	0.70635	6.36	0.08263	3.62	0.57	511.8	17.8	543	27	674	112	**512**	**18**
155.8	549	3	0.57351	13.90	0.08264	2.47	0.18	511.9	12.1	460	52	210	318	**512**	**12**
249.9	1134	1	0.67769	3.32	0.08321	1.36	0.41	515.2	6.7	525	14	570	66	**515**	**7**
367.5	5287	1	0.67820	5.22	0.08332	2.85	0.55	515.9	14.1	526	21	568	95	**516**	**14**
222.9	272	1	0.64582	4.68	0.08349	3.50	0.75	516.9	17.4	506	19	456	69	**517**	**17**
588.9	5376	7	0.65880	4.07	0.08351	2.62	0.64	517.1	13.0	514	16	500	69	**517**	**13**
958	2534	10	0.66307	4.29	0.08366	2.16	0.50	517.9	10.7	516	17	510	82	**518**	**11**
244.5	4359	1	0.70323	5.66	0.08368	4.56	0.81	518.0	22.7	541	24	638	72	**518**	**23**
190.6	1462	2	0.66925	3.97	0.08382	3.55	0.89	518.9	17.7	520	16	526	39	**519**	**18**
82.94	131	3	0.68938	7.22	0.08401	4.26	0.59	520.0	21.3	532	30	586	127	**520**	**21**
72.96	730	2	0.65105	8.85	0.08477	3.60	0.41	524.5	18.1	509	35	441	180	**525**	**18**
945.2	10992	2	0.68078	2.78	0.08485	2.32	0.84	525.0	11.7	527	11	537	33	**525**	**12**
164.7	810	1	0.64770	6.00	0.08496	2.75	0.46	525.6	13.9	507	24	424	119	**526**	**14**
281.3	4417	1	0.76904	3.66	0.08511	2.25	0.62	526.5	11.4	579	16	792	60	**527**	**11**
1026	2331	2	0.67215	3.79	0.08531	2.30	0.61	527.7	11.6	522	15	497	66	**528**	**12**
491.8	630	5	0.67071	4.69	0.08576	3.16	0.67	530.4	16.1	521	19	481	77	**530**	**16**
261.4	1109	2	0.66465	7.99	0.08592	5.69	0.71	531.4	29.0	517	32	457	125	**531**	**29**
396.6	6046	2	0.71668	3.38	0.08604	2.40	0.71	532.1	12.2	549	14	618	51	**532**	**12**
219.4	4192	2	0.74393	5.58	0.08611	4.06	0.73	532.5	20.8	565	24	697	82	**533**	**21**
402.8	5557	2	0.70821	4.25	0.08631	2.10	0.49	533.7	10.8	544	18	586	80	**534**	**11**
62.04	297	0	0.67205	6.27	0.08641	3.93	0.63	534.3	20.2	522	26	468	108	**534**	**20**
603.8	7016	2	0.69027	3.63	0.08671	2.53	0.70	536.0	13.0	533	15	520	57	**536**	**13**
212.1	3581	1	0.71285	3.00	0.08674	1.34	0.45	536.2	6.9	546	13	589	58	**536**	**7**
866.4	12524	4	0.70119	3.93	0.08683	2.66	0.68	536.8	13.7	539	16	551	63	**537**	**14**
202.5	3097	3	0.74507	4.17	0.08718	2.56	0.61	538.8	13.2	565	18	674	71	**539**	**13**
1237	4681	5	0.69576	4.39	0.08738	2.77	0.63	540.0	14.3	536	18	520	75	**540**	**14**
23.24	216	7	0.69806	8.20	0.08787	2.79	0.34	542.9	14.6	538	34	515	169	**543**	**15**
324.6	5754	2	0.74506	3.31	0.08841	2.37	0.72	546.1	12.4	565	14	644	50	**546**	**12**
705.9	1103	8	0.70896	4.80	0.08923	2.04	0.43	551.0	10.8	544	20	516	95	**551**	**11**
916.1	7017	2	0.71343	6.59	0.08931	3.22	0.49	551.5	17.0	547	28	527	126	**551**	**17**
722.2	9505	5	0.76130	9.14	0.08938	3.10	0.34	551.9	16.4	575	40	666	184	**552**	**16**
1103	7825	19	0.77395	2.85	0.09068	1.87	0.66	559.6	10.0	582	13	671	46	**560**	**10**
606.4	2006	2	0.74753	11.39	0.09071	5.58	0.49	559.8	29.9	567	50	595	216	**560**	**30**
1382	1981	35	0.75653	9.04	0.09090	6.39	0.71	560.9	34.3	572	40	616	138	**561**	**34**
737.5	7729	2	0.72689	6.66	0.09090	6.00	0.90	560.9	32.2	555	28	530	63	**561**	**32**
1265	6333	14	0.72825	5.29	0.09091	2.71	0.51	560.9	14.5	556	23	534	100	**561**	**15**
686.9	12621	4	0.76918	5.06	0.09203	1.18	0.23	567.5	6.4	579	22	626	106	**568**	**6**
785.5	5236	4	0.75468	6.14	0.09214	3.37	0.55	568.2	18.3	571	27	582	112	**568**	**18**
196.3	3073	2	0.82424	4.82	0.09235	3.47	0.72	569.4	18.9	610	22	766	70	**569**	**19**
598.2	6583	4	0.80263	6.33	0.09262	3.38	0.53	571.0	18.5	598	29	703	114	**571**	**18**
200.3	2804	1	0.80016	5.55	0.09327	3.48	0.63	574.9	19.2	597	25	682	92	**575**	**19**
370.6	2664	3	0.77820	5.37	0.09398	1.91	0.36	579.1	10.6	584	24	605	109	**579**	**11**
198.7	3202	2	0.86186	5.97	0.09404	3.73	0.63	579.4	20.7	631	28	821	97	**579**	**21**
1328	1427	5	0.72174	10.68	0.09422	8.24	0.77	580.5	45.7	552	45	435	152	**580**	**46**
314.6	6061	2	0.81451	3.88	0.09426	1.57	0.40	580.7	8.7	605	18	697	76	**581**	**9**
340.4	1087	5	0.86365	7.97	0.09489	3.39	0.43	584.4	18.9	632	38	807	151	**584**	**19**
618.8	2374	4	0.82001	8.13	0.09576	6.42	0.79	589.5	36.2	608	37	678	107	**590**	**36**
1201	3229	2	0.81144	7.86	0.09763	7.06	0.90	600.5	40.5	603	36	614	75	**601**	**40**
341.5	6156	4	0.88529	8.08	0.10096	3.14	0.39	620.0	18.6	644	39	728	158	**620**	**19**
673.5	5819	7	0.89578	6.81	0.10249	5.25	0.77	629.0	31.5	649	33	721	92	**629**	**31**
868.5	3534	6	0.87799	7.67	0.10432	5.62	0.73	639.7	34.2	640	36	641	112	**640**	**34**
723.1	5705	6	1.03012	5.88	0.11214	4.67	0.79	685.2	30.3	719	30	826	75	**685**	**30**
981.2	11927	1	1.13473	4.31	0.11536	3.97	0.92	703.8	26.5	770	23	967	34	**704**	**26**
336.6	8503	5	1.65277	5.18	0.16451	4.72	0.91	981.8	43.0	991	33	1010	43	**1010**	**43**

			Isotopic ratios					Apparent ages (Ma)							
U	206Pb	U/Th	207Pb*		206Pb*		error	206Pb*		207Pb*		206Pb*		Best age	
(ppm)	204Pb		235U	(%)	238U	(%)	corr.	238U	±(Ma)	235U	±(Ma)	207Pb*	±(Ma)		±(Ma)
CJ															
718.8	16625	3	1.78956	3.15	0.17542	1.81	0.57	1041.9	17.4	1042	21	1041	52	**1041**	**52**
619.9	9113	15	1.79513	6.58	0.17552	6.08	0.93	1042.4	58.6	1044	43	1046	50	**1046**	**50**
180.6	4998	1	1.91664	3.91	0.18649	2.50	0.64	1102.3	25.3	1087	26	1056	60	**1056**	**60**
81.05	2652	1	1.83495	5.10	0.17430	3.95	0.77	1035.8	37.8	1058	34	1104	65	**1104**	**65**
79.77	1624	2	1.72882	3.51	0.16238	2.32	0.66	970.0	20.9	1019	23	1127	53	**1127**	**53**
121.6	3775	2	2.04945	2.61	0.18993	1.99	0.76	1121.0	20.5	1132	18	1154	33	**1154**	**33**
138.3	5562	1	2.44135	2.82	0.21463	1.37	0.48	1253.5	15.6	1255	20	1257	48	**1257**	**48**
85.93	5506	2	2.18859	3.12	0.19057	2.74	0.88	1124.4	28.2	1177	22	1276	29	**1276**	**29**
40.03	79	1	0.94745	9.68	0.07791	6.26	0.65	483.6	29.2	677	48	1387	142	**1387**	**142**
30.07	88	22	0.98795	7.83	0.08094	5.86	0.75	501.7	28.3	698	40	1394	100	**1394**	**100**
HB															
182	342	1	0.09251	11.47	0.01224	3.54	0.31	78.5	2.8	90	10	404	245	**78**	**3**
47.2	49	3	0.54133	4.32	0.06327	2.23	0.52	395.5	8.6	439	15	676	79	**395**	**9**
84.4	135	6	0.59472	3.81	0.07564	1.89	0.50	470.0	8.6	474	14	492	73	**470**	**9**
135.3	157	9	0.62816	4.99	0.08010	1.48	0.30	496.7	7.1	495	20	487	105	**497**	**7**
358.1	304	1	0.64457	2.27	0.08013	1.65	0.73	496.9	7.9	505	9	542	34	**497**	**8**
796.7	2655	2	0.65747	3.43	0.08265	2.71	0.79	511.9	13.3	513	14	518	46	**512**	**13**
393.1	4662	2	0.66428	2.54	0.08357	1.92	0.76	517.4	9.5	517	10	517	36	**517**	**10**
244	4061	1	0.69599	2.31	0.08361	1.68	0.73	517.6	8.4	536	10	617	34	**518**	**8**
481.6	6237	2	0.67768	3.18	0.08409	2.80	0.88	520.5	14.0	525	13	547	33	**520**	**14**
251	4466	2	0.67451	2.69	0.08409	1.39	0.52	520.5	7.0	523	11	536	50	**520**	**7**
555.9	6225	2	0.66928	2.18	0.08419	1.34	0.62	521.1	6.7	520	9	517	38	**521**	**7**
295	4674	2	0.68232	2.75	0.08426	1.84	0.67	521.5	9.2	528	11	557	45	**522**	**9**
286.8	4730	2	0.67379	3.16	0.08437	2.51	0.79	522.2	12.6	523	13	527	42	**522**	**13**
420.9	2258	2	0.66121	2.74	0.08445	1.86	0.68	522.6	9.3	515	11	483	44	**523**	**9**
335.5	371	1	0.69151	3.85	0.08449	2.62	0.68	522.9	13.2	534	16	580	61	**523**	**13**
403.5	7452	4	0.67210	5.82	0.08455	2.81	0.48	523.3	14.1	522	24	516	112	**523**	**14**
240.3	4672	8	0.68756	2.40	0.08458	1.00	0.42	523.4	5.0	531	10	566	47	**523**	**5**
323.5	4725	4	0.67665	2.42	0.08481	1.00	0.41	524.8	5.0	525	10	525	48	**525**	**5**
295.7	3986	23	0.68000	3.06	0.08510	1.94	0.64	526.5	9.8	527	13	528	52	**526**	**10**
186.9	2832	1	0.68431	3.31	0.08516	2.49	0.75	526.9	12.6	529	14	540	48	**527**	**13**
329.1	4290	2	0.67456	2.22	0.08520	1.86	0.84	527.1	9.4	523	9	508	26	**527**	**9**
391	6364	4	0.69527	2.83	0.08534	2.36	0.83	527.9	11.9	536	12	570	34	**528**	**12**
212	3438	2	0.68860	1.85	0.08537	1.00	0.54	528.1	5.1	532	8	549	34	**528**	**5**
392	4641	3	0.68229	2.75	0.08540	1.84	0.67	528.3	9.3	528	11	528	45	**528**	**9**
612	5632	2	0.69314	1.64	0.08545	1.00	0.61	528.5	5.1	535	7	561	28	**529**	**5**
184.3	3102	3	0.68213	3.86	0.08545	2.88	0.74	528.6	14.6	528	16	526	57	**529**	**15**
272.6	1336	3	0.65074	7.10	0.08548	1.76	0.25	528.7	8.9	509	28	421	154	**529**	**9**
523.5	8287	2	0.69525	4.52	0.08568	3.61	0.80	530.0	18.4	536	19	562	59	**530**	**18**
327.6	4958	1	0.68774	2.17	0.08579	1.48	0.68	530.6	7.5	531	9	535	35	**531**	**8**
427.6	6579	5	0.68813	1.80	0.08580	1.44	0.80	530.6	7.3	532	7	536	24	**531**	**7**
450.1	5690	1	0.68993	2.30	0.08582	1.49	0.65	530.8	7.6	533	10	541	38	**531**	**8**
429.1	5984	2	0.68380	1.48	0.08582	1.00	0.68	530.8	5.1	529	6	522	24	**531**	**5**
342.3	5758	2	0.67241	3.09	0.08591	1.26	0.41	531.3	6.4	522	13	482	62	**531**	**6**
245	4173	4	0.70345	1.61	0.08599	1.00	0.62	531.8	5.1	541	7	579	27	**532**	**5**
435.2	5298	3	0.70665	2.53	0.08604	1.19	0.47	532.1	6.1	543	11	588	49	**532**	**6**
204.8	3952	2	0.67738	3.86	0.08616	2.85	0.74	532.8	14.6	525	16	492	57	**533**	**15**
401.1	6049	1	0.70374	2.13	0.08624	1.29	0.61	533.2	6.6	541	9	574	37	**533**	**7**
424.8	7608	1	0.69877	2.29	0.08638	1.91	0.83	534.1	9.8	538	10	555	28	**534**	**10**
296.3	4430	2	0.68835	2.60	0.08641	1.46	0.56	534.3	7.5	532	11	521	47	**534**	**8**
255.2	3584	1	0.67191	4.11	0.08642	1.42	0.35	534.3	7.3	522	17	468	85	**534**	**7**
545	7607	3	0.69753	2.36	0.08652	1.91	0.81	534.9	9.8	537	10	548	30	**535**	**10**
290.2	5394	3	0.72032	3.08	0.08683	2.03	0.66	536.8	10.4	551	13	609	50	**537**	**10**
1388	17694	2	0.70675	1.73	0.08684	1.41	0.82	536.8	7.3	543	7	568	22	**537**	**7**
371.6	6323	2	0.73923	5.79	0.08700	2.37	0.41	537.8	12.2	562	25	661	113	**538**	**12**
276.6	4111	2	0.70493	2.26	0.08703	1.69	0.75	537.9	8.7	542	9	558	33	**538**	**9**
198.6	3813	2	0.70467	2.87	0.08706	1.97	0.69	538.1	10.2	542	12	556	46	**538**	**10**
375.5	7458	2	0.71129	3.01	0.08734	2.50	0.83	539.8	12.9	546	13	569	36	**540**	**13**
384.6	7594	2	0.70271	2.33	0.08742	1.57	0.67	540.3	8.1	540	10	541	38	**540**	**8**
266.7	2338	1	0.71250	4.29	0.08743	3.68	0.86	540.3	19.1	546	18	571	48	**540**	**19**
309.2	546	1	0.72219	2.64	0.08753	2.04	0.77	540.9	10.6	552	11	598	36	**541**	**11**

			Isotopic ratios					Apparent ages (Ma)							
U	206Pb	U/Th	207Pb*		206Pb*		error	206Pb*		207Pb*		206Pb*		Best age	
(ppm)	204Pb		235U	(%)	238U	(%)	corr.	238U	±(Ma)	235U	±(Ma)	207Pb*	±(Ma)		±(Ma)
HB															
347.1	5662	2	0.71988	2.49	0.08754	1.82	0.73	541.0	9.4	551	11	590	37	**541**	**9**
608.2	8909	3	0.69490	2.31	0.08759	1.86	0.80	541.3	9.6	536	10	512	30	**541**	**10**
295.1	5377	2	0.72750	3.61	0.08804	2.01	0.56	543.9	10.5	555	15	601	65	**544**	**10**
321.8	6008	2	0.73008	3.42	0.08812	2.24	0.66	544.4	11.7	557	15	607	56	**544**	**12**
282.6	3896	2	0.73439	3.56	0.08874	1.40	0.39	548.1	7.4	559	15	604	71	**548**	**7**
509.5	5201	2	0.72323	4.77	0.08902	1.10	0.23	549.7	5.8	553	20	564	101	**550**	**6**
278.5	4715	2	0.70511	2.39	0.08902	1.00	0.42	549.8	5.3	542	10	509	48	**550**	**5**
174.8	3192	2	0.73926	2.67	0.08915	1.64	0.61	550.5	8.7	562	12	609	46	**550**	**9**
231.7	1522	2	0.68123	6.32	0.08918	1.68	0.27	550.7	8.9	528	26	429	136	**551**	**9**
428.1	7272	2	0.71162	3.59	0.08964	2.57	0.72	553.4	13.7	546	15	514	55	**553**	**14**
364	1512	2	0.71087	4.25	0.08973	1.56	0.37	553.9	8.3	545	18	509	87	**554**	**8**
687.9	8269	2	0.71223	3.86	0.08976	1.77	0.46	554.1	9.4	546	16	513	75	**554**	**9**
572.6	4758	2	0.72643	2.81	0.08990	1.29	0.46	554.9	6.9	554	12	552	55	**555**	**7**
185.6	3900	2	0.80088	6.59	0.08996	1.85	0.28	555.3	9.8	597	30	760	133	**555**	**10**
235.7	3457	2	0.73035	1.80	0.09002	1.07	0.59	555.6	5.7	557	8	561	32	**556**	**6**
150.4	2307	2	0.74937	3.58	0.09025	2.71	0.76	557.0	14.5	568	16	612	50	**557**	**14**
306.8	4390	23	0.71940	3.35	0.09030	1.88	0.56	557.3	10.0	550	14	521	61	**557**	**10**
481	8764	3	0.76430	3.96	0.09041	2.21	0.56	558.0	11.8	576	17	650	70	**558**	**12**
329.7	4298	2	0.76708	3.17	0.09108	2.20	0.69	561.9	11.9	578	14	642	49	**562**	**12**
365.2	2158	2	0.74527	2.42	0.09142	1.57	0.65	563.9	8.5	565	10	572	40	**564**	**8**
423.6	7861	4	0.76308	3.38	0.09174	2.59	0.77	565.8	14.0	576	15	615	47	**566**	**14**
365.8	7132	2	0.75115	4.57	0.09229	3.13	0.69	569.1	17.1	569	20	568	72	**569**	**17**
223.8	4626	4	0.78171	4.51	0.09278	1.52	0.34	572.0	8.3	586	20	643	91	**572**	**8**
159.4	3238	2	0.76138	4.06	0.09317	2.53	0.62	574.3	13.9	575	18	577	69	**574**	**14**
893.4	11611	2	0.86971	4.33	0.10327	3.90	0.90	633.6	23.5	635	20	642	40	**634**	**24**
963.8	1248	4	1.50208	5.03	0.15631	4.06	0.81	936.2	35.4	931	31	919	61	**919**	**61**
435.4	9101	2	1.63953	3.75	0.16258	1.63	0.43	971.1	14.7	986	24	1018	68	**1018**	**68**
123.4	3964	1	1.76151	3.29	0.17373	2.62	0.80	1032.6	25.0	1031	21	1029	40	**1029**	**40**
285.9	6445	3	1.75928	4.15	0.17041	3.69	0.89	1014.4	34.6	1031	27	1065	38	**1065**	**38**
583.2	3107	1	1.76806	7.35	0.16988	6.55	0.89	1011.4	61.3	1034	48	1081	67	**1081**	**67**
35.86	1316	1	1.84504	4.53	0.17392	2.68	0.59	1033.7	25.6	1062	30	1120	73	**1120**	**73**
131.1	4756	2	1.92368	1.73	0.18127	1.00	0.58	1073.9	9.9	1089	12	1120	28	**1120**	**28**
94.17	3070	1	1.91088	2.87	0.17928	2.33	0.81	1063.0	22.8	1085	19	1129	34	**1129**	**34**
222.5	7003	1	2.27120	2.51	0.20327	2.10	0.83	1192.9	22.8	1203	18	1222	27	**1222**	**27**
207.3	6153	1	2.45389	1.57	0.21501	1.00	0.64	1255.5	11.4	1259	11	1264	24	**1264**	**24**
327.6	18438	2	5.16293	3.08	0.31668	2.77	0.90	1773.5	42.9	1847	26	1930	24	**1930**	**24**
666.5	27693	4	6.18398	1.99	0.32423	1.54	0.77	1810.3	24.3	2002	17	2206	22	**2206**	**22**
LW2-A															
428.7	4448	1	0.64695	3.58	0.07912	2.45	0.68	490.9	11.6	507	14	578	57	**491**	**12**
70.67	1121	1	0.82625	8.05	0.08379	3.13	0.39	518.7	15.6	612	37	972	152	**519**	**16**
811.5	12442	2	0.68001	2.04	0.08441	1.41	0.69	522.4	7.1	527	8	546	32	**522**	**7**
785.4	11596	7	0.69515	3.44	0.08637	2.57	0.75	534.0	13.2	536	14	544	50	**534**	**13**
56.82	670	1	0.78584	4.88	0.08783	2.17	0.44	542.7	11.3	589	22	771	92	**543**	**11**
101.9	1495	22	0.72877	4.46	0.08950	2.84	0.64	552.6	15.0	556	19	569	75	**553**	**15**
136.9	1723	1	0.79914	5.35	0.09022	2.78	0.52	556.9	14.8	596	24	750	97	**557**	**15**
39.46	476	1	0.94927	8.10	0.09033	4.29	0.53	557.5	22.9	678	40	1101	138	**557**	**23**
607.2	3879	1	0.77738	7.27	0.09059	3.69	0.51	559.0	19.7	584	32	682	134	**559**	**20**
147.2	1492	2	0.79401	3.40	0.09061	1.35	0.40	559.2	7.2	593	15	727	66	**559**	**7**
191.5	3269	285	0.74999	3.70	0.09119	2.37	0.64	562.6	12.8	568	16	591	62	**563**	**13**
36.19	493	0	0.95068	9.42	0.09147	5.52	0.59	564.2	29.8	678	47	1079	153	**564**	**30**
459.8	7231	4	0.78270	3.23	0.09167	2.60	0.80	565.4	14.0	587	14	672	41	**565**	**14**
1250	17658	3	0.75442	2.67	0.09182	1.27	0.47	566.3	6.9	571	12	589	51	**566**	**7**
892.7	11644	5	0.77966	3.18	0.09210	2.50	0.79	568.0	13.6	585	14	653	42	**568**	**14**
220.1	2884	1	0.75114	6.61	0.09229	3.07	0.46	569.1	16.7	569	29	568	127	**569**	**17**
65.98	1263	1	0.74908	6.09	0.09266	2.51	0.41	571.3	13.7	568	27	553	121	**571**	**14**
13.71	1610	5	0.69364	9.40	0.09282	6.54	0.70	572.2	35.8	535	39	379	152	**572**	**36**
138.8	1808	1	0.84053	4.52	0.09395	2.89	0.64	578.8	16.0	619	21	771	73	**579**	**16**
73.81	1250	0	0.77548	8.55	0.09446	1.48	0.17	581.9	8.2	583	38	587	183	**582**	**8**
336.6	4565	2	0.82876	2.75	0.09567	1.70	0.62	589.0	9.5	613	13	702	46	**589**	**10**
183.6	2718	1	0.86132	3.94	0.09716	3.14	0.80	597.7	17.9	631	18	751	50	**598**	**18**
666.7	8025	1	0.80602	1.61	0.09718	1.00	0.62	597.9	5.7	600	7	609	27	**598**	**6**

			Isotopic ratios					Apparent ages (Ma)							
U	206Pb	U/Th	207Pb*		206Pb*		error	206Pb*		207Pb*		206Pb*		Best age	
(ppm)	204Pb		235U	(%)	238U	(%)	corr.	238U	±(Ma)	235U	±(Ma)	207Pb*	±(Ma)		±(Ma)
LW2-A															
666.7	8025	1	0.80602	1.61	0.09718	1.00	0.62	597.9	5.7	600	7	609	27	**598**	**6**
223.5	3031	6	0.83828	3.29	0.09728	1.89	0.57	598.4	10.8	618	15	691	57	**598**	**11**
365.2	5208	1	0.82081	3.58	0.09825	1.83	0.51	604.1	10.6	609	16	625	66	**604**	**11**
430.5	4731	1	0.85802	3.54	0.09845	2.66	0.75	605.3	15.4	629	17	715	50	**605**	**15**
418.6	1278	2	0.84820	7.52	0.09901	6.09	0.81	608.6	35.4	624	35	679	94	**609**	**35**
182.5	2274	2	0.87021	3.35	0.09961	2.15	0.64	612.1	12.6	636	16	720	54	**612**	**13**
202.5	3428	5	0.95621	4.34	0.10025	3.02	0.70	615.8	17.7	681	22	904	64	**616**	**18**
238	4177	2	0.89414	3.40	0.10356	1.51	0.45	635.3	9.2	649	16	695	65	**635**	**9**
315	5666	1	0.92171	2.85	0.10372	2.62	0.92	636.2	15.9	663	14	756	24	**636**	**16**
719.4	1447	3	1.18570	9.11	0.11159	7.92	0.87	681.9	51.3	794	50	1123	90	**682**	**51**
347.6	3702	2	1.00066	2.43	0.11602	1.95	0.80	707.6	13.1	704	12	693	31	**708**	**13**
1492	1466	3	1.14183	7.05	0.11825	5.58	0.79	720.5	38.0	773	38	929	89	**720**	**38**
286.3	3029	1	1.06476	6.36	0.12094	2.67	0.42	735.9	18.6	736	33	737	122	**736**	**19**
169.9	3120	2	1.43916	2.49	0.14621	2.03	0.82	879.7	16.7	905	15	969	29	**880**	**17**
159.5	2134	1	1.42701	7.43	0.14840	5.27	0.71	892.0	43.9	900	44	921	108	**892**	**44**
310.6	10151	9	1.48725	4.16	0.14975	2.35	0.57	899.5	19.8	925	25	987	70	**900**	**20**
529.5	8593	2	1.59812	3.21	0.15970	1.02	0.32	955.1	9.0	969	20	1002	62	**1002**	**62**
127.7	2752	1	1.55242	4.26	0.15293	4.04	0.95	917.4	34.6	951	26	1031	27	**1031**	**27**
689.2	3843	16	1.67073	4.94	0.16012	4.46	0.90	957.4	39.7	997	31	1087	42	**1087**	**42**
155.7	4516	2	1.66018	2.26	0.15859	1.98	0.87	948.9	17.4	993	14	1093	22	**1093**	**22**
1207	14227	1	2.01866	3.88	0.19207	3.32	0.86	1132.6	34.5	1122	26	1101	40	**1101**	**40**
401.1	8014	1	2.02857	4.00	0.19067	2.17	0.54	1125.0	22.4	1125	27	1125	67	**1125**	**67**
173.5	3654	1	1.93231	3.94	0.17881	3.46	0.88	1060.5	33.8	1092	26	1156	37	**1156**	**37**
518.9	13853	3	1.92161	2.29	0.17680	1.90	0.83	1049.4	18.4	1089	15	1168	25	**1168**	**25**
256.4	7530	2	2.28218	4.29	0.20664	3.88	0.90	1210.9	42.8	1207	30	1199	36	**1199**	**36**
248.3	6491	1	2.33672	2.36	0.20958	1.54	0.65	1226.6	17.2	1224	17	1218	35	**1218**	**35**
49.01	1430	3	1.92278	6.13	0.16280	2.96	0.48	972.3	26.8	1089	41	1331	104	**1331**	**104**
33.02	572	1	1.21679	13.95	0.10255	8.32	0.60	629.4	49.9	808	78	1339	217	**1339**	**217**
443.6	3451	1	2.80561	3.19	0.23071	2.14	0.67	1338.2	25.9	1357	24	1387	45	**1387**	**45**
18.58	801	1	2.57291	7.25	0.20883	3.95	0.55	1222.6	44.0	1293	53	1412	116	**1412**	**116**
177.3	6463	2	3.04603	2.01	0.24183	1.43	0.71	1396.2	18.0	1419	15	1454	27	**1454**	**27**
176.7	7399	1	3.30029	3.01	0.25988	2.11	0.70	1489.2	28.1	1481	23	1470	41	**1470**	**41**
60.61	2570	1	3.14242	1.71	0.24735	1.00	0.59	1424.8	12.8	1443	13	1470	26	**1470**	**26**
147.3	5463	2	3.37649	2.20	0.26154	1.00	0.46	1497.7	13.4	1499	17	1501	37	**1501**	**37**
315.9	4990	1	3.08401	2.99	0.23474	1.59	0.53	1359.3	19.5	1429	23	1534	48	**1534**	**48**
411.4	18076	2	3.71390	3.66	0.27964	2.57	0.70	1589.5	36.1	1574	29	1554	49	**1554**	**49**
121.9	4557	1	3.29468	4.64	0.24685	2.07	0.45	1422.2	26.5	1480	36	1563	78	**1563**	**78**
480.2	10228	2	3.63638	2.94	0.27215	1.84	0.63	1551.7	25.4	1558	23	1565	43	**1565**	**43**
305	9412	2	3.81893	3.84	0.28474	1.53	0.40	1615.2	21.9	1597	31	1572	66	**1572**	**66**
339.1	13955	2	5.51713	1.88	0.34374	1.04	0.55	1904.6	17.1	1903	16	1902	28	**1902**	**28**
237.7	15227	1	5.65546	3.16	0.34857	2.09	0.66	1927.8	34.8	1925	27	1921	42	**1921**	**42**
274.2	13151	2	6.06286	3.52	0.35696	1.86	0.53	1967.7	31.6	1985	31	2003	53	**2003**	**53**
160.3	9830	1	7.67816	2.20	0.40695	1.00	0.45	2201.0	18.6	2194	20	2188	34	**2188**	**34**
429.6	9955	2	6.90777	4.12	0.35924	2.93	0.71	1978.6	49.9	2100	37	2221	50	**2221**	**50**
502.6	17235	7	6.05380	5.53	0.31397	1.95	0.35	1760.2	30.0	1984	48	2225	90	**2225**	**90**
283	11023	2	7.73143	2.52	0.39838	2.21	0.88	2161.6	40.6	2200	23	2236	21	**2236**	**21**
60.19	2126	1	6.83135	4.66	0.35187	3.56	0.76	1943.5	59.7	2090	41	2237	52	**2237**	**52**
421.4	11738	3	8.29185	3.74	0.42115	2.53	0.68	2265.7	48.3	2263	34	2261	48	**2261**	**48**
152.2	8757	2	7.42703	1.42	0.35150	1.00	0.70	1941.8	16.8	2164	13	2382	17	**2382**	**17**
73.47	5502	1	9.10521	3.98	0.42663	2.61	0.66	2290.5	50.4	2349	36	2399	51	**2399**	**51**
430	21252	1	10.66801	2.66	0.47160	1.60	0.60	2490.6	33.1	2495	25	2498	36	**2498**	**36**
913.4	48186	13	10.73048	1.93	0.47340	1.28	0.66	2498.4	26.5	2500	18	2501	24	**2501**	**24**
64.03	6890	1	12.10778	2.87	0.48097	2.68	0.94	2531.5	56.2	2613	27	2676	17	**2676**	**17**
307	11111	1	13.41546	3.96	0.52739	2.39	0.60	2730.4	53.2	2709	37	2694	52	**2694**	**52**
450.8	14131	1	13.08150	6.14	0.51092	1.80	0.29	2660.5	39.2	2686	58	2704	97	**2704**	**97**
260.3	16087	2	13.24324	2.84	0.51393	2.01	0.71	2673.4	44.0	2697	27	2715	33	**2715**	**33**
86.3	5033	2	13.29528	2.60	0.51522	1.51	0.58	2678.9	33.1	2701	25	2717	35	**2717**	**35**
160.9	11400	1	11.63077	2.34	0.44499	1.70	0.72	2373.0	33.7	2575	22	2738	27	**2738**	**27**
103.3	8737	2	14.49784	6.42	0.54185	5.92	0.92	2791.2	134.2	2783	61	2777	41	**2777**	**41**
68.8	5855	2	12.48545	3.34	0.46172	2.60	0.78	2447.2	53.0	2642	31	2794	34	**2794**	**34**
98.24	1294	2	13.41919	3.72	0.46718	1.90	0.51	2471.2	38.9	2710	35	2893	52	**2893**	**52**

			Isotopic ratios					Apparent ages (Ma)							
U	206Pb	U/Th	207Pb*		206Pb*		error	206Pb*		207Pb*		206Pb*		Best age	
(ppm)	204Pb		235U	(%)	238U	(%)	corr.	238U	±(Ma)	235U	±(Ma)	207Pb*	±(Ma)		±(Ma)
LW2-A															
483.7	27800	4	14.93123	6.78	0.50260	3.12	0.46	2625.0	67.3	2811	65	2947	97	**2947**	**97**
119.4	8539	1	17.42231	2.81	0.58398	1.21	0.43	2965.0	28.8	2958	27	2954	41	**2954**	**41**
539.8	12759	5	17.91941	2.56	0.58957	1.48	0.58	2987.7	35.3	2985	25	2984	34	**2984**	**34**
81.99	8627	23	18.82073	5.35	0.60465	4.42	0.83	3048.5	107.3	3033	52	3022	48	**3022**	**48**
118.1	11090	2	25.14877	2.32	0.66974	2.04	0.88	3304.9	52.8	3314	23	3320	17	**3320**	**17**
541	27405	1	30.83114	1.61	0.71358	1.00	0.62	3471.9	26.8	3514	16	3538	19	**3538**	**19**
LW2-B															
229.2	3345	1	0.70746	2.81	0.08669	1.21	0.43	535.9	6.2	543	12	574	55	**536**	**6**
214.3	2490	2	0.69569	3.11	0.08762	1.30	0.42	541.5	6.8	536	13	514	62	**541**	**7**
313.1	4262	2	0.72494	3.57	0.08867	2.55	0.72	547.7	13.4	554	15	578	54	**548**	**13**
61.36	708	0	0.70745	3.27	0.08924	2.25	0.69	551.0	11.9	543	14	511	52	**551**	**12**
14.19	232	0	0.80309	19.42	0.08927	4.93	0.25	551.2	26.1	599	88	782	398	**551**	**26**
34.29	685	3	0.97531	6.89	0.08977	2.70	0.39	554.2	14.3	691	35	1167	126	**554**	**14**
563.9	6201	1	0.72258	2.06	0.08993	1.26	0.61	555.1	6.7	552	9	540	36	**555**	**7**
218	3446	3	0.87123	5.59	0.09028	3.74	0.67	557.2	19.9	636	26	928	85	**557**	**20**
41.79	649	2	0.77340	8.03	0.09032	3.29	0.41	557.4	17.6	582	36	678	157	**557**	**18**
73.95	1398	0	0.79653	6.46	0.09079	2.99	0.46	560.2	16.0	595	29	729	122	**560**	**16**
258.3	3519	1	0.73233	3.92	0.09083	3.48	0.89	560.5	18.7	558	17	547	39	**560**	**19**
114.2	1619	1	0.73745	4.37	0.09109	1.36	0.31	562.0	7.3	561	19	557	91	**562**	**7**
346.8	4647	14	0.74401	2.87	0.09128	1.65	0.58	563.1	8.9	565	12	571	51	**563**	**9**
375.7	5060	1	0.74978	2.98	0.09162	1.84	0.62	565.1	10.0	568	13	580	51	**565**	**10**
80.4	932	1	0.72524	6.39	0.09177	3.71	0.58	566.0	20.1	554	27	504	115	**566**	**20**
144.2	1804	1	0.73460	5.15	0.09196	3.46	0.67	567.1	18.8	559	22	527	84	**567**	**19**
295	6189	1	0.77381	3.79	0.09251	2.42	0.64	570.4	13.2	582	17	627	63	**570**	**13**
891	1218	1	0.74496	4.04	0.09320	1.98	0.49	574.5	10.9	565	18	529	77	**574**	**11**
122.7	1628	2	0.73849	5.42	0.09330	4.40	0.81	575.0	24.2	562	23	507	70	**575**	**24**
339	1674	2	0.74314	3.91	0.09386	1.31	0.34	578.3	7.3	564	17	508	81	**578**	**7**
77.87	1039	2	0.72793	7.34	0.09462	2.82	0.38	582.8	15.7	555	31	444	151	**583**	**16**
428.9	5571	1	0.78105	3.21	0.09482	2.17	0.67	584.0	12.1	586	14	594	51	**584**	**12**
107.9	2082	1	0.80762	3.53	0.09509	2.71	0.77	585.5	15.2	601	16	660	48	**586**	**15**
119.8	2235	3	0.82064	5.24	0.09660	3.59	0.69	594.5	20.4	608	24	661	82	**594**	**20**
100	1315	1	0.88089	6.20	0.09667	2.71	0.44	594.9	15.4	641	30	809	117	**595**	**15**
242.1	4605	1	0.83072	4.63	0.09671	3.21	0.69	595.1	18.3	614	21	684	71	**595**	**18**
294.4	4280	345	0.83983	2.82	0.09850	1.25	0.44	605.6	7.2	619	13	668	54	**606**	**7**
377.1	6244	2	0.83588	3.94	0.09894	3.28	0.83	608.2	19.0	617	18	649	47	**608**	**19**
504.1	7188	1	0.82838	2.81	0.09913	2.03	0.72	609.3	11.8	613	13	625	42	**609**	**12**
259.5	3012	2	0.82647	3.47	0.10002	2.02	0.58	614.5	11.8	612	16	601	61	**614**	**12**
223.5	3081	3	0.83775	3.79	0.10008	2.65	0.70	614.9	15.6	618	18	629	58	**615**	**16**
126.8	2794	1	0.87106	4.51	0.10012	1.54	0.34	615.1	9.0	636	21	712	90	**615**	**9**
155.4	2743	0	0.85166	4.94	0.10028	4.21	0.85	616.1	24.7	626	23	660	56	**616**	**25**
828.9	8268	3	0.82589	4.15	0.10047	3.27	0.79	617.2	19.3	611	19	590	55	**617**	**19**
1138	12977	32	0.86258	3.12	0.10206	2.35	0.75	626.5	14.0	632	15	650	44	**626**	**14**
238	3514	2	0.84159	3.48	0.10232	2.89	0.83	628.0	17.3	620	16	591	42	**628**	**17**
49.95	707	1	0.83751	5.87	0.10253	1.89	0.32	629.2	11.3	618	27	576	121	**629**	**11**
707.3	9650	4	1.02337	3.73	0.10840	3.17	0.85	663.5	20.0	716	19	883	40	**663**	**20**
703.8	10530	4	0.94650	3.14	0.10974	2.51	0.80	671.2	16.0	676	15	693	40	**671**	**16**
277	4122	3	1.07557	2.48	0.11908	1.73	0.70	725.2	11.9	741	13	791	37	**725**	**12**
256.7	3414	3	1.18496	3.38	0.12888	2.88	0.85	781.5	21.2	794	19	828	37	**782**	**21**
324.4	6874	4	1.27536	3.15	0.13811	2.03	0.65	834.0	15.9	835	18	837	50	**834**	**16**
303.3	5342	2	1.42291	3.85	0.14861	2.91	0.76	893.1	24.3	899	23	912	52	**912**	**52**
530	10119	4	1.51127	4.92	0.15699	4.24	0.86	940.0	37.1	935	30	923	51	**923**	**51**
485	9292	3	1.52704	4.05	0.15853	3.47	0.86	948.6	30.6	941	25	924	43	**924**	**43**
115.5	2696	2	1.42185	2.13	0.14654	1.51	0.71	881.6	12.4	898	13	939	31	**939**	**31**
512.1	13693	3	1.54804	3.07	0.15824	2.14	0.70	947.0	18.8	950	19	956	45	**956**	**45**
231.5	8738	2	1.56986	3.85	0.15941	1.66	0.43	953.5	14.8	958	24	970	71	**970**	**71**
664.2	2803	1	1.57146	5.25	0.15856	4.60	0.88	948.8	40.6	959	33	983	51	**983**	**51**
130.1	2734	4	1.50406	4.59	0.15174	3.04	0.66	910.7	25.8	932	28	983	70	**983**	**70**
413.5	9951	2	1.50299	5.22	0.15088	2.74	0.53	905.9	23.2	932	32	993	90	**993**	**90**
79.97	1975	1	1.33419	4.33	0.13347	3.23	0.75	807.6	24.5	861	25	1000	59	**1000**	**59**
647.2	10731	8	1.66874	6.22	0.16648	5.15	0.83	992.7	47.4	997	40	1006	71	**1006**	**71**
386.4	9917	2	1.70268	3.67	0.16940	2.55	0.70	1008.8	23.8	1010	23	1011	53	**1011**	**53**

			Isotopic ratios					Apparent ages (Ma)							
U	206Pb	U/Th	207Pb*		206Pb*		error	206Pb*		207Pb*		206Pb*		Best age	
(ppm)	204Pb		235U	(%)	238U	(%)	corr.	238U	±(Ma)	235U	±(Ma)	207Pb*	±(Ma)		±(Ma)
LW2-B															
186.9	1876	1	1.76444	4.56	0.17551	2.25	0.49	1042.4	21.6	1032	30	1012	81	**1012**	**81**
1511	7314	5	1.73983	5.74	0.16866	4.93	0.86	1004.7	45.9	1023	37	1064	59	**1064**	**59**
394	6389	3	1.84949	3.85	0.17758	3.46	0.90	1053.8	33.7	1063	25	1083	34	**1083**	**34**
257.2	11061	4	1.94360	3.17	0.18610	2.02	0.64	1100.2	20.5	1096	21	1088	49	**1088**	**49**
275.2	5691	2	1.77328	4.97	0.16955	4.00	0.80	1009.6	37.3	1036	32	1091	59	**1091**	**59**
181.9	4518	2	1.64485	4.00	0.15717	3.49	0.87	941.0	30.5	988	25	1092	39	**1092**	**39**
482.1	5501	3	2.00211	3.37	0.19046	2.94	0.87	1123.9	30.3	1116	23	1101	33	**1101**	**33**
83.28	2138	0	2.16129	2.88	0.19949	2.39	0.83	1172.6	25.6	1169	20	1161	32	**1161**	**32**
88.17	2625	1	2.08444	3.42	0.19180	1.68	0.49	1131.1	17.5	1144	24	1168	59	**1168**	**59**
84.72	2301	1	2.31918	3.47	0.20511	1.98	0.57	1202.7	21.7	1218	25	1246	56	**1246**	**56**
179.7	5683	2	2.27485	3.56	0.20004	1.44	0.40	1175.5	15.4	1205	25	1257	64	**1257**	**64**
309.6	12133	2	2.51833	4.41	0.22047	3.38	0.77	1284.3	39.3	1277	32	1266	55	**1266**	**55**
63.21	2260	97	2.39398	4.17	0.20772	3.25	0.78	1216.7	36.0	1241	30	1283	51	**1283**	**51**
40.52	2228	1	2.68915	5.54	0.23180	4.80	0.87	1343.9	58.2	1325	41	1296	54	**1296**	**54**
18.26	326	0	1.06300	11.61	0.09137	3.51	0.30	563.6	18.9	735	61	1301	216	**1301**	**216**
585.5	693	1	3.02187	9.48	0.24117	7.79	0.82	1392.8	97.6	1413	72	1444	103	**1444**	**103**
379.5	9206	2	3.64673	3.26	0.27159	2.87	0.88	1548.9	39.5	1560	26	1575	29	**1575**	**29**
403.1	20325	7	3.76633	3.10	0.27844	1.33	0.43	1583.5	18.7	1586	25	1588	52	**1588**	**52**
362.1	19509	3	3.85004	4.53	0.28263	3.67	0.81	1604.6	52.2	1603	37	1602	49	**1602**	**49**
192.7	6468	1	4.41745	3.07	0.30415	2.26	0.74	1711.9	34.0	1716	25	1720	38	**1720**	**38**
122	6545	1	4.92852	2.42	0.32186	1.81	0.75	1798.8	28.4	1807	20	1817	29	**1817**	**29**
88.47	4084	1	5.27076	3.34	0.33306	2.52	0.75	1853.2	40.6	1864	29	1876	40	**1876**	**40**
142.4	7438	2	5.74075	3.08	0.35108	1.69	0.55	1939.7	28.4	1938	27	1935	46	**1935**	**46**
592.6	20399	4	4.98083	3.17	0.29788	2.57	0.81	1680.8	38.0	1816	27	1975	33	**1975**	**33**
340.7	18417	2	6.38097	4.87	0.36585	4.27	0.88	2009.8	73.7	2030	43	2050	41	**2050**	**41**
359.5	16515	2	6.00127	4.72	0.34318	3.61	0.77	1901.9	59.5	1976	41	2054	54	**2054**	**54**
134.8	7482	2	7.08096	4.11	0.38188	2.64	0.64	2085.1	47.0	2122	37	2157	55	**2157**	**55**
509.1	19688	3	7.54389	4.40	0.38791	4.18	0.95	2113.1	75.3	2178	39	2240	24	**2240**	**24**
101.3	5529	2	6.27099	4.20	0.30966	3.49	0.83	1739.1	53.2	2014	37	2310	40	**2310**	**40**
627.9	29359	3	8.75525	3.43	0.41294	3.13	0.91	2228.3	59.0	2313	31	2388	24	**2388**	**24**
73	5075	1	9.93673	3.09	0.39825	2.02	0.65	2161.0	37.2	2429	29	2662	39	**2662**	**39**
303.8	9244	2	10.64396	3.38	0.42359	3.02	0.89	2276.7	58.0	2493	31	2673	25	**2673**	**25**
125.3	6968	2	12.86159	3.24	0.50462	2.66	0.82	2633.6	57.6	2670	31	2697	30	**2697**	**30**
434.5	24005	2	12.53814	3.94	0.48733	3.37	0.86	2559.1	71.2	2646	37	2712	34	**2712**	**34**
455.8	26789	1	13.60263	2.84	0.52526	2.16	0.76	2721.4	48.0	2722	27	2723	30	**2723**	**30**
82.79	5738	2	13.89051	4.25	0.52975	3.36	0.79	2740.4	75.1	2742	40	2744	43	**2744**	**43**
339.1	11546	1	14.72533	2.96	0.54011	2.30	0.78	2783.9	52.1	2798	28	2808	30	**2808**	**30**
383.3	14061	13	11.36825	3.40	0.41483	2.67	0.79	2236.9	50.5	2554	32	2816	34	**2816**	**34**
318.4	23724	2	17.21856	2.58	0.58009	1.73	0.67	2949.1	40.9	2947	25	2946	31	**2946**	**31**
76.45	5457	1	18.19414	2.36	0.58187	1.90	0.80	2956.4	45.0	3000	23	3029	22	**3029**	**22**
343.6	10302	2	27.10073	5.09	0.68970	4.79	0.94	3381.5	126.1	3387	50	3390	27	**3390**	**27**
339.4	21407	1	25.11400	2.34	0.63668	1.32	0.56	3176.0	33.0	3313	23	3396	30	**3396**	**30**
LW2-C															
258.1	1443	1	0.34317	11.64	0.04132	1.93	0.17	261.0	4.9	300	30	612	249	**261**	**5**
298.4	5172	2	0.69993	5.52	0.08280	3.81	0.69	512.8	18.8	539	23	650	86	**513**	**19**
474.5	7497	24	0.71350	2.89	0.08694	1.47	0.51	537.4	7.6	547	12	586	54	**537**	**8**
1017	10192	4	0.71016	2.24	0.08782	1.99	0.89	542.6	10.4	545	9	554	22	**543**	**10**
86.54	1547	1	0.87375	8.28	0.08812	3.97	0.48	544.4	20.7	638	39	983	148	**544**	**21**
271.4	4204	4	0.73975	4.99	0.08880	3.22	0.64	548.4	16.9	562	22	619	82	**548**	**17**
630.9	8353	2	0.73075	3.78	0.08918	2.36	0.62	550.7	12.4	557	16	583	64	**551**	**12**
178.3	2451	3	0.77180	4.03	0.08948	2.98	0.74	552.5	15.8	581	18	693	58	**552**	**16**
83.64	1576	1	0.85673	5.38	0.09121	3.54	0.66	562.7	19.1	628	25	872	84	**563**	**19**
223.2	3422	2	0.79834	3.78	0.09234	2.84	0.75	569.3	15.5	596	17	698	53	**569**	**15**
412.5	6089	1	0.75355	3.22	0.09267	2.29	0.71	571.3	12.5	570	14	566	49	**571**	**13**
146.5	2488	2	0.85333	3.69	0.09269	2.34	0.63	571.4	12.8	626	17	831	60	**571**	**13**
150.8	2464	1	0.80382	5.22	0.09303	2.16	0.42	573.4	11.9	599	24	697	101	**573**	**12**
58.61	947	1	0.82533	5.92	0.09335	3.47	0.59	575.3	19.1	611	27	746	101	**575**	**19**
472.1	8685	3	0.78536	2.98	0.09345	2.25	0.76	575.9	12.4	589	13	638	42	**576**	**12**
391	5683	1	0.77357	5.18	0.09397	3.69	0.71	579.0	20.4	582	23	593	79	**579**	**20**
614.8	1829	6	0.78257	6.11	0.09419	1.65	0.27	580.2	9.1	587	27	613	127	**580**	**9**
250	2761	2	0.79003	5.51	0.09425	2.62	0.48	580.6	14.5	591	25	632	104	**581**	**15**

			Isotopic ratios					Apparent ages (Ma)							
U	206Pb	U/Th	207Pb*		206Pb*		error	206Pb*		207Pb*		206Pb*		Best age	
(ppm)	204Pb		235U	(%)	238U	(%)	corr.	238U	±(Ma)	235U	±(Ma)	207Pb*	±(Ma)		±(Ma)
LW2-C															
68.06	1057	1	0.83108	5.79	0.09475	1.94	0.33	583.5	10.8	614	27	729	116	**584**	**11**
374.5	4009	0	0.76798	4.52	0.09475	3.05	0.67	583.6	17.0	579	20	559	73	**584**	**17**
1020	9207	5	0.77859	4.64	0.09496	3.03	0.65	584.8	16.9	585	21	584	76	**585**	**17**
155.1	3199	2	0.84290	3.97	0.09507	2.19	0.55	585.5	12.2	621	18	752	70	**585**	**12**
95.33	1577	1	0.87068	3.70	0.09530	1.23	0.33	586.8	6.9	636	17	815	73	**587**	**7**
655.1	8843	5	0.82079	5.80	0.09531	5.28	0.91	586.9	29.6	608	27	690	51	**587**	**30**
97.86	1813	0	0.89307	6.80	0.09558	2.93	0.43	588.5	16.5	648	33	861	127	**588**	**16**
1251	5847	81	0.77984	3.84	0.09576	2.80	0.73	589.5	15.8	585	17	569	57	**590**	**16**
1189	7079	2	0.80291	3.88	0.09741	2.31	0.60	599.2	13.2	598	18	596	68	**599**	**13**
295.4	3554	0	0.80215	3.34	0.09756	2.64	0.79	600.1	15.1	598	15	590	44	**600**	**15**
234.9	3255	1	0.88047	4.42	0.09766	3.45	0.78	600.7	19.8	641	21	787	58	**601**	**20**
205.3	3015	1	0.86694	4.74	0.09959	2.49	0.52	612.0	14.5	634	22	713	86	**612**	**15**
138.6	2804	1	0.90897	3.94	0.10106	2.25	0.57	620.6	13.3	657	19	782	68	**621**	**13**
416.3	6687	1	0.85800	4.51	0.10177	3.53	0.78	624.8	21.0	629	21	644	60	**625**	**21**
216.7	1906	2	0.90541	8.00	0.10239	2.89	0.36	628.4	17.3	655	39	746	158	**628**	**17**
265.2	5064	1	1.17410	3.02	0.12133	2.01	0.66	738.2	14.0	789	17	934	46	**738**	**14**
437	8303	2	1.46036	2.57	0.14914	1.35	0.53	896.2	11.3	914	15	958	45	**958**	**45**
120.6	3040	1	1.53890	2.90	0.15560	1.26	0.44	932.3	10.9	946	18	978	53	**978**	**53**
308.6	8917	2	1.53021	3.16	0.15407	1.95	0.62	923.8	16.8	943	19	987	51	**987**	**51**
371.4	8092	4	1.70989	6.62	0.16792	5.74	0.87	1000.6	53.2	1012	42	1037	67	**1037**	**67**
209.3	6520	3	1.69243	6.06	0.16440	4.59	0.76	981.2	41.7	1006	39	1059	80	**1059**	**80**
52.76	1195	1	1.32528	4.63	0.12731	1.67	0.36	772.5	12.2	857	27	1082	87	**1082**	**87**
413.7	11164	5	1.84281	2.63	0.17581	1.89	0.72	1044.0	18.3	1061	17	1096	37	**1096**	**37**
492.5	11254	4	1.92729	5.01	0.18317	3.56	0.71	1084.3	35.5	1091	34	1103	71	**1103**	**71**
231.8	5730	1	1.92887	6.28	0.17840	3.41	0.54	1058.2	33.3	1091	42	1157	105	**1157**	**105**
28.1	426	0	1.08044	11.92	0.09682	7.09	0.59	595.7	40.3	744	63	1220	189	**1220**	**189**
132.8	4637	1	2.31326	3.16	0.20538	2.49	0.79	1204.2	27.3	1216	22	1238	38	**1238**	**38**
150.2	4923	2	2.37003	5.07	0.20916	2.89	0.57	1224.3	32.2	1234	36	1250	82	**1250**	**82**
61.39	2271	1	2.70716	5.91	0.22248	5.03	0.85	1295.0	59.1	1330	44	1388	59	**1388**	**59**
271.5	8249	1	3.22884	4.14	0.25797	2.22	0.54	1479.4	29.4	1464	32	1442	67	**1442**	**67**
77.53	3058	2	3.43844	4.63	0.26026	1.78	0.38	1491.2	23.7	1513	36	1544	80	**1544**	**80**
329.5	4661	2	3.02279	4.48	0.22635	3.88	0.87	1315.3	46.1	1413	34	1564	42	**1564**	**42**
1360	5244	2	3.31134	9.98	0.24757	9.10	0.91	1425.9	116.4	1484	78	1567	77	**1567**	**77**
256.4	13056	3	3.86750	3.92	0.28083	3.42	0.87	1595.5	48.3	1607	32	1622	36	**1622**	**36**
518.3	3971	3	3.97457	6.11	0.28860	2.38	0.39	1634.5	34.4	1629	50	1622	105	**1622**	**105**
127.7	6549	2	5.89706	4.07	0.35151	2.94	0.72	1941.8	49.3	1961	35	1981	50	**1981**	**50**
239.4	12727	1	6.99328	2.57	0.38047	1.63	0.64	2078.5	29.0	2111	23	2142	35	**2142**	**35**
665.2	35849	12	10.12291	3.48	0.45282	1.69	0.49	2407.8	34.0	2446	32	2478	51	**2478**	**51**
431.5	23472	2	11.32872	9.07	0.46400	4.14	0.46	2457.2	84.7	2551	85	2626	134	**2626**	**134**
203.4	11832	2	11.03206	6.02	0.43822	5.42	0.90	2342.7	106.5	2526	56	2676	43	**2676**	**43**
236.1	13935	3	12.81531	4.30	0.50042	2.73	0.64	2615.6	58.8	2666	41	2705	55	**2705**	**55**
285.1	27339	2	13.57504	2.65	0.52654	1.07	0.40	2726.8	23.7	2721	25	2716	40	**2716**	**40**
185.5	11549	21	11.96468	3.41	0.45114	1.00	0.29	2400.3	20.0	2602	32	2762	54	**2762**	**54**
187.6	4901	2	13.77037	10.86	0.49319	10.42	0.96	2584.4	221.9	2734	103	2846	50	**2846**	**50**
171.7	13670	1	23.41292	4.57	0.64633	1.81	0.40	3213.8	45.8	3244	45	3263	66	**3263**	**66**
148.7	13230	2	22.80704	5.86	0.60095	3.77	0.64	3033.7	91.3	3219	57	3336	70	**3336**	**70**
LW															
218.1	2390	1	0.45039	4.26	0.06005	2.87	0.67	376.0	10.5	378	13	387	71	**376**	**10**
489.7	7078	9	0.70878	3.84	0.08768	2.71	0.71	541.8	14.1	544	16	553	59	**542**	**14**
60.09	893	1	0.67144	5.91	0.08845	3.18	0.54	546.4	16.7	522	24	414	111	**546**	**17**
56.63	804	1	0.73871	6.81	0.08858	2.96	0.43	547.1	15.5	562	29	621	133	**547**	**16**
141.8	2340	1	0.71752	3.56	0.09004	1.76	0.49	555.8	9.4	549	15	522	68	**556**	**9**
332.8	6624	8	0.77460	3.38	0.09005	2.40	0.71	555.8	12.8	582	15	687	51	**556**	**13**
141.9	2536	1	0.74021	4.41	0.09033	1.97	0.45	557.5	10.5	563	19	583	86	**558**	**11**
529.5	10135	2	0.72914	2.08	0.09120	1.61	0.77	562.7	8.7	556	9	529	29	**563**	**9**
132	2823	1	0.75334	3.11	0.09177	1.67	0.54	566.0	9.0	570	14	587	57	**566**	**9**
399.5	9910	2	0.76854	3.44	0.09184	1.32	0.38	566.4	7.1	579	15	628	69	**566**	**7**
346	5303	8	0.72427	3.21	0.09222	2.06	0.64	568.7	11.2	553	14	490	54	**569**	**11**
276.8	3575	0	0.76253	3.20	0.09247	1.06	0.33	570.2	5.8	575	14	596	66	**570**	**6**
65.77	1331	1	0.70974	7.16	0.09299	5.97	0.83	573.2	32.8	545	30	427	88	**573**	**33**
223.3	3364	2	0.73658	4.76	0.09312	3.60	0.76	574.0	19.8	560	21	506	69	**574**	**20**

			Isotopic ratios					Apparent ages (Ma)							
U	206Pb	U/Th	207Pb*		206Pb*		error	206Pb*		207Pb*		206Pb*		Best age	
(ppm)	204Pb		235U	(%)	238U	(%)	corr.	238U	±(Ma)	235U	±(Ma)	207Pb*	±(Ma)		**±(Ma)**
LW															
223.3	3364	2	0.73658	4.76	0.09312	3.60	0.76	574.0	19.8	560	21	506	69	**574**	**20**
384.9	6531	4	0.76932	3.07	0.09346	1.71	0.56	576.0	9.4	579	14	593	55	**576**	**9**
73.81	1481	3	0.75714	7.20	0.09396	6.04	0.84	578.9	33.4	572	32	546	86	**579**	**33**
66.1	1226	1	0.73248	8.21	0.09445	2.86	0.35	581.8	15.9	558	35	462	171	**582**	**16**
251.1	4111	2	0.78605	4.10	0.09447	2.33	0.57	581.9	12.9	589	18	616	73	**582**	**13**
253.3	4049	1	0.79111	2.03	0.09449	1.04	0.51	582.1	5.8	592	9	629	38	**582**	**6**
76.03	1521	1	0.78842	6.04	0.09470	2.87	0.48	583.3	16.0	590	27	617	115	**583**	**16**
299.4	5533	4	0.78427	4.69	0.09559	1.59	0.34	588.5	8.9	588	21	586	96	**588**	**9**
257.8	4089	1	0.79932	3.20	0.09582	1.88	0.59	589.9	10.6	596	14	622	56	**590**	**11**
1052	21147	98	0.79474	4.47	0.09604	2.20	0.49	591.2	12.4	594	20	604	84	**591**	**12**
112	2989	1	0.82185	4.57	0.09605	2.05	0.45	591.2	11.6	609	21	676	87	**591**	**12**
563.3	7448	1	0.79549	1.82	0.09641	1.10	0.60	593.3	6.2	594	8	598	31	**593**	**6**
202.9	2433	0	0.79190	4.27	0.09644	2.98	0.70	593.5	16.9	592	19	587	67	**594**	**17**
185.7	3403	1	0.77675	4.13	0.09648	3.21	0.78	593.8	18.2	584	18	544	57	**594**	**18**
164.3	2597	1	0.80818	5.19	0.09671	1.46	0.28	595.1	8.3	601	24	625	107	**595**	**8**
552.3	8184	1	0.81035	1.54	0.09702	1.03	0.67	596.9	5.9	603	7	624	25	**597**	**6**
286.5	5678	5	0.79748	3.47	0.09712	2.02	0.58	597.5	11.5	595	16	587	61	**598**	**12**
184.6	2619	1	0.80849	2.88	0.09720	1.00	0.35	598.0	5.7	602	13	615	58	**598**	**6**
136.1	2215	1	0.80263	2.90	0.09735	1.33	0.46	598.8	7.6	598	13	596	56	**599**	**8**
176.3	2806	1	0.80390	4.02	0.09737	1.82	0.45	599.0	10.4	599	18	599	78	**599**	**10**
102	1748	1	0.84242	4.42	0.09807	2.72	0.62	603.1	15.7	620	21	684	74	**603**	**16**
796	7690	3	0.81244	1.58	0.09831	1.00	0.63	604.5	5.8	604	7	601	27	**605**	**6**
299.5	5580	1	0.83084	2.96	0.09836	1.86	0.63	604.8	10.8	614	14	649	49	**605**	**11**
332.2	4675	0	0.83428	2.81	0.09852	1.98	0.71	605.7	11.5	616	13	654	43	**606**	**11**
58.11	1675	1	0.81692	9.38	0.09856	5.21	0.56	606.0	30.1	606	43	608	169	**606**	**30**
73.49	1460	7	0.81899	7.00	0.09857	3.23	0.46	606.0	18.7	607	32	613	134	**606**	**19**
37.69	632	1	0.80264	7.99	0.09858	3.16	0.40	606.1	18.3	598	36	569	160	**606**	**18**
161.8	1653	0	0.85313	5.96	0.10084	2.23	0.37	619.3	13.2	626	28	652	119	**619**	**13**
112.7	2260	7	0.85772	4.94	0.10202	1.39	0.28	626.2	8.3	629	23	638	102	**626**	**8**
1014	5182	1	0.87511	4.74	0.10401	1.97	0.42	637.8	11.9	638	22	640	93	**638**	**12**
151.3	3848	1	0.99258	3.34	0.11317	2.62	0.79	691.1	17.2	700	17	729	44	**691**	**17**
676.9	10205	31	1.00949	4.52	0.11608	3.44	0.76	708.0	23.0	709	23	711	63	**708**	**23**
239.6	5454	4	1.39534	5.11	0.14678	4.90	0.96	882.9	40.4	887	30	897	31	**883**	**40**
472.5	9996	6	1.46007	3.31	0.14863	1.85	0.56	893.3	15.4	914	20	965	56	**893**	**15**
237.9	5765	2	1.51946	3.15	0.15507	1.46	0.46	929.3	12.7	938	19	959	57	**929**	**13**
717.3	18085	2	1.51065	2.79	0.15646	0.99	0.35	937.1	8.6	935	17	929	54	**937**	**9**
318.1	11008	2	1.65324	8.34	0.16501	7.70	0.92	984.6	70.3	991	53	1005	65	**1005**	**65**
461.3	10217	2	1.65688	8.48	0.16505	7.75	0.91	984.8	70.8	992	54	1009	70	**1009**	**70**
370.2	10666	3	1.68641	3.05	0.16795	2.25	0.74	1000.8	20.8	1003	19	1009	42	**1009**	**42**
609.3	16878	2	1.74563	2.33	0.17279	2.09	0.89	1027.4	19.8	1026	15	1021	21	**1021**	**21**
215.4	5729	1	1.73246	4.58	0.17012	3.18	0.70	1012.8	29.8	1021	29	1038	66	**1038**	**66**
295	3643	2	1.52114	6.11	0.14931	2.51	0.41	897.1	21.0	939	37	1038	113	**1038**	**113**
484	11025	1	1.85934	2.79	0.18194	1.75	0.63	1077.6	17.4	1067	18	1045	44	**1045**	**44**
178.6	6064	2	1.89624	3.59	0.18491	2.48	0.69	1093.8	24.9	1080	24	1052	52	**1052**	**52**
389.7	7688	2	1.63266	9.23	0.15906	8.64	0.94	951.5	76.4	983	58	1054	66	**1054**	**66**
224.7	5455	2	1.89429	3.63	0.18272	2.18	0.60	1081.8	21.7	1079	24	1074	58	**1074**	**58**
176.3	4145	5	1.57362	4.52	0.15010	3.37	0.75	901.5	28.3	960	28	1096	60	**1096**	**60**
204.6	6012	1	1.89926	4.14	0.18033	3.37	0.81	1068.8	33.2	1081	28	1105	48	**1105**	**48**
115.6	3229	1	1.91296	2.14	0.18145	1.75	0.82	1074.9	17.4	1086	14	1107	25	**1107**	**25**
717.3	3893	3	1.84812	4.83	0.17460	4.46	0.92	1037.4	42.7	1063	32	1115	37	**1115**	**37**
152.2	3391	2	2.18161	3.16	0.20001	1.31	0.41	1175.4	14.0	1175	22	1175	57	**1175**	**57**
408.8	15537	2	2.21735	4.94	0.20181	2.34	0.47	1185.0	25.3	1187	35	1189	86	**1189**	**86**
50.07	2008	1	2.04435	4.34	0.18560	2.81	0.65	1097.5	28.4	1130	30	1194	65	**1194**	**65**
74.54	3450	1	2.14758	4.46	0.19126	2.48	0.56	1128.2	25.7	1164	31	1232	73	**1232**	**73**
104.3	4991	2	2.31856	3.02	0.20544	1.54	0.51	1204.5	16.9	1218	21	1242	51	**1242**	**51**
85.02	4303	1	2.24820	3.12	0.19832	1.02	0.33	1166.3	10.8	1196	22	1251	58	**1251**	**58**
252.5	6327	2	2.14370	3.49	0.18853	2.39	0.68	1113.4	24.4	1163	24	1257	50	**1257**	**50**
189.2	5922	1	1.89441	3.21	0.14745	2.67	0.83	886.7	22.1	1079	21	1492	34	**1492**	**34**
161.2	6372	1	3.44279	6.71	0.26105	3.31	0.49	1495.2	44.1	1514	53	1541	110	**1541**	**110**
1598	44366	93	3.60108	2.99	0.27128	2.35	0.79	1547.3	32.3	1550	24	1553	35	**1553**	**35**
257.4	10625	2	3.67078	5.14	0.27459	4.82	0.94	1564.1	67.0	1565	41	1566	33	**1566**	**33**

			Isotopic ratios					Apparent ages (Ma)							
U	206Pb	U/Th	207Pb*		206Pb*		error	206Pb*		207Pb*		206Pb*		Best age	
(ppm)	204Pb		235U	(%)	238U	(%)	corr.	238U	±(Ma)	235U	±(Ma)	207Pb*	±(Ma)		**±(Ma)**
LW															
376.8	1865	1	3.30637	4.82	0.24507	3.01	0.62	1413.0	38.1	1483	38	1584	70	**1584**	**70**
942.1	25208	4	3.63144	6.53	0.26865	6.01	0.92	1533.9	82.0	1556	52	1587	48	**1587**	**48**
548.2	18777	4	3.53947	5.75	0.26012	5.12	0.89	1490.4	68.1	1536	46	1599	49	**1599**	**49**
138	5536	1	3.57811	1.76	0.26090	1.15	0.66	1494.4	15.3	1545	14	1614	25	**1614**	**25**
164.1	10578	1	3.93413	2.49	0.28353	1.58	0.64	1609.1	22.5	1621	20	1636	36	**1636**	**36**
181.8	4558	1	4.65343	3.40	0.30903	1.97	0.58	1735.9	30.0	1759	28	1786	50	**1786**	**50**
616.2	1643	1	5.23931	7.28	0.33538	6.86	0.94	1864.4	111.0	1859	62	1853	44	**1853**	**44**
571.9	26841	1	5.38607	4.57	0.34177	2.70	0.59	1895.2	44.4	1883	39	1869	67	**1869**	**67**
23.88	1840	1	5.32091	4.29	0.32583	3.26	0.76	1818.1	51.6	1872	37	1933	50	**1933**	**50**
160	10879	1	5.74671	2.23	0.34791	1.35	0.61	1924.6	22.5	1938	19	1953	32	**1953**	**32**
95.78	6709	3	7.19043	3.63	0.38634	3.24	0.89	2105.8	58.3	2135	32	2164	28	**2164**	**28**
154.2	11705	1	7.63570	3.97	0.38047	3.40	0.86	2078.5	60.5	2189	36	2294	35	**2294**	**35**
75.07	7502	1	8.92469	4.47	0.43466	1.00	0.22	2326.7	19.5	2330	41	2334	75	**2334**	**75**
273	19918	2	9.63283	3.98	0.44860	3.06	0.77	2389.0	61.0	2400	37	2410	43	**2410**	**43**
200	6583	1	12.25424	2.44	0.50214	1.60	0.66	2623.0	34.5	2624	23	2625	31	**2625**	**31**
119.8	9973	1	12.53970	2.10	0.49630	1.78	0.85	2597.9	38.0	2646	20	2682	18	**2682**	**18**
203.2	13186	2	12.84694	3.54	0.50003	2.54	0.72	2613.9	54.5	2668	33	2710	41	**2710**	**41**
259.3	22175	1	13.47872	2.52	0.52277	2.00	0.80	2710.9	44.3	2714	24	2716	25	**2716**	**25**
1466	91862	13	13.56987	2.38	0.52509	1.10	0.46	2720.7	24.5	2720	23	2720	35	**2720**	**35**
126	12088	2	13.93784	3.92	0.53238	1.89	0.48	2751.5	42.3	2745	37	2741	57	**2741**	**57**
164.3	3379	1	11.56709	3.49	0.44023	2.16	0.62	2351.7	42.6	2570	33	2747	45	**2747**	**45**
80.53	7148	2	14.72048	3.18	0.54208	1.83	0.58	2792.1	41.5	2797	30	2801	43	**2801**	**43**
125.1	13171	1	19.30416	3.36	0.58993	2.61	0.78	2989.1	62.3	3057	32	3102	34	**3102**	**34**
MT															
86.86	1355	2	0.73615	5.37	0.07953	1.97	0.37	493.3	9.4	560	23	842	104	**493**	**9**
154.6	2300	2	0.75646	3.12	0.08303	1.51	0.48	514.2	7.5	572	14	809	57	**514**	**7**
444.1	5364	1	0.68270	3.26	0.08481	1.00	0.31	524.8	5.0	528	13	544	68	**525**	**5**
1360	14336	2	0.71059	7.89	0.08924	7.24	0.92	551.1	38.3	545	33	520	68	**551**	**38**
1158	865	1	0.73863	12.11	0.09192	4.23	0.35	566.9	22.9	562	52	540	249	**567**	**23**
526.7	665	2	1.24276	7.46	0.12003	4.31	0.58	730.7	29.8	820	42	1071	123	**1071**	**123**
83.96	2516	1	2.50747	6.04	0.21234	2.63	0.44	1241.3	29.7	1274	44	1330	105	**1330**	**105**
175	3135	1	4.03488	7.38	0.27709	1.93	0.26	1576.7	27.1	1641	60	1725	131	**1725**	**131**
347.1	6316	1	4.31541	6.33	0.29513	5.28	0.83	1667.1	77.5	1696	52	1733	64	**1733**	**64**
137.7	6869	1	4.77996	3.43	0.31872	1.06	0.31	1783.5	16.6	1781	29	1779	59	**1779**	**59**
46.65	3140	2	4.72361	6.89	0.31254	2.72	0.40	1753.2	41.8	1771	58	1793	115	**1793**	**115**
194.6	12300	1	5.24740	3.69	0.33240	1.49	0.41	1850.0	24.0	1860	31	1872	61	**1872**	**61**
326.3	10744	1	5.72688	5.32	0.35328	3.54	0.67	1950.2	59.6	1935	46	1920	71	**1920**	**71**
92.74	8038	1	14.62706	4.14	0.54204	2.98	0.72	2792.0	67.5	2791	39	2791	47	**2791**	**47**
107.3	12765	2	14.88501	5.15	0.55066	1.21	0.23	2827.9	27.7	2808	49	2794	82	**2794**	**82**

Notes:

• All uncertainties are reported at the 1-sigma level, and include only measurement errors. Systematic errors would increase age uncertainties by 1-2%.

• U concentration and U/Th are calibrated relative to NIST SRM 610 and are accurate to ~20%.

• Common Pb correction is from 204Pb, with composition interpreted from Stacey and Kramers (1975) and uncertainties of 1.0 for 206Pb/ 204Pb, 0.3 for 207Pb/ 204Pb, and 2.0 for 208Pb/ 204Pb.

• U/Pb and 206Pb/ 207Pb fractionation is calibrated relative to fragments of a large Sri Lanka zircon of 564 ± 4 Ma (2-sigma).

• U decay constants and composition as follows: 238U = 9.8485 x 10 -10, 235U = 1.55125 x 10 -10, 238U/ 235U = 137.88

Appendix D. Extracted detrital zircon U-Pb ages.

SORTED BY AGE					SORTED BY # GRAINS (SIGNIFICANCE)				
Min. Age	Max. Age	# Grains	Peak Age	# Grains	Min. Age	Max. Age	# Grains	Peak Age	# Grains
BN									
508	685	52	531	11	508	685	52	586	39
772	1149	17	586	39	772	1149	17	531	11
1155	1580	10	844	7	1155	1580	10	844	7
2195	2293	2	893	7	2195	2293	2	893	7
2355	2410	1	1006	5	2355	2410	1	1048	6
2450	2479		1048	6	2531	2626	1	1006	5
2531	2626	1	1333	5	2450	2479		1333	5
			1493	5				1493	5
			2238	4				2238	4
			2552	3				2552	3
BR									
481	702	46	533	16	481	702	46	588	25
708	718		555	23	735	1334	34	555	23
722	726		588	25	1397	1506	3	533	16
735	1334	34	680	4	708	718		943	11
1365	1376		800	6	722	726		800	6
1397	1506	3	943	11	1365	1376		1138	6
1764	1789		1138	6	1764	1789		1248	5
1898	1908		1248	5	1898	1908		680	4
			1461	3				1461	3
CJ									
449	708	67	530	43	449	708	67	530	43
937	1220	6	1039	5	937	1220	6	1039	5
HB									
483	602	71	530	51	483	602	71	530	51
947	1266	9	1112	6	947	1266	9	1112	6
			1248	3				1248	3
LW									
513	645	42	570	28	513	645	42	570	28
657	666		596	27	869	1367	21	596	27
869	1367	21	895	4	1491	1708	7	1101	13
1491	1708	7	935	7	1765	2003	5	1027	10
1735	1761		1027	10	2628	2792	5	935	7
1765	2003	5	1101	13	2324	2364	1	1602	7
2324	2364	1	1602	7	657	666		2694	5
2628	2792	5	1858	4	1735	1761		895	4
			1941	4				1858	4
			2694	5				1941	4
LW2-A									
508	668	26	564	15	508	668	26	564	15
698	734	2	596	15	1400	1652	8	596	15
860	940	3	712	3	2642	2798	6	1471	8
1021	1259	5	888	4	1021	1259	5	2683	5
1400	1652	8	1188	4	860	940	3	888	4
1897	1958	2	1471	8	2926	3036	3	1188	4
2194	2256	1	1909	3	698	734	2	712	3
2453	2501	2	2234	3	1897	1958	2	1909	3
2510	2549		2499	3	2453	2501	2	2234	3
2642	2798	6	2683	5	2194	2256	1	2499	3
2926	3036	3	2981	3	2510	2549		2981	3

SORTED BY AGE					SORTED BY # GRAINS (SIGNIFICANCE)				
Min. Age	Max. Age	# Grains	Peak Age	# Grains	Min. Age	Max. Age	# Grains	Peak Age	# Grains
LW2-B									
522	666	36	563	20	522	666	36	563	20
701	703		608	18	808	1385	26	608	18
808	1385	26	836	5	2658	2783	4	953	14
1504	1692	3	953	14	1504	1692	3	1076	14
1796	1796		1076	14	2047	2132	2	1267	7
1843	1875		1267	7	701	703		836	5
1946	1956		1580	4	1796	1796		1580	4
1968	2027		2054	3	1843	1875		2715	4
2047	2132	2	2715	4	1946	1956		2054	3
2658	2783	4			1968	2027			
LW2-C									
520	647	29	583	23	520	647	29	583	23
885	1704	16	991	7	885	1704	16	991	7
2636	2815	2	1080	7	2636	2815	2	1080	7
			1232	4				1439	5
			1439	5				1232	4
			1613	4				1613	4
			2713	3				2713	3
MT									
521	535	1	525	3	1605	1994	6	1788	6
1605	1994	6	1788	6	521	535	1	525	3
SAL1633									
478	771	27	489	4	478	771	27	545	13
903	1245	10	545	13	903	1245	10	598	9
			598	9				1072	6
			711	4				489	4
			923	3				711	4
			1072	6				923	3
			1194	3				1194	3
SAL1636									
468	644	25	490	4	468	644	25	553	11
649	658		523	6	950	1218	6	599	8
950	1218	6	553	11	1786	1869	2	523	6
1786	1869	2	599	8	649	658		490	4
			1000	4				1000	4
			1139	3				1139	3
			1821	3				1821	3
SAL1639									
491	668	22	516	9	491	668	22	561	12
			561	12				516	9
			604	9				604	9
SAL1641									
461	803	64	488	13	461	803	64	518	24
815	822		518	24	826	1122	18	488	13
826	1122	18	561	11	1532	1686	3	590	13
1124	1248	2	590	13	1124	1248	2	561	11
1532	1686	3	721	6	815	822		1059	8
			880	4				721	6
			949	6				949	6
			1059	8				880	4
			1185	3				1185	3
			1621	3				1621	3
SAL282									
96	110	5	102	5	96	110	5	102	5
522	554	3	539	3	522	554	3	539	3
606	638	2	622	3	644	699	3	622	3
644	699	3	676	3	983	1072	3	676	3
727	728		1035	3	606	638	2	1035	3
983	1072	3			727	728			

Appendix E. Raw point count data from Byrd Glacier and Ross Sea samples.

Sample ID	qtz	pyr	kspar	plag	cal	oli	musc	biot	chlor	iron ore	opaq	unknown other	pmict	silt/s. s.	mudst clayst	maf	int	fel	marble l. s.	meta	ext	*n*
Byrd Glacier																						
BN-A	3	2	1	2	0	0	0	0	0	0	0	1	0	0	0	200	4	0	0	0	0	213
BN-B	4	0	8	2	0	0	0	0	0	0	1	4	0	0	0	420	0	0	0	0	0	439
BN-C	2	16	2	2	0	0	0	0	0	0	0	1	0	0	0	345	1	0	0	0	0	369
BN	**9**	**18**	**11**	**6**	**0**	**0**	**0**	**0**	**0**	**0**	**1**	**6**	**0**	**0**	**0**	**965**	**5**	**0**	**0**	**0**	**0**	**1021**
												0							0	0		
BR-A	3	3	0	1	0	0	0	0	0	0	0	0	0	4	0	307	0	0	0	9	0	327
BR-B	7	0	0	3	0	0	0	0	0	0	0	0	0	7	1	127	0	0	0	23	0	168
BR-C	0	1	0	1	0	0	0	0	1	0	0	3	3	3	0	121	0	1	0	1	0	135
BR Avg.	**10**	**4**	**0**	**5**	**0**	**0**	**0**	**0**	**1**	**0**	**0**	**3**	**3**	**14**	**1**	**555**	**0**	**1**	**0**	**33**	**0**	**630**
												0							0	0		
CJ-B	95	4	54	32	0	0	0	11	0	0	1	8	1	0	0	37	34	92	0	12	0	381
CJ-C	38	2	42	29	0	0	0	9	0	0	1	12	0	0	0	18	72	107	0	66	1	397
CJ Avg.	**133**	**6**	**96**	**61**	**0**	**0**	**0**	**20**	**0**	**0**	**2**	**20**	**1**	**0**	**0**	**55**	**106**	**199**	**0**	**78**	**1**	**778**
												0							0	0		
HB-B	19	0	8	20	0	0	0	8	0	0	0	5	0	0	0	1	49	39	0	19	0	168
HB-C	15	0	10	35	0	0	0	14	0	0	0	3	0	0	0	0	63	44	0	27	0	211
HB Avg.	**34**	**0**	**18**	**55**	**0**	**0**	**0**	**22**	**0**	**0**	**0**	**8**	**0**	**0**	**0**	**1**	**112**	**83**	**0**	**46**	**0**	**379**
												0							0	0		
LW-A1	151	3	15	6	0	0	0	0	0	0	2	7	335	27	0	27	6	25	0	22	0	626
LW-A2	21	0	3	3	0	0	0	0	0	0	0	0	66	0	0	26	2	18	0	14	0	153
LW-B	124	4	4	3	0	0	0	0	0	0	2	3	672	9	3	4	2	20	2	7	0	859
LW Avg.	**296**	**7**	**22**	**12**	**0**	**0**	**0**	**0**	**0**	**0**	**4**	**10**	**1073**	**36**	**3**	**57**	**10**	**63**	**2**	**43**	**0**	**1638**
												0							0	0		
LW2-A	277	7	11	6	0	0	0	0	0	0	1	3	294	15	1	149	8	51	1	29	0	853
LW2-B	119	7	5	3	0	0	0	0	0	0	1	2	163	6	0	12	5	34	0	9	0	366
LW2-C	44	2	5	1	0	0	0	0	0	0	2	1	117	6	0	9	1	24	2	10	1	225
LW2-D	105	7	11	1	1	0	0	0	0	0	2	1	190	10	0	5	2	33	1	5	0	374
LW2 Avg.	**268**	**16**	**21**	**5**	**1**	**0**	**0**	**0**	**0**	**0**	**5**	**4**	**470**	**22**	**0**	**26**	**8**	**91**	**3**	**24**	**1**	**965**

Appendix E. Raw point count data from Byrd Glacier and Ross Sea samples.

Sample ID	qtz	pyr	kspar	plag	cal	oli	musc	biot	chlor	iron ore	opaq	unknow n other	pmict	silt/s. s.	mudst clayst	maf	int	fel	marble l. s.	meta	ext	*n*
MT-A	0	0	0	0	0	0	0	0	0	0	0	0	180	23	3	0	1	0	66	5	0	278
MT-B	0	0	0	0	0	0	0	0	0	0	0	0	43	14	0	0	0	0	217	5	0	279
MT-C	0	0	0	0	0	0	0	0	0	0	0	0	250	23	3	0	0	0	62	6	0	344
MT Avg.	**0**	**0**	**0**	**0**	**0**	**0**	**0**	**0**	**0**	**0**	**0**	**0**	**473**	**60**	**6**	**0**	**1**	**0**	**345**	**16**	**0**	**901**
Ross Sea																						
NPB94-07-39 (100-102cm) SAL283	4	0	1	1	0	0	0	0	0	0	2	1	131	1	0	0	0	0	0	1	0	**142**
NPB94-01-02 (50-52cm) SAL372	41	1	25	12	0	1	0	0	0	0	6	4	113	3	2	5	12	17	30	31	30	**333**
NBP94-01-02 (111-116cm) SAL1633	9	2	2	0	0	0	0	0	0	0	3	0	285	0	2	3	0	0	0	10	0	**316**
NPB94-01-02 (150-152cm) SAL374	29	0	8	11	0	0	0	1	0	0	8	2	14	3	4	14	7	12	0	21	17	**151**
												0							0	0		
ELT27-14 (47-50cm) SAL1634	33	2	11	7	0	0	0	0	0	0	0	2	230	4	1	7	10	13	1	30	1	**352**
ELT27-14 (63-66)cm SAL1635	64	1	9	26	0	0	0	0	0	0	2	0	407	2	3	19	10	16	1	51	10	**621**
ELT27-14 (105-109cm) SAL1636	66	2	6	3	0	0	0	0	0	0	1	1	195	6	5	17	0	19	0	28	0	**349**
ELT27-14 (164-170cm SAL1637	60	0	20	10	0	0	0	0	0	0	2	1	406	2	1	13	7	32	1	46	4	**605**
ELT32-20 (64-69cm) SAL1638	29	2	12	12	0	0	0	0	0	0	0	1	303	9	3	36	18	26	1	44	1	**497**
ELT32-20 (132-134cm) SAL1639	0	0	7	3	0	0	0	0	0	0	1	1	1149	4	0	6	6	4	0	5	2	**1188**
												0							0	0		
ELT32-21 (54-58cm) SAL1640	166	1	52	59	1	0	0	0	0	0	3	6	360	66	13	19	47	104	9	181	3	**1090**
ELT32-21 (104-108cm) SAL1641	136	1	32	25	0	0	0	0	0	0	0	0	485	35	21	21	24	54	3	116	4	**957**
ELT32-21 (154-160cm) SAL1642	26	0	14	7	0	0	0	0	0	0	2	2	1082	16	2	3	7	20	0	57	0	**1238**

Appendix F. Raw pebble classification data from Byrd Glacier and Ross Sea samples.

Sample ID	Icf	Ici	Icm	Iff	Ifi	Ifm	Mg	Ms	Mp	Mq	Mm	Sm	Ss	Sc	Sw	Sch	Sl	Other	TOTAL
Byrd Glacier																			
BN-A	0	0	59	0	0	0	0	0	0	6	0	0	8	0	0	0	0	0	73
BN-B	0	0	118	0	0	7	0	0	0	0	0	0	6	0	0	0	0	0	131
BN-C	0	0	102	0	0	2	0	0	0	0	0	0	7	0	0	0	0	0	111
BN	**0**	**0**	**279**	**0**	**0**	**9**	**0**	**0**	**0**	**6**	**0**	**0**	**21**	**0**	**0**	**0**	**0**	**0**	**315**
												0							0
BR-A	0	0	76	0	0	0	0	0	0	0	0	0	14	0	0	0	0	0	90
BR-B	0	0	96	0	0	0	0	0	0	0	0	0	18	0	0	0	0	0	114
BR-C	0	0	80	0	0	0	0	0	0	0	0	0	26	0	0	0	0	0	106
BR Avg.	**0**	**0**	**252**	**0**	**0**	**0**	**0**	**0**	**0**	**0**	**0**	**0**	**58**	**0**	**0**	**0**	**0**	**0**	**310**
CJ-A	23	25	4	0	0	8	36	16	0	0	0	0	0	0	0	0	0	0	112
CJ-B	20	9	0	0	0	0	38	12	0	0	0	0	1	0	0	0	0	3	83
CJ-C	22	10	6	0	0	7	36	15	0	0	0	0	0	0	2	0	0	0	98
CJ Avg.	**65**	**44**	**10**	**0**	**0**	**15**	**110**	**43**	**0**	**0**	**0**	**0**	**1**	**0**	**2**	**0**	**0**	**3**	**293**
HB-A	**11**	**0**	**0**	**0**	**0**	**0**	**54**	**60**	**0**	**0**	**0**	0	**0**	**0**	**0**	**0**	**0**	**0**	125
HB-B	17	0	0	0	0	0	23	49	0	0	0	0	0	0	0	0	0	0	89
HB-C	5	0	0	0	0	0	48	47	0	0	0	0	0	0	0	0	0	0	100
HB Avg.	**33**	**0**	**0**	**0**	**0**	**0**	**125**	**156**	**0**	**0**	**0**	**0**	**0**	**0**	**0**	**0**	**0**	**0**	**314**
												0							
LW-A	1	24	57	0	0	11	10	5	0	2	0	0	2	0	6	0	0	0	118
LW-B	2	25	3	0	0	0	5	0	0	7	0	0	5	0	40	0	0	0	87
LW Avg.	**3**	**49**	**60**	**0**	**0**	**11**	**15**	**5**	**0**	**9**	**0**	**0**	**7**	**0**	**46**	**0**	**0**	**0**	**205**
												0							
LW2-A	1	0	51	0	0	11	6	0	0	18	0	0	11	0	34	0	2	0	134
LW2-B	2	0	45	0	0	3	6	1	0	14	0	0	5	0	31	1	0	0	108
LW2-C	6	0	68	0	0	0	6	4	0	19	0	0	7	0	7	0	0	0	117
LW2 Avg.	**9**	**0**	**164**	**0**	**0**	**14**	**18**	**5**	**0**	**51**	**0**	**0**	**23**	**0**	**72**	**1**	**2**	**0**	**359**

Appendix F (cont.) Raw pebble classification data from Byrd Glacier and Ross Sea s

Sample ID	qtz	pyr	kspar	plag	cal	oli	musc	biot	chlor	iron ore	opaq	unknow n other	gwacke	silt/s. s.	mudst clayst	maf	int	fel	marble l. s.
MT-A	0	0	1	0	0	0	0	0	0	0	3	0	0	0	0	0	102	0	106
MT-B	0	0	0	0	0	0	0	0	0	0	0	0	0	0	0	0	124	0	124
MT-C	0	0	0	0	0	0	0	0	0	0	1	0	1	0	0	0	95	0	97
MT Avg.	**0**	**0**	**1**	**0**	**0**	**0**	**0**	**0**	**0**	**0**	**4**	**0**	**1**	**0**	**0**	**0**	**321**	**0**	**327**

Appendix G-1. Particle size statistical data using SYSAT 8.0.

Complete Discriminant Analysis of Particle Size Data

Variables:

fCLAY: Fine Clay
mCLAY: Medium Clay
cCLAY: Course Clay

vfSILT: Very Fine Silt
fSILT: Fine Silt
mSILT: Medium Silt
cSILT: Course Silt

vfSAND: Very Fine Sand
fSAND: Fin Sand
mSAND: Medium Sand
cSAND: Course Sand
vcSAND: Very Course Sand

Group Frequencies

Group 1:	24
Group 2:	5
Group 3:	6
Group 4:	4

Group Means

	1	2	3	4
fCLAY:	13.7	14.9	0.03	0.3
mCLAY:	7.2	6.2	0.2	1.4
cCLAY:	11	7	0.5	1.7
vfSILT:	13.2	6.8	0.8	2.2
fSILT:	13.2	6.2	1.2	2.8
mSILT:	10.4	5.5	2.2	3.7
cSILT:	8.2	6.4	4.5	5.3
vfSAND:	6.5	7.2	12.5	7.5
fSAND:	5.6	8.1	25	10
mSAND:	5.2	9.7	27.5	17
cSAND:	3.8	13.3	18.2	28.4
vcSAND:	2	8.9	7.5	19.4

Between Group *F*-matrix -- df = 11 25

	1	2	3	4
1	0			
2	5.8	0		
3	55.1	28.3	0	
4	21	6.8	19.3	0

Wilks' Lambda

Lambda =	0.0002	df =	11	3	25	
Appx. *F* =	35.26	df =	33	74	prob =	0

Appendix G-1 (cont.). Particle size statistical data using SYSAT 8.0.

Complete Discriminant Analysis of Particle Size Data

Classification Functions

	1	2	3	4
Constant	-2412.2	-2430.6	-2673.8	-2452
fCLAY:	52.6	53.7	61.1	54.8
mCLAY:	-6.8	-9.8	-53.6	-29.1
cCLAY:	138	144.4	187.2	167.6
vfSILT:	-83.1	-90.8	-123.2	-115.8
fSILT:	191	195	211.9	212.4
mSILT:	-71	-71.8	-59.6	-78.3
cSILT:	127.1	125.8	110.8	127.5
vfSAND:	-7.5	-6.3	2.5	-6.7
fSAND:	93.3	923	96,7	93.6
mSAND:	14.7	14.6	18.2	14.3
cSAND:	93.8	95.5	98.4	97.4
vcSAND:	0	0	0	0

Variable	*F*-to-remove	Tolerance	Variable	*F*-to-enter	Tolerance
fCLAY:	4.75	0.057	**vcSAND**	5843.1	0.00003
mCLAY:	5.26	0.03			
cCLAY:	4.46	0.006			
vfSILT:	6.75	0.004			
fSILT:	12.12	0.003			
mSILT:	34.14	0.004			
cSILT:	47.58	0.011			
vfSAND:	-8.6	0.021			
fSAND:	11.29	0.034			
mSAND:	10.84	0.105			
cSAND:	1.16	0.044			

Classification Matrix

	1	**2**	**3**	**4**	**%Correct**
1	24	0	0	0	100
2	0	5	0	0	100
3	0	0	6	0	100
4	0	0	0	4	100
Total	**24**	**5**	**6**	**4**	**100**

Jackknifed Classification Matrix

	1	**2**	**3**	**4**	**%Correct**
1	22	2	0	0	92
2	1	4	0	0	80
3	0	0	6	0	100
4	0	0	0	4	100
Total	**23**	**6**	**6**	**4**	**92**

Eigenvalues

25.56	7.08	0.9

Canonical Correlations

0.981	0.936	0.689

Cumulative Proportion of Total Dispersion

0.762	0.973	1

Appendix G-1 (cont.). Particle size statistical data using SYSAT 8.0.

Complete Discriminant Analysis of Particle Size Data

Wilks's Lamda = 0.002
Approx. *F* = 15.08 df = 33, 74 p-tail = 0.0000

Philai's Trace = 2.31
Approx. *F* = 8.26 df = 33, 81 p-tail = 0.0000

Lawley-Hotelling Trace = 33.538
Approx. *F* = 24.05 df = 33, 71 p-tail = 0.0000

Canonical Discriminant Functions - standardized by within variance

	1	2	3
fCLAY:	2.2	0.7	1.1
mCLAY:	-3.6	-0.2	1
cCLAY:	7.1	-1.2	-1.8
vfSILT:	-6.3	3	2.6
fSILT:	4.6	-3.3	-3.7
mSILT:	1.7	3.5	3.1
cSILT:	-2	-1.6	-1.9
vfSAND:	1.9	1.1	1.6
fSAND:	0.7	0.5	-0.2
mSAND:	0.86	0.92	0.51
cSAND:	1.2	-0.7	0.47
vcSAND:	.	.	.

Appendix G-2. Particle size statistical data using SYSAT 8.0.

Forward Stepwise Discriminant Analysis of Particle Size Data with Alpha-to-Enter=0.150 and Alpha-to-remove=0.150

Groups 1 - 4

Variables:

fCLAY: Fine Clay
mCLAY: Medium Clay
cCLAY: Course Clay

vfSILT: Very Fine Silt
fSILT: Fine Silt
mSILT: Medium Silt
cSILT: Course Silt

vfSAND: Very Fine Sand
fSAND: Fin Sand
mSAND: Medium Sand
cSAND: Course Sand
vcSAND: Very Course Sand

Group Frequencies

Group 1:	24
Group 2:	5
Group 3:	6
Group 4:	4

Group Means

	1	2	3	4
fCLAY:	13.7	14.9	0.03	0.3
mCLAY:	7.2	6.2	0.2	1.4
cCLAY:	11	7	0.5	1.7
vfSILT:	13.2	6.8	0.8	2.2
fSILT:	13.2	6.2	1.2	2.8
mSILT:	10.4	5.5	2.2	3.7
cSILT:	8.2	6.4	4.5	5.3
vfSAND:	6.5	7.2	12.5	7.5
fSAND:	5.6	8.1	25	10
mSAND:	5.2	9.7	27.5	17
cSAND:	3.8	13.3	18.2	28.4
vcSAND:	2	8.9	7.5	19.4

Group Classification Functions

	1	2	3	4
fCLAY:	0	0	0	0
mCLAY:	0	0	0	0
cCLAY:	0	0	0	0
vfSILT:	0	0	0	0
fSILT:	0	0	0	0
mSILT:	0	0	0	0
cSILT:	0	0	0	0
vfSAND:	0	0	0	0
fSAND:	0	0	0	0
mSAND:	0	0	0	0
cSAND:	0	0	0	0
vcSAND:	0	0	0	0

Between Group *F*-matrix -- df = 5 31

	1	2	3	4
1	0			
2	12.9	0		
3	88.2	47.2	0	
4	42	11.6	42.6	0

Appendix G-2 (cont.). Particle size statistical data using SYSAT 8.0.

Forward Stepwise Discriminant Analysis of Particle Size Data with Alpha-to-Enter=0.150 and Alpha-to-remove=0.150

Groups 1 - 4

Wilks' Lambda

Lambda =	0.0054	df =	5	3	35	
Appx. *F* =	31.9712	df =	15	85	prob =	0

Variable	*F*-to-remove	Tolerance	Variable	*F*-to-enter	Tolerance
mCLAY:	25.9	0.39	**fCLAY**	1.13	0.551
vfSILT:	9.94	0.629	**cCLAY**	0.38	0.19
cSILT:	12.46	0.365	**fSILT**	0.34	0.33
cSAND:	5.28	0.23	**mSILT**	0.43	0.379
vcSAND:	4.12	0.409	**vfSAND**	0	0.428
			fSAND	0.38	0.428
			mSAND	1.12	0.186

Classification Matrix

	1	2	3	4	%Correct
1	24	0	0	0	100
2	0	5	0	0	100
3	0	0	6	0	100
4	0	0	0	4	100
Total	**24**	**5**	**6**	**4**	**100**

Jackknifed Classification Matrix

	1	2	3	4	%Correct
1	23	1	0	0	96
2	0	5	0	0	100
3	0	0	6	0	100
4	0	0	0	4	100
Total	**23**	**6**	**6**	**4**	**97**

Appendix G-3. Particle size statistical data using SYSAT 8.0.

Forward Stepwise Discriminant Analysis of Particle Size Data with Alpha-to-Enter=0.150 and Alpha-to-remove=0.150

Subgroups A and B

Variables:

fCLAY: Fine Clay
mCLAY: Medium Clay
cCLAY: Course Clay

vfSILT: Very Fine Silt
fSILT: Fine Silt
mSILT: Medium Silt
cSILT: Course Silt

vfSAND: Very Fine Sand
fSAND: Fin Sand
mSAND: Medium Sand
cSAND: Course Sand
vcSAND: Very Course Sand

Group Frequencies

Group 1:	9
Group 2:	15

Group Means

	1	**2**
fCLAY:	12.2	14.6
mCLAY:	6.8	7.5
cCLAY:	10.3	11.4
vfSILT:	11.2	14.4
fSILT:	9.7	15.3
mSILT:	7.7	12.1
cSILT:	7.4	8.6
vfSAND:	7.7	5.8
fSAND:	8.9	3.6
mSAND:	8.4	3.3
cSAND:	6.2	2.4
vcSAND:	3.4	1.2

Group Classification Functions

	1	**2**
Constant	**-0.693**	**-0.693**
fCLAY:	0	0
mCLAY:	0	0
cCLAY:	0	0
vfSILT:	0	0
fSILT:	0	0
mSILT:	0	0
cSILT:	0	0
vfSAND:	0	0
fSAND:	0	0
mSAND:	0	0
cSAND:	0	0
vcSAND:	0	0

(After final step)

Between Group *F*-matrix -- df = 5 31

	1	**2**
1	0	
2	34.523	0

Appendix G-3 (cont.). Particle size statistical data using SYSAT 8.0.

Forward Stepwise Discriminant Analysis of Particle Size Data with Alpha-to-Enter=0.150 and Alpha-to-remove=0.150

Groups 1 - 4

Wilks' Lambda

Lambda =	0.2332	df =	2	1	22	
Appx. *F* =	34.523	df =	2	21	prob =	0

Variable	*F*-to-remove	Tolerance
fSILT	41.13	0.997
vcSAND	3.21	0.997

Variable	*F*-to-enter	Tolerance
fCLAY	0.61	0.793
mCLAY	0.21	0.531
cCLAY	0.1	0.788
vfSILT	0.47	0.881
mSILT	0.33	0.411
cSILT	0.4	0.993
vfSAND	0.69	0.746
fSAND	1.72	0.382
mSAND	0	0.755
cSAND	0.03	0.388

Classification Matrix

	1	2	%Correct
1	9	0	100
2	0	15	100
Total	**9**	**15**	**100**

Jackknifed Classification Matrix

	1	2	%Correct
1	9	0	100
2	1	14	93
Total	**10**	**14**	**96**

Appendix G-4. Particle size statistical data using SYSAT 8.0.

Backward Stepwise Discriminant Analysis of Particle Size Data with Alpha-to-Enter=0.150 and Alpha-to-remove=0.150

Subgroups A and B

Variables:

fCLAY: Fine Clay
mCLAY: Medium Clay
cCLAY: Course Clay

vfSILT: Very Fine Silt
fSILT: Fine Silt
mSILT: Medium Silt
cSILT: Course Silt

vfSAND: Very Fine Sand
fSAND: Fin Sand
mSAND: Medium Sand
cSAND: Course Sand
vcSAND: Very Course Sand

Group Frequencies

Group 1:	9
Group 2:	15

Group Means

	1	**2**
fCLAY:	12.2	14.6
mCLAY:	6.8	7.5
cCLAY:	10.3	11.4
vfSILT:	11.2	14.4
fSILT:	9.7	15.3
mSILT:	7.7	12.1
cSILT:	7.4	8.6
vfSAND:	7.7	5.8
fSAND:	8.9	3.6
mSAND:	8.4	3.3
cSAND:	6.2	2.4
vcSAND:	3.4	1.2

Group Classification Functions

	1	**2**
Constant	**-6591.4**	**-6882.6**
fCLAY:	84.9	83
mCLAY:	336.4	357.6
cCLAY:	-80.25	-95
vfSILT:	234.1	246.1
fSILT:	268.2	281.5
mSILT:	-136.3	-155.1
cSILT:	390	414.9
vfSAND:	0.3	-5.9
fSAND:	190.9	193
mSAND:	85.3	87.5
cSAND:	194.7	196.4
vcSAND:	0	0

(After final step)

Between Group *F*-matrix -- df = 5 31

	1	**2**
1	0	
2	21.543	0

Appendix G-4 (cont.). Particle size statistical data using SYSAT 8.0.

Forward Stepwise Discriminant Analysis of Particle Size Data with Alpha-to-Enter=0.150 and Alpha-to-remove=0.150

Groups 1 - 4

Wilks' Lambda

Lambda =	0.1162	df =	6	1	22	
Appx. *F* =	21.5433	df =	6	17	prob =	0

Variable	*F*-to-remove	Tolerance	Variable	*F*-to-enter	Tolerance
mCLAY	11.7	0.07	**fCLAY**	0.71	0.313
cCLAY	13.9	0.0181	**fSILT**	0	0.02
vfSILT	27.7	0.026	**vfSAND**	0.08	0.161
mSILT	3.66	0.137	**fSAND**	0.47	0.265
cSILT	19.39	0.077	**cSAND**	1.6	0.236
mSAND	10.7	0.185	**vcSAND**	0.83	0.24

Classification Matrix

	1	2	%Correct
1	9	0	100
2	0	15	100
Total	**9**	**15**	**100**

Jackknifed Classification Matrix

	1	2	%Correct
1	8	1	89
2	0	15	100
Total	**8**	**16**	**96**

Appendix G-5. Particle size statistical data using SYSAT 8.0.

Forward Stepwise Discriminant Analysis of Particle Size Data with Alpha-to-Enter=0.150 and Alpha-to-remove=0.150

Ross Sea Till Groups 1 and 2

Variables:

fCLAY: Fine Clay
mCLAY: Medium Clay
cCLAY: Course Clay

vfSILT: Very Fine Silt
fSILT: Fine Silt
mSILT: Medium Silt
cSILT: Course Silt

vfSAND: Very Fine Sand
fSAND: Fin Sand
mSAND: Medium Sand
cSAND: Course Sand
vcSAND: Very Course Sand

Group Frequencies

Group 1:	11
Group 2:	5

Group Means

	1	**2**
fCLAY:	15.2	13.8
mCLAY:	7.2	6.3
cCLAY:	10.3	9
vfSILT:	13.5	10.9
fSILT:	15.5	10.7
mSILT:	13	8.8
cSILT:	9.3	8
vfSAND:	5.9	7.6
fSAND:	3.6	7.5
mSAND:	3	6
cSAND:	2.4	6.8
vcSAND:	1.1	4.6

Group Classification Functions

	1	**2**
Constant	**-0.693**	**-0.693**
fCLAY:	0	0
mCLAY:	0	0
cCLAY:	0	0
vfSILT:	0	0
fSILT:	0	0
mSILT:	0	0
cSILT:	0	0
vfSAND:	0	0
fSAND:	0	0
mSAND:	0	0
cSAND:	0	0
vcSAND:	0	0

(After final step)

Between Group *F*-matrix -- df = 5 31

	1	**2**
1	0	
2	17.415	0

Appendix G-5 (cont.). Particle size statistical data using SYSAT 8.0.

Forward Stepwise Discriminant Analysis of Particle Size Data with Alpha-to-Enter=0.150 and Alpha-to-remove=0.150

Groups 1 - 4

Wilks' Lambda

Lambda =	0.1868	df =	3	1	14	
Appx. *F* =	17.4152	df =	3	12	prob =	0.0001

Variable	*F*-to-remove	Tolerance	Variable	*F*-to-enter	Tolerance
mSILT	11.7	0.07	**fCLAY**	0.02	0.559
vfSAND	13.9	0.0181	**mCLAY**	0.44	0.658
mSAND	27.7	0.026	**cCLAY**	0.03	0.385
			vfSILT	0.66	0.158
			fSILT	0.49	0.186
			cSILT	0.02	0.377
			fSAND	0.49	0.275
			cSAND	0.06	0.561
			vcSAND	0.55	0.734

Classification Matrix

	1	2	%Correct
1	9	0	100
2	0	15	100
Total	**9**	**15**	**100**

Jackknifed Classification Matrix

	1	2	%Correct
1	11	0	100
2	0	5	100
Total	**11**	**5**	**100**

Appendix H. Averaged point count statistical data using SYSAT 8.0.

Complete Discriminant Analysis of Averaged Point Count Data

Variables:

Qtz:	Quartz
Pyrx:	Pyroxene
Feld:	Felspar
Biot:	Biotite
Opaq:	Opaque
Pmict:	Polymict
SiltSS:	Siltstone/Sandstone
Mudst:	Mudstone/Claystone
M:	Mafic Igneous
Int+Fel:	Intermediate and Felsic Igneous
Meta:	Metamorphic
Ext:	Extrusive Igneous
Lime	Limestone/Marble/Calcite

Group Frequencies

Group 1:	4
Group 2:	7
Group 3:	8
Group 4:	4

Group Means

	1	2	3	4
Qtz:	1.72	11.67	18.44	16.97
Pyrx:	0.08	0.28	0.44	0.07
Feld:	1.17	4.5	11.7	12.05
Biot:	0	0	0.13	0.34
Opaq:	0.53	0.16	0.79	3.65
Pmict:	91.8	61.1	28.4	16.2
SiltSS:	0.74	1.43	3.13	3.79
Mudst:	0.12	0.55	0.73	1.18
M:	0.42	4.08	0.84	4.11
Int+Fel:	1.03	6.75	20.35	15.6
Meta:	1.9	8.71	11.62	10.36
Ext:	0.28	0.45	1.91	14.77
Lime	0.00	0.14	0.85	0.07

Between Group *F*-matrix -- df = 12 8

	1	2	3	4
1	0			
2	8.79	0		
3	40.94	30.516	0	
4	50.67	48.84	12.42	0

Wilks' Lambda

Lambda =	0.0001	df =	12	3	19	
Appx. *F* =	15.483	df =	36	24	prob =	0

Appendix H (cont.). Averaged point count statistical data using SYSAT 8.0.

Complete Discriminant Analysis of Averaged Point Count Data

Classification Functions

	1	2	3	4
Constant	-74302.6	-72766.3	-68563	-68435.1
Qtz:	1509	1495.4	1451.2	1448.3
Pyrx:	1275.3	1286.4	1242.8	1223.4
Feld:	1294	1283.3	1249.2	1247.9
Biot:	3968.7	3961.9	3858.5	3854.3
Opaq:	1450	1415.6	1389.1	1413.9
Pmict:	1494.7	1478.7	1434.6	1431.6
SiltSS:	1266.9	1248.7	1219.3	1227.1
Mudst:	1093.3	1060.8	1048.9	1065.5
M:	1388.5	1379.2	1334.2	1328.1
Int+Fel:	1385.6	1369.5	1331	1330.5
Meta:	1567.6	1555.6	1506.6	1499.9
Ext:	1392.9	1380.7	1342.4	1343.4
Lime	0	0	0	0

Variable	*F*-to-remove	Tolerance	Variable	*F*-to-enter
Qtz:	320.6	0.004	**Lime**	12.49
Pyrx:	3.62	0.3196		
Feld:	114.56	0.0215		
Biot:	7.31	0.1519		
Opaq:	15.42	0.075		
Pmict:	425.17	0.0016		
SiltSS:	36.64	0.0373		
Mudst:	5.48	0.135		
M:	80.77	0.214		
Int+Fel:	141.82	0.0038		
Meta:	193.71	0.0068		
Ext:	-3.16	0.0093		

Classification Matrix

	1	2	3	4	%Correct
1	4	0	0	0	100
2	0	7	0	0	100
3	0	0	8	0	100
4	0	0	0	4	100
Total	**4**	**7**	**8**	**4**	**100**

Jackknifed Classification Matrix

	1	2	3	4	%Correct
1	4	0	0	0	100
2	0	7	0	0	100
3	0	0	7	1	88
4	0	0	0	4	100
Total	**4**	**7**	**7**	**5**	**96**

Eigenvalues

117.35	17.4	4.65

Canonical Correlations

0.996	0.972	0.907

Cumulative Proportion of Total Dispersion

0.842	0.967	1

Appendix H (cont.). Averaged point count statistical data using SYSAT 8.0.

Complete Discriminant Analysis of Averaged Point Count Data

Wilks's Lamda = 0.000
Approx. *F* = 15.718 df = 36, 24 p-tail = 0.0000

Philai's Trace = 2.76
Approx. *F* = 9.59 df = 36, 30 p-tail = 0.0000

Lawley-Hotelling Trace = 139.395
Approx. *F* = 25.814 df = 36, 20 p-tail = 0.0000

Canonical Discriminant Functions - standardized by within variance

	1	2	3
Qtz:	10.18	4.8	6.6
Pyrx:	0.72	-0.432	0.77
Feld:	3.85	1.98	2.69
Biot:	1.03	0.26	1.26
Opaq:	1.05	2.92	0.6
Pmict:	16.59	8.6	9.15
SiltSS:	2.42	2.91	1.62
Mudst:	0.49	1.76	1.62
M:	0.49	1.756	-0.41
Int+Fel:	10.07	6.47	5.44
Meta:	8.25	2.68	5.35
Ext:	6	3.62	4.81
Lime	.	.	.

Appendix H-2. Averaged point count statistical data using SYSAT 8.0.

Forward Stepwise Discriminant Analysis of Averaged Point Count Data

Subgroups A - D

Variables:

Qtz:	Quartz
Pyrx:	Pyroxene
Feld:	Felspar
Biot:	Biotite
Opaq:	Opaque
Polymict:	Greywacke
SiltSS:	Siltstone/Sandstone
Mudst:	Mudstone/Claystone
M:	Mafic Igneous
Int+Fel:	Intermediate and Felsic Igneous
Meta:	Metamorphic
Ext:	Extrusive Igneous
Lime	Limestone/Marble/Calcite

Group Frequencies

Group 1:	4
Group 2:	7
Group 3:	8
Group 4:	4

Group Means

	1	2	3	4
Qtz:	1.72	11.67	18.44	16.97
Pyrx:	0.08	0.28	0.44	0.07
Feld:	1.17	4.5	11.7	12.05
Biot:	0	0	0.13	0.34
Opaq:	0.53	0.16	0.79	3.65
Polymict:	91.8	61.1	28.4	16.2
SiltSS:	0.74	1.43	3.13	3.79
Mudst:	0.12	0.55	0.73	1.18
M:	0.42	4.08	0.84	4.11
Int+Fel:	1.03	6.75	20.35	15.6
Meta:	1.9	8.71	11.62	10.36
Ext:	0.28	0.45	1.91	14.77
Lime	0	0.136	0.85	0.07

Group Classification Functions

	1	2	3	4
Constant	**-1.386**	**-1.386**	**-1.386**	**-1.386**
Qtz:	0	0	0	0
Pyrx:	0	0	0	0
Feld:	0	0	0	0
Biot:	0	0	0	0
Opaq:	0	0	0	0
Polymict:	0	0	0	0
SiltSS:	0	0	0	0
Mudst:	0	0	0	0
M:	0	0	0	0
Int+Fel:	0	0	0	0
Meta:	0	0	0	0
Ext:	0	0	0	0
Lime	0	0	0	0

Appendix H-2 (cont.) Averaged point count statistical data using SYSAT 8.0.

Forward Stepwise Discriminant Analysis of Averaged Point Count Data

Subgroups A - D

Between Group *F*-matrix -- df = 6 14

	1	2	3	4
1	0			
2	12.52	0		
3	42.79	25.07	0	
4	79.7	76.53	31.8	0

Wilks' Lambda

Lambda =	0.001	df =	6	3	19
Appx. *F* =	23.6213	df =	18	40	prob = 0

Variable	*F*-to-remove	Tolerance	Variable	*F*-to-enter	Tolerance
Opaq:	17.79	0.2384	**Qtz:**	0.49	0.3988
Polymict:	13.91	0.3401	**Pyrx:**	0.18	0.97485
SiltSS:	4.2	0.4151	**Feld:**	1.66	0.74454
M:	3.01	0.7098	**Biot:**	0.35	0.62476
Int+Fel:	2.94	0.2515	**Mudst:**	1.54	0.41608
Ext:	7.49	0.7383	**Meta:**	0.71	0.48348
			Lime	0.32	0.74838

Classification Matrix

	1	2	3	4	%Correct
1	4	0	0	0	100
2	0	7	0	0	100
3	0	0	8	0	100
4	0	0	0	4	100
Total	**4**	**7**	**8**	**4**	**100**

Jackknifed Classification Matrix

	1	2	3	4	%Correct
1	4	1	0	0	100
2	0	7	0	0	100
3	0	0	7	1	88
4	0	0	0	4	100
Total	**4**	**7**	**7**	**1**	**96**

Appendix I. Averaged point count principle component loadings using Aabel 2.2.

Subgroups A - D

	PC_1[L]	PC_2[L]	PC_3[L]	PC_4[L]	PC_5[L]	PC_6[L]
EigenValues	898.33	40.87	17.92	10.78	6.87	2.8
Varience(%)	91.65	4.17	1.83	1.1	0.7	0.29
Variance(Cum. %)	91.65	95.82	97.65	98.75	99.45	99.73
-						
Qtz	0.21	0.32	0.42	0.64	0.11	0.36
Pyrx	0	0.02	0	0.02	0.01	0.03
F	0.14	-0.02	-0.07	-0.23	0.82	-0.24
Biot	0	-0.01	0	-0.01	0	-0.04
Opaq	0.02	-0.14	0.05	0.04	0.11	-0.07
Polymict	-0.92	0.13	-0.1	0.06	0.03	0.08
Siltstone/SS	0.04	-0.01	-0.09	-0.14	-0.16	0.06
mud/clayst	0.01	-0.02	0.07	-0.03	-0.03	-0.01
M	0.01	-0.14	0.38	0.08	-0.37	-0.74
Int+Fel	0.25	0.48	-0.69	0.08	-0.25	-0.14
Meta	0.11	0.13	0.31	-0.68	-0.24	0.39
Ext	0.1	-0.77	-0.3	0.19	-0.12	0.29
Lime/Marble	0.01	0.05	-0.04	-0.03	-0.06	0.03

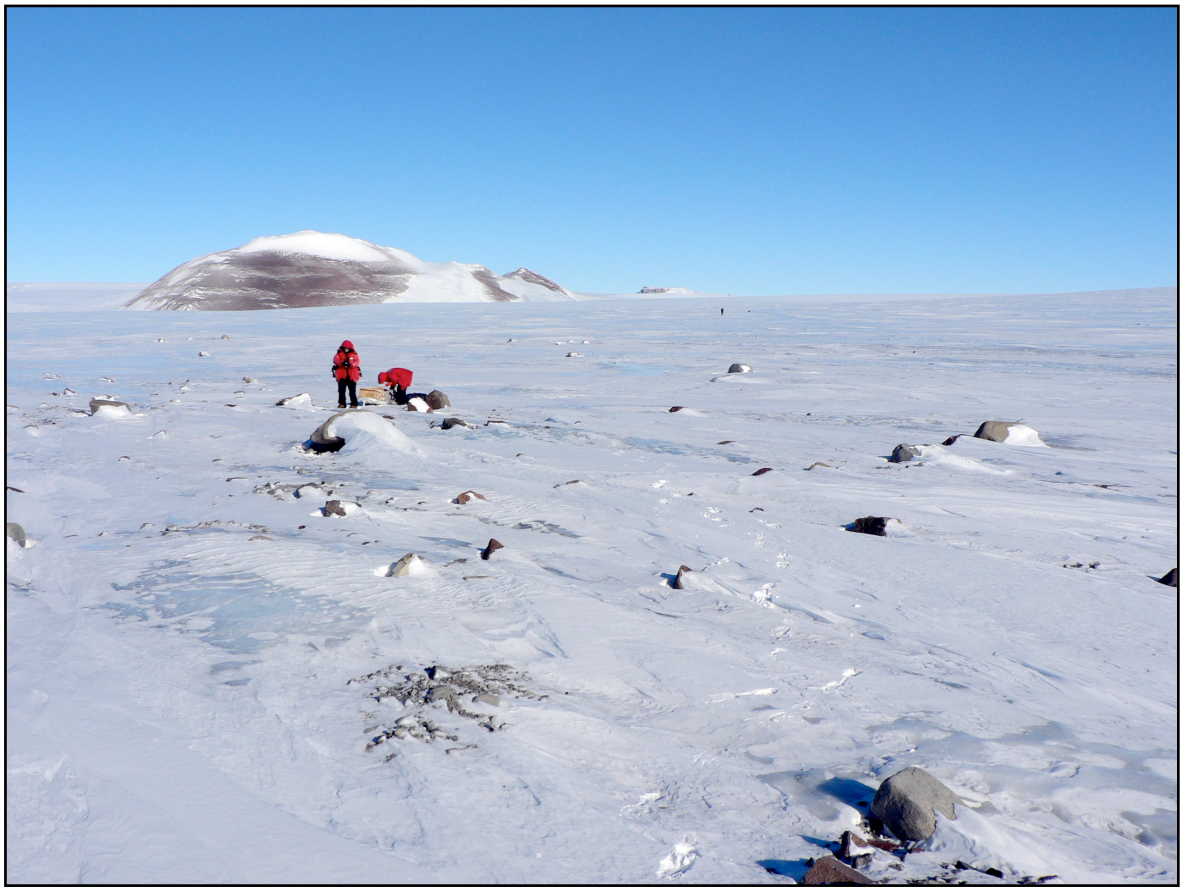

Plate 1: Lonewolf Nunatak site (LW). Glacial till can be seen exposed at surface of ice due to ablation. (Photo: 10/27/2005, 1/800, f 4.0, ISO 80)

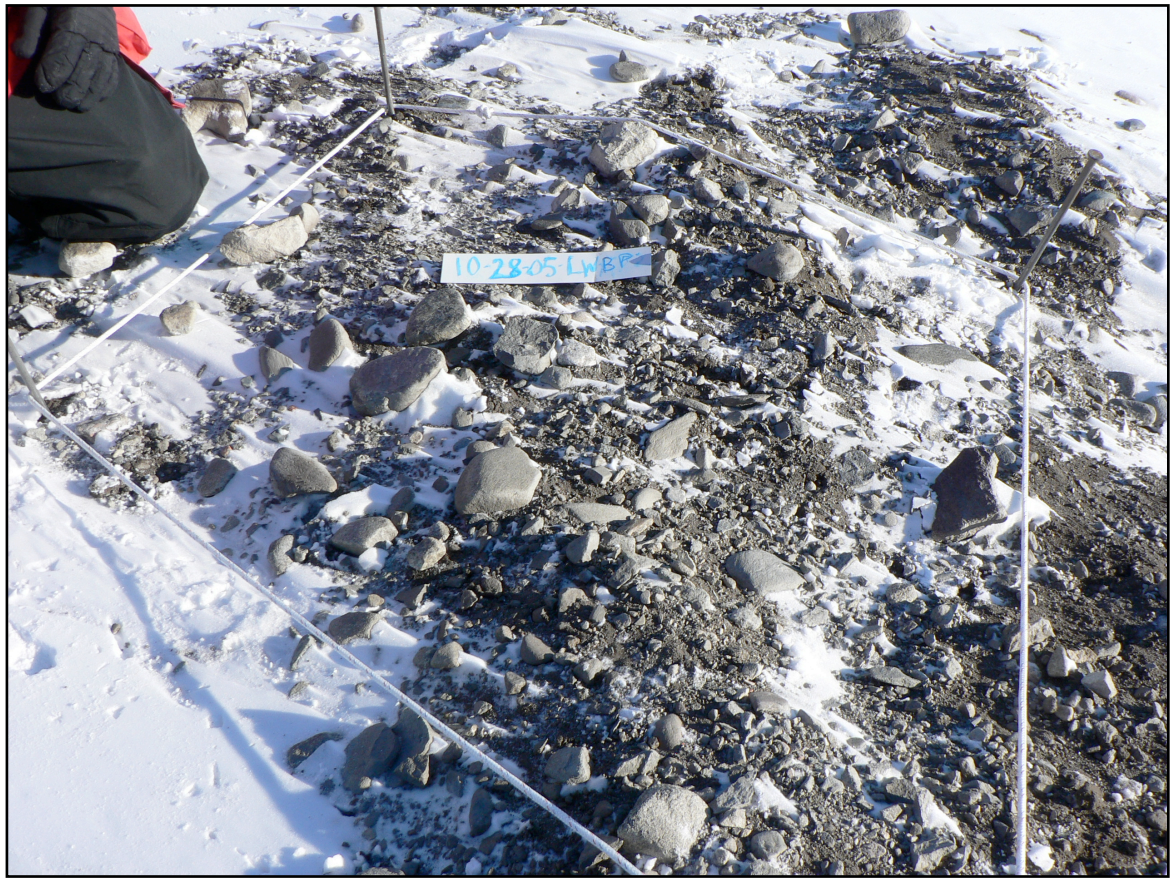

Plate 2: Lonewolf Nunatak site (LW). Sub-sample LW-B. (Photo: 10/28/2005, 1/400, f 4.5, ISO 80)

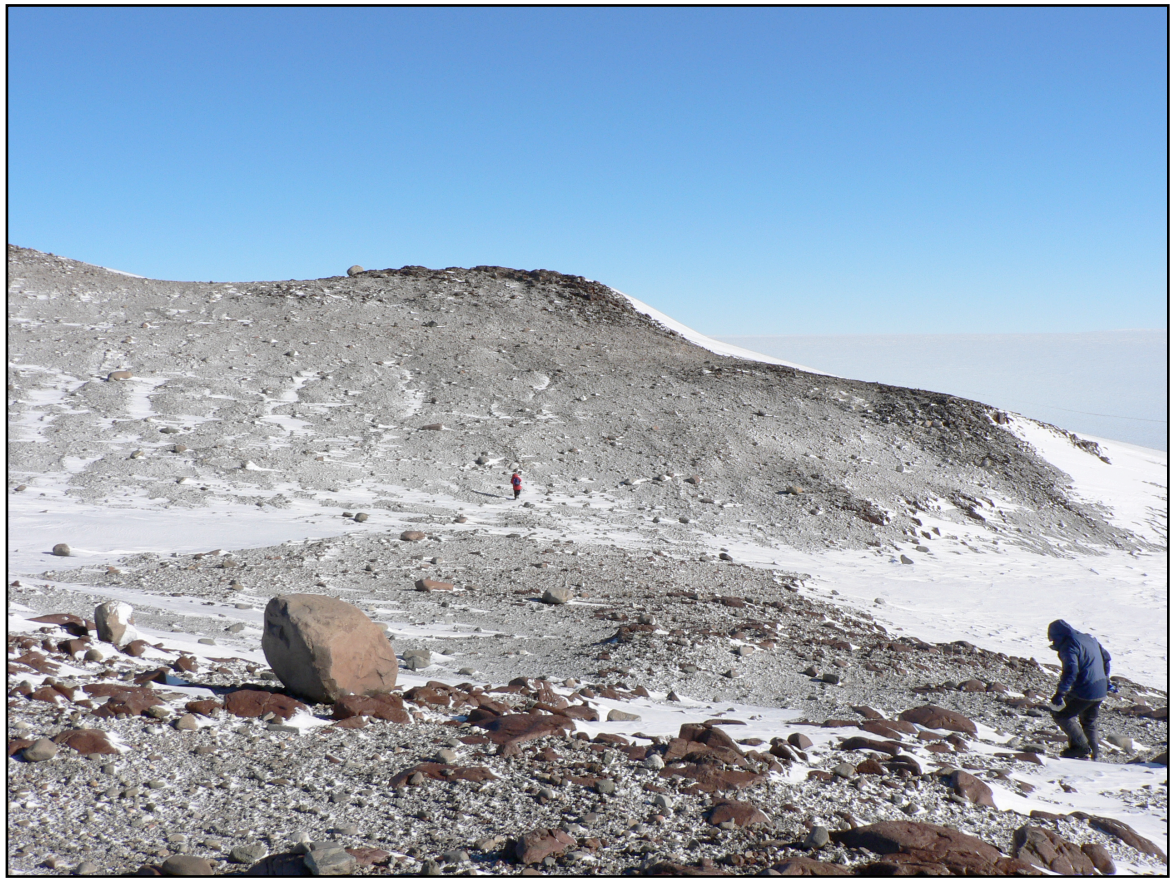

Plate 3: Lonewolf Nunatak site (LW2). (Photo: 10/28/2005, 1/400, f 4.5, ISO 80)

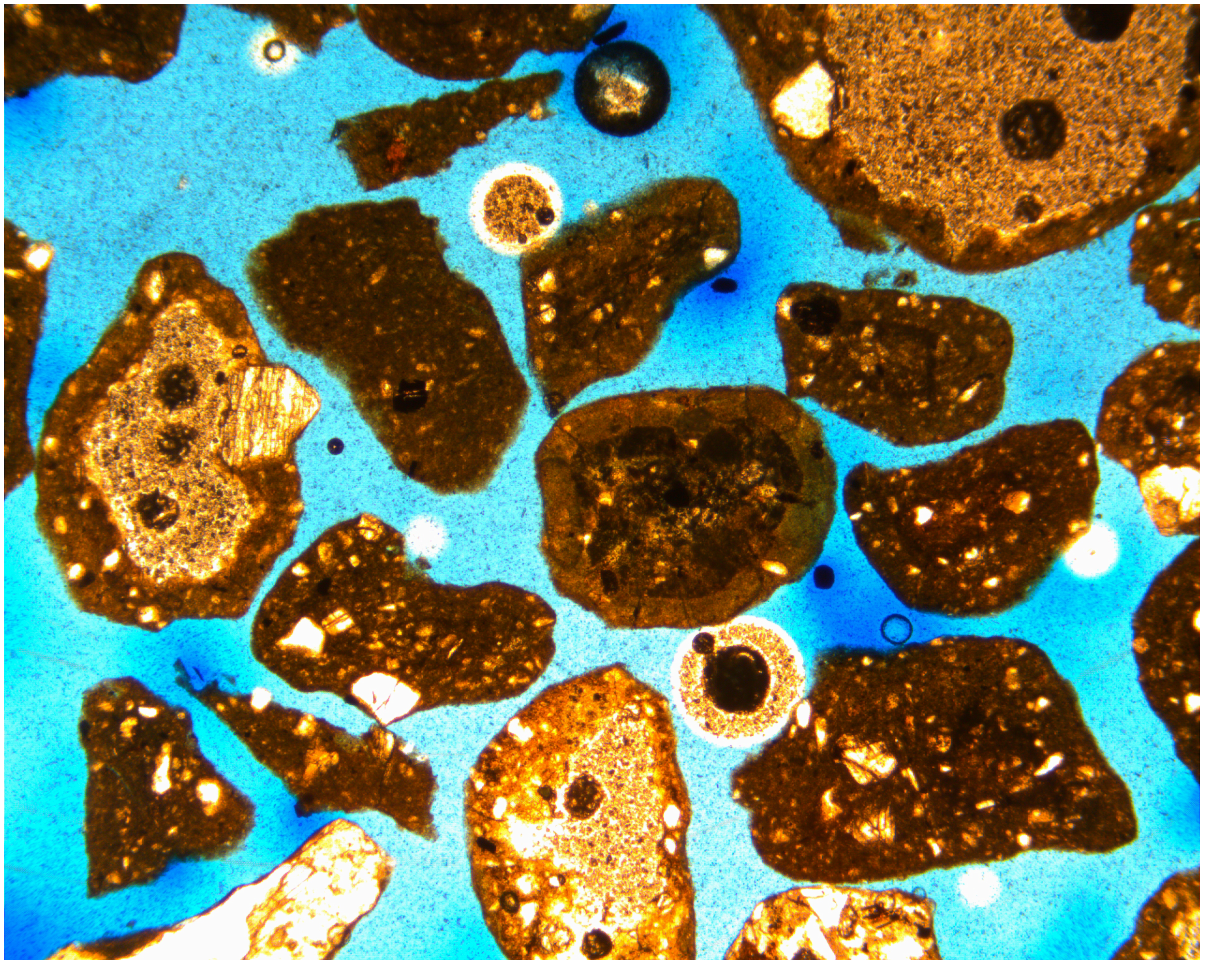

Plate 4: Polymict grains from sample NBP94-01-02(SAL1633). (x31.25)

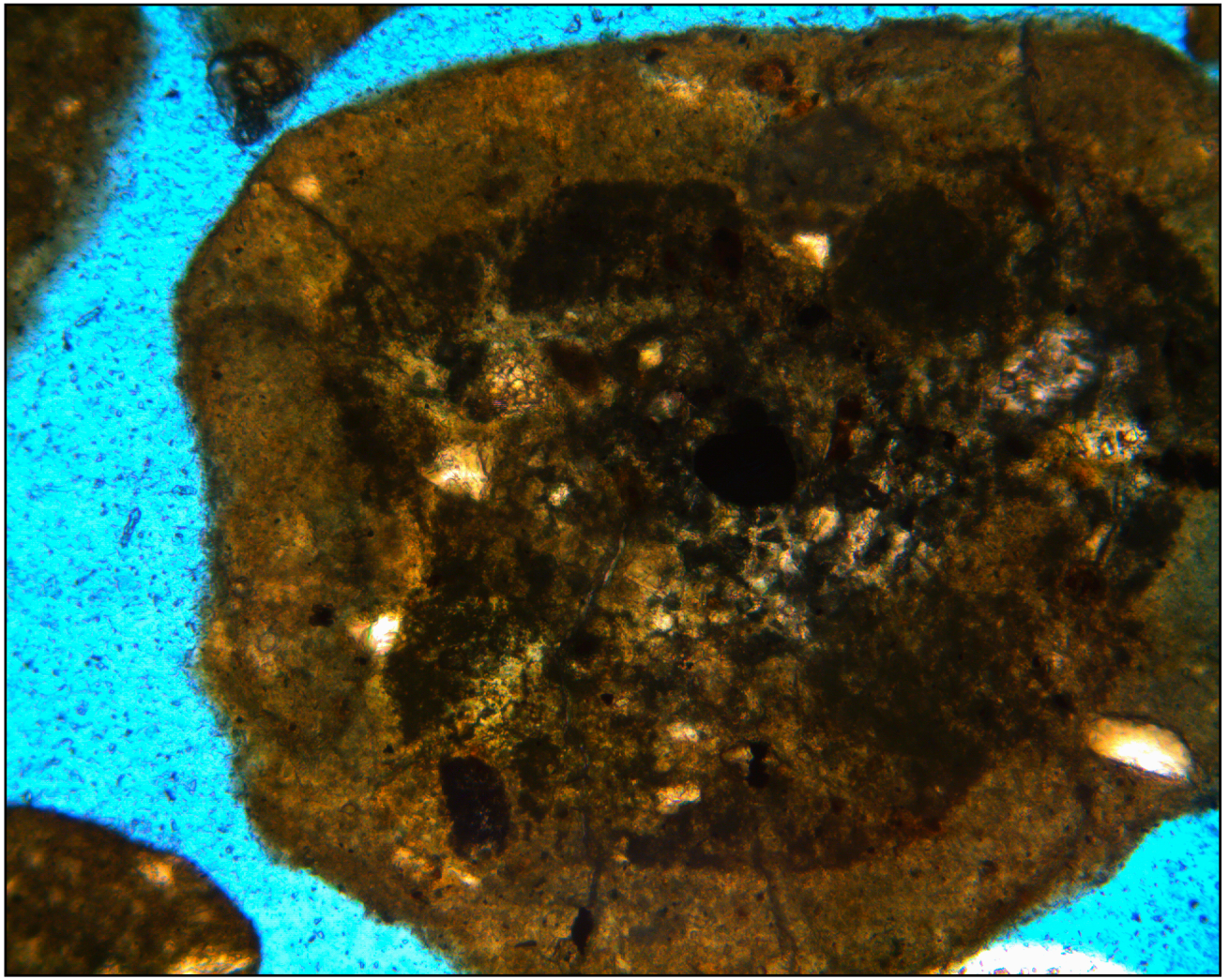

Plate 5: Polymict grains from sample NBP94-01-02(SAL1633). (x120.5)

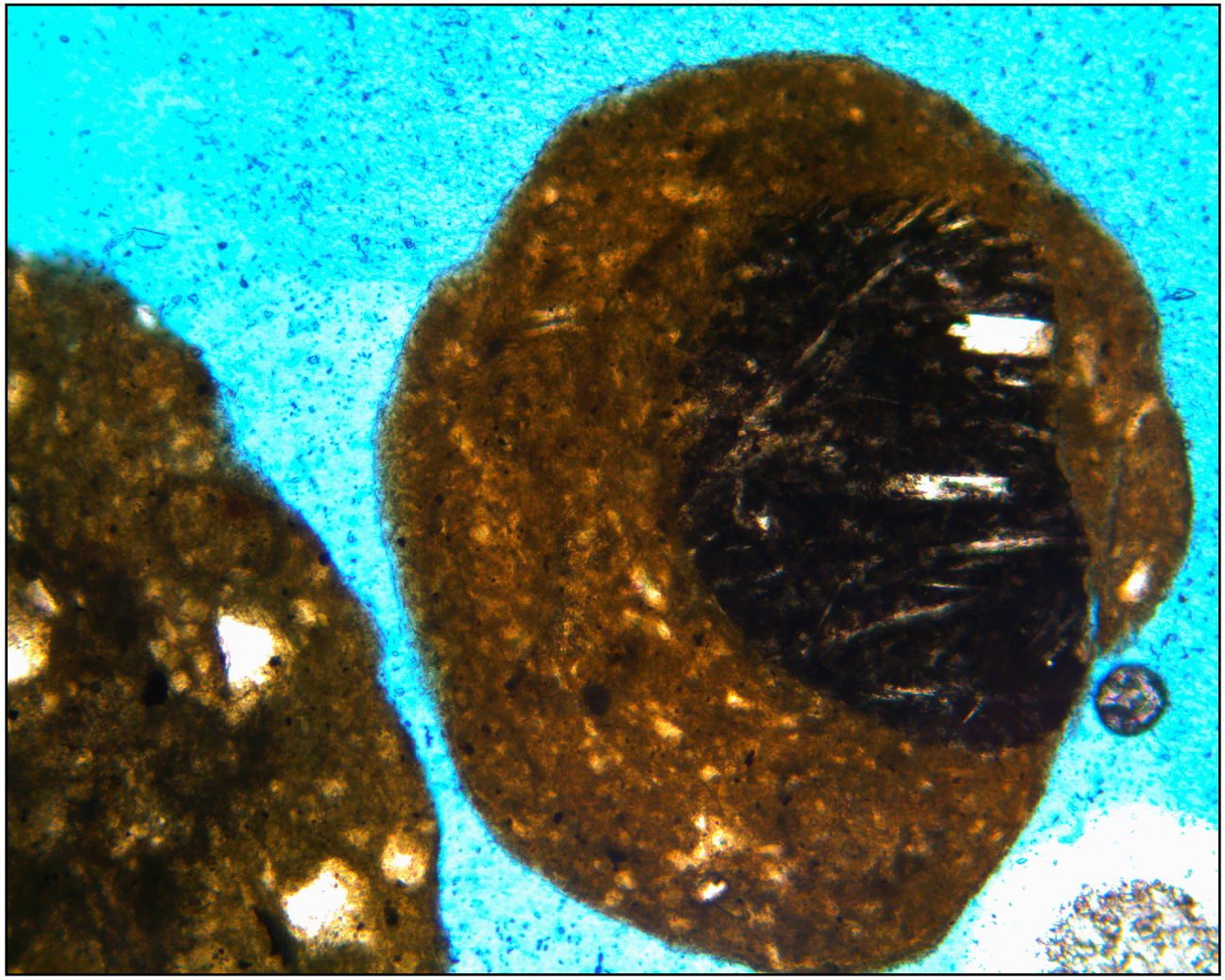

Plate 6: Polymict grains from sample NBP94-01-02(SAL1633). (x120.5)

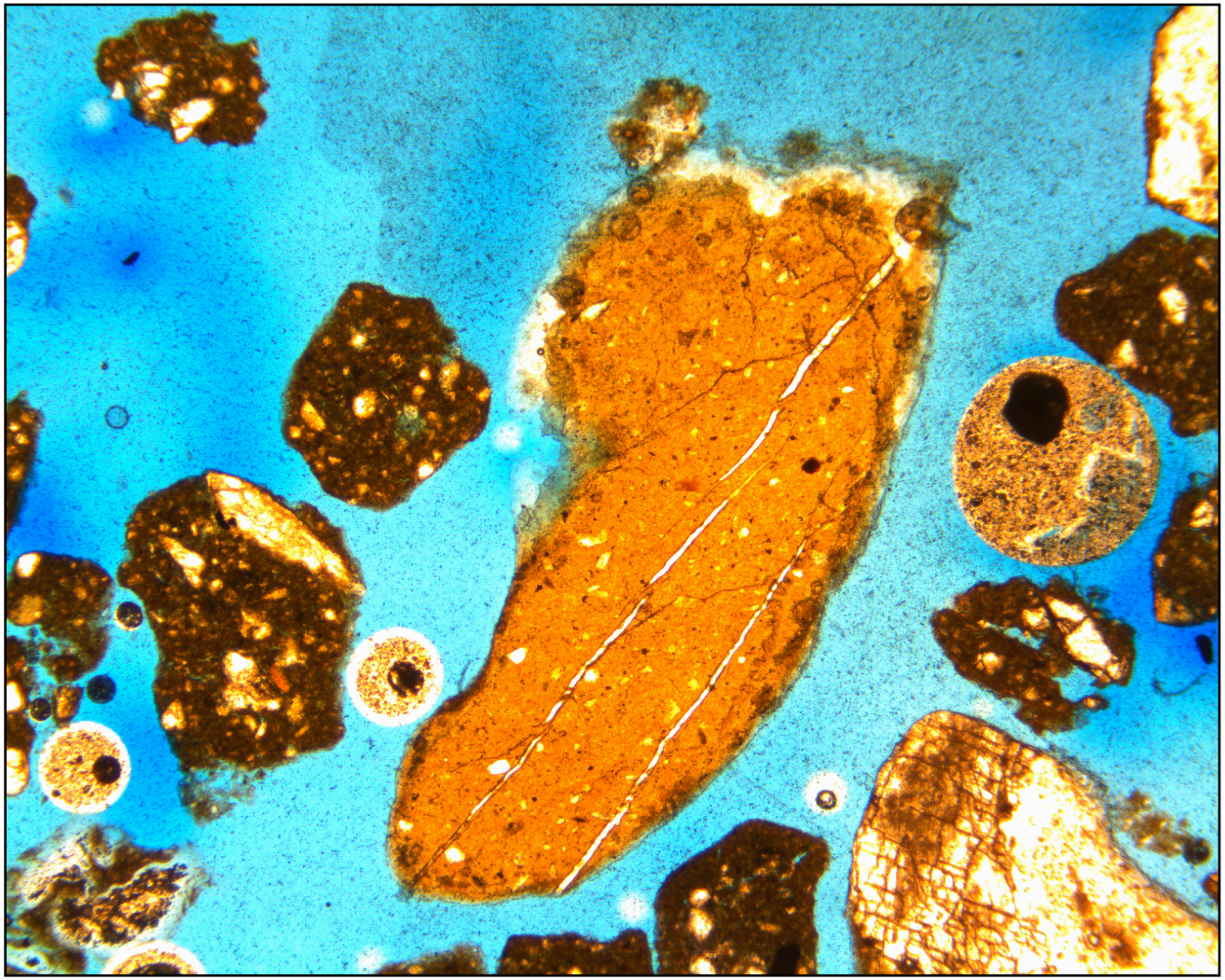

Plate7: Polymict grains from sample NBP94-01-02(SAL1633). Note veins within polymict. Veins are composed of opal. (x120.5)

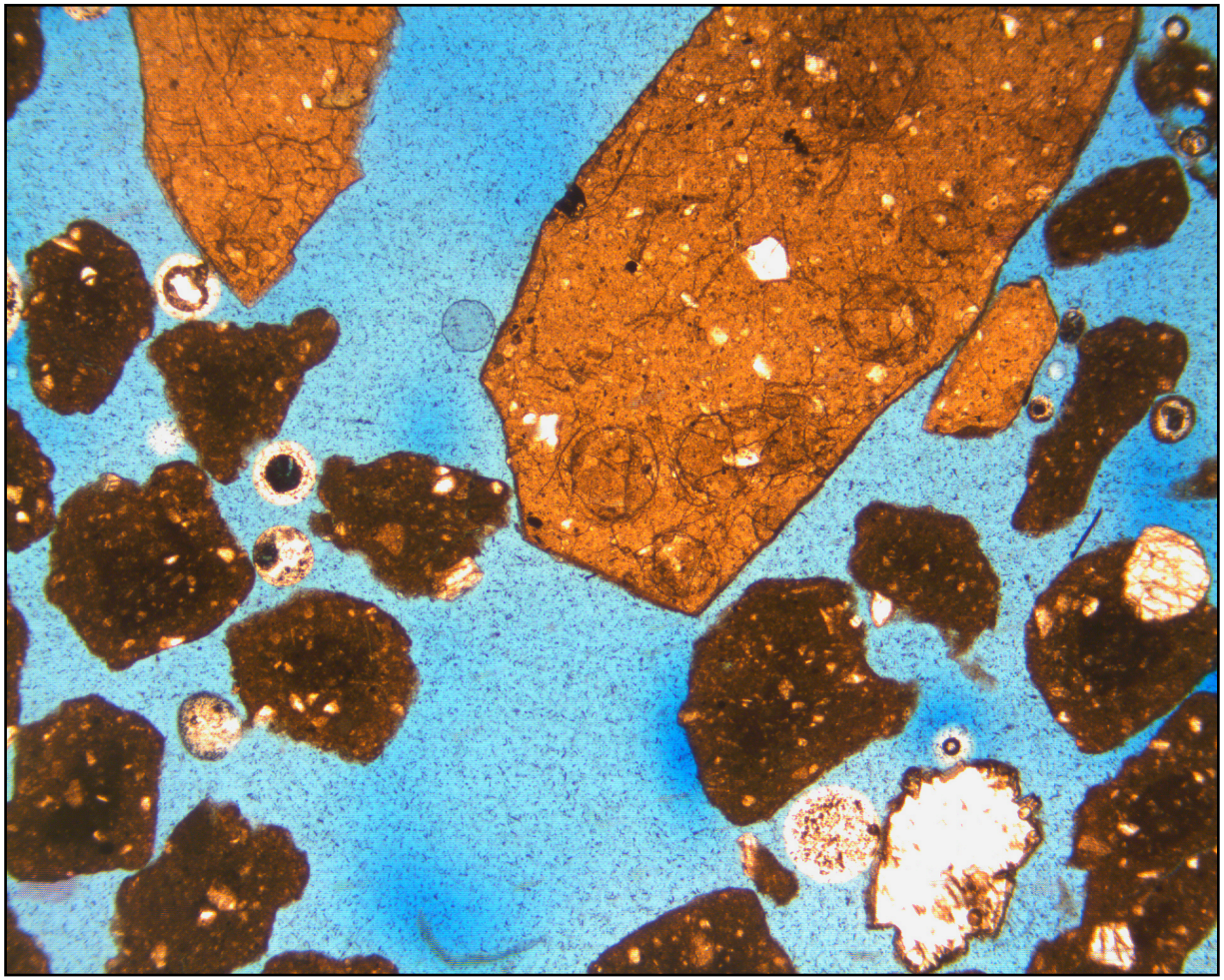

Plate 8: Polymict grains from sample ELT32-20(SAL1639). (x31.25)

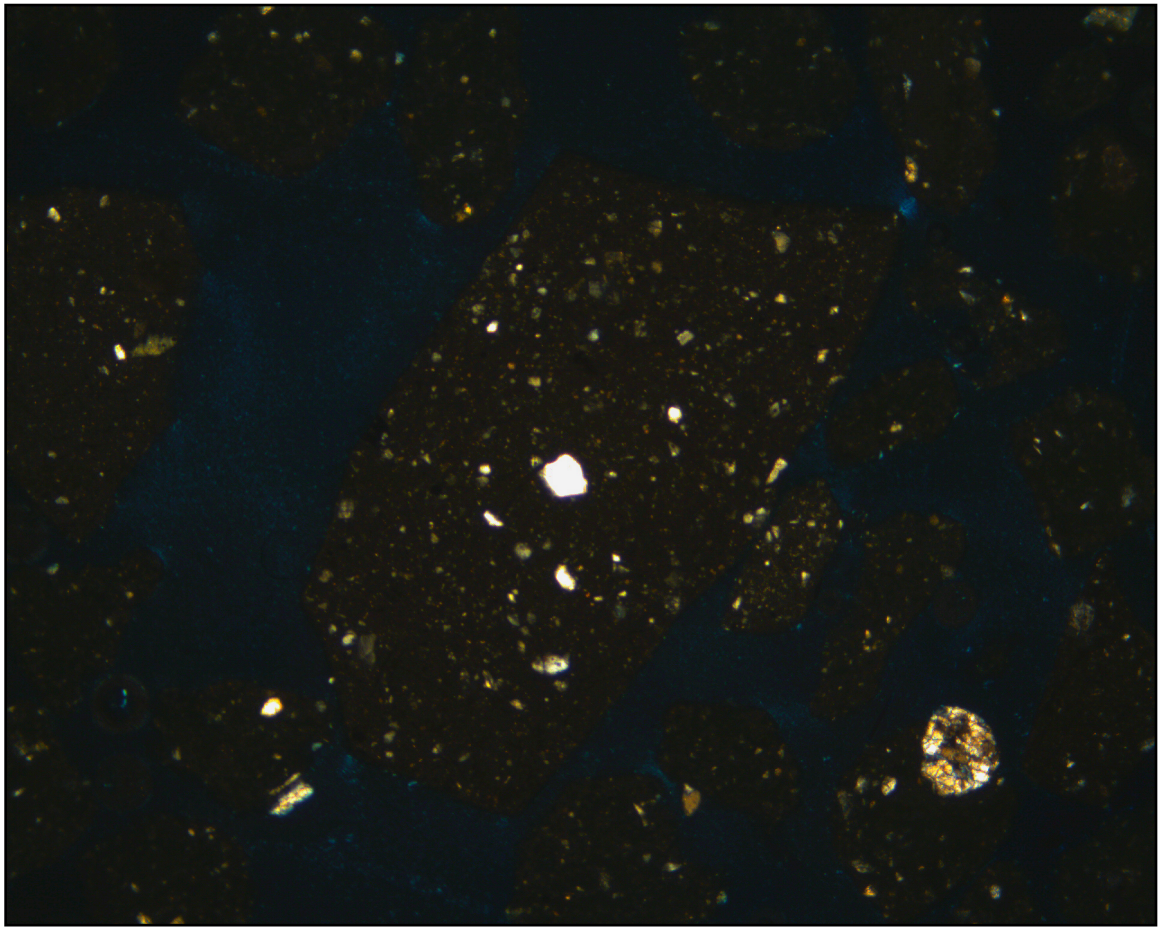

Plate 9: Polymict grains from sample ELT32-20(SAL1639) in cross-polar light.
(x31.25)

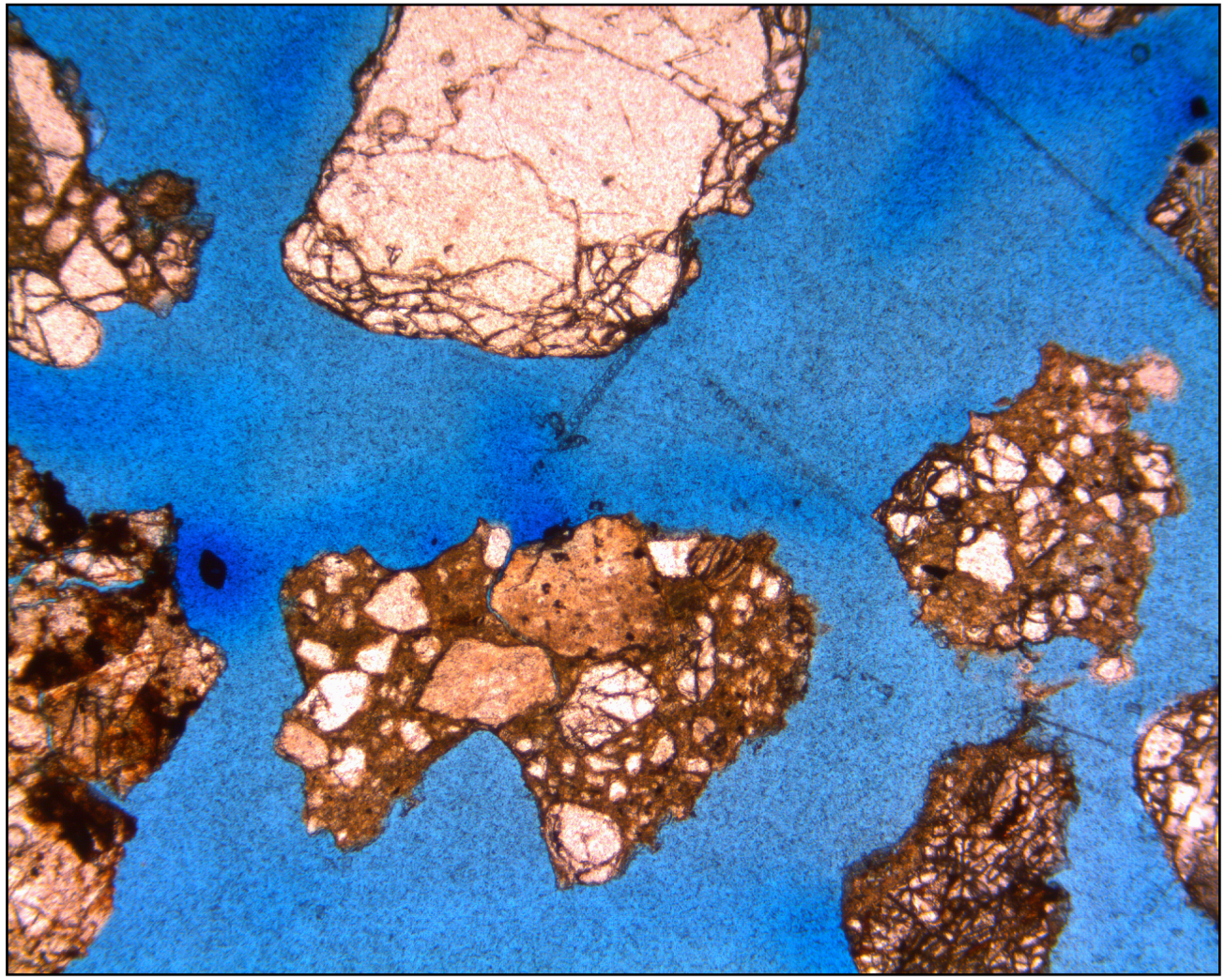

Plate 10: Polymict grains from sample SAL1580 from the Lonewolf Nunataks in plane light. (x31.25)

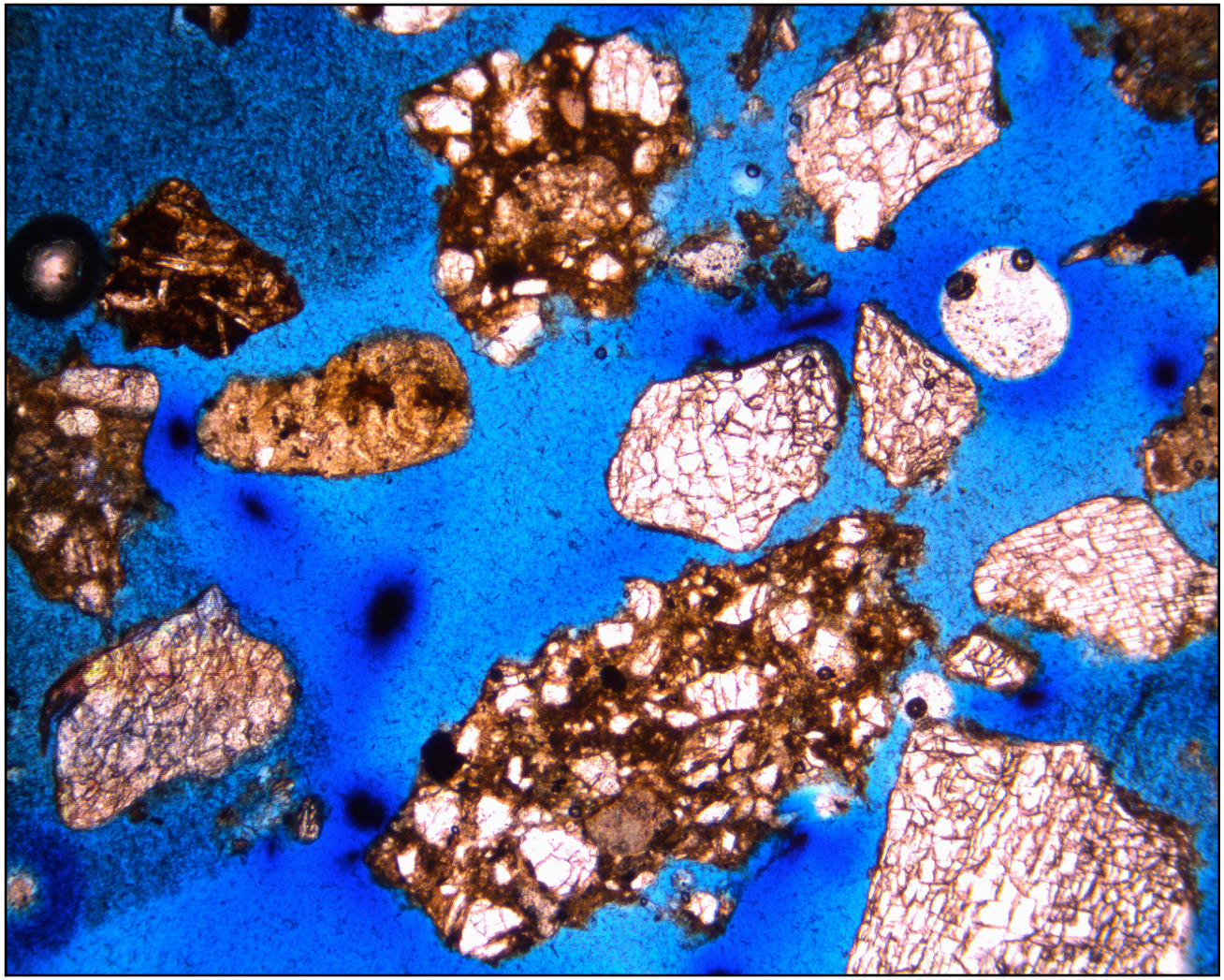

Plate 11: Polymict grains from sample SAL1581 from the Lonewolf Nunataks in plane light. (x31.25)

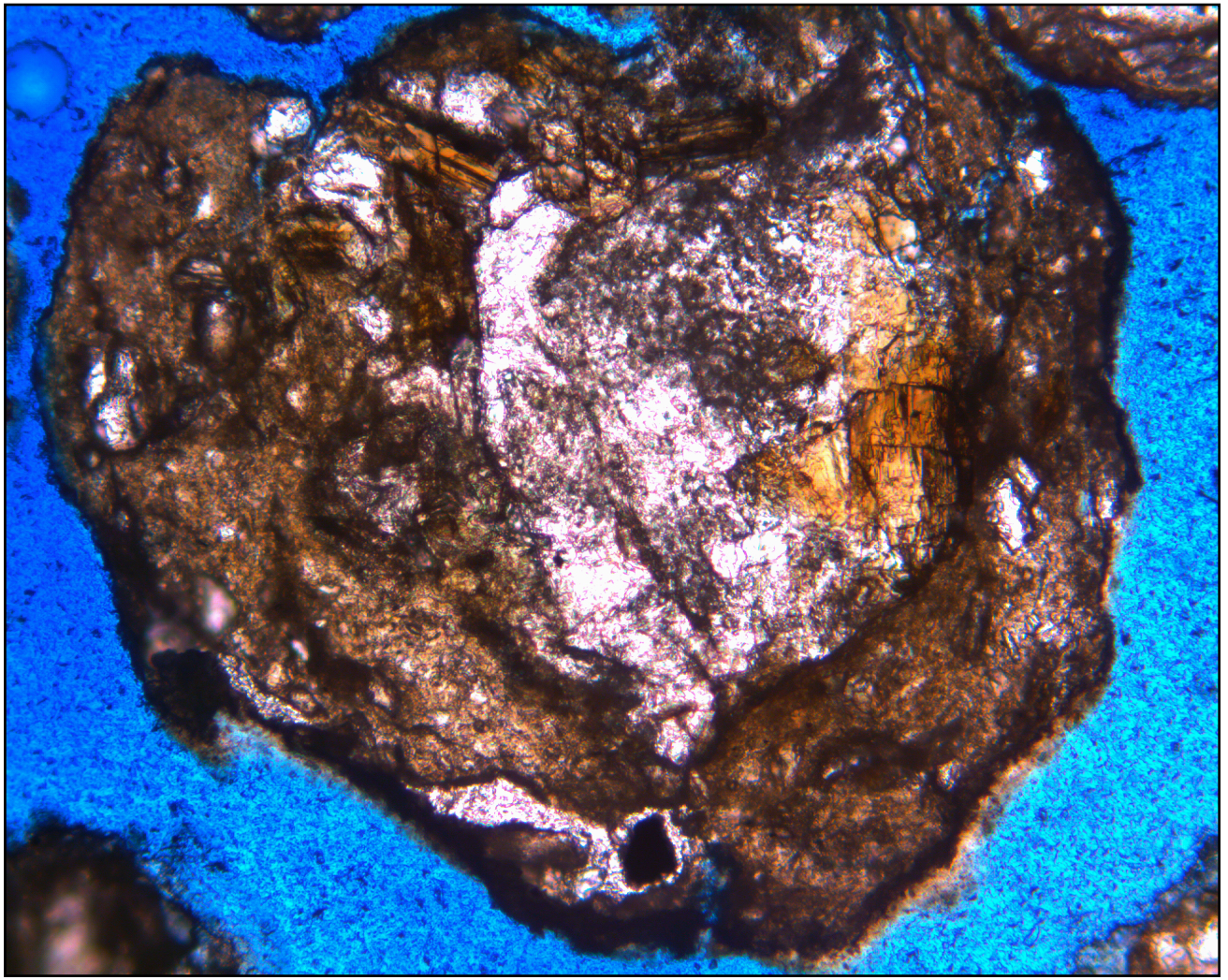

Plate 12: Polymict grains from sample SAL1580 from the Lonewolf Nunataks in plane light. (x120.5)

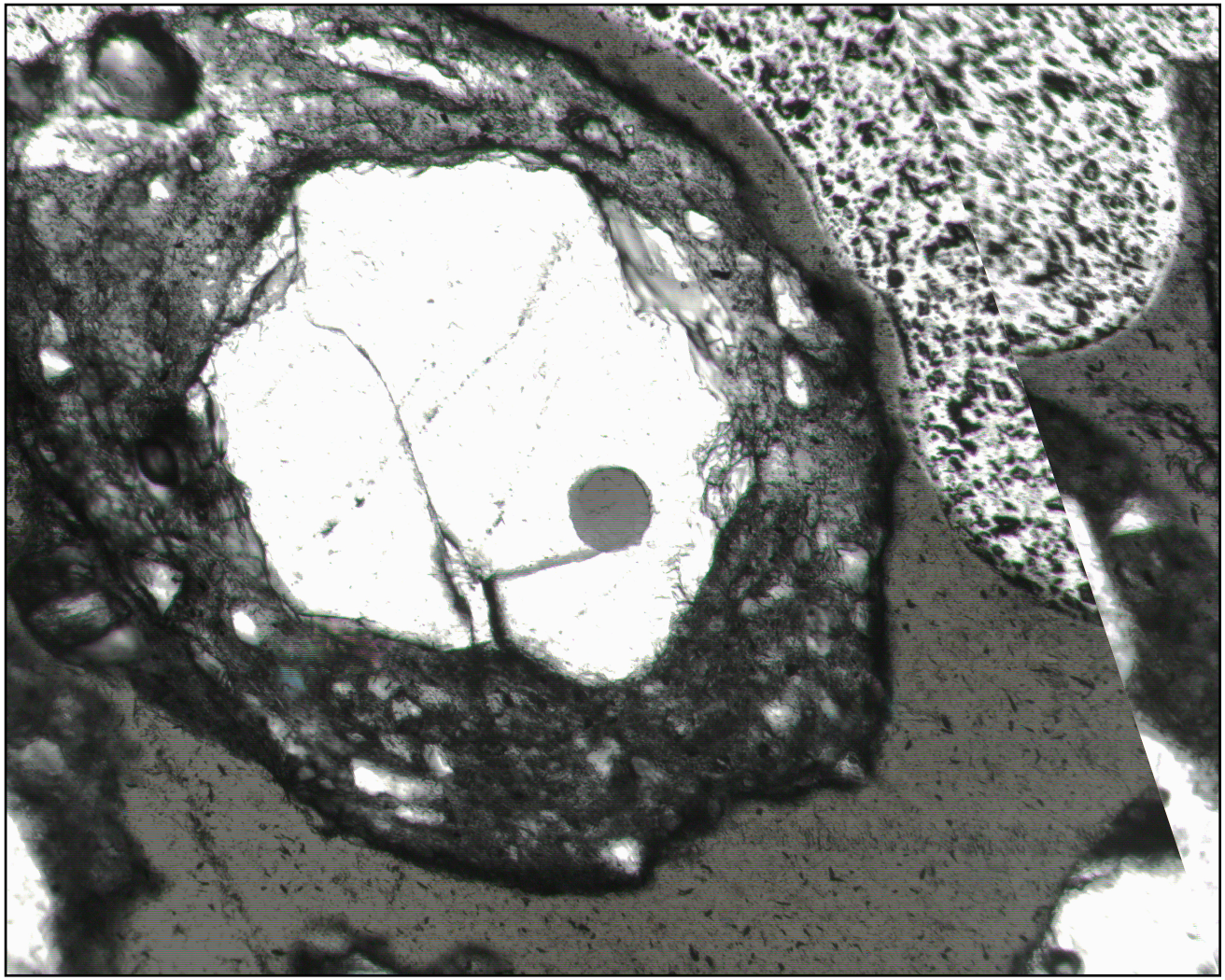

Plate 13: Polymict grains from sample SAL1579 from the Lonewolf Nunataks in plane light. (x120.5)

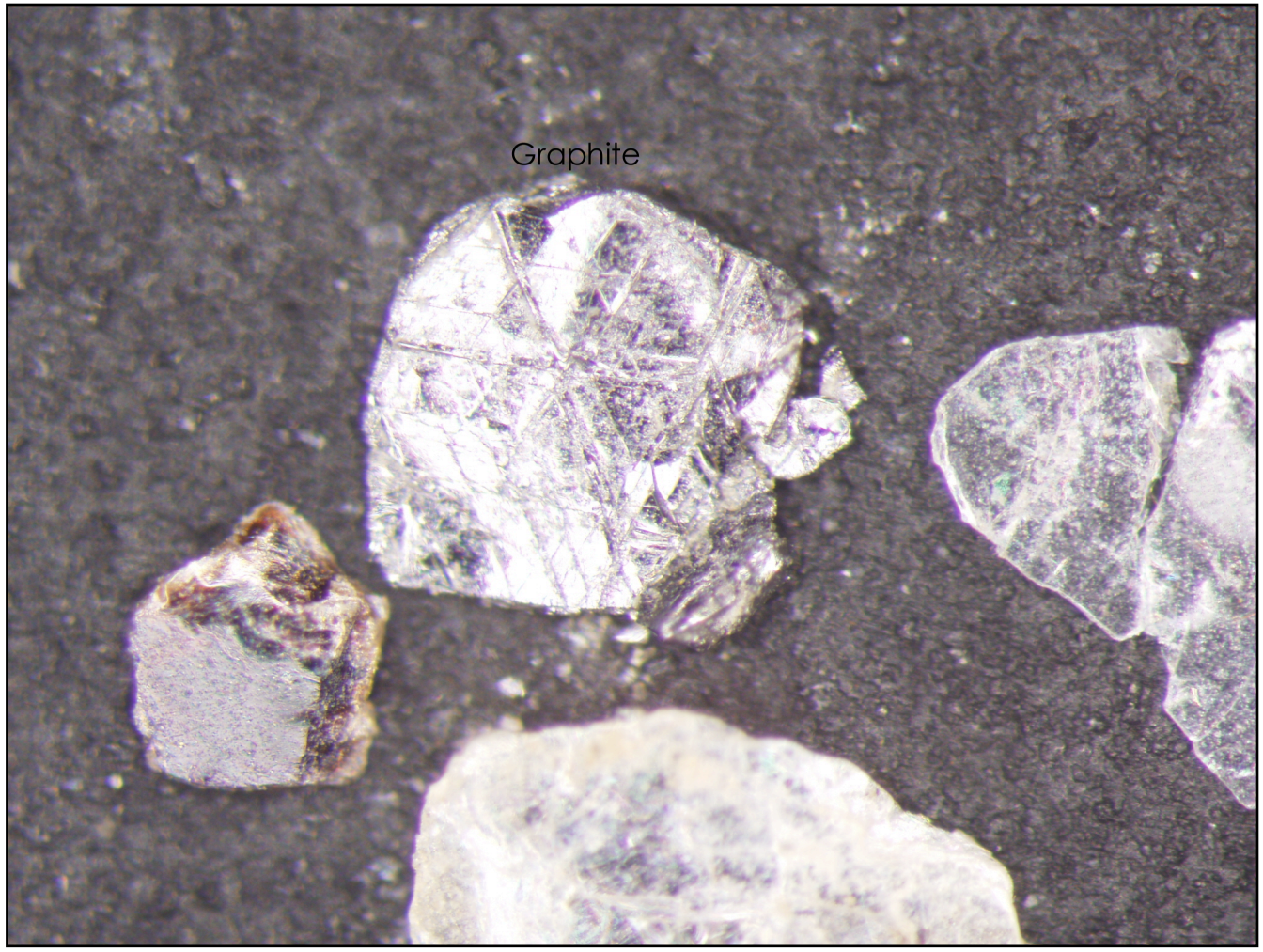

Plate 14: Graphite from CJ sample site. Notice the hexagonal cleavage planes. (x50)

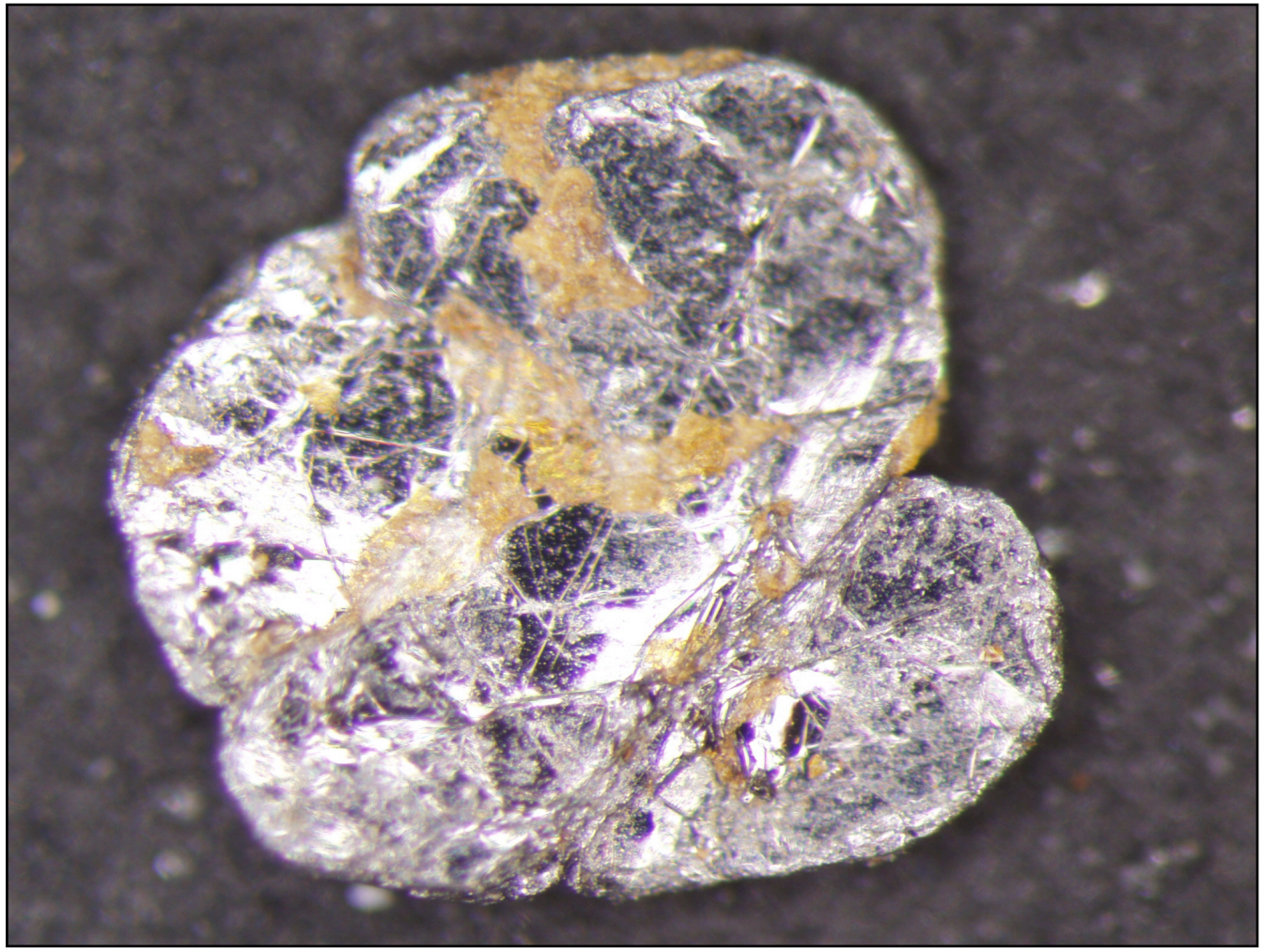

Plate 15: Graphite from HB sample site. Notice the hexagonal cleavage planes. (x108.5)

References

Alley, R.B., and Whillians, I.M., 1991, Changes in the West Antarctic Ice-Sheet: Science, vol. 254, pp. 959–963

Alley, R.B., and Bindschadler, R.A., 2001, The West Antarctic ice sheet and sea-level change: *in* Alley, R.B., and Binschadler, R.A., eds., The West Antarctic ice sheet: behavior and environment: Antarctic Research Series, vol. *77*, Washington, D.C., American Geophysical Union, pp. 1–11

Anderson, J.B., Kurtz, D., Weaver, F., and Weaver, M., 1982, Sedimentation on the West Antarctic Continental Margin, *in* Craddock, C., *ed.*, Antarctic Geoscience: University of Wisconsin Press, Madison, pp. 1003–1012

Anderson, J.B., Brake, C., Domack, E.D., Myers, N., and Singer, J., 1983, Sedimentary dynamics on the Antarctic Continental Shelf, *in* Oliver, R.L., James, P.R., and Jago, J.B., *eds.*, Antarctic Earth Science: Australian Academy of Science, Canberra, pp. 387–389

Anderson, J.B., Brake, C.F., and Myers, N.C., Sedimentation on the Ross Sea continental shelf, Antarctica. Marine Geology, 1984. 57: pp. 295–333.

Anderson, J.B., Shiip, S.S., Bartek, L.R., and Reid, D.E., 1992, Evidence for a grounded ice sheet on the Ross Sea continental shelf during the Late Pleistocene and preliminary paleodrainage reconstruction, Contributions to Antarctic Research Series III, Antarctic Research Series, vol. 57, pp. 39-62

Anderson, J.B., 1999, Antarctic Marine Geology: Cambridge University Press, New York, 289 p.

Anderson, J.B., Shiip, S.S., Lowe, A.L., Wellner, J.S., Mosola, A.B., 2001, The Antarctic Ice Sheet during the Last Glacial Maximum and its subsequent retreat history: A review: Quaternary Science Reviews, vol. 21, pp. 49–70

Arne, D.C., Kelly, P.R., Brown, R.W., and Gleadow, A.J.W., 1993, Reconnaissance apatite fission-track data from East Antarctic Shield, *in* Findlay, R.H., Unrug, R., Banks, M.R., and Veevers, J.J., *eds.*, Gondwana Eight: Assembly, Evolution and Dispersal: Balkema, Hobart, pp. 605–611

Australian Antarctic Data Centre, 2000, Polar Stereographic Map of Antarctica

Ballance, P.F., and Watters, W.A., 2002, Hydrothermal alteration, contact metamorphism, and authigenesis in Ferrar Supergroup and Beacon Supergroup rocks, Carapace Nunatak, Allan Hills, and Coombs Hills, Victoria Land, Antarctica: New Zealand Journal of Geology and Geophysics, vol. 45, pp. 71–84

Baroni, C., and Fasano, F., 2006, Micromorphological evidence of warm-based glacier deposition from the Ricker Hills Tillite (Victoria Land, Antarctica): Quaternary Science Reviews, vol. 25, pp. 976–992

Barrett, P.J., 1972, Stratigraphy and petrology of the mainly fluvial Permian and Triassic part of the Beacon Supergroup, Beardmore Glacier area, *in* Adie R.J., *ed.*, Antarctic geology and geophysics, International Union of Geological Sciences Series B-1, pp. 365–372

Barrett, P.J., 1991, The Devonian to Jurassic Beacon Supergroup of the Transantarctic Mountains and correlatives in other parts of Antarctica, *in* Tingey, R.J., ed. The geology of Antarctica: Oxford Monographs on Geology and Geophysics 17, Clarenden Press, pp. 120–149

Bentley, C.R., 1981, Variations in valley glacier activity in the Transantarctic Mountains as indicated by associated flow bands in the Ross Ice Shelf: *in* Allison, I., ed., Sea Level, Ice, and Climate Change, International Association of Hydrological Sciences, no. 131, pp. 247–251

Bentley, C.R., 1997, Rapid sea-level rise soon from West Antarctic Ice Sheet Collapse?, Science, vol. 275, pp. 1077–1078

Bernet, M., and Gaupp, R., 2005, Diagenetic history of Triassic sandstone from the Beacon Supergroup in central Victoria Land, Antarctica: New Zealand Journal of Geology & Geophysics, vol. 48, pp. 447–458

Bindschadler, R., 1997a, Actively surging West Antarctic ice streams and their response characteristics: Annals of Glaciology, vol. 24, pp. 409–414

Bindschadler, R., 1997b, West Antarctic Ice Sheet Collapse?: Science, vol. 276, pp. 662–664

Borg, S., 1989, Studies of granites and metamorphic rocks, Byrd Glacier area: Antarctic Journal of the United States, vol. 24, pp. 19–21

Borg, S.G., and DePaulo, D.J., 1991, A tectonic model of the Antarctic Gondwana margin with implications for southeastern Australia: isotopic and geochemical evidence: Tectonophysics, vol. 196, pp. 339–mi359

Carter, R.M., Landis, C.A., and Norris, R.J., 1974, Suggestions towards a high-level nomenclature for New Zealand rocks: Journal of the Royal Society of New Zealand, vol. 4., pp. 5–18

Collins, A., and Pisarevsky, S.A., 2005, Amalgamating eastern Gondwana: the evolution of the Circum-Indian Orogens: Earth Science Reviews, vol. 71, pp. 229–270

Collinson, J.W., and Pennington, D.C., 1986, Stratigraphy and petrology of Permian and Triassic fluvial deposits in northern Victoria Land, Antarctica: Antarctic Research Series, vol. 46, pp. 211–242

Conway, H., Hall, B.L., Denton, G.H., Gades, A.M., and Waddington, E.D., 1999, Past and future grounding-line retreat of the West Antarctic Ice Sheet: Science, vol. 286, pp. 280–283

Cox, S.C., Parkinson, D.L., Allibone, A.H., and Cooper, A.F., 2000, Isotopic character of Cambro-Ordovician plutonism, southern Victoria Land, Antarctica: New Zealand Journal of Geology and Geophysics, vol. 43, pp. 501–520

Davey, F.J., 2004, Ross Sea Bathymetry, 1:2,000,000, version 1.0, Institute of Geological & Nuclear Sciences geophysical map 16, Institute of Geological & Sciences Limited, Lower Hutt, New Zealand

Denton, G.H., and Hughes, T.J., 2000, Reconstruction of the Ross ice drainage system, Antarctica, at the last glacial maximum: Geografiska Annaler, vol. 82, no. 2/3, pp. 143–166

Denton, G.H., and Hughes, T.J., 2002, Reconstructing the Antarctic Ice Sheet at the Last Glacial Maximum: Quaternary Science Reviews, vol. 21, pp. 193–202

Domack, E.W., Jacobson, E.A., Shipp, S., and Anderson, J.B., 1999, Late Pleistocene-Holocene retreat of the West Antarctic Ice-Sheet system in the Ross Seaa: Part 2-Sedimentologic and stratigraphic signature: GSA Bulletin, vol. 111, no. 10, pp. 1517–1536

Farmer, G.L., Licht, K., Swope, R.J., and Andrews, J., 2006, Isotopic constraints on the provenance of fine-grained sediment in LGM tills from the Ross Embayment, Antarctica: Earth and Planetary Science Letters, vol. 249, pp. 90–107

Federico, L., Giovanni, C., and Crispini, L., 2006, The Ross orogeny of the Transantarctic Mountains: a northern Victoria Land perspective: International Journal of Earth Sciences, vol. 95, pp. 759–770

Fitzgerald, P.G., and Gleadow, A.J.W., 1988, Fission-track geochronology, tectonics and structure of the Transantarctic Mountains in northern Victoria Land, Antarctica: Chemical Geology, vol. 73, pp. 169–198

Fleming, K., Johnson, P., Zwart, D., Yokoyama, Y., Lambeck, K., and Chapell, J., 1998, Refining the eustatic sea-level curve since the Last Glacial Maximum using far- and intermediate- field sites: Earth and Planetary Letters, vol. 163, pp. 327–342

Geslin, J. K., Link, P. K., and Fanning, C. M., 1999, High-precision provenance determination using detrital-zircon ages and petrography of Quaternary sands on the eastern Snake River Plain, Idaho: Geology, vol. 27, pp. 295–298

Gehrels, G., Valencia, V., and Pullen, A., 2006, Detrital zircon geochronology by laser-ablation multicollector ICPMS at the Arizona Laserchron Center, *in* Loszewski, T., and Huff, W., *eds.,* Geochronology: Emerging Opportunities: Paleontological Society Papers, vol. 12, pp. 67–76

Gogineni, S., Paden, J., Akins, T., Allen, C. Braaten, D., and Jezek, K, 2006, Synthetic aperture radar imaging of sub-surface interfaces in glacial ice: Thirteenth Annual WAIS Workshop, Eatonville, Washington

Goodge, J.W., and Dallmeyer, R.D., 1992, $^{40}Ar/^{39}Ar$ mineral age constraints on the Paleozoic tectonothermal evolution of high-grade basement rocks within the Ross orogen, central Transantarctic Mountains: Journal of Geology, vol. 100, pp. 91–106

Goodge, J.W., Hansen, V.L., Peacock, S.M., Smith, B.K., Walker, N.W., 1993a, Kinematic evolution of the Miller Range shear zone, central Transantarctic Mountains, Antarctica, *in* Yoshida, Y., Kaminuma, K., Shiraishi, K., *ed.*, Recent progress in Antarctic earth science: Tokyo, Terra Scientific, pp. 203–209

Goodge, J.W., Walker, N.W., and Hansen, V.L., 1993b, Neoproterozoic-Cambrian basement-involved orogenesis, within the Antarctic margin of Gondwana: Geology, vol. 21, no. 1, pp. 37–40

Goodge, J.W., Myrow, P., Williams, I.S., and Bowring, S.A., 2002. Age and provenance of the Beardmore Group, Antarctica: Constraints on Rodinia supercontinent breakup: Journal of Geology, vol. 110, pp. 393–406.

Goodge, J.W., and Fanning, C.M., 2002, Precambrian crustal history of the Nimrod Group, central Transantarctic Mountains: Royal Society of New Zealand Journal, vol. 35, pp. 43–50

Goodge, J.W., Williams, I. S., and Myrow, P., 2004, Provenance of Neoproterozoic and lower Paleozoic siliciclastic rocks of the central Ross orogen, Antarctica: Detrital record of rift-, passive-, and active-margin sedimentation. G.S.A. Bulletin, vol. 116(no. 9/10), pp. 1253–1279.

Goodge, J.W., and Vervoort, J.D., 2006, Origin of Mesoproterozoic A-type granites in Laurentia: Hf isotope evidence: Earth and Planetary Science Letters, vol. 243, pp. 711–731

Goodge, J.W., Brecke, D.V., Fanning, C.M., Vervoort, J.D., Williams, I.S., and Myrow, P., 2007, Pieces of Laurentia in East Antarctica, Cooper, A.K., and Raymond, C.R., *eds.*, *in* USGS Open-File Report 2007-1047, Extended Abstract 055, 1–4

Grikurov, G.E., 1982, Structure of Antarctica and outline of its evolution, *in* Craddock, C., *ed.*, Antarctic Geoscience: University of Wisconsin Press, Madison, pp. 791–804

Grindley, G.W., and Laird, M.G., 1969, Geology of the Shackleton Coast, Antarctica, *in* Bushnell, V.C., and Craddock,C., *eds.*, Geologic map of Antarctica: New York, American Geographical Society, Antarctica Map Folio Series, folio 12, sheet 15, scale 1:1000000

Grousset, F.E., Labeyrie, L., Sinko, J.A., Cremer, M., Bond, G., Duprat, J., Cortijo, E., and Huon, S., 1993, Patterns of ice-rafted detritus in the glacial North Atlantic (40–55°N): Paleoceanography, vol. 8, pp. 175–192

Guynn, J., 2006, Comparison of detrital zircon age distribution using the K-S test: Department of Geosciences, University of Arisona, Tucson, 10 p.

Gwiazda, R.H., Hemming, S.R., and Broecker, W.S., 1996, The provenance of ice-rafted debris in Heinrich layer 2, Paleoceanography, vol. 11, pp. 77–93

Halpin, J.A., Gerakiteys, C.L., Clarke, G.L., Belousova, E.A., and Griffin, W.L., 2005, In-situ U-Pb geochronology and Hf isotope analysis of the Rayner Complex, east Antarctica: Contributions to Mineralogy and Petrology, vol. 148, pp. 689–706

Hemming, S.R., Broecker, W.S., Sharp, W.D., Bond, G.C., Gwiazda, R.H., MaManus, J.F., Klas, M., and Hajdas, I., 1998, Provenance of Heinrich layers in core V28-82, northeastern Atlantic: $^{40}Ar/^{39}Ar$ ages of ice-rafted horneblende, Pb isotopes in feldspar grains, and Nd-Sr-Pb isotopes in the fine sediment fraction: Earth and Planetary Science Letters, vol. 164, pp. 317–333

Hemming, S.R., Gwiazda, R.H., Andrews, J.T., Broecker, W.S., Jennings, A.E., and Onstott, T.C., 2000, $^{40}Ar/^{39}Ar$ ages and Pb-Pb study of individual horneblende and feldspar grains from southeastern Baffin Island glacial sediments: Implications for the provenance of Heinfich layers: Canadian Journal of Earth Sciences, vol. 37, pp. 879–890

Hemming, S.R., Hall, C.M., Biscaye, P.E., Higgins, S.M., Bond, G.C., McManus, J.F., Barber, D.C., Andrews, J.T., and Broecker, W.S., 2002, $^{40}Ar/^{39}Ar$ ages and ^{40}Ar concentrations of fine-grained sediment fractions from North Atlantic Heinrich layers: Chemical Geology, vol. 182, pp. 583–603

Holcombe, R.J., Stephens, C.J., Fielding, C.R., Gust, D., Little, T.A., Silwa, R., Kassan, McPhie, J., and Ewart, A.E., 1997, Tectonic evolution of the northern New England Fold Belt: the Permian-Triassic Hunter -Bowen event: Geological Society of Australia Special Paper, no. 19, pp. 52–65

Hollin, J.T., 1962, On the glacial history of Antarctica: Journal of Glaciology, vol. 4, pp. 173–195

Hughes, T.J., 1973, Is the West Antarctic Ice Sheet disintegrating?: Journal of Geophysical Research, vol. 78, pp. 7884–7909

Jahns, E., 1994, Evidence for a fluidized till deposit on the Ross Sea continental shelf: Antarctic Journal of the U.S., vol. 29, pp. 139–141

Jacobs, J., Fanning, C.M., Henjes-Kunst, F., Olesch, M., and Paech, H., 1998, Continuation of the Mozambique Belt into East Antarctica: Grenville-age metamorphism and polyphase Pan-African high-grade events in central Dronning Maud Land: Journal of Geology, vol. 102, pp. 47–65

Johnson, G.L., Vanney, J.R., and Hayes, P., 1982, The Antarctic continental shelf: A review, *in* Craddock, C., *ed.*, Antarctic Geoscience: University of Wisconsin Press, Madison, pp. 505–510

Kamenev, E.N., 1982, Antarctica's oldest metamorphic rocks in the Fyfe Hills, Enderby Land, *in* Craddock, C., *ed.*, Antarctic Geoscience: University of Wisconsin Press, Madison, pp. 505–510

Kellogg, T.B., Truesdale, R.S., and Osterman, L.E., 1979, Late Quaternary extent of the West Antarctic Ice Sheet: new evidence from Ross Sea cores: Geology, vol. 7, pp. 249–253

Laird, M.G., 1987, Lower-mid-Paleozoic sedimentation and tectonic patterns on the paleo-Pacific margin of Antarctica: *in* Thomson, M.R.A., Crame, J.A., and Thomson, J.W., eds., Geological Evolution of Antarctica: Cambridge, Cambridge University Press, pp. 177–185

Lederer, J.R., 2003, Provenance of last glacial maximum till from the Ross Embayment, Antarctica: M.S. Thesis, Indiana University, 72 p.

Licht, K.J., Jennings, A.E., Andrews, J.T., and Williams, K.M., 1996, Chronology of late Wisconsin ice retreat from the western Ross Sea, Antarctica: Geology, vol. 23, no. 3, pp. 223–226

Licht, K.J., 1999, Investigations into the late Quaternary history of the Ross Sea, Antarctica (PhD Dissertation): Boulder, University of Colorado, 234 p.

Licht, K.J., Dunbar, N.W., Andrews, J.T., and Jennings, A.E., 1999, Distinguishing subglacial till and glacial marine diamictons in the western Ross Sea, Antarctica: Implications for a last glacial maximum grounding line: Geological Society of America Bulletin, vol. 111, no. 1, pp. 91–103

Licht, K.J., and Fastook, J., 1998, Constraining a numerical ice sheet model with geologic data over one ice sheet advance/retreat cycle in the Ross Sea: Chapman Conference on the West Antarctic Ice Sheet, University of Maine, pp. 25–26

Licht, K.J., Jennings, A.E., Andrews, J.T., and Williams, K.M., 1996, Chronology of the Late Wisconsin ice retreat from the western Ross Sea, Antarctica: Geology, vol. 24, pp. 223–226

Licht, K.J., 2004, The Ross Sea's contribution to eustatic sea level during meltwater pulse 1A: Sedimentary Geology, vol. 165, pp. 343–353

Licht, K.J., Lederer, J. R., and Swope, R. J., 2005, Provenance of LGM glacial till (sand fraction) across the Ross Embayment, Antarctica: Quaternary Science Reviews, vol. 24, pp. 1499–1520

Lisker, F., 1996, Geodynamik des Westantarktischen Riftsystems basierend auf Apatit-Spalts-puranalysen: Berichte zur Polarforschung, vol. 198, Kamloth, Bremerhaven, 108 p.

Lisker, F., 2002, Review of fission track studies in northern Victoria Land, Antarctica - passive margin evolution versus uplift of the Transantarctic Mountains: Tectonophysics, vol. 349, pp. 57–73

Ludwig, K.R., 2003, Isoplot 3.00: Berkeley Geochronology Center, Special Publication no. 4, 70 p.

MacAyeal, D.R., 1992, Irregular oscillations of the West Antarctic Ice-Sheet: Nature, vol. 359, pp. 29–32

Mercer, J.H., 1978, West Antarctic Ice Sheet and CO_2 greenhouse effect: A threat of disaster: Nature, vol. 271, pp. 321–325

Meert, J.G., 2003, A synopsis of events related to the assembly of eastern Gondwana: Tectonophysics, vol. 362, pp. 1–40

Mikhalsky, E.V., Beliatsky, B.V., Savva, E.V., Wetzel, H.U., Fedorov, L.V., Weiser, T., and Hahne, K., 1997, Reconnaissance geochronologic data on poly-metamorphic and igneous rocks of the Humboldt Mountains, central Queen Maud Land, East Antarctica, *in* Ricci, C.A., ed., The Antarctic Region: Geological Evolution and Processes: Terra Antarctica Publication, Siena, pp. 45–53

Moores, E.M., 1991, Southwest U.S. - East Antarctic (SWEAT) connection: A hypothesis: Geology, vol. 19, pp. 425–428

Mukasa, S.B., and Dalziel, I.W.D., 2000, Marie Byrd Land, West Antarctica: Evolution of Gondwana's Pacific margin constrained by zircon U/Pb geochronology and feldspar common-Pb isotopic compositions: GSA Bulletin, vol. 112, no. 4, pp. 611–627

Oppenheimer, M., 1998, Global warming and the stability of the West Antarctic Ice Sheet: Nature, vol. 393, pp. 325–332

Pankhurst, R.J., Weaver, S.D., Bradshaw, J.D., Storey, B.C., and Ireland, T.R., 1998, Geochronology and geochemistry of pre-Jurrasic superterranes in Marie Byrd Land, Antarctica: Journal of Geophysical Research, vol. 103, n0. B2, pp. 2529–2547

Pell, S.D., Williams, I.S., and Chivas A.R., 1997, The use of protolith zircon-age finger prints in determining the protosource areas for some Australian dune sands: Sedimentary Geology, vol, 109, pp. 233–260

Phillips, G., Wilson, C.J.L., Campbell, I.H., and Allen, C.M., 2006, U-Th-Pb detrital zircon geochronology from the southern Prince Charles Mountains, East Antarctica - Defining the Archaean to Neoproterozoic Ruker Provence: Precambrian Research, vol. 148, pp. 292–306

Ravich, M.G., 1982, The lower Precambrian of Antarctica - review paper, *in* Craddock, C., *ed.*, Antarctic Geoscience: University of Wisconsin Press, Madison, pp. 65–71

Schafer, T., 1998, Thermo-tektonische Entwicklung von Oates Land und der Shackleton range (Antarktis) basierend auf Apatit-Spalts-puranalysen: Berichte zur Polarforschung, vol. 263, Kamloth, Bremerhaven, 107 p.

Scherer, R.P., Aldahan, A., Tulaczyk, S., Possnert, G., Englehardt, H., and Kamb, B., 1998, Pleistocene collapse of the West Antarctic Ice Sheet, Science, vol. 281, pp. 82–85

Scambos, T.A., Bohlander, J.A., Shuman, C.A., and Skvarca, P., 2004, Glacier acceleration and thinning after ice shelf collapse in the Larsen B embayment, Antarctica: Geophysical Research Letters, vol. 31, no. 18, 4 p.

Shipp, S.S., Anderson, J.B., and Domack, E.W., 1999, Late Pleistocene-Holocene retreat of the West Antarctic Ice-Sheet system in the Ross Sea: Part 1-Geophysical results: GSA Bulletin, vol. 111, no. 10, pp. 1486–1516

Sircombe, K.N., 2000, Quantitative comparison of large sets of geochronological data using multivariate analysis: A provenance example from Australia: Geochimica et Cosmochimica Acta, vol. 94, no. 9, pp. 1593–1616

Sobotovich, E.V., Kamenev, E.N., Komaristyy, A.A., and Rudnik, V.A., 1976, The oldest rocks in Antarctica (Enderby Land): International Geological Review, vol. 18, pp. 371–388

Stacey, J.S., and Kramers, J.D., 1975, Approximation of terrestrial lead isotope evolution by a two-stage model: Earth and Planetary Science Letters, vol. 26, pp. 207–221

Stearns, L., and Hamilton, G., 2005, A new velocity map for Byrd Glacier, East Antarctica, from sequential ASTER satellite imagery: Annuls of Glaciology, vol. 41, no. 1, pp. 71–76

Stump, E., Edgerton, D.G., and Korsch, R.J., 2002, Geological relationships at Cotton Plateau, Nimrod Glacier Area, bearing on the tectonic development of the Ross Orogen, Transantarctic Mountains, Antarctica: Terra Antarctica, vol. 9, no. 1, pp. 3–18.

Stump, E., Gootee, B.F., Talarico, F., Van Schmus, W.R., Brand, P.K., Foland, K.A., and Fanning, C.M., 2004, Correlation of Byrd and Selborne Groups, with implications for the Byrd Glacier discontinuity, central Transantarctic Mountains, Antarctica: New Zealand Journal of Geology & Geophysics, vol. 47, pp. 157–171

Stump, E., Gootee, B.F., and Talarico, F., 2006, Tectonic model for development of the Byrd Glacier discontinuity and surrounding regions of the Transantarctic Mountains during the Neoproterozoic-early Paleozoic: International Symposium on Antarctic Earth Sciences, vol. 9, pp. 181–190

Stuiver, M., Denton, G.H., Hughes, T.J., and Fastook, J.L., 1981, History of the marine ice sheets in West Antarctica during the last glaciation: A working hypothesis, *In* Denton, G.H., and Hughes, T.J., eds., The Last Great Ice Sheets: New York, Wiley-Interscience, pp. 487–496

Suggate, R.P., 1978, The Geology of New Zealand, Vols. 1 and 2: New Zealand Geological Survey, Wellington

Suttner, L.J., 1974, Sedimentary petrographic provinces: an evaluation, *in* Ross, C.A., *ed.*, Paleogeographic Provinces and Provinciality: SEPM Special Publication, v. 21, pp. 1486–1516

Suttner, L.J., Basu, A., and Mack, G.H., 1981, Climate and the origin of quartz arenites: Journal of Sedimentary Petrology, v. 51, no. 4, pp. 1235–1246

ten Brink, U.S., Schneider, C., and Johnson, A.H., 1995, Morphology and stratal geometry of the Antarctic continental shelf: Insights from models, *in* Cooper, A.K., and Davey, F.J., *eds.*, The Antarctic continental margin, Earth Science Series,k Volume 5B,: Geology and Geophysics of the Western Ross Sea: Houston, Circum-Pacific Council for Energy and Mineral Resources, pp. 1–24

Tingey, R.J., 1991, The regional geology of Archaean and Proterozoic rocks in Antarctica, in Tingey, R.J., ed. The geology of Antarctica: Oxford Monographs on Geology and Geophysics 17, Clarenden Press, pp. 1–73

Thomas, R.H., 1979, Effect of climate warming on the West Antarctic ice sheet: Nature, vol. 277, no. 5695, pp. 355–358

Thomas, R.H., 1979, The dynamics of marine ice sheets: Journal of Glaciology, vol. 24, pp. 167–177

Thomas, R.H., Sanderson, T.J.O., and Rose, K.E., 1979, Effect of climatic warming on the West Antarctic Ice Sheet: Nature, vol. 277, pp. 355–358

van der Veen, C.J., Response of a marine ice sheet to changes at the grounding line: Quaternary Research, vol. 24, pp. 257–267

Weertman, J., 1974, Stability of the junction of an ice sheet and an ice shelf: Journal of Glaciology, vol. 13, no. 6, pp. 543–544

Wilhelm, S., 1994, Geochemische und quantitative petrographische Untersuchungen (Kristall-größenverteilung) an Ferrar-Sills und Kirkpatrick-Flows, Victoria Land, Antarktis: Unpublished Masters thesis, Johannes-Gutenberg Universität Mainz, Germany, 172 p.

Wilson, M., 1989, Igneous petrogenesis, a global tectonic approach: New York, Chapman and Hall, 466 p.

CURRICULUM VITAE

Emerson Fowler Palmer
epalmer@ldeo.columbia.edu
emersonpalmer@mac.com

Education

- **M.S. Geology** - February 2008 Indiana University, Indianapolis, IN
- **B.A. Geology** - 2005 Indiana University, Indianapolis, IN
- **Graduate Certificate in GIS** - 2008 Indiana University, Indianapolis, IN

Professional Experience

Research Assistant (Sept. 2007 - present)

Lamont-Doherty Earth Observatory of Columbia University
Geochemistry Division
Ar Thermochronometry Laboratory

Field Geologist (November - December 2007)

Indiana Geological Survey at Indiana University
Antarctic Field Season 2007 - Taylor Valley, Antarctica
Science Group: I-133
Principle Investigator: Dr. Michael Prentice

Graduate Research Assistant (August 2005 - 2007)

IUPUI Department of Earth Sciences

Research Project Synopsis: A comparative provenance study of Antarctic glacial material from the Byrd and Nimrod Glaciers with Ross Sea marine sediments using sand petrography, particle size analysis, and U/Pb age dating of detrital zircons.

Research Advisor: Dr. Kathy Licht (317-278-1343)

Laboratory Technician (December 2003 - May 2005)

Sediment Analysis Laboratory - IUPUI

Field and Laboratory Research Intern (January 2005 - August 2005)

Center for Earth and Environmental Sciences - IUPUI

Awards and Grants

IU Travel Fellowship (2006)
2006 American Geophysical Union Annual Meeting - $800

IUPUI Graduate Student Organization Educational Enhancement Grant (2006)
Grant for graduate students to assist in research, training, or research presentation at national conferences - $500

Center for Earth and Environmental Science Distinguished Student Award (2005)
Award for outstanding undergraduate student assisting in CEES sponsored research - $500

Indiana Geology and Gem Society Scholarship (2004)
Scholarship to support a qualified undergraduate Geology major who is not within twelve months of graduation following beginning of Fall semester - $1000

Undergraduate Research Opportunities Program Grant (2004)
Program supporting undergraduate research with a faculty mentor - $3000

Topic: A Comparative Geochemical Study of the Palms and White Tank Granites in Joshua Tree National Park - *Dr. Andrew Barth advising*

Deans List
Fall 2003, Spring 2003, Fall 2004

Distinguished Hoosier Award Gov. Evan Bayh (1990)

Publications

Palmer, E.F., and Licht, K., 2007, Sand Petrography and U/Pb Detrital Geochronology of Late Quaternary Tills from the Byrd Glacier and Central/Western Ross Sea, Antarctica: in Cooper, A.K., and Raymond C.R. et al., eds., A Keystone in a Changing World - Online Proceedings of the 10th ISAES X, USGS OFR-2007-1047, ExtendedAbstract 134, 1-3

Licht, K., and Palmer, E.F., 2007, Characteristics of Till Transported by the Byrd and Nimrod Glaciers, Antarctica: in Cooper, A.K., and Raymond C.R. et al., eds., A Keystone in a Changing World - Online Proceedings of the 10th ISAES X, USGS OFR-2007-1047, Extended Abstract 114, 1-3

Brown, K.L., Palmer, E.F., and Barth, A.P., 2007 Depth-Dependent Geochemical Changes in Late Cretaceous Granitic Rocks, Transverse Ranges, Southern California: Geological Society of America Abstracts with Programs, vol.39, no. 6

Wiengand, B.A., Barth, A.P., Wooden, J.L., Palmer, E.F., and Brown, K.L., 2007, Sr and Nd isotopic evolution in Late Cretaceous lower to upper crustal granitic rocks from the Transverse Ranges, Southern California: Geological Society of America Abstracts with Programs, vol. 39, no. 6

Palmer, E.F., Brown, K.L., Wiegand, B., Wooden, J.L., Needy, S.K., and Barth, A.P., 2006, A Geochemical Comparison of Plutonic Granitoids to Deeper Sheeted Plutonic Rocks: Eastern Transverse Ranges, Southern California, Geological Society of America Abstracts with Programs, vol. 38, no. 7

Palmer, E.F., Licht, K., and Swope, R.J., 2006, Rock, Till, and Ice: A Provenance Study of the Byrd Glacier, Antarctica, Eos Trans. AGU, 87(52), Fall Meet. Suppl., Abstract V31D-0627

Fohey, N., Barth, A.P., Wooden, J., and Palmer, E.F., 2006, A Geochemical Comparison of Voluminous Ignimbrites from the Sidewinder Volcanic Series to Exposed Contemporaneous Plutons, Southern California, Geological Society of America Abstracts with Programs, vol. 38, no. 7

Licht, K., Swope, R.J., and Palmer, E.F., 2006, Evolution of Till During Transport Down the Byrd and Nimrod Glaciers, Antarctica, Geological Society of America Abstracts with Programs, vol. 38, no. 7

Professional Societies

Geological Society of America
American Geophysical Union
American Association of Petroleum Geologists

Teaching Experience

- Physical Geology Laboratory, IUPUI (Fall 2004)

Field Experience

Field Equipment

22 HP Hydraulic Coring Drill with 4.5 meter mast and compressed air chip removal system, YSI Multi-Parameter Water Quality Monitor, Hydrolab, Brunton Transit Compass, Trimble GPS, Trimble Total Station

- **Surface Sampling and Permafrost Coring of Glacial Sediment in Taylor Valley, Antarctica** (November - December, 2007)
- **Field Mapping in San Bernardino Mountains, California** (June, 2006)
- **Sample Collection at Byrd and Nimrod Glaciers, Antarctica** (November, 2005)
- **Sample Collection and Field Mapping in Joshua Tree National Park, California** (December, 2004; May, 2004; May 2005; May 2006)
- **Sample and Spectrographic Data Collection at Geist Reservoir, Indiana** (June, 2005)

International Meetings and Professional Workshops

2007

- 10th International Symposium of Antarctic Earth Sciences - August 2007

2006

- Sequence Stratigraphy Short Course, Geological Society of America Annual Meeting, Philadelphia, PA - October 2006
- Geological Society of America Annual Meeting, Philadelphia, PA - October 2006
- Transantarctic Mountains Workshop, The Ohio State University - September, 2006

2005

- Western Antarctic Ice Sheet Initiative Workshop (WAIS), Sterling, VA - September, 2005

2004

- Geological Society of America Annual Meeting, Denver, CO - October, 2004

Student Organizations

Graduate Student Government

- School of Science Student Council - Earth Sciences Representative (2007)
- Geology Club Student Council Representative (2004)

Undergraduate Student Government

- School of Science Senator (2005)
- Geology Club Student Council Representative (2004)

Geology Club

- President (2005)
- USGS House Representative (2004)

School of Science Student Council

- Geology Club Representative (2004, 2005)
- Public Relations Officer (2005)